VIRGINIA TECH

CENTER FOR COMPOSITE MATERIALS AND STRUCTURES

Structural Efficiency Study of Composite Wing Rib Structures

Gary D. Swanson
Zafer Gurdal
James H. Starnes, Jr.

Virginia Polytechnic
Institute
and
State University

Blacksburg, Virginia
24061
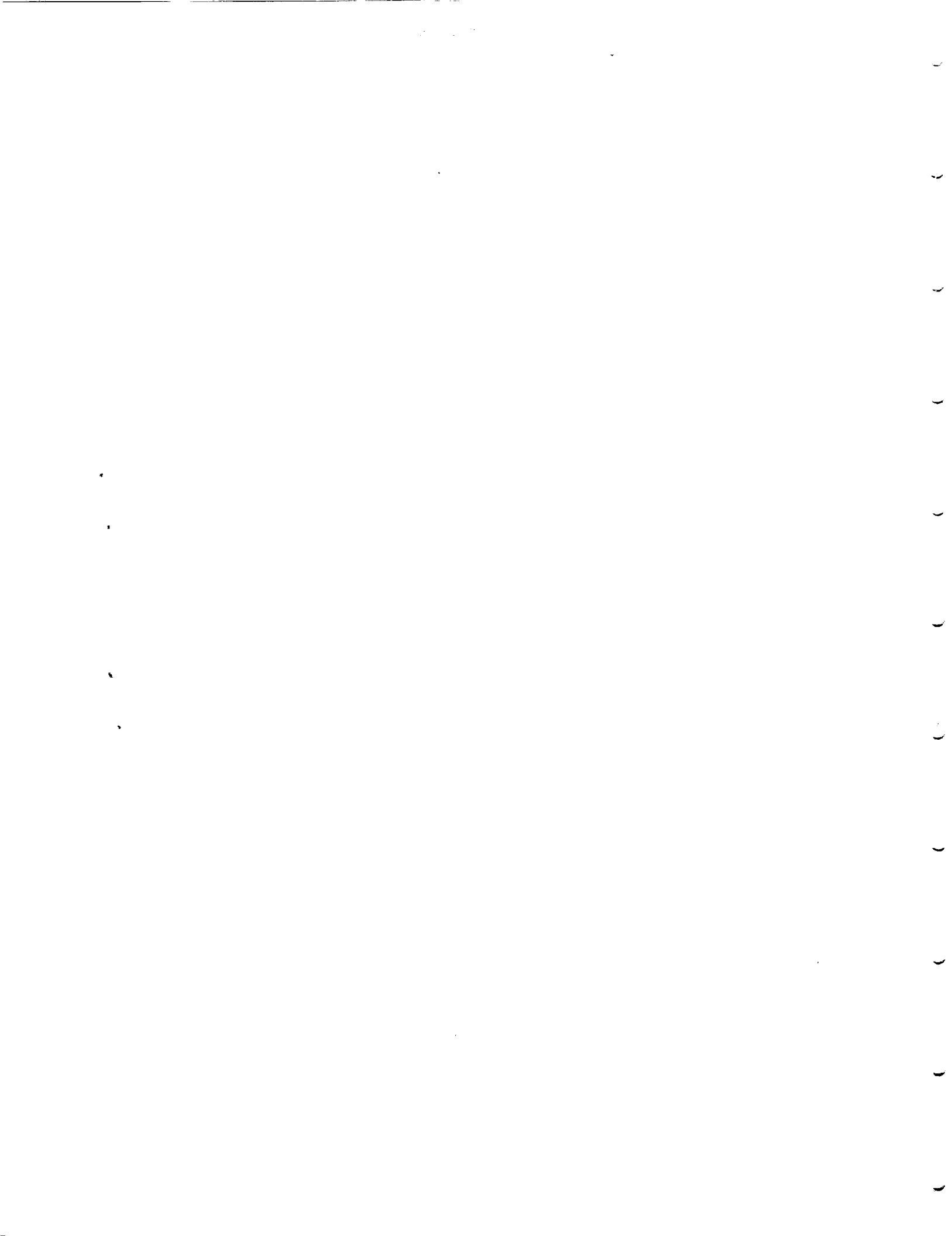
September 1988

College of Engineering
Virginia Polytechnic Institute and State University
Blacksburg, Virginia 24061

September 1988

CCMS-88-18
VPI-E-88-29

Structural Efficiency Study of
Composite Wing Rib Structures

Gary D. Swanson[1]
Zafer Gurdal[2]
James H. Starnes, Jr.[3]

[1] Graduate Student, Department of Engineering Science and Mechanics,
Virginia Polytechnic Institute and State University

[2] Assistant Professor, Department of Engineering Science and Mechanics,
Virginia Polytechnic Institute and State University

[3] Head, Structural Mechanics Branch, NASA Langley Research Center

Structural Efficiency Study of Composite Wing Rib Structures

(ABSTRACT)

A series of short stiffened panel designs which may be applied to a preliminary design as-sessment of an aircraft wing rib is presented. The computer program PASCO is used as the primary design and analysis tool to assess the structural efficiency and geometry of a tailored corrugated panel, a corrugated panel with a continuous laminate, a hat stiffened panel, a blade stiffened panel, and an unstiffened flat plate. To correct some of the shortcomings in the PASCO analysis when shear is present, a two step iterative process using the computer program VICON is used. The loadings considered include combinations of axial compression, shear, and lateral pressure. The loading ranges considered are broad enough such that the designs presented may be applied to other stiffened panel applications. An assessment is made of laminate variations, increased spacing, and non-optimum geometric variations, in-cluding a beaded panel, on the design of the panels.

Acknowledgements

Table of Contents

List of Figures

List of Tables

1.0 Introduction

1.1 Composite Materials for Aircraft Applications

Advanced design concepts are currently being studied to exploit the potential benefits of composite materials for primary aircraft structures applications. The use of composite materials challenges the designer to exploit the additional design flexibility of tailoring structural stiffnesses by changing fiber orientations or laminate stacking sequences, a design feature that is not available with metals. This additional design flexibility, along with the increased stiffness-to-weight and strength-to-weight ratio of composite materials, often allows a composite structure to be lighter in weight than a comparable metallic structure. If the structural weight is reduced, either the payload or the fuel weight of the aircraft can be increased which would add to the aircraft's performance. For example, if the structural weight saved is replaced by additional fuel, longer flying ranges are achieved. NASA initiated a program in late 1975, called the Aircraft Energy Efficiency (ACEE) Program [1], to accelerate the technologies that show potential for increased fuel efficiency. One of the areas studied was composite materials applications to aircraft structures, supporting the concept that structural weight saved can be transformed into better performance [2].

The history of composite materials usage in aircraft structures [3] indicates that composite materials applications have long been considered for aircraft structures. In the past, lack of adequate knowledge on the efficient use of these novel materials, along with the limited available material properties, often constrained the design such that it was significantly overweight. With the development of new stiffer fibers and an increased awareness of proper applications, composite materials will be an important part of future primary aircraft structures. Current applications of composite materials to aircraft structures are, however, limited by high acquisition costs and by more complex design and analysis requirements compared to similar structures made from metallic materials. These restrictions have limited the application of composite materials in transport aircraft to secondary structures such as fairings and control surfaces. While these composite secondary structures have saved weight compared to their metallic counterparts, they account for only a small fraction of the total structural weight. Primary aircraft structures such as the wing, fuselage, and empennage must be considered for composite material applications in order to obtain weight savings that will significantly increase aircraft performance. Fighter aircraft such as the AV-8B [4] make extensive use of composite materials in the primary structure. Since fighter type aircraft are extremely weight critical, the significantly higher cost of developing these composite structures is usually justified. However, due to the size and cost of a transport type aircraft, the transition from a metallic structure to a composite structure is a very big step. The physical size of the structure present in a transport aircraft requires additional care in the design process because of manufacturing constraints. The cost of fabricating primary aircraft structural components will have to be low enough that the increased material and design costs can be justified. Therefore, a dedicated effort to determine the best design and fabrication techniques for the large structures associated with transport aircraft primary structures is important. Changing the conventional metallic designs to innovative, cost and weight saving composite designs will assure the advancing performance characteristics of future aircraft systems.

1.2 Primary Aircraft Structures

Past studies on the application of composite structures to primary aircraft structures summarize the state of the art for particular areas of technology. Fuselage technology studies by Jackson et al. [5] and Davis et al. [6], summarize the general concepts that must be addressed when designing a large aircraft fuselage with composite materials. A fuselage design study by Dickson and Biggers [7] presents typical fuselage structure designs (based on available loads and criteria) which could be built with composite materials. Many of the ideas expressed in these reports can be used in the application of composite materials to other primary structures.

Studies on the design of aircraft wings using composite materials were conducted under the ACEE program by Watts [8] and Harvey et al. [9]. Criteria for design, manufacturing and available fabrication procedures, and conceptual designs were discussed and evaluated in References 8 and 9, a necessary first step for applying composite materials to this type of structure. This preliminary work identifies the technology deficiencies which may limit the current application of composite materials to transport type primary aircraft structures. Since composite materials applications to primary aircraft structures are not common, further research is needed in this area.

1.3 Aircraft Wing and Rib Structures

The present study concentrates specifically on the application of composite materials to a primary aircraft structural subcomponent, namely a wing rib. Typically, a wing rib is a short, stiffened panel, that separates the upper and lower wing skin panels, as shown in Figure 1. Many configurations are possible to satisfy the structural requirements of a wing rib. For ex-
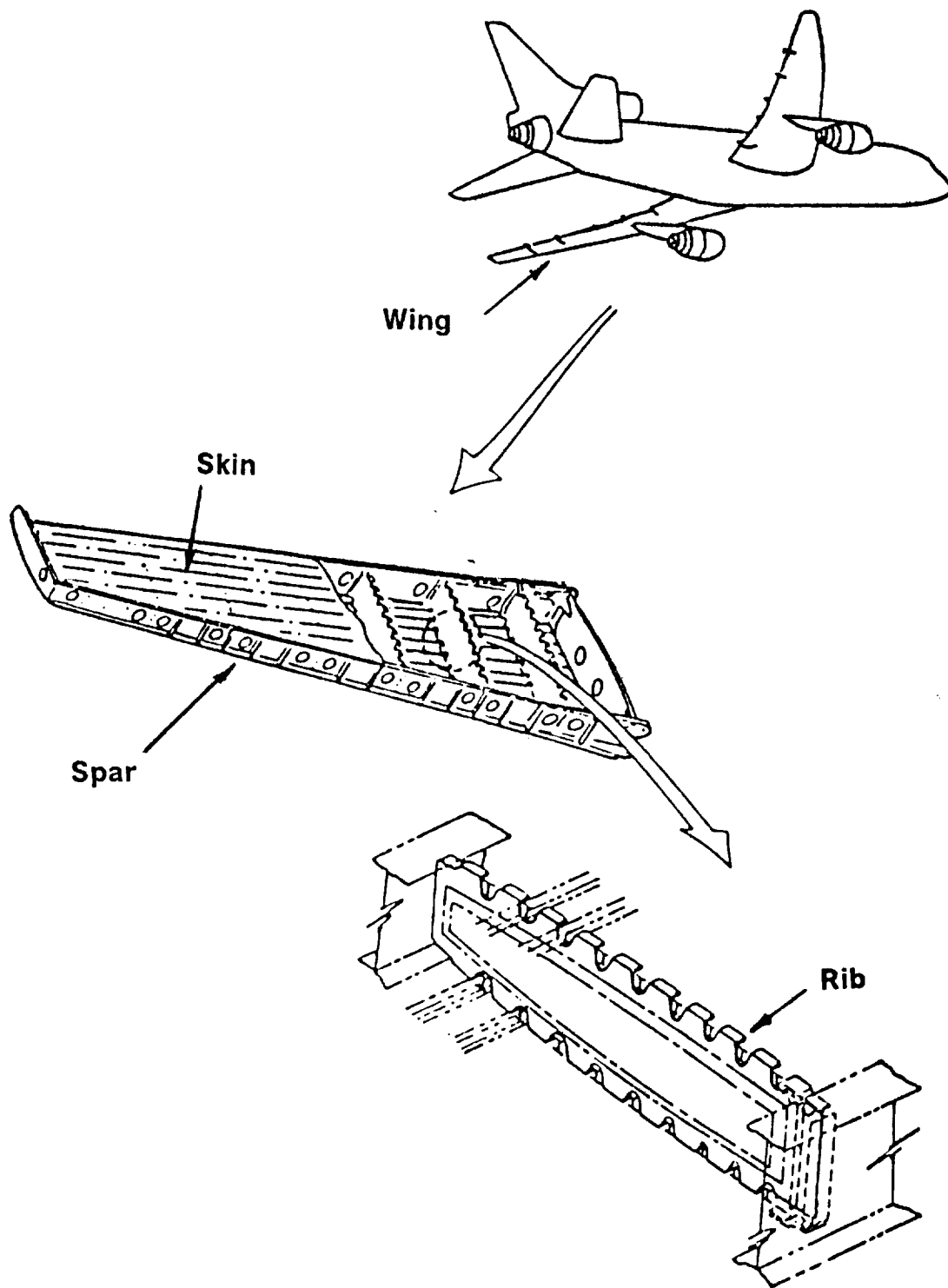
Figure 1. General Wing Structure Diagram.

Labels in figure: Wing, Skin, Spar, Rib

ample, in Figure 2, several wing rib configurations are presented that illustrate some of the many ways that a wing rib can be constructed. The solid rib concept shown in Figure 2 is typical of the current proposed applications of composite materials to transport aircraft wing rib structures.

In service, a wing is subjected to air loads which bend and twist the entire wing structure. This twisting becomes more severe as the wing is swept further aft, a configuration common in most transport aircraft. The bending load is resisted primarily by compression and tension in the upper and lower wing skins and spar caps. Wing bending also creates axial compressive loading in the wing ribs that resists the tendency for the wing skins to collapse. The twisting load is resisted by a torque box, which consists of the wing skins, spars, and ribs. Wing attachments such as flaps, ailerons, and engines are usually attached to the ribs, introducing significant shearing loads in the ribs. Transport aircraft also typically carry fuel in portions of the wing structure. Thus, the rib which closes out the fuel cell will have significant lateral pressure loads applied to it, along with axial compressive and shearing loads.

1.4 Stiffened Panel Design Review

The analysis and design of stiffened composite panels is often based on a computerized analysis procedure. Many of the currently available procedures have been used to evaluate different configurations and are discussed in the following section. Past studies discussing different configurations which exhibit potential cost savings due to manufacturability are also discussed.

Analysis Codes: Past studies using computerized design procedures to obtain stiffened panel designs and analyses have economically provided accurate results. Early stiffened panel design and optimization studies using composite materials were carried out using computer programs like AESOP (Automated Engineering and Scientific Optimization Program)

Chordwise direction

Wing thickness direction
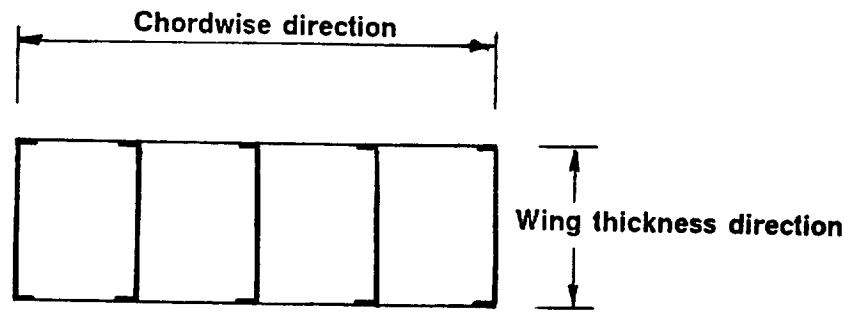
1. MULTISPAR
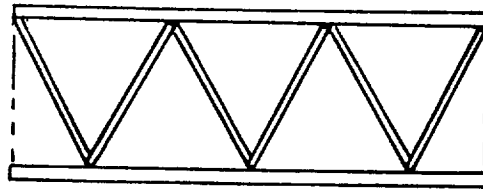
2. TRUSSES
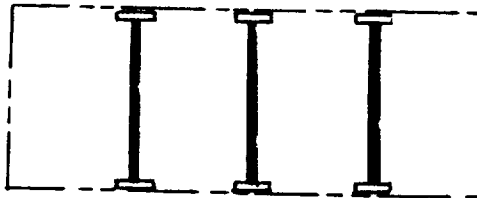
3. POST
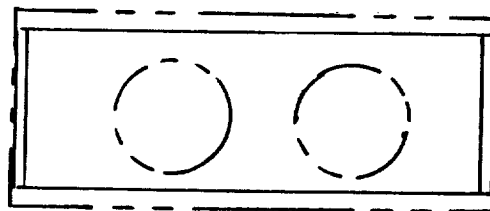
4. SOLID RIB

Figure 2. Examples of Wing Rib Structural Configurations [9].

[10,11], and the results were compared with aluminum panels. These early studies in composite materials applications stimulated further research to find ways to exploit the potential of designing lighter weight structures with composite materials. Other approaches included using a stiffened panel analysis program for biaxial loading called BUCLASP2 (A Computer Program for the Instability Analysis of Biaxially Loaded Composite Panels) to design stiffened panels [12]. Studies of panels designed using BUCLASP2 were compared with results from other analysis procedures and with experimental data [13-15], and showed an even greater potential for the use of composite materials. Another computer program, PANDA2 [16], has been developed and is also being used to design stiffened panels for multiple loading conditions. The analysis procedures mentioned have been used to design stiffened panels, fulfilling the need for economical, accurate analyses during the design process. Other analysis procedures currently being used include an analysis code developed by Williams and Anderson called VIPASA (Vibration and Instability of Plate Assemblies including Shear and Anisotropy) [17,18]. VIPASA is capable of modeling anisotropic plate properties and includes their effect on the natural frequencies and buckling loads of prismatic assemblies of thin, flat rectangular plates which are connected along their edges. Anderson et al. incorporated VIPASA into the computer program PASCO (Panel Analysis and Sizing Code) [19-21], currently one of the most widely used programs for the study of stiffened panels using composite materials. PASCO was written to economically design optimum stiffened panels made up of linked plate elements. Studies leading up to the development of PASCO included the design of stiffened panels by Stroud and Agranoff [22] using a simplified buckling analysis to obtain the optimum design. For comparison, Stroud et al. [23] used the more rigorous buckling analysis of VIPASA to provide an evaluation of the analysis method. Later studies by Stroud et al. [24] have revealed some shortcomings of the PASCO analysis by comparing the results of a PASCO generated design with the finite element codes EAL [25] and STAGS [26]. The results of these studies indicated that PASCO may generate questionable designs when shear or anisotropy is present. Other recent work involving PASCO includes the design and analysis of different corrugated panel configurations by Davis et al. [27], with curved caps and beaded

webs, and a study of the sensitivity of the buckling loads to bow type imperfections of an optimized panel design by Stroud et al. [28].

As a possible solution to the shortcomings in VIPASA, Williams et al. recently developed the computer program VICON [29] based on earlier work of Williams and Anderson [30,31]. VICON (VIPASA with constraints) adds the user-defined option of specifying constraints at any arbitrary point on the panel. Later work was done by the same authors using VICON to show how the computation time can be reduced by considering laterally repetitive cross sections in a stiffened panel [32]. Anderson and Williams also used VICON to evaluate another approach to a finite length plate [33]. VICON was shown to provide an improved analysis over VIPASA due to a more accurate definition of the boundary conditions at the loaded ends when shear is present.

Configurations: Many studies have been performed on configurations and materials systems that may potentially reduce the fabrication costs of composite materials applications to primary aircraft structures. The corrugated panel, long recognized for its structurally efficient shape, has been studied for many years because of its buckling and shear resistant properties [34-41]. The application of composite materials to this particular configuration is potentially very important [22,23,42] since economical manufacturing techniques which take advantage of the corrugated panel geometry can reduce the production cost.

A corrugated panel is a primary candidate for thermoplastic materials application to primary aircraft structures. The use of thermoplastic materials for primary composite aircraft structures is of interest because of potential low cost manufacturing techniques, high toughness (damage tolerance), and higher operating temperatures. Work on the advancement of thermoplastic materials by Johnston et al. [43,44] and Christensen et al. [45] emphasize the benefits of using this type of material. The application of thermoplastics to aircraft structures has been studied, for example, by Goad [46] and Hoggatt et al. [47], but the application has yet to be realized in production.

Other structural concepts which have been considered in past studies simultaneously combine the efficiency of a stiffened structure with the superior properties of an advanced

composite materials system in a manner consistent with automated manufacturing technology. These concepts include the orthogrid [48] and the isogrid [49-52] panel configurations. Because of their overall properties, these concepts are suited for use in primary aircraft structures.

1.5 Present Study

The present study focuses on the optimum design of wing rib panels made of composite materials. The baseline model considered for a typical wing rib panel in the present study is that of a center wing box rib of the Lockheed C-130 transport aircraft. In the past, stiffened panel structural efficiency studies have concentrated on long or semi-infinite panels. However, because of the short length (measured in the wing thickness direction) of the wing rib compared to its width (measured in the chordwise direction), it is expected that boundary conditions will play a much more important role in the design process for ribs. Much of the stiffened panel design work mentioned earlier used the analysis tools available to either show the accuracy of the analysis code or the relative efficiency of a stiffened panel concept. None of the studies mentioned have included an stiffened panel optimization study specifically for wing rib panels loaded with combinations of axial compression, shear, and especially lateral pressure. This study concentrates on the application of specific configurations to an aircraft wing rib panel, with the additional consideration of economical manufacturing techniques. To accomplish this, minimum weight rib panel designs which have the potential for being economically manufactured have been optimized to satisfy buckling and strength constraints for a wide range of loading conditions. Due to the wide loading range considered, the study is expected to provide information for buckling resistant stiffened panel designs for many different applications.

2.0 Design Study Approach

2.1 Design Approach

When considering a preliminary wing rib design, many constraints that are related to the panel fabrication, and interaction of the rib with the global wing structure should be considered without over constraining the design. The designer must carefully consider what limits to put on specific design constraints to develop the best possible design. The constraints considered in the present study of an aircraft wing rib sub-component include those associated with buckling, material, and geometric limits. The material limits for the present study include a material failure criterion and a minimum ply thickness. The material failure criterion chosen is the maximum strain failure criterion [53] commonly used for composite materials. The other material constraint used in the present study, minimum ply thickness, is based on the fact that a design would not be realistic if the ply design thicknesses are less than the minimum material ply thickness available. This practical limit is expected to have a significant effect on the design efficiency for lightly loaded stiffened panels. The effect of having a discrete thickness due to an integer number of plies in the laminate is also evaluated. The buckling criterion used in the present study is based on the common design practice used for

wing structures that does not allow the components to buckle at limit loads. This philosophy is based on the aerodynamically critical shape of the wing structure and the effects that a buckled skin or a stiffness loss caused by a buckled rib may have on its performance. Thus, the design of the wing rib does not consider any postbuckling capability of the panel. The buckling constraints imposed in this study include both global and local buckling modes. The only geometric constraint included in the present study is a minimum width restriction placed on the individual plate elements which make up the panel model. This constraint represents a practical manufacturing limit for stiffened panels.

The objective of the design study is to achieve a minimum-weight rib panel for the specified loadings and design constraints. Thicknesses of plies with different ply orientations in the different sections of the panel are used as design variables. Also, individual plate element widths are used as sizing variables to determine the best cross sectional geometry. The optimization code used in PASCO (CONMIN [54]) provides the optimization capability required to achieve a minimum-weight design.

Since carbon fibers in an epoxy matrix will most likely dominate the aircraft primary structure applications in the near future, a typical graphite-epoxy composite material is chosen for the material system in this study. One of the goals of this study is to determine trends for preliminary rib design. Different material properties may affect the efficiency results and alter the geometry of the optimized designs, but the design trends as a function of individual design variables are assumed to be representative. Therefore, Hercules AS4/3502 preimpregnated graphite-epoxy tape was chosen as a typical graphite-epoxy material, and is the only material considered for this study. Typical properties of the Hercules AS4 graphite fiber pre-impregnated with Hercules 3502 350°F cure thermosetting epoxy resin are presented in Table 1. Since thermoplastic composite material properties have many characteristics similar to thermoset composite material properties, the results of this study can also be used for preliminary design trends for thermoplastic applications. Applications of thermoplastic materials are considered in this study because of their potential manufacturing cost reduction benefits.

Table 1. AS4/3502 Graphite-Epoxy Material Properties Used

Longitudinal Modulus, $E_1 = 18.5 \times 10^6 \dfrac{lb}{in^2}$

Transverse Modulus, $E_2 = 1.64 \times 10^6 \dfrac{lb}{in^2}$

Shear Modulus, $G_{12} = 0.87 \times 10^6 \dfrac{lb}{in^2}$

Major Poisson's Ratio, $v_{12} = 0.30$

Longitudinal Coefficient of Thermal Expansion, $\alpha_1 = 0.25 \times 10^{-6} \dfrac{in}{in°F}$

Transverse Coefficient of Thermal Expansion, $\alpha_2 = 16.2 \times 10^{-6} \dfrac{in}{in°F}$

Longitudinal Tensile Strain Allowable, $\varepsilon_x = 0.0085$

Longitudinal Compressive Strain Allowable, $\varepsilon_x = 0.0085$

Transverse Tensile Strain Allowable, $\varepsilon_y = 0.0085$

Transverse Compressive Strain Allowable, $\varepsilon_y = 0.0085$

Shearing Strain Allowable, $\varepsilon_y = 0.0140$

Density, $\rho = 0.057 \dfrac{lb}{in^3}$

2.2 Panel Configurations

As was discussed in Chapter 1, for a global wing configuration that uses the rib-spar design concept, the rib is an integral part of the load carrying capability of the wing. Lack of current rib design trends may result in over-designed ribs that add unnecessary weight to the structure. Therefore, a better understanding of the rib design trends will be useful to the designer and will contribute to the efficient design of composite wing rib structures. The wing rib panel concepts considered in this study are based on some guidelines drawn from economical manufacturing techniques. Since manufacturability and cost are of great concern in the aerospace industry, the present study concentrates only on designs that are practical and applicable to cost effective manufacturing techniques. As a result of these considerations, a corrugated panel is chosen for further study and compared to other, more common configurations. A corrugated panel is relatively easy to manufacture since it has continuous plies which run throughout the configuration that form integral stiffeners without requiring fasteners. It is also suitable for the thermoforming process which is a potentially economical manufacturing technique for thermoplastic materials. Different configurations using various combinations of corrugated panels and flat face sheets were initially considered and are illustrated in Figure 3. Included are a simple corrugation (3a), corrugated panels with one and two face sheets (3b-3c), two similar corrugated panels attached at the caps (3d), two similar corrugated panels separated by a face sheet (3e), and finally, two corrugated panels shifted with respect to one another by half of the corrugation repeating element width and separated by a face sheet (3f). The number of panels actually evaluated in the present design study, however, is reduced to include fewer configurations. This is necessary in order to carry out a fairly complete preliminary design study with the limited resources available. The configurations chosen are based on the ability of the configurations to be modeled by the design program, their manufacturability, the lack of obvious inherent weight penalties associated with some configurations, and practical considerations such as maintainability and inspectability.
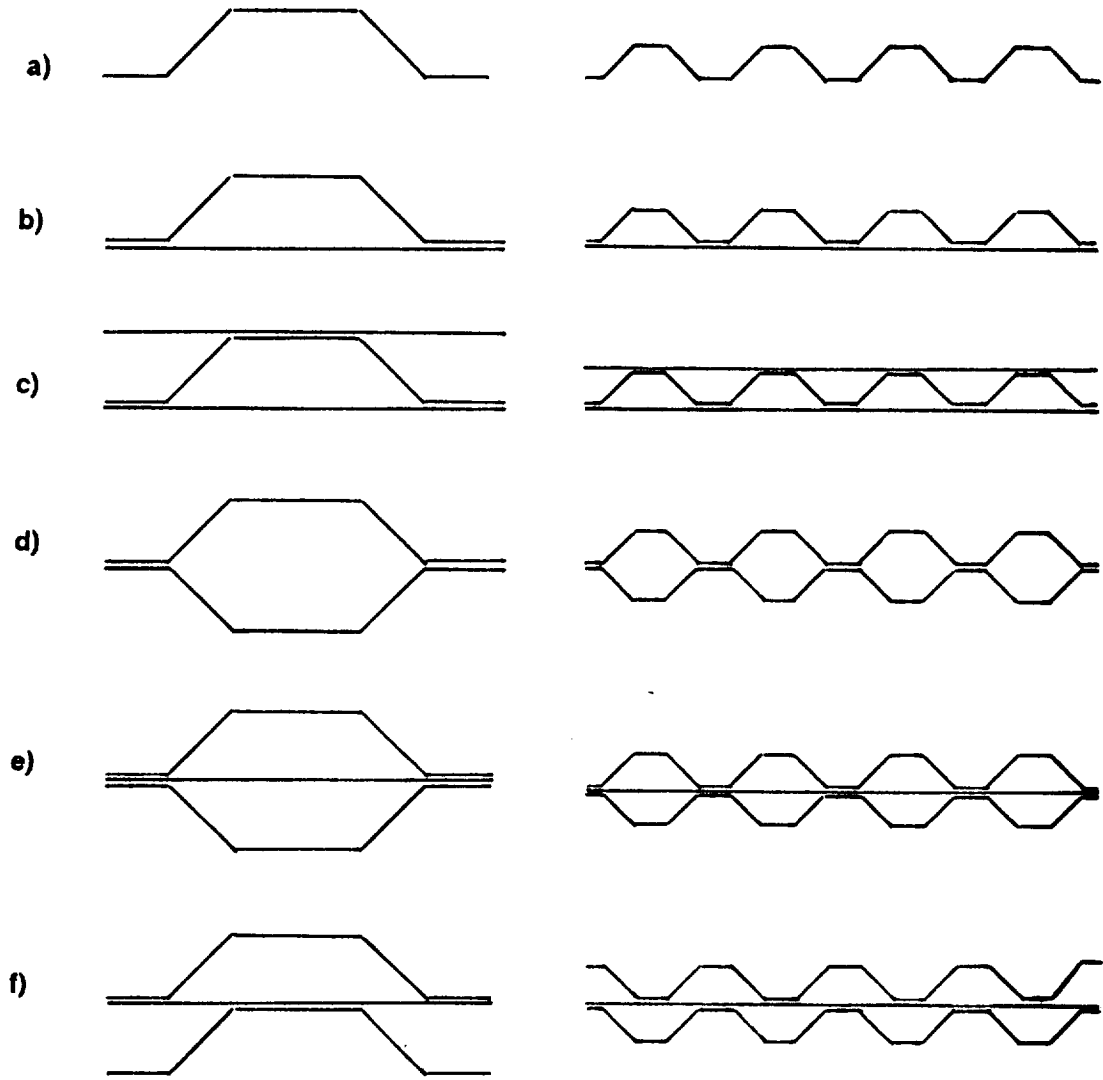
Figure 3. Configurations Considered for Study.

Of all the original configurations presented in Figure 3, only three are considered for further study. The configurations omitted from the present study are not practical in that they either have inherent weight penalties (3d-3e) or their ability to be manufactured and inspected is not reliable. Specifically, some of the configurations (3c,3f) that have blind connections (accessible from one side only) are not considered due to potential quality control, assembly costs, and inspectability problems. The configurations chosen for the study are shown in Figure 4. Included are a corrugated panel with tailored laminates in the cap and webs, a corrugated panel with a continuous laminate throughout its length and width (suitable for thermoplastic thermoforming applications) and a tailored corrugated panel with a face sheet, often referred to as a hat stiffened panel. Also included in the study is a blade stiffened panel, the most commonly used composite stiffened pane considered for a wing rib application, and a flat unstiffened plate, for comparison. The latter configurations are used as baseline designs for evaluating the corrugated panel concepts.

The general approach to the current study includes a comparison of how each config- uration relates to the others for various loading conditions and other non-optimum geometric variations. The various loading conditions considered are combinations of axial compression, shear, and out-of-plane or normal pressure. Non-optimum geometric variations considered in the present study include the effect of variations in blade stiffener spacing, corrugation web angle, and laminate ply layup on the structural efficiency.

2.3   Design and Analysis Tools

The PASCO program is chosen as the primary sizing and analysis tool for this study. PASCO has the generality to include the loading conditions considered, to model the chosen configurations, and to apply the design constraints of interest. PASCO is computationally ef-

a) Tailored Corrugated Panel

b) Corrugated Panel with a Continuous Laminate

c) Hat Stiffened Panel

d) Blade Stiffened Panel

e) Unstiffened Flat Plate
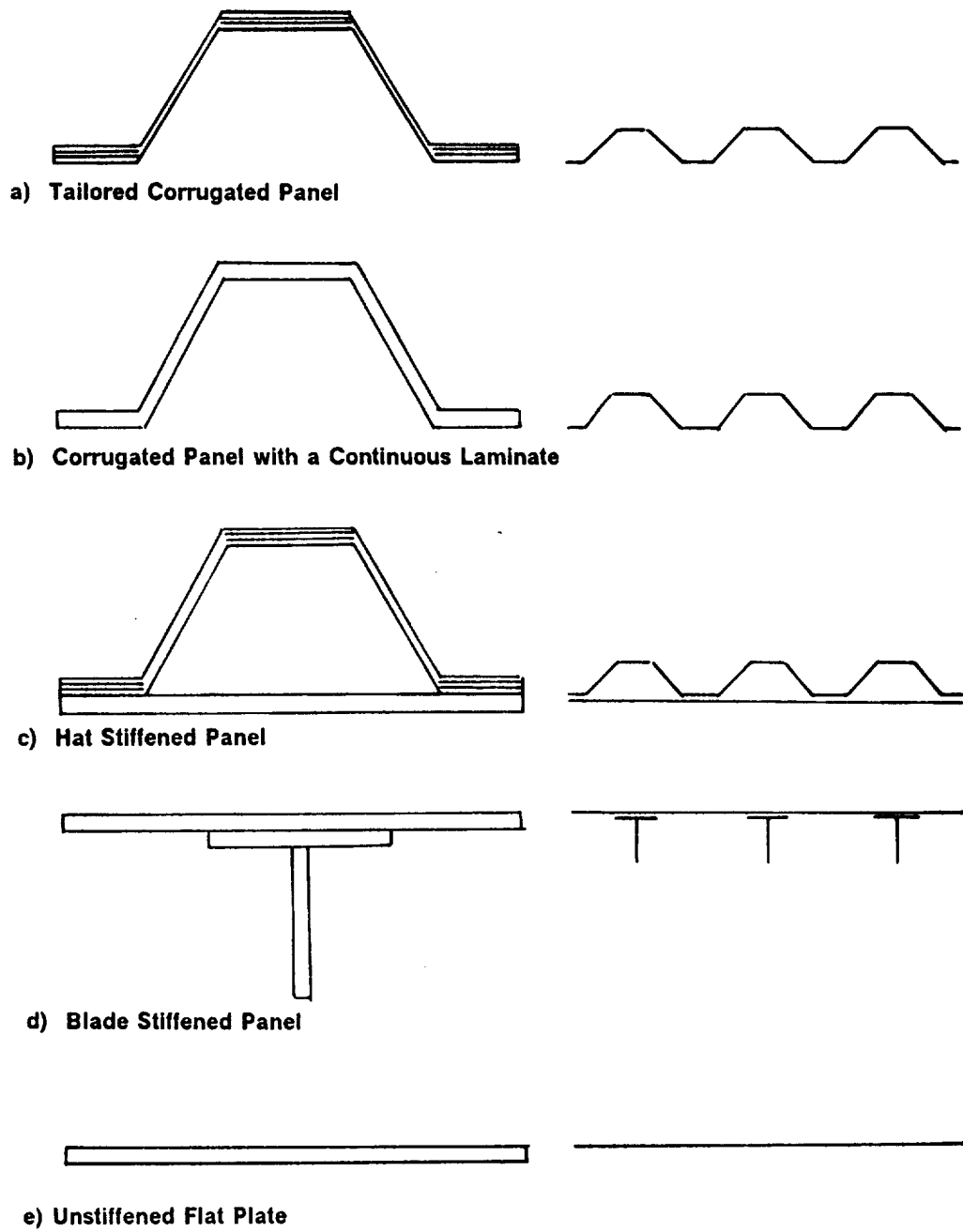
Figure 4.   Configurations Studied.

ficient which allows the large number of design cases required for a study of this nature to be performed at a reasonable computational cost.

2.3.1 PASCO

2.3.1.1 Theory and Shortcomings

PASCO is a computer program developed for use in the design and analysis of stiffened panel structures which can be modeled by a series of linked plate elements. The panel being designed by PASCO may be loaded by any combination of in-plane axial and shear loads, out-of-plane pressure, and applied moments as shown in Figure 5. PASCO can also account for a bow type imperfection. PASCO consists of a buckling analysis program (VIPASA), a non-linear mathematical programming optimizer (CONMIN [54]), and analyses for material failure and other constraints. VIPASA uses linked plate elements to model the panel and maintains continuity of the buckling pattern between adjoining plate elements. Each individual plate element can be loaded with any combination of N_x , N_y, and N_{xy} as illustrated in Figure 6. The buckling displacement, w, assumed in the VIPASA analysis is of the general form:

$$w = f_1(y) \cos \frac{\pi x}{\lambda} - f_2(y) \sin \frac{\pi x}{\lambda}$$

(3.1)

where λ is the buckling half-wavelength and the functions $f_1(y)$ and $f_2(y)$ are such that equilibrium of the governing differential equations [20] are satisfied, while allowing boundary conditions to be defined on the lateral edges of the panel. In-plane displacements u and v are specified in a similar fashion. Boundary conditions on the panel ends perpendicular to the stiffeners are assumed to be simply supported and cannot be changed. This simple support boundary condition is inherent in the analysis for an orthotropic plate with no applied shear.
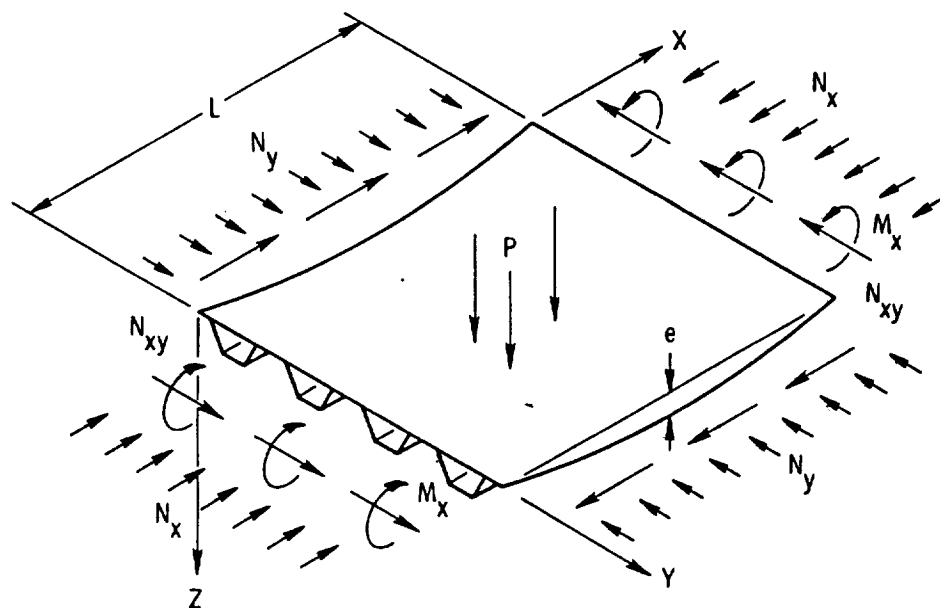
Figure 5. Bow-type imperfection, Applied Loading, and Coordinate System used in PASCO [24].
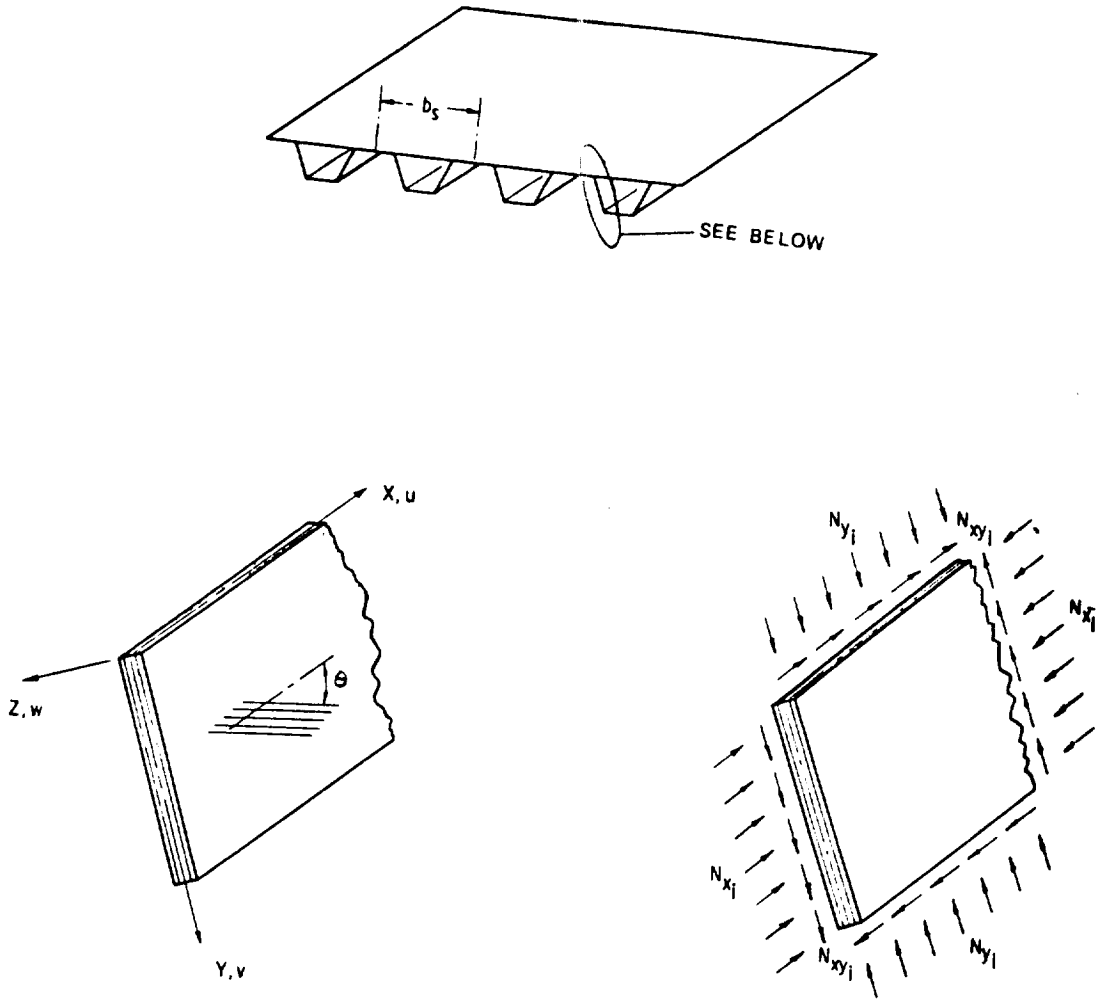
Figure 6. Plate Element Coordinate System and Loading   [21].

The assumed buckling displacement of equation (3.1) corresponds to a series of straight nodal lines that are perpendicular to the longitudinal panel axis, as shown in Figure 7, and satisfy the simple support boundary conditions. The VIPASA analysis is considered accurate for this condition in the sense that it is the exact solution of the plate equations satisfying the Kirchoff-Love hypothesis. However, when shear is applied to the panels, the buckling pattern consists of a series of skewed nodal lines, each spaced by a distance λ, as shown in Figure 8. When skewed nodal lines are present, the simple support boundary conditions assumed for the panel ends may no longer be applicable. When only a single buckling half wave of length λ forms along the panel length, L, the difference in the assumed skewed deformation shape and the actual straight edge condition is much more pronounced than if many waves form along the panel length. Thus, the VIPASA solution when shear is present is still considered accurate for the case when many buckling waves form along the panel length. For the case of the buckling wave length equal to the panel length, however, the VIPASA buckling analysis can severely underestimate the buckling load when shear is applied.

2.3.1.2 Smeared Stiffness Solution

A procedure based on a smeared stiffness representation of the stiffened panels can be used to obtain a more accurate solution for the global buckling mode ($\lambda =$ L) when shearing loads are present. By rotating the panel properties 90°, one can form an infinitely wide panel with simple supports on the ends with finite length. However, since VIPASA can only analyze a panel with a uniform cross section in the infinite direction (no transverse discrete stiffeners are allowed), it cannot solve the problem in this form. The properties of the discrete stiffeners must be smeared to form an equivalent orthotropic plate. The smeared stiffness approach was shown in Reference 24 to be an improved solution but not always a conservative one. The smeared stiffener solution also ignores any local buckling in the stiffeners which may
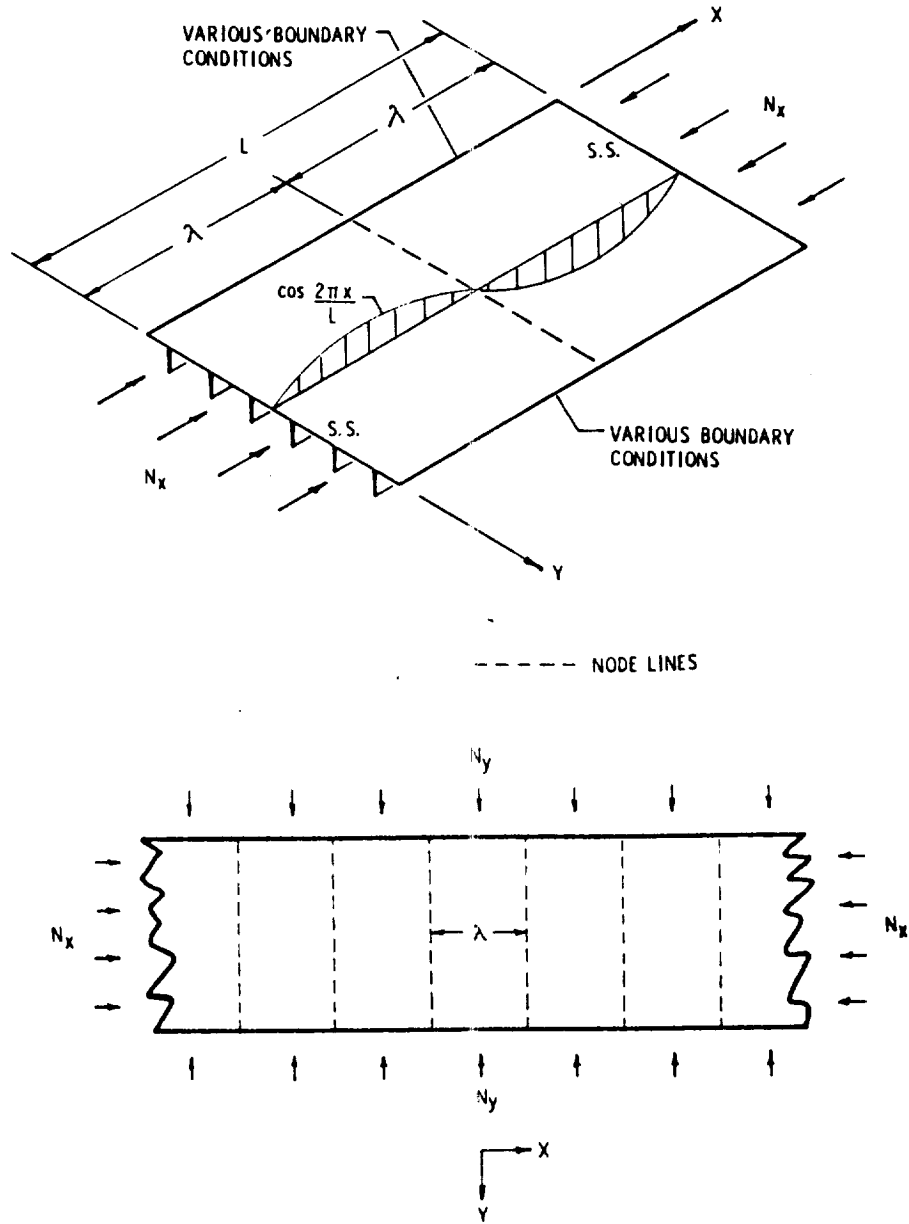
Figure 7. PASCO Buckling Nodes with No Applied Shear [24].
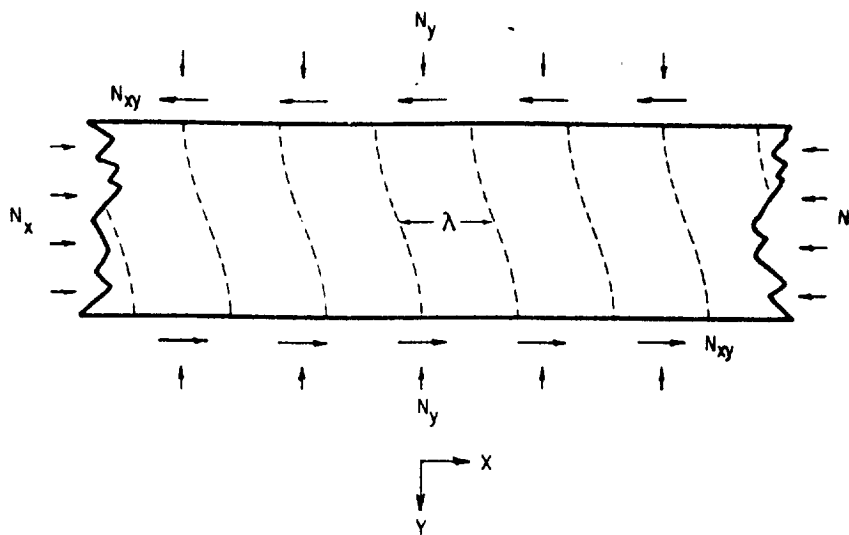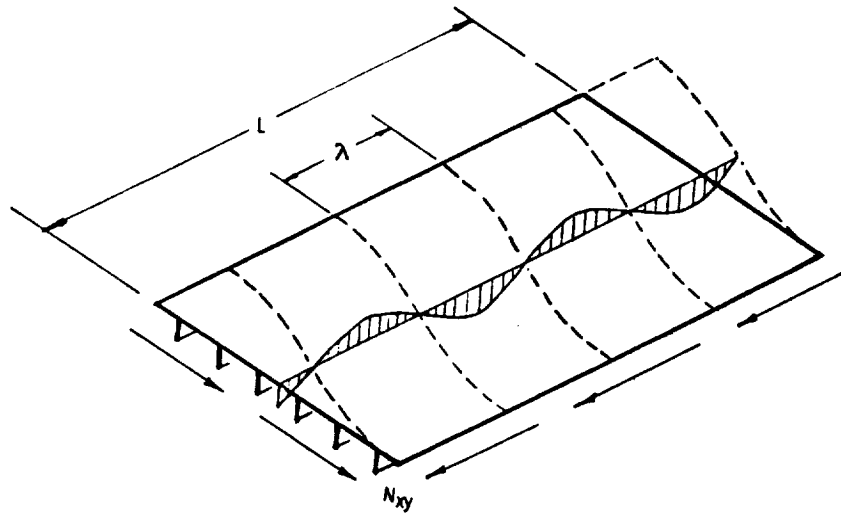
Figure 8. PASCO Skewed Buckling Nodes Due to Applied Shear [24].

occur, thus, this method should only be used with caution, and an alternative solution should be sought.

2.3.1.3 Applied Pressure

As an additional feature, PASCO accounts for the application of out-of-plane pressure to the stiffened panel. PASCO uses a beam column approach to account for the interaction of the in-plane loads with the out-of-plane pressure load [55]. The effect of the interaction is included during the analysis as an applied moment with a magnification factor β:

$$M = \frac{P \times L^2}{8} \times \beta$$

where $\beta = \frac{8}{\pi^2 \times \gamma}\left[\sec\frac{\pi}{2}\sqrt{\gamma} - 1\right]$, $\gamma = \frac{N_x}{N_{xcr}}$, and P is the lateral pressure. When shear is present, N_{xcr} is assumed to be the buckling load corresponding to the buckling half wavelength λ equal to L. Since this value of N_{xcr} corresponds to the overall buckling mode that PASCO determines incorrectly when shear is present, the moment applied due to a given value of pressure is also in error. Calculation of the magnification factor, β, is automatic in PASCO and cannot be modified. In order to apply the corrected value of the bending moment, therefore, one can modify the input value of the design pressure, P. The applied moment due to the pressure, including the effect of the magnification factor β, forces the sizing code to increase the overall buckling load corresponding to $\lambda = L$ to be a non-critical value which, in turn, causes a local buckling mode to become critical. The structural efficiency and geometric effects of increasing pressure for various combinations of N_x and N_{xy} on the configurations studied will be described in the following chapters.

The shortcomings of PASCO present a problem with respect to its applicability to the current study of short, longitudinally stiffened panel configurations. The boundary conditions on a short panel may play a more important role in the buckling response than a longer panel,

Design Study Approach

requiring the boundary conditions to be accounted for more accurately. To correct the short-comings in PASCO, the panel must retain the full cross sectional detail to account for local stiffener buckling, while at the same time, maintain the simple support boundary conditions at the loaded edges. The smeared stiffener solution in PASCO does not account for this detail and an improved analysis (VICON) is used to account for these important effects.

2.3.2 VICON

A recently developed computer program, VICON (VIPASA with constraints), modifies the VIPASA buckling analysis program to include supports at arbitrary locations along the panel length. This is accomplished by coupling the desired end constraints with the VIPASA stiffness matrix for different buckling wavelength responses through the method of Lagrangian multipliers. By specifying the supports at intervals corresponding to the ends of the desired panel length, the simple support boundary conditions will be approximated at the panel ends when shear is applied.

In order to include the modifications of the VICON analysis in the PASCO design, a two step iterative design process is used. PASCO is first run to generate a design based on the smeared orthotropic stiffness solution which is then analyzed using VICON. The PASCO design load for the overall buckling mode ($\lambda = L$) is then reduced by the ratio of the original PASCO design load to the VICON buckling load for the same overall mode shape. The reduction is introduced to PASCO by means of a safety factor, CLAM(λ), described in the User's Manual [19]. CLAM(1) corresponds to the overall buckling load and adjusts the $\lambda = L$ load used in the design. The panel is redesigned using PASCO with this correction for the overall buckling load and the resulting design is again checked using VICON. This iterative process is continued until the analyses converge.

2.4 Panel Modeling

The modeling of the panels shown in Figure 4 for input into the PASCO program includes specifying the laminate layup, the overall repeating element geometry, and the applied constraints. The panel size and typical loads chosen for this study are based on an inboard wing rib for a transport aircraft. The rib dimensions of 28 inches high by 80 inches wide were chosen based on dimensions obtained for a typical fuel closeout rib for the C-130 aircraft. The laminate ply layup specification is the first consideration for the modeling. For PASCO, both the lamina ply orientation angles and ply thicknesses can be used as design variables. For the current study, only thicknesses are used as design variables and the ply angle orientations are chosen as conventional values and not varied. For the models chosen, the laminates which define the plate elements consist of laminates made up of layers with orientations of ±45°, 0°, and 90°, where the +45° and -45° plies are assumed to be of equal thickness. Only balanced symmetric laminates are used since PASCO can only model plate elements made up of this type of laminate. Hence, only one half the laminate must be defined in the input file. Practical layup constraints are applied, such as using ±45° plies as the outermost lamina to improve damage tolerance, and using continuous fibers throughout the cross section where possible to minimize the stress concentrations which occur at the ply termination points.

The geometry of the repeating elements, and thus the overall cross-sectional panel geometry, is left to vary by using the individual plate element widths as design variables. Since the total panel width is restrained to 80 inches, the panel model is adjusted in width by changing the number of repeating elements. To determine the number of repeating elements for the optimum design, the number of repeating elements is first fixed at a value that is assumed to result in a panel width near 80 inches. As the panel dimensions are changed by optimizing the repeating element widths, the total panel width changes accordingly. Repeating elements are then added or removed as necessary to provide the total panel width closest

to 80 inches. Within the PASCO model, symmetry is used wherever possible to reduce the number of unknowns in the problem.

2.4.1 PASCO Models

The first panel chosen for modeling is the corrugated panel with different laminates in the caps and webs, providing the opportunity for the optimizer to tailor the stiffnesses of different sections of the panel. The panel will be referred to as a tailored corrugated panel and the details of the model are shown in Figure 9. This particular model is similar to the models used in past studies [22-24]. The geometry of the repeating element is defined by the plate widths b_1, b_2, and b_3, where both the upper and lower corrugation caps are assumed to be of equal width due to symmetry. The corrugated panel web angle (θ) is a dependent variable and is defined using the plate element widths, b_2 and b_3, to define the cosine of the angle between them, as shown in Figure 9. Two different laminates, both with common $\pm 45°$ plies are used to define this configuration. The panel webs are made of only $\pm 45°$ plies. These $\pm 45°$ plies run continuously across the width of the entire panel cross section to reduce both manufacturing costs and any stress concentrations that occur at the $\pm 45°$ ply termination points. In the plate elements which make up the caps, $0°$ plies are included between the layers of $\pm 45°$ fibers continuing from the webs. Thus, both laminates can be defined by two thicknesses, T_1 and T_2, relating to the $45°$ and $0°$ plies, respectively. The plies of similar orientation are all collected together in the analysis to reduce the number of design variables. A sample PASCO input file for this model is shown in Figure 10. In PASCO, for cases when only axial compression load is applied ($N_{xy}=0.0$), the anisotropic terms are omitted by default from the analysis, even though the laminates may contain some off axis plies which are grouped together making the anisotropic terms D_{16} and D_{26} of an appreciable magnitude. This grouping effect may cause unconservative buckling calculations due to the anisotropic bend-

$\theta = \cos^{-1}\dfrac{b_3}{b_2}$

$2b_1$

$2b_1$

b_2

b_3

$[\pm 45^\circ, 0^\circ]_s$

$2T_1 (45^\circ)$

$2T_2 (0^\circ)$

$2T_1 (45^\circ)$

$4T_1 (45^\circ)$

$[\pm 45^\circ]_s$

$2T_1 (45^\circ)$

$2T_2 (0^\circ)$

$2T_1 (45^\circ)$

$[\pm 45^\circ, 0^\circ]_s$

Legend:

0° plies

45° plies
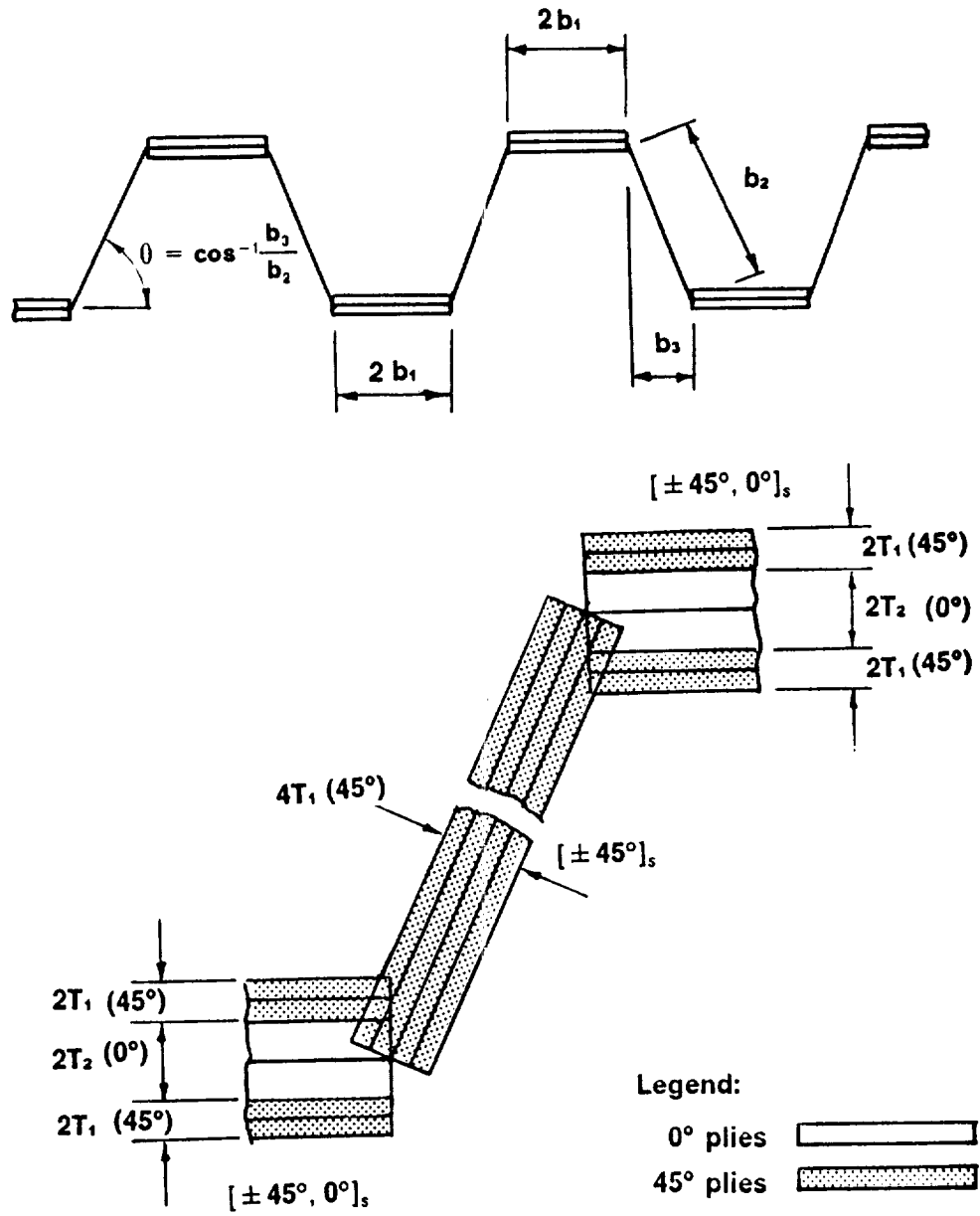
Figure 9. Tailored Corrugated Panel Model.

```
***** PASCO MODEL 5A CASE 002 *****
$CONDAT
$
$PANEL
GRANGE =  10,
MAXJJJ = 10,
LINK =  0,
EL =  28,
B =  -0.2296,-2.175, 3*1.E30,-0.710,
BL =  .10, .10, .10, .10, .10, .10,
T =  -.005, -.005, -.0050,
TL =  .005, .005,
THET =  45,  0, 0,
KWALL(1,1) =  1,-1, 2,
KWALL(1,2) =  1,-1,3,
IWALL =  1,2,1,2,1,
HCARD =  4,-7,2,-6,2,
        4,-8,7,90,0,
        4,-9,4,6,2,
        4,-10,9,-90,0,
        6,11,1,8,3,10,5,
NOBAY =  16,
AB(1,1) =   0, 1, 0,-1,
AB(1,2) =   1, 0, 0, 0,-1,
AB(1,3) =  2, 0,-1,
MINLAM =  28,
NLAM =  1,2,4,7,14,28,
IBC =  1,
IP =  2,
NX =  100.,
$
$MATER
E1 =  18.5E6,  E2 = 1.64E6,  E12 = .87E6,  ANU1 = .30,  RHO = .0570,
ALFA1 =  0.25E-6, ALFA2 = 16.2E-6,
ALLOW =  2,  .00850,-.00850,  .00850,-.00850, .0140,
$
*
```

Figure 10.   Tailored Corrugated Panel PASCO Input Data File.

ing stiffnesses that are present. The effect of these neglected terms will be discussed in more detail later in the analysis and results section.

The corrugated panel with a continuous laminate is modeled in a similar way to the tailored corrugated panel, except the laminate is defined to be the same for all the plate elements. The model used is shown in Figure 11 and a sample PASCO input file for this configuration is presented in Figure 12. In this case, a $[\pm 45°, 0°, 90°]_s$ laminate is chosen to define the properties of the laminate. Thus, three thicknesses T_1, T_2, and T_3, referring to the 45°, 0°, and 90° plies, respectively, are used to define the optimized laminate. The plate width variables b_1, b_2, and b_3, used to define the cross sectional geometry for the tailored corrugated panel, are also used to define the geometry of the corrugated panel with a continuous laminate.

The hat stiffened panel model is similar to the corrugated panels discussed earlier, since it is essentially a tailored corrugated panel attached to a flat face sheet. The model detail is shown in Figure 13 and a sample PASCO input file is shown in Figure 14. The geometry is defined by four plate element width variables, b_1, b_2, b_3, and b_4. The symmetry argument used to define equal cap widths in the corrugated panels is no longer valid since the geometry of the hat stiffened panel is not symmetric about the neutral axis. Therefore the upper cap is defined by b_3 and the lower cap by $2b_1$. The laminates are defined in a manner similar to that of the corrugated panel except that the thickness of the 0° plies in the lower and upper caps can be different. Thus, T_1, T_2, and T_3 define the thickness of the 45° plies, the 0° plies in the lower cap, and the 0° plies in the upper cap used in the corrugated panel laminates. The thicknesses T_4, T_5, and T_6 define the 45°, 0°, and 90° lamina thicknesses in the skin elements. The skin elements are offset from the corrugated panel lower caps, a feature available in PASCO and discussed in the User's Manual [19]. The offset simulates the actual attachment of the skin and corrugated panel to each other to form the hat stiffened panel.

The blade stiffened panel geometry is defined by b_1, b_2, and b_3 as shown in Figure 15, and a sample PASCO input file for this configuration is shown in Figure 16. Three laminates are used to define the blade stiffened panel. The first is the skin panel, defined by a
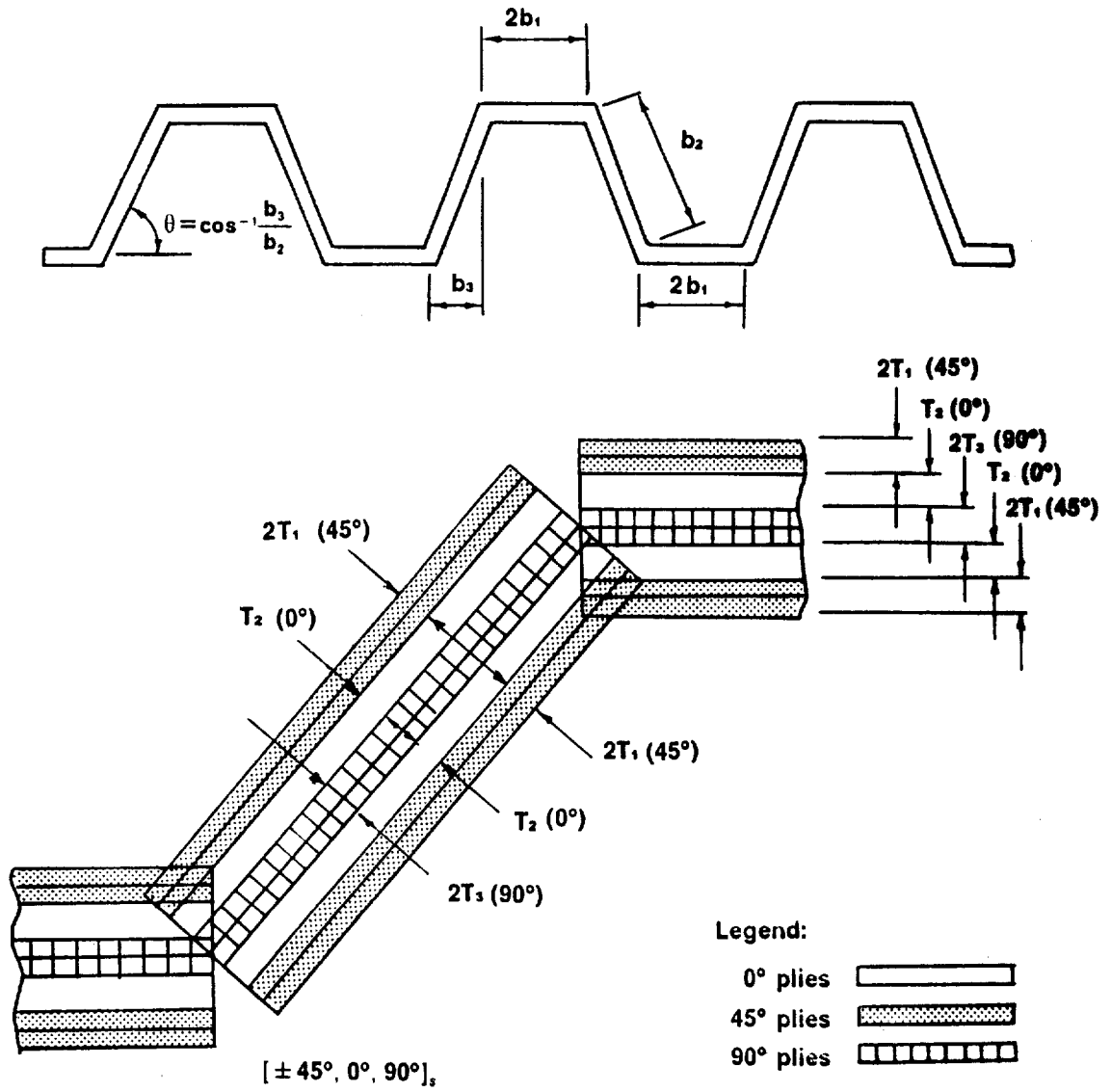
Figure 11. Corrugated Panel with a Continuous Laminate Model

```
***** PASCO MODEL 9A 200 *****
$CONDAT
$
$PANEL
GRANGE= 10,
MAXJJJ=10,
LINK= 0,
EL= 28,
B= -2.4740,-1.798, 4*1.E30,-0.042,
BL= .10, .10, .10, .10, .10, .10,
T= .005, .005, .005,
TL= .005, .005, .005,
THET= 45, 0, 90,
KWALL(1,1)= 1,-1, 2, 3,
IWALL= 1,1,1,1,1,
HCARD= 4,-7,2,6,2,
       4,-9,4,-6,2,
       6,11,1,7,3,9,5,
NOBAY= 6,
AB(1,1)=  0, 1, 0,-1,
AB(1,2)=  1, 0, 0, 0,-1,
AB(1,3)=  2, 0,-1,
AB(1,4)=  0, 1, 0, 0, 0,-1,-1,
MINLAM= 28,
NLAM= 1,2,4,7,14,28,
IBC= 1,
IP= 2,
NX= 100.,
$
$MATER
E1= 18.5E6, E2=1.64E6, E12=.87E6, ANU1=.30, RHO=.0570,
ALFA1= 0.25E-6, ALFA2=16.2E-6,
ALLOW= 2, .00850,-.00850, .00850,-.00850, .0140,
$
*
```

Figure 12.   Corrugated Panel with a Continuous Laminate PASCO Input Data File.
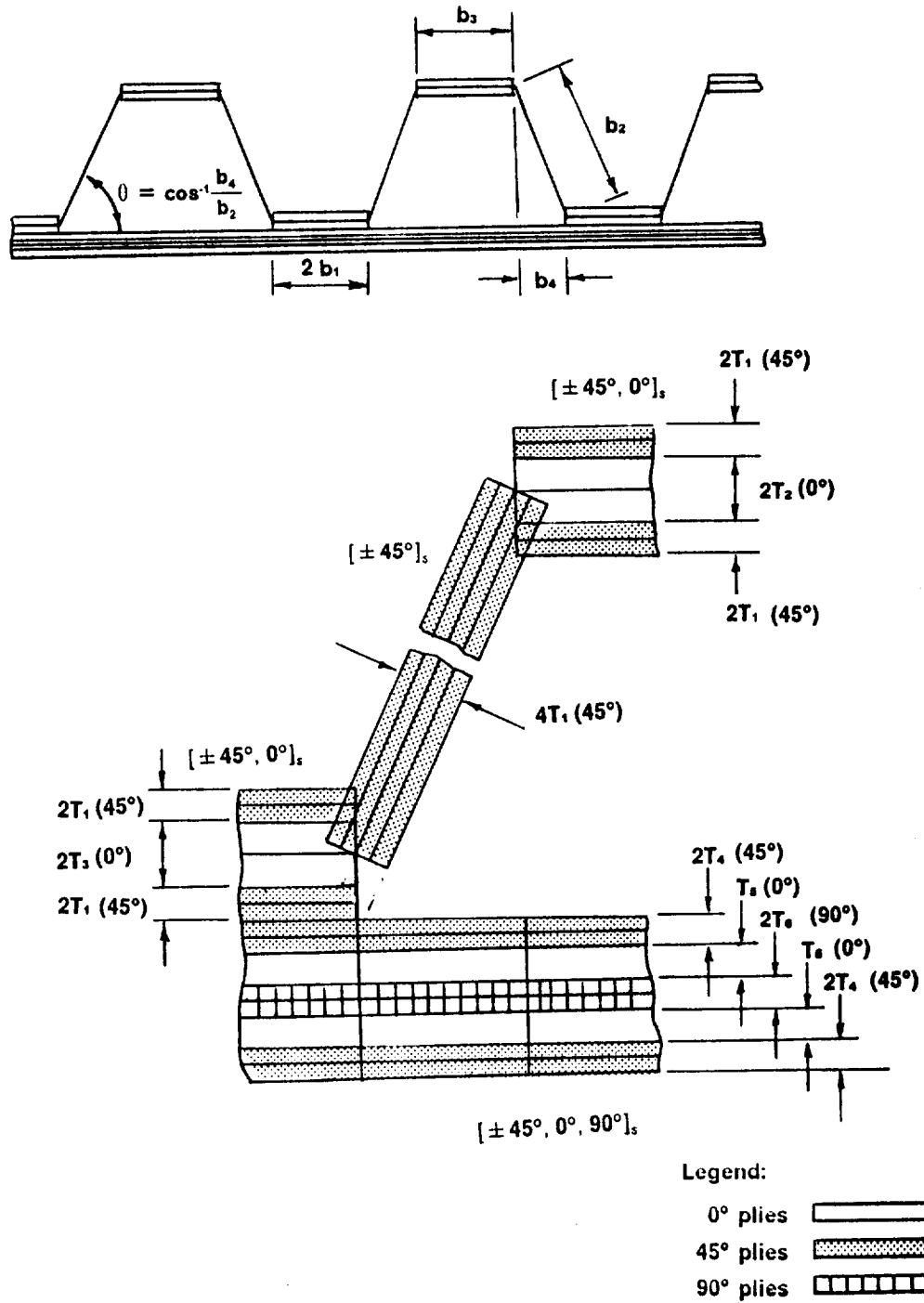
Figure 13. Hat Stiffened Panel Model.

```
***** PASCO MODEL 6A CASE 002 *****
$CONDAT
$
$PANEL
MAXJJJ = 10,
GRANGE = 10,
LINK = 0,
EL = 28,
B =   0.1000,-2.654,-0.1832, 7*1.E30,-0.045,
BL(1) = .10, .10, .10, .10, .10, .10, .10, .10, .10, .10, .005,
T = -.005, .005, .005, .005, .005, .005, 1.E30,  -.005,
TL = .005, .005, .005, .005, .005, .005, .005,
THET =  45, 0, 0, 45, 0, 90, 0, 0,
KWALL(1,1) =  1,-1, 2,
KWALL(1,2) =  1,-1, 8,
KWALL(1,3) =  1,-1, 3,
KWALL(1,4) =  4,-4, 5, 6,
IWALL =  1,2,3,2,1,4,4,4,4,4,
HCARD =  4,-11,2,7,2,
        4,-12,4,-7,2,
        6,-13,-1,0,7,0,7,
        6,-14,-11,0,7,0,0,
        6,-15,-12,0,0,0,7,
        6,-16,-5,0,7,0,7,
        4,17,14,3,15,
        4,18,7,8,9,
        7,19,6,-13,18,-17,10,-16,
NOBAY =  14,
AT(1,1) =   2, 1, 0, 2, 1, 1,-1,
AB(1,2) =   0, 1, 0,-1,
AB(1,3) =   1, 0, 0, 0,-1,
AB(1,4) =   1, 0, 0, 0, 0,-1,
AB(1,5) =   0, 1, 0, 0, 0, 0,-1, 0, 0, 0,-1,
AB(1,6) =   0, 0, 1, 0, 0, 0, 0,-1,
AB(1,7) =   0, 0, 0, 0, 0, 0, 1, 0,-1,
AB(1,8) =   1, 0, 0, 0, 0, 0, 0, 0, 0,-1,
MINLAM =  28,
NLAM =  1,2,4,7,14,28,
IBC =  1,
IP =  2,
NX =  100.,
$
$MATER
E1 =  18.5E6,  E2 = 1.64E6,  E12 = .87E6,  ANU1 = .30,  RHO = .0570,
ALFA1 =  0.25E-6, ALFA2 = 16.2E-6,
ALLOW =  2,  .00850,-.00850,  .00850,-.00850, .0140,
$
.
```

Figure 14.   Hat Stiffened Panel PASCO Input Data File.
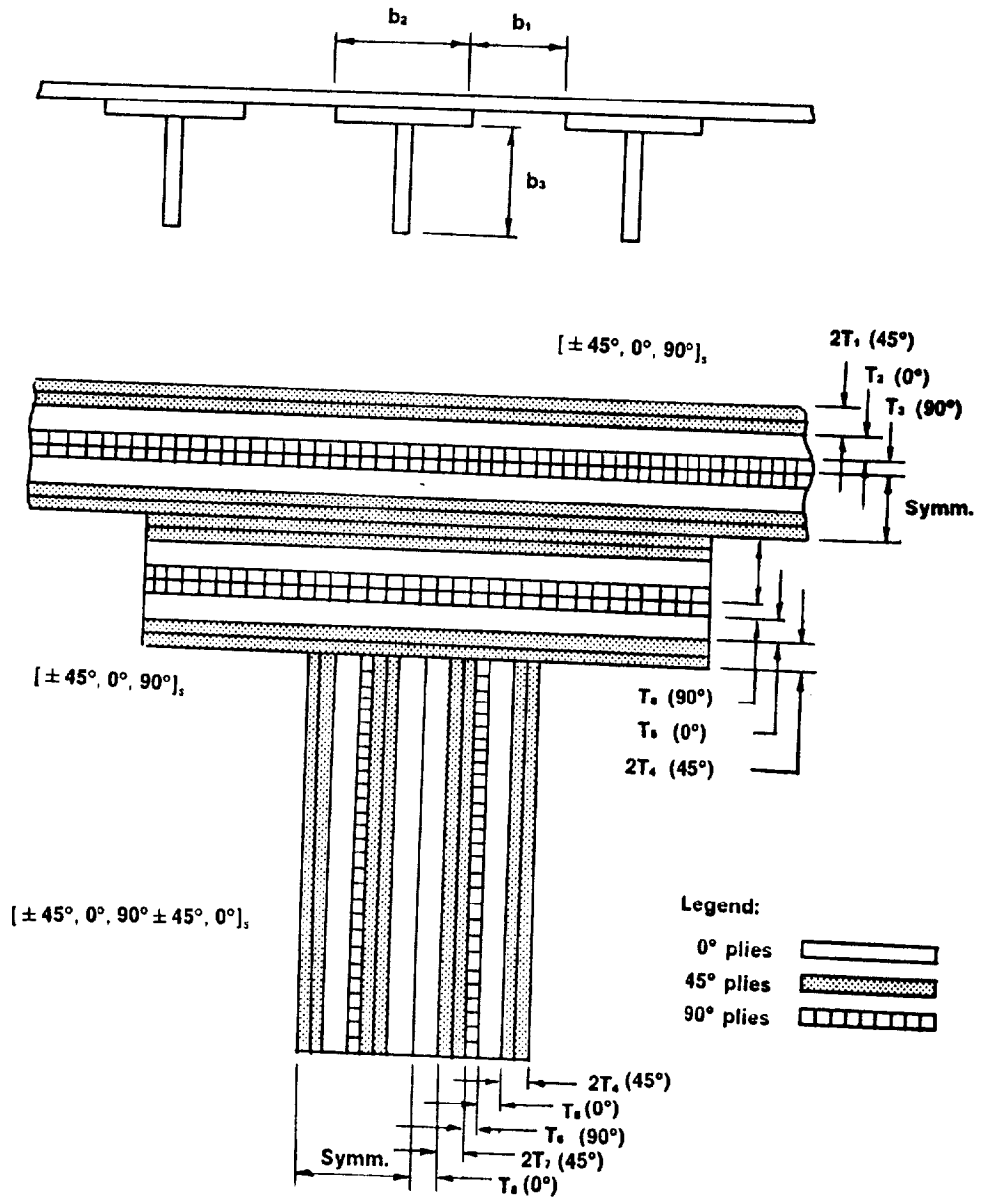
Figure 15. Blade Stiffened Panel Model.

```
***** PASCO MODEL 7A CASE 002 *****
$CONDAT
$
$PANEL
MAXJJJ= 10,
GRANGE= 10,
LINK= 0,
EL= 28,
B= -2.858,  0.750, 4*1.E30, -0.630,
BL(1)= .01, .75, .01, .01, .01, .01, .01,
T= .00500, .00500, .00500, .00500, .00500, .00500,-.00600,-.00629,
     2*1.E30,
TL= .005, .005, .005, .005, .005, .005, .005, .005,
THET= 45, 0, 90, 45, 0, 90, 45, 0,
KWALL(1,1)= 1,-1, 2, 3,
KWALL(1,2)= 4,-4, 5, 6,
KWALL(1,3)= 4,-4, 5, 6, 7,-7, 8,
IWALL= 1,1,1,1,2,2,3,
HCARD= 6, -8,-5, 0,-9, 0,-9,
       6, -9,-6, 0,-9, 0,-9,
       6,-10,-7, 0, 0,10, 0,
       4,-11,10,90, 0,
       2,121,11,
       8, 12, 1, 2,-8, 3,-9,-121, 4, ⹁
NOBAY= 11,
AB(1,1)=  0, 1,-1,
AB(1,2)=  1, 0, 0,-1,
AB(1,3)=  0, 1, 0, 0,-1,
AB(1,4)=  0, 1, 0, 0, 0,-1,
AT(1,5)=  2, 1, 1, 2, 1, 1, 0, 0,-1,
AT(1,6)=  2, 1, 1, 4, 2, 2, 0, 0, 0,-1,
MINLAM= 28,
NLAM= 1,2,4,7,14,28,
IBC= 1,
IP= 2,
NX= 100.,
CLAM(1)=  1.0,
SHEAR= 0.,
$
$MATER
E1= 18.5E6,  E2=1.64E6,  E12=.87E6,  ANU1=.30,  RHO=.0570,
ALFA1= 0.25E-6, ALFA2=16.2E-6,
ALLOW= 2,  .00850,-.00850,  .00850,-.00850, .01400,
$
```

Figure 16.   Blade Stiffened Panel PASCO Input Data File.

$[\pm 45°, 0°, 90°]_s$ laminate where T_1, T_2, and T_3 define the 45°, 0°, and 90° lamina thicknesses, respectively. The flange of the blade stiffener is also defined as a $[\pm 45°, 0°, 90°]_s$ laminate with independent ply thicknesses T_4, T_5, and T_6 defining the 45°, 0°, and 90° lamina thicknesses, respectively. The blade itself is defined such that the lower half of the flange laminate is continuous into the blade. This feature is shown schematically in Figure 17. Therefore, the laminate defining the blade is a $[\pm 45°, 0°, 90°, \pm 45°, 0°]_s$ laminate where the first $\pm 45°$, 0°, and 90° plies are continuous from the flange and are again defined by T_4, T_5, and T_6, respectively. The added 45° and 0° plies are defined by T_7 and T_8, respectively, and allow the blade properties to be independent of the flange properties.

The unstiffened flat plate is defined by a laminate of $[\pm 45°, 0°, 90°]_s$ where T_1, T_2, and T_3 define the 45°, 0°, and 90° lamina thicknesses, respectively, and is shown in Figure 18. A sample PASCO input is presented in Figure 19.

For the case where increased stiffener spacing is desired, plate widths are required to be specified either in absolute dimensions or as a function of other plate widths. PASCO provides an option that allows the plate widths to be linked relative to one another. The corrugated panel can be modeled such that the space between the corrugations, essentially the lower cap, is a function or multiple of the width of the span formed by the upper cap and webs. By increasing the ratio of the spacing of the corrugations to the corrugation width, a configuration is defined which is referred to as a beaded panel. This beaded panel concept is shown in Figure 20 and a sample PASCO input file is presented in Figure 21. This panel is potentially easy to manufacture using thermoplastic materials since it can be thermoformed or stamped into its final form.

As previously discussed, PASCO accounts for applied lateral pressure by applying a bending moment to the panel cross section. Since PASCO can only apply constant N_x, N_y, and N_{xy} to any single plate element, the model must be modified in such a way to account for the variation of the in-plane loads across the plate depth resulting from the applied moment. For the case of a stiffened panel with applied pressure, each model is altered by replacing the single plate element representing the corrugation web or the blade with a series of three
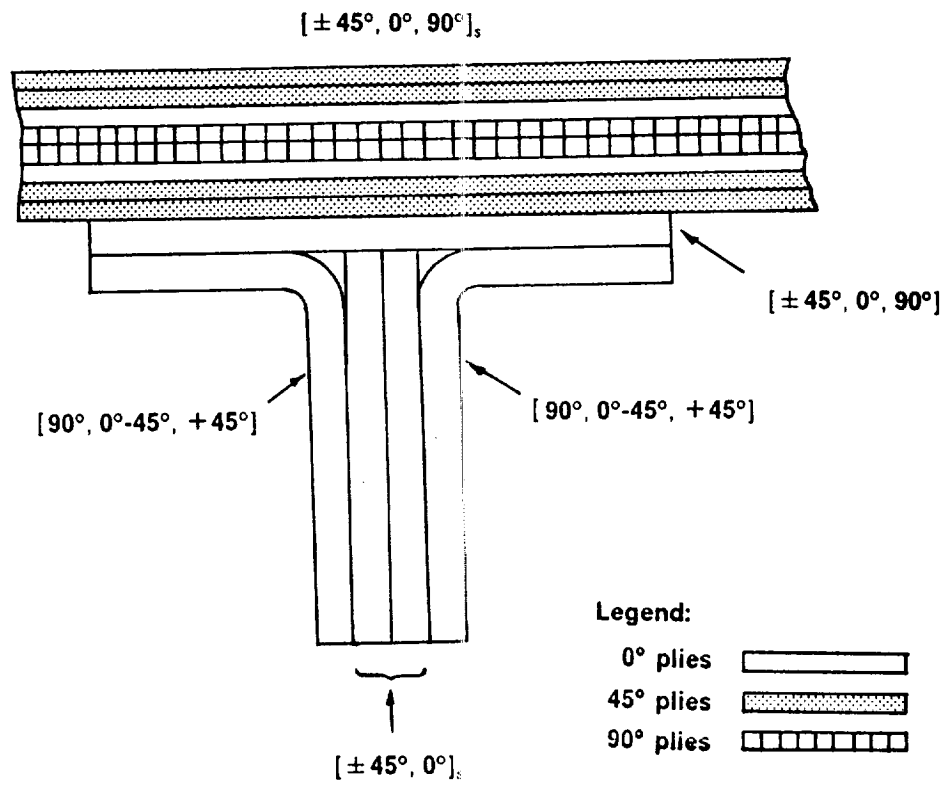
Figure 17. Blade Stiffened Panel Laminate Schematic Diagram.

Design Study Approach
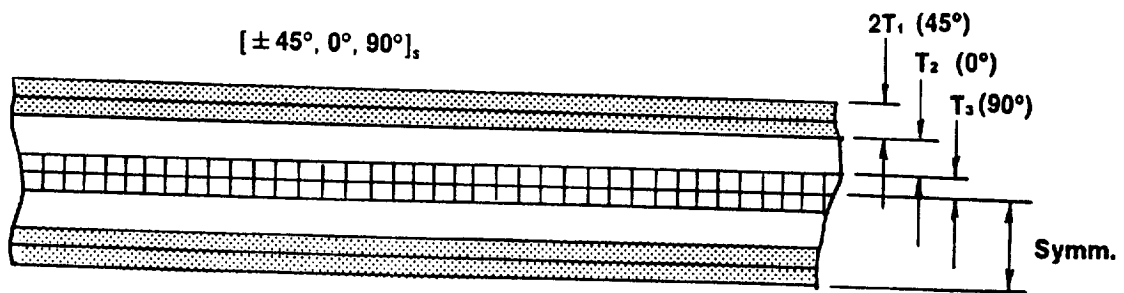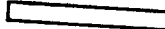
Figure 18. Unstiffened Flat Plate Model.

```
***** PASCO MODEL 8A 001   FLAT SHEET *****
$CONDAT
$
$PANEL
GRANGE= 10,
LINK= 0,
EL= 28,
B= 5.00, 5.00,
T=  -.0075, -0.0090, -0.005,
THET= 45, 0, 90,
KWALL(1,1)= 1,-1,2,3,
IWALL= 1,1,
HCARD= 4,-3,1,400,-2,
      4,-4,2,-400,-2,
      3,5,3,4,
NOBAY= 8,
MINLAM= 28,
NLAM= 1,2,4,7,14,28,
IBC= 1,
IP= 2,
NX= 10.,
CLAM(1)= 1.0,
$
$MATER
E1= 18.5E6,  E2=1.64E6,  E12=.87E6,  ANU1=.30,  RHO=.0570,
ALFA1= 0.25E-6, ALFA2=16.2E-6,
ALLOW= 1, -204.E3, 211.E3, -21.4E3, 6.1E3, 13.8E3,
$
*
```

Figure 19.   Unstiffened Flat Plate PASCO Input Data File.

$$\psi = \text{Bead Ratio}$$

$$\theta = \cos^{-1}\frac{b_3}{b_2}$$

Legend:

0° plies

45° plies
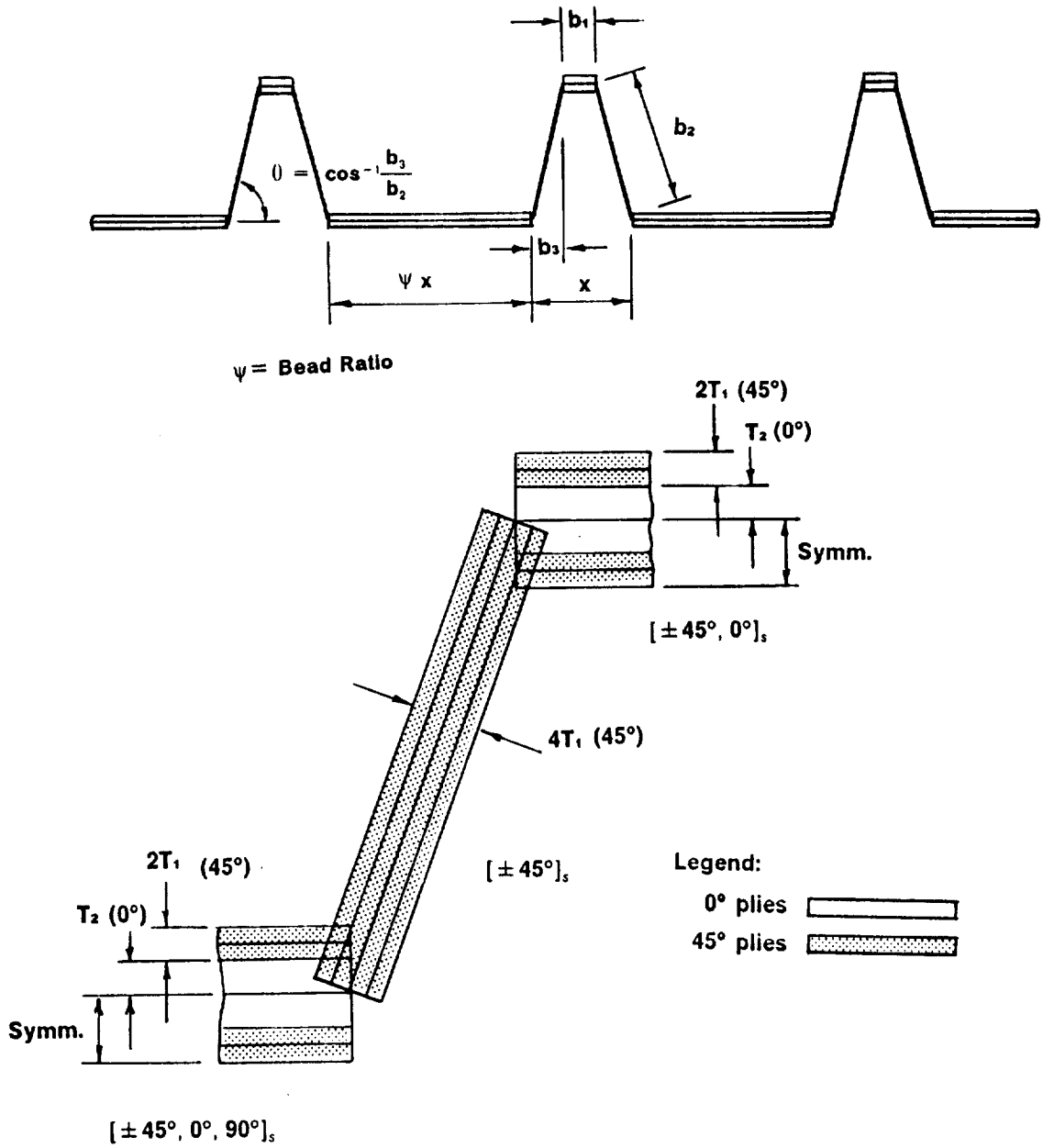
Figure 20. Beaded Panel Model.

```
***** PASCO MODEL 5A 701 (BEADED RATIO = 1.0) *****
$CONDAT
$
$PANEL
GRANGE= 10,
MAXJJJ= 10,
LINK= 0,
EL= 28,
B=  1.E30,-2.04766,-1.22414, 2*1.E30,-0.75320,
BL= .10, .10, .10, .10, .10, .10,
T= -.011, -.125,
TL= .005, .005,
THET= 45, 0,
KWALL(1,1)= 1,-1, 2,
KWALL(1,2)= 1,-1,
IWALL= 1,2,1,2,1,
HCARD= 4,-7,2,6,2,
       4,-9,4,-6,2,
       6,11,1,7,3,9,5,
NOBAY= 15,
AB(1,1)= -1, 0,.5, 0, 0, 1,
AB(1,2)=  0, 1, 0,-1,
AB(1,3)=  1, 0, 0, 0,-1,
MINLAM= 28,
NLAM= 1,2,4,7,14,28,
IBC= 1,
IP= 2,
NX= 28000.,
CLAM(1)= 1.0000,
SHEAR= 0,
$
$MATER
E1=  18.5E6,  E2=1.64E6,  E12= .87E6,  ANU1=.30,  RHO=.0570,
ALFA1= 0.25E-6, ALFA2=16.2E-6,
ALLOW= 2, .00850,-.00850, .00850,-.00850, .01400,
$
*
```

Figure 21. Beaded Panel PASCO Input Data File.

linked plate elements as shown in Figure 22. The N_x applied to each of these elements can then be varied to simulate the moment due to the applied pressure.

2.4.2 Applied Loads

The loadings applied to the PASCO models include the in-plane loads N_x, and N_{xy} applied to each individual plate element making up the panel model. The axial loading, N_x is by definition a compressive load. The buckling response of the panel to a shearing load, however, is dependent on the sign of the applied load. Since the positive 45° lamina is on the outermost layer, the laminate can resist buckling in shear better when the outermost 45° layer is in compression in the fiber direction, which occurs when positive shear is applied. The difference in buckling loads is due to the change in sign of the anisotropic bending stiffnesses D_{16} and D_{26}. To be conservative, a negative shear is applied to the laminates for all the loading cases considered in this study since the +45° lamina is the outermost lamina and this results in the lowest buckling load. The response of a positive shear applied to a $[+45°, -45°]_s$ laminate is the same as applying a negative shear to a $[-45°, +45°]_s$ laminate.

The magnitude of the loading range selected for study is based on a typical loading of a inboard wing rib fuel closeout cell for a large transport aircraft. Typical loadings for a fuel closeout rib of this type are axial compressive loads of $N_x=$ 200 to 300 lb/in, shear loads of N_{xy} up to 500 lb/in, and pressure loads of up to 15 lb/in^2. Worst case loadings of N_x and N_{xy} of 1000 lb/in are considered to be the maximum attainable. These loads are estimated for a panel with a height of 28 inches even though ribs located near the wing tip can be loaded differently and be considerably shorter in length. To include all of these loadings, a load index of N_x/L is used to define the loads. A range of N_x/L from about 0.3 to 1000 lb/in^2 is chosen to represent the entire loading range expected and to include additional loading above and below these typical loadings to help describe the trends. When other subcomponents, such as a wing skin, are considered, this loading range is also within reason. The range of N_{xy} studied
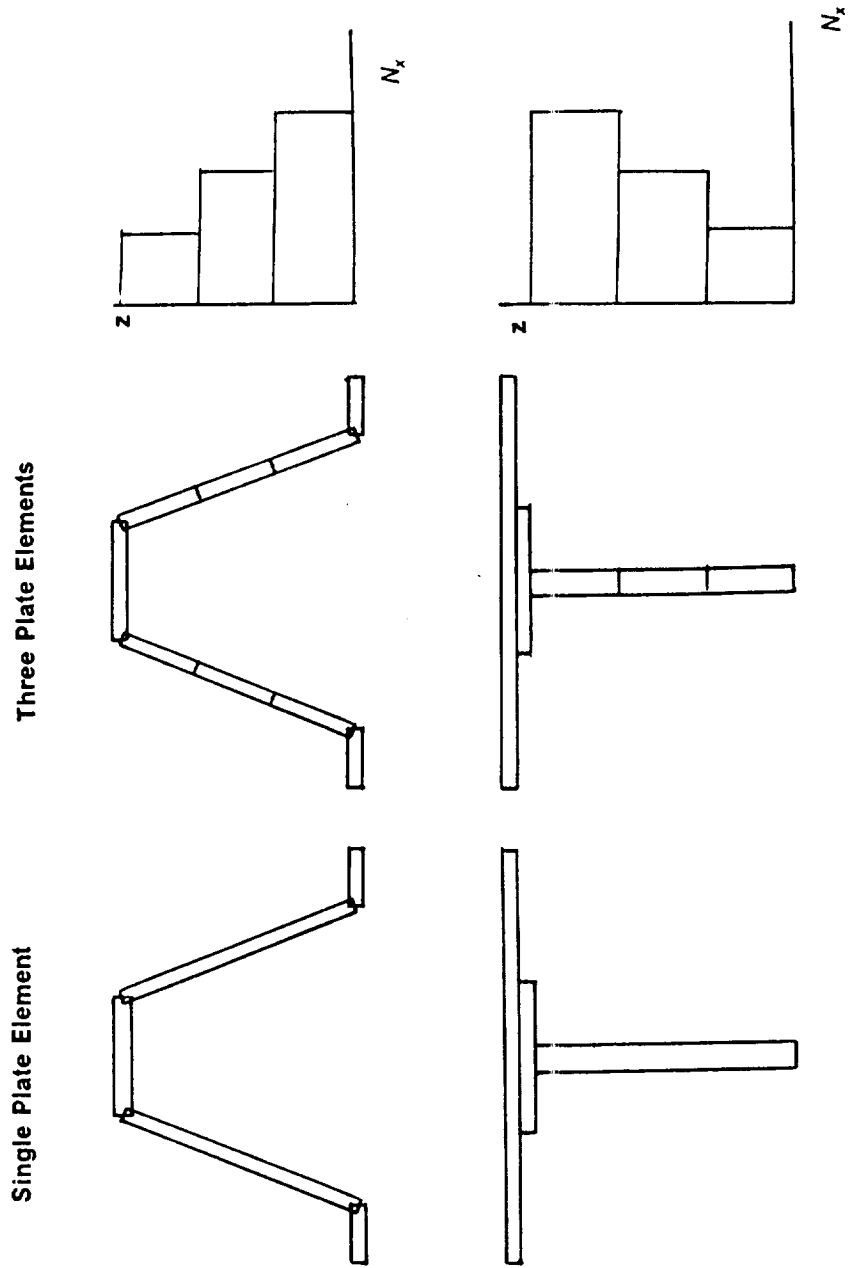
Figure 22. PASCO Model Change for Applied Moment due to Pressure

is chosen to be a ratio of the applied axial load. Shear load ratios of $N_{xy}/N_x =$ 0.0, 0.3, 0.6, and 1.0 are investigated. Even though a pressure of 15 lb/in² is considered typical, peak pressures due to fuel sloshing or impact can be considerably higher. Thus, values of applied pressure up to 45 lb/in² are included to investigate the effects of higher pressure on the design trends. In summary, N_x/L is applied between 0.3 and 1000 lb/in². For each value of N_x/L, shear is applied by keeping the ratios of N_{xy}/N_x equal to 0.0, 0.3, 0.6, and 1.0. Finally, pressure effects are investigated by applying lateral pressures of 0., 15., 30., and 45. lb/in² to each combination of N_x and N_{xy}. The results for these loading conditions are presented in the following chapter.

3.0 Design Study Results

Minimum weight, buckling resistant wing rib panel configurations are designed for various loading conditions using the computer program PASCO, including considerations for maximum allowable material strain, and minimum ply thicknesses. Results are presented for the selected configurations discussed in Chapter 2, which include a corrugated panel with tailored laminates, a corrugated panel with a single continuous laminate, a corrugated panel with a face sheet, and a blade stiffened panel. A flat, unstiffened plate is also included for comparison. For each of these configurations, results are presented for various combinations of loading which include an axial compressive load, combined axial compression and out-of-plane pressure, combined axial compression and shear, and finally, combined axial compression, shear, and out-of-plane pressure. Effects of these loading conditions on the geometry and individual lamina thicknesses of the panels are determined. The results are presented in two forms including standard structural efficiency diagrams and charts showing the detailed cross sectional geometries of the repeating elements that make up the panel cross section. The structural efficiency diagrams show the weight index, W/LA, as a function of the applied axial load index, N_x/L, where W is the panel weight, A is the panel area, L is the length, and N_x is the axial compressive stress resultant. The curves presented represent a series of designs which form a lower bound of weight for a given panel configuration designed

to carry the indicated load. The curves are generated by determining the minimum mass design for several loading conditions and fitting a curve to these data points using a cubic spline.

3.1 Axial Compression Loading

The first loading condition considered is an axial compressive load acting alone. Since PASCO is an adequate analytical tool for simply supported panels loaded only in axial compression, the panel designs presented in this section are considered accurate. The effect of an axial compression load on the structural efficiency and geometry of all the panel configurations considered in the present study is shown in Figure 23 and Figure 24. For comparison, similar configurations which were designed using simplified buckling equations [22] are also presented. Since slightly different material properties, geometric constraints, and panel lengths are used in Reference 22, some differences exist between the present results and those published in Reference 22, especially at the lower loading levels where minimum gage ply thicknesses are active in the present study. However, in general, the trends observed in both studies are similar.

3.1.1 Lightly Loaded Panels

For lightly loaded panels, in the loading range less than $N_x/L = 100$ lb/in^2, the tailored corrugated panel is noticeably more efficient than the other configurations (see Figure 23). For example, at $N_x/L = 1.0$ lb/in^2, the tailored corrugated panel is nearly half the weight of the corrugated panel with a continuous laminate, slightly less than half the weight of the blade stiffened panel, and almost a third of the weight of the hat stiffened panel. All of these con-
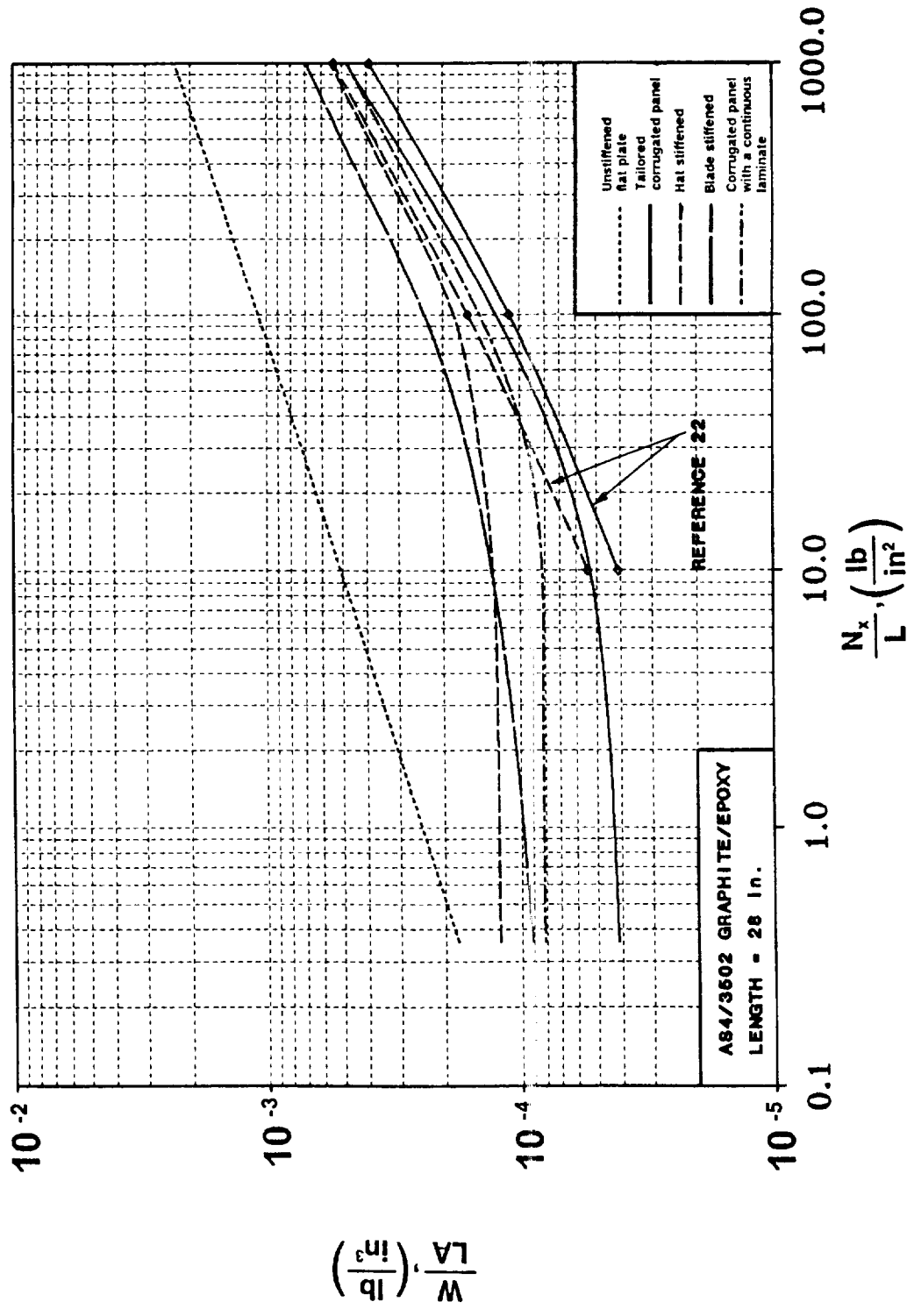
Figure 23. Structural Efficiency Curves for Axial Compression Loaded Configurations.

$N_x = 10. \frac{lb}{in}$	100.	1000.	10000.	28000.
Tailored Corrugated Panel				
Corrugated Panel with a Continuous Laminate				
Hat Stiffened Panel				
Blade Stiffened Panel				

Refer to Tables 3, 15, 26, and 36 for actual dimensions.

Figure 24. Geometry of Axial Compression Loaded Configurations.

figurations, excluding the unstiffened flat plate, are constrained by the same minimum gage ply thickness of 0.005 inches on all of the plies which make up each individual laminate. The unstiffened flat plate increases its ply thicknesses above the minimum gage constraint even at the lightest load to achieve enough bending stiffness to resist buckling, with the 0° fibers dominating the design. The large weight differences in the stiffened panels are due largely to the modeling of the laminates that define the panel geometry. Since all of the individual plies are at a minimum gage thickness of 0.005 inches for this light loading, the weight of the panel is almost directly proportional to the number of layers in the cross section and is independent of the intensity of the loading. For an axial compression load of $N_x/L = 1.0$ lb/in², for example, the tailored corrugated panel consists of 4 plies, the corrugated panel with a continuous laminate consists of 8 plies, the blade stiffened panel consists of 8 plies, and the hat stiffened panel consists of 10 plies, each proportional to the respective panel weights observed at the same applied load.

For loads approaching $N_x/L = 10.0$ lb/in², the tailored corrugated panel and the blade stiffened panel both show some increase in structural weight, even though the laminates all remain constrained by minimum gage ply thicknesses. The weight increase in this loading range, N_x/L between 1.0 and 10.0 lb/in², for the tailored corrugated panel is attributed to changes in the optimum corrugation angle. The increase in the blade stiffener weight can be attributed to the decreased spacing of the stiffeners and the slight increase in the stiffener depth, since all of the laminates remain constrained by minimum gage ply thickness constraints. These geometry changes in the blade stiffened panel essentially add material to the entire panel cross section as opposed to the other configurations which basically change their geometric configuration.

3.1.2 Bent Plate

The optimum design of the tailored corrugated panel for very light loads consists of a minimum thickness $[\pm 45°]_s$ laminate with small regular bends along its width (see Figure 24). This configuration will henceforth be referred to as a bent plate design. Further analysis of a flat $[\pm 45°]_s$ laminate with slight bends (i.e. bent plate) addresses the effect of these bends on the panel buckling load and is shown in Figure 25. The optimum design of the bent plate is such that the local buckling (buckling of the individual bend sections) and the global buckling modes occur simultaneously. The local buckling mode is critical for panel designs with plate elements wider than the plate element widths of the optimum configuration, and the global mode is critical for panels with plate element widths shorter than that of the optimum design. The bent plate design idealizes the optimized tailored corrugated panel (for very light loads) by disregarding the corrugation caps which are constrained by a minimum width limit of 0.10 inches and a minimum ply thickness limit of 0.005 inches on all of the plies. The effect of these minimized cap widths on the structural efficiency is negligible as can be seen by comparing the optimized tailored panel for $N_x = 10$ lb/in (indicated by a solid circular symbol) to the idealized bent plate solution shown in Figure 25. Thus, the geometry of the bent plate is shown to provide the largest contribution to the increased buckling capability over that of the flat plate. For example, a bend angle (θ) of 1° for a plate with 10 inch wide plate elements increases the buckling load by more than 200% compared to the unstiffened flat plate. The optimized bent plate designs, however, disregard any modal interaction between the global and local buckling modes which will reduce the buckling load. Therefore, the optimum bent plate design should be used with caution. The bent plate configuration is of particular interest because of the possibility of adopting a simple manufacturing method for production. This same bent plate configuration, with an flat face sheet attached, essentially describes the geometry of the lightly loaded ($N_x/L = 1.0$ lb/in²) hat stiffened panel.
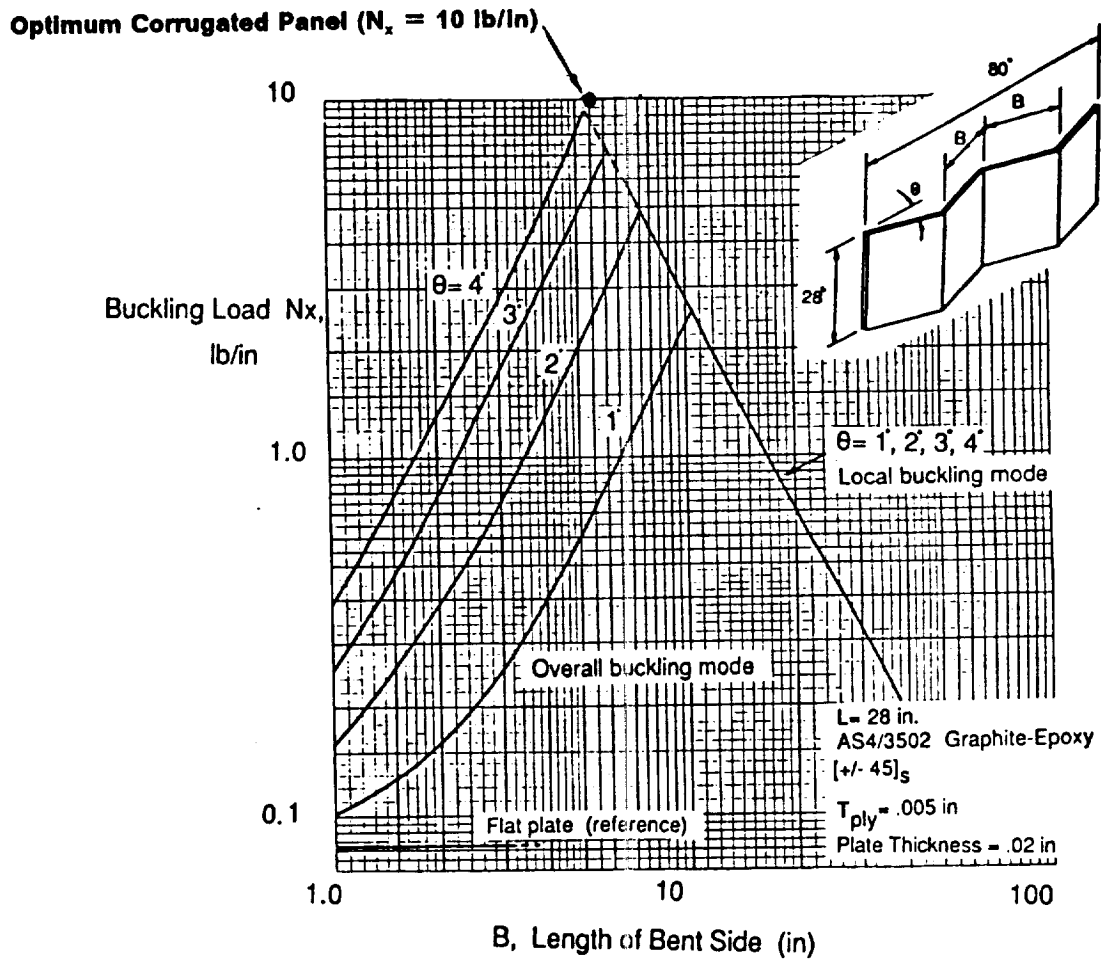
Figure 25. Geometry Effect on Buckling Load of a Bent Plate.

3.1.3 Heavily Loaded Panels

In the loading range between $N_x/L = 10$ and 100 lb/in^2, each of the configurations undergo cross sectional geometry changes to carry the applied load with minimum added weight. The repeating element geometries change, as shown in Figure 24, such that the repeating element widths decrease, increasing the number of stiffeners present in the panel, and the stiffener depths increase, adding to the amount of material present in the panel, while the optimum individual ply thicknesses remain at the minimum ply thickness. These changes in the cross sectional geometry cause different amounts of weight increase for different configurations for this moderate increase in loading from $N_x/L = 10$ to 100 lb/in^2. In this loading range, the tailored corrugated panel, the corrugated panel with a continuous laminate, the hat stiffened panel, and the blade stiffened panel increase their weights by 141%, 83%, 38%, and 85%, respectively. At loadings of N_x/L above 200 lb/in^2, the minimum gage ply thickness constraints are no longer active and the structural weight indices (W/LA) of the panel configurations become larger with increased loading. For loadings near $N_x/L = 1000$ lb/in^2, both the material failure constraint and the buckling constraint are active for the optimum design. The cross sectional geometries, Figure 24, show an increased thickness of 0° fibers in the caps of the tailored corrugated panel and the hat stiffened panel, an increased stiffener thickness in the blade stiffened panel, and an increased laminate thickness in the corrugated panel with a continuous laminate. For loads above $N_x/L = 200$ lb/in^2, the structural efficiencies of the panels are similar, with the tailored corrugated panel and the corrugated panel with a continuous laminate approaching the same weight near $N_x/L = 1000$ lb/in^2 (Figure 23).

The flat plate, as expected, increases its ply thicknesses with increasing load from the lowest loading level considered to achieve enough bending stiffness to resist buckling, with 0° fibers dominating the design.

3.2 Axial Compression and Pressure Loads

The same panel configurations considered in the previous section are also subjected to combined axial compression and out-of-plane pressure. This very important loading condition was often neglected in previous studies. The PASCO analysis used in the present study converts pressure loading to a moment applied at the loaded ends of the panel. The applied moment is equal to the maximum moment that occurs at the mid-span of a uniformly loaded beam. To account for the interaction of the in-plane axial compression loads and the out-of-plane pressure, PASCO uses a magnification factor, β, obtained using a beam column approach. This factor was discussed in Chapter 2. The application of pressure using PASCO should, however, be used with caution [20,55] since the approach used does not consider any nonlinear effects.

As discussed briefly in Chapter 2, to incorporate the pressure moment into the design, the PASCO models are slightly modified to allow varying axial loads along the depth of the panels to simulate a moment applied to the entire cross section. The corrugation web is changed from a single plate element to three connected plate elements. Similar modeling changes are made to the hat and blade stiffened panels.

3.2.1 Tailored Corrugated Panel

The effect of lateral pressure is most pronounced at the low end of the loading range as shown in the structural efficiency diagram presented in Figure 26. For loading intensities of up to $N_x/L =$ 10 lb/in², the effect of introducing a lateral pressure causes the structural weight index to increase substantially. Specifically, for $N_x/L =$ 1.0 lb/in², an applied pressure of 45 lb/in² increased the structural weight 190% over a panel designed without the applied pressure. Since there is little bending stiffness in the panel designed without the applied pressure,
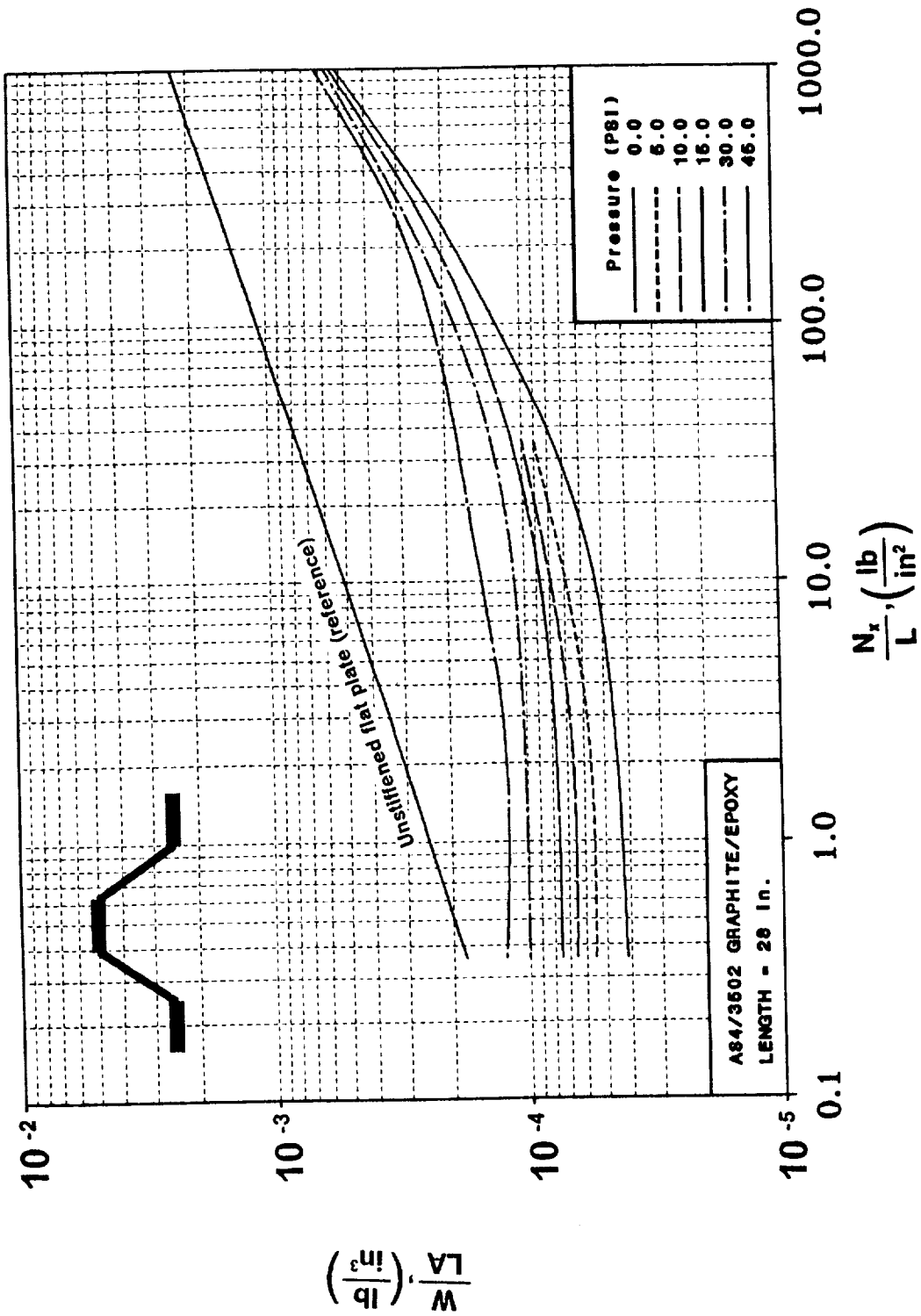
Figure 26. Structural Efficiency Curves of a Tailored Corrugated Panel Loaded by Pressure.

the moment due to even a small amount of applied pressure can cause a significant change in the geometry to create the bending stiffness needed to resist the additional load. Additional weight is also added by increased ply thicknesses necessary to resist material failure. As the magnitude of the applied pressure increases, the increase in weight for each unit of pressure increase becomes smaller. For N_x/L near 1000 lb/in², any increase in pressure has only a small effect on the weight parameter. Specifically, for $N_x/L=$ 1000. lb/in², an applied pressure of 45 lb/in² increased the structural weight only 20% over a panel designed without pressure. The reduced sensitivity of the highly loaded panels to pressure changes indicates the existence of sufficient bending stiffness in those high axial compression loaded panels so that only relatively small changes in the cross sectional geometry and ply thicknesses are needed to resist the additional moment due to the applied pressure.

The effect of lateral pressure on the geometry of the tailored corrugated panel is shown in Figure 27. For all loading combinations with a non-zero applied pressure, material failure is critical for the 0° plies in the cap. The most dramatic geometry changes occur at the lower pressure levels (P less than 15 lb/in²), explaining the weight increase noted earlier. Without the pressure, the optimized panels assume the bent plate configuration with just enough bending stiffness to resist buckling under the small axial compression load. For the lower axial compression loads near $N_x/L=1.0$ lb/in², the additional bending stiffness necessary to resist the moment resulting from the applied pressure is large compared to the bending stiffness present in the panel designed without pressure. At the higher loading levels near $N_x/L=$ 1000. lb/in², the bending stiffness necessary to resist the additional moment due to the pressure is relatively small when compared to the bending stiffness capability of the panel designed for axial loads alone. For increasing pressure at the low axial compression load levels near $N_x/L=10$ lb/in², the web angle and cap width increases, while the repeating element width decreases. As the applied pressure is further increased, less change in the geometry is needed to provide the required bending stiffness and, hence, a smaller weight increase for a unit pressure increase is observed. The geometry for $N_x/L=1000$ lb/in² has

Refer to Tables 3, 7, 8, and 9 in Appendix A for actual dimensions.

Figure 27. Geometry of Tailored Corrugated Panels Loaded by Pressure.

smaller repeating element widths for applied pressure of up to 15 lb/in² but changes little for pressures above that.

3.2.2 Corrugated Panel with a Continuous Laminate

The corrugated panel with a continuous laminate through its length and width is subjected to the increasing pressure along with the applied axial compression load. The effects of the applied pressure on the structural efficiency and geometry are shown in Figure 28 and Figure 29, respectively. At low loading levels, near $N_x/L = 10$ lb/in², the structural weight of the panel is greater than that of the tailored corrugated panel. The increased weight at this load level is a result of the minimum gage limitations active on both configurations, with more plies required to define the continuous laminate corrugated panel than required for the tailored corrugated panel. Although the continuous laminate corrugated panel is heavier than the tailored corrugated panel at the lower loading levels, the geometry of the both configurations respond similarly to increasing amounts of applied pressure. For higher axial compression loadings near $N_x/L = 1000$ lb/in², the structural efficiency of the corrugated panel with a continuous laminate is very close to the structural efficiency of the tailored corrugated panel. As the intensity of the pressure is increased at this higher loading level, similar to the trends observed for the corrugated panel with tailored laminates, only small changes in the structural efficiency is observed. The small weight changes resulting from increased pressure with high axial compression loading leads to the observation that the corrugated panel configuration is insensitive to changes in the laminate properties. That is, changes in the laminates may change the stress distribution within the cross section, but the panel weight is not severely effected. The effect of different laminates in corrugated panel configurations will be addressed with more detail in Chapter 4.

Design Study Results
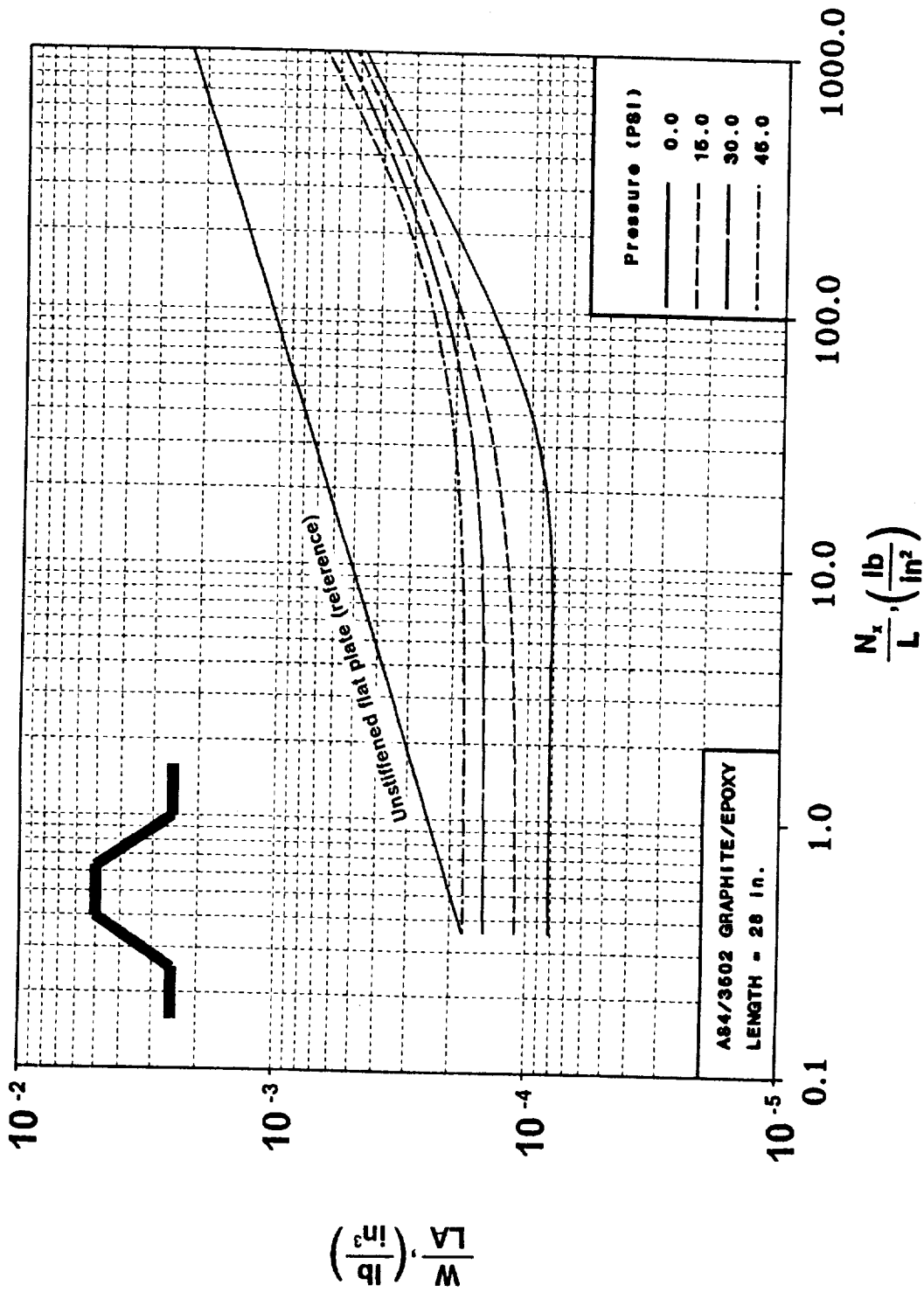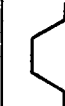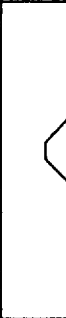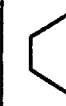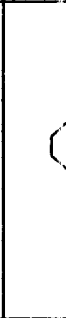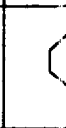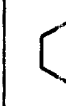
Figure 28. Structural Efficiency Curves for a Corrugated Panel with a Continuous Laminate Loaded by Pressure.

Refer to Tables 36 through 39 in Appendix D for actual dimensions.

Figure 29. Geometry of Corrugated Panels with a Continuous Laminates Loaded by Pressure.

3.2.3 Hat Stiffened Panel

The changes in the hat stiffened panel geometry are similar to the changes in the corrugated panel configurations mentioned previously when subjected to a compressive load and to an increasing level of applied pressure. The effect of applied pressure on structural efficiency is shown in Figure 30. For a lightly loaded panel (N_x/L less than 10 lb/in^2), even a small amount of applied pressure (5 lb/in^2) causes the weight to increase. This increase, however, is less than the increase observed at the same load level for the corrugated panels discussed previously. The weight of the panel increases 75% for $N_x/L = 1.0$ lb/in^2 as the applied pressure is increased from 0 to 45 lb/in^2. At the high load levels near $N_x/L = 1000$ lb/in^2, only an 18% weight increase is observed for pressure increases between 0 and 45 lb/in^2. This reduction in the sensitivity to pressure for the higher loads is attributed to the high stiffness of the panels designed for $N_x/L = 1000$ lb/in^2. The hat stiffened panel geometry, shown in Figure 31, has similar trends to the corrugated panel geometries shown previously. For the lightly loaded panels, an applied pressure load of up to 15 lb/in^2 results in significant changes in the geometry such as reduced repeating element widths and deeper hats. The resulting geometries are quite different from the nearly flat bent plate design for the panel without the pressure. The cross sectional geometry, however, is less affected as the pressure increased from 15 to 45 lb/in^2. At the very high loading levels near $N_x/L = 1000$ lb/in^2, very little difference in the geometry is observed other than a ply thickness increase in the caps and skin to account for the active material failure constraint. The spacing between hats, where the skin and stiffeners are attached, is not constrained in the present study (only a minimum plate element width is imposed to keep a zero plate width from occurring) and for many cases in this study, this dimension appears unreasonably small. Further study to assure the integrity of the attachment of the components is necessary.
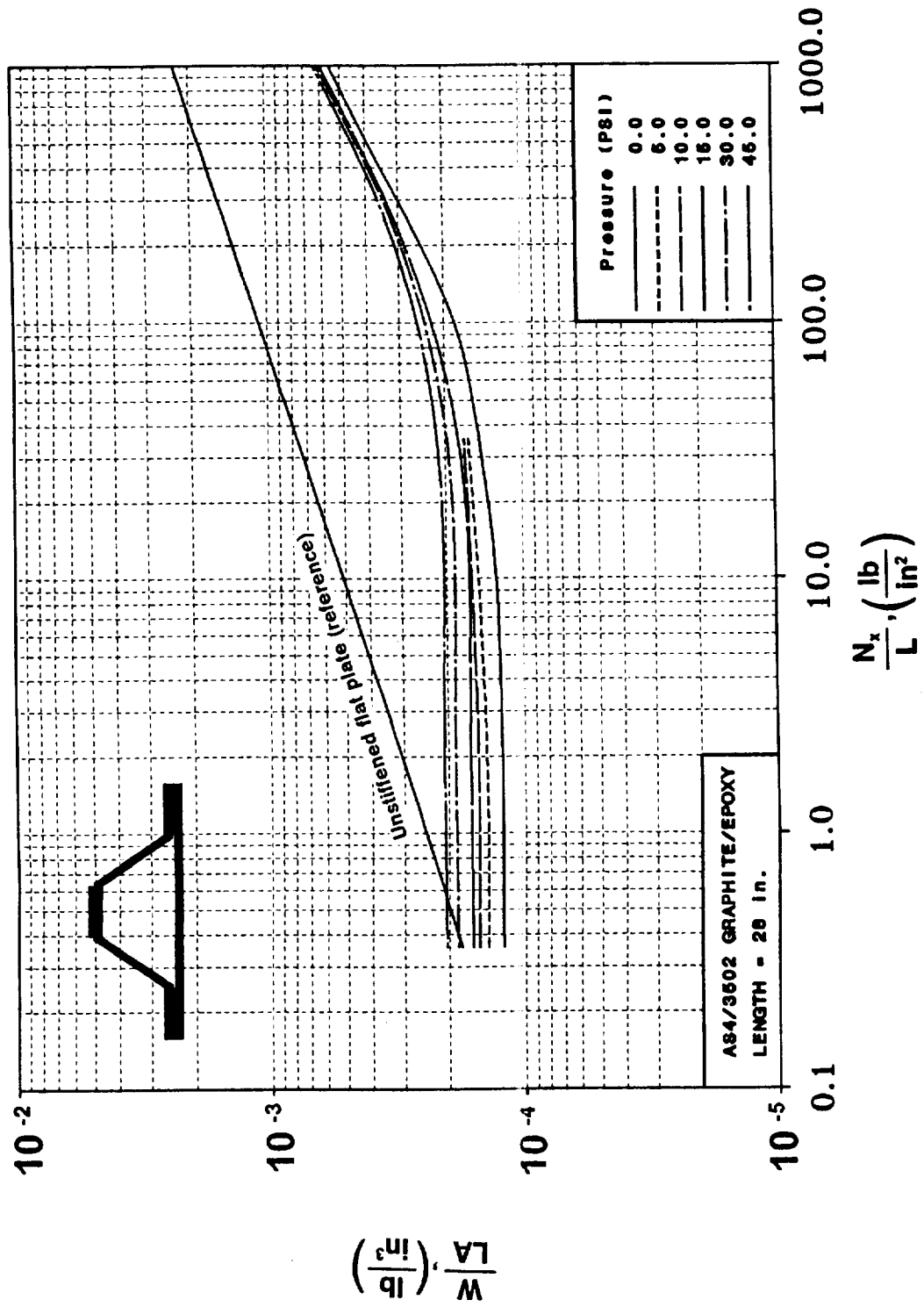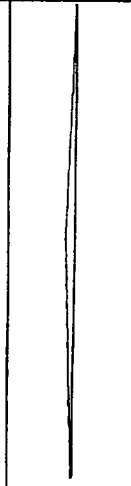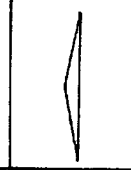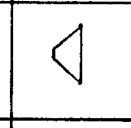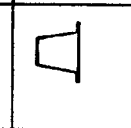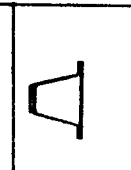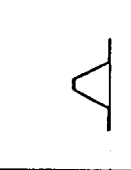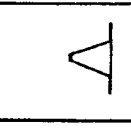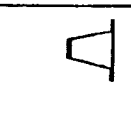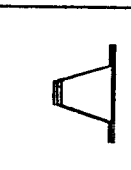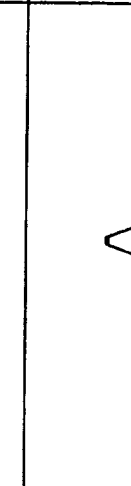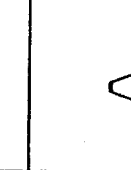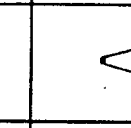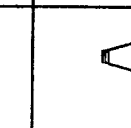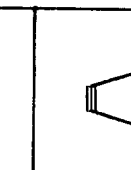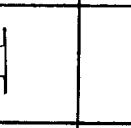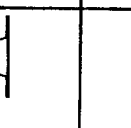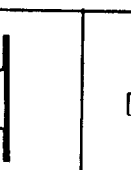
Figure 30. Structural Efficiency Curves of a Hat Stiffened Panel Loaded by Pressure.

$N_x = 10. \frac{lb}{in}$	100.	1000.	10000.	28000.
P = 0 psi				
15 psi				
30 psi				
45 psi				

Refer to Tables 15, 19, 20, and 21 in Appendix B for actual dimensions.

Figure 31. Geometry of Hat Stiffened Panel Loaded by Pressure.

3.2.4 Blade Stiffened Panel

The blade stiffened panel, in general, follows the trends set by the previously described configurations, both in structural weight and geometry, as shown in Figure 32 and Figure 33, respectively. The structural efficiencies of these panels are similar to the others in that a noticeable weight increase accompanies the application of pressure of up to 15 lb/in^2 at the low end of the axial loading range near $N_x/L = 10.0$ lb/in^2, and the amount of weight increase becomes smaller as the applied pressure intensity increases to 45 lb/in^2. Increasing the pressure from 0 to 45 lb/in^2 for $N_x = 1.0$ lb/in^2 results in nearly a 200% increase in weight. At the lightly loaded levels (N_x/L under 10 lb/in^2), when no pressure is applied, the panel is designed with small, widely spaced stiffeners. When pressure is applied to this lightly loaded design, the stiffener spacing decreases significantly and each stiffener increases its depth, adding much material to the total cross section, hence, increasing the weight. As the applied loads increase to $N_x/L = 1000$ lb/in^2, design changes in the configuration due to applied pressure are less noticeable, again noting that the design for the highly loaded panels possess enough bending stiffness to carry the applied pressure without drastic geometric changes. Increasing the applied pressure from 0 to 45 lb/in^2 at this load level ($N_x/L = 1000.$ lb/in^2) results in only a 14% structural weight increase.

3.2.5 Comments

To aid in the evaluation of the effectiveness of the panel configurations to resist the applied pressure, the configurations being studied are compared in the structural efficiency diagrams shown in Figure 34, for four different pressure levels, 0, 15, 30, and 45 lb/in^2. The relative efficiencies for the configurations considered for no applied pressure was discussed previously and show that the tailored corrugated panel is the most efficient, followed by the
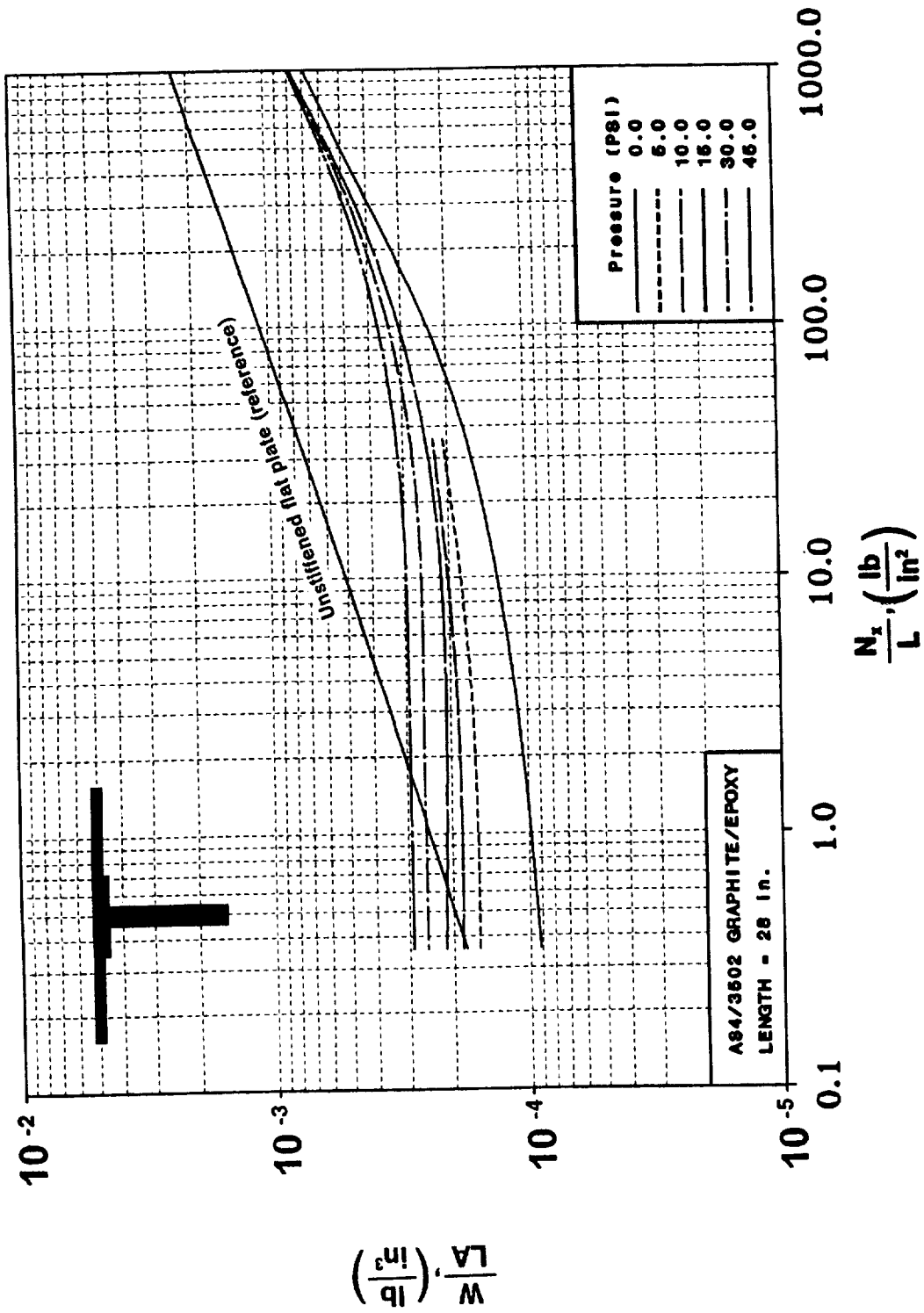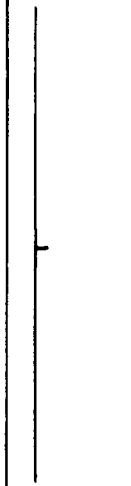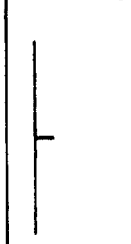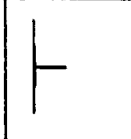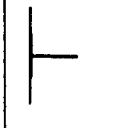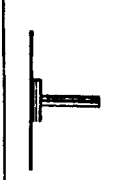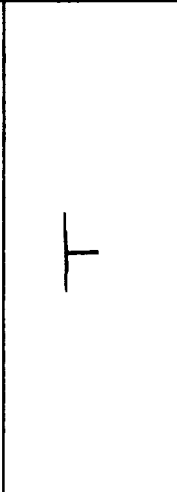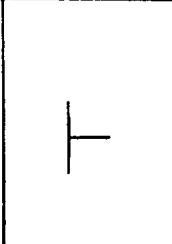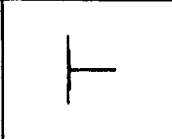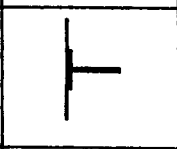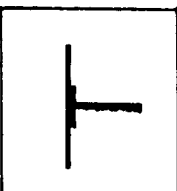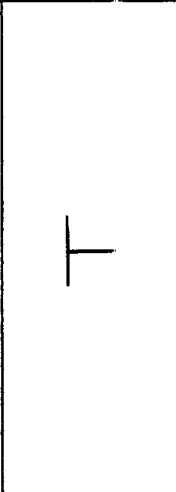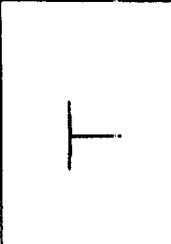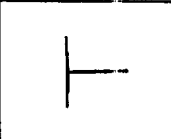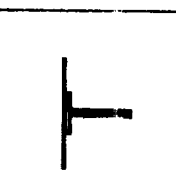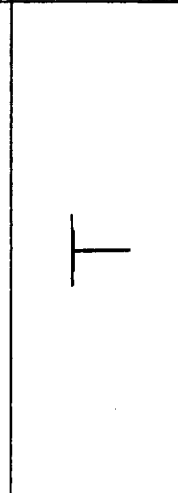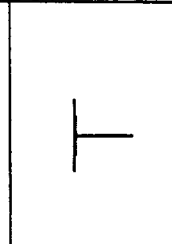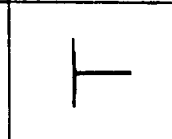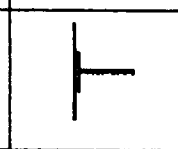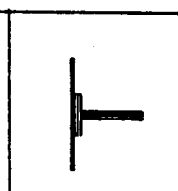
Figure 32. Structural Efficiency Curves of a Blade Stiffened Panel Loaded by Pressure.

$N_x = 10. \frac{lb}{in}$ | 100. | 1000. | 10000. | 28000.

P = 0 psi

15 psi

30 psi

45 psi

Refer to Tables 26, 30, 31, and 32 in Appendix C for actual dimensions.

Figure 33. Geometry of Blade Stiffened Panels Loaded by Pressure.
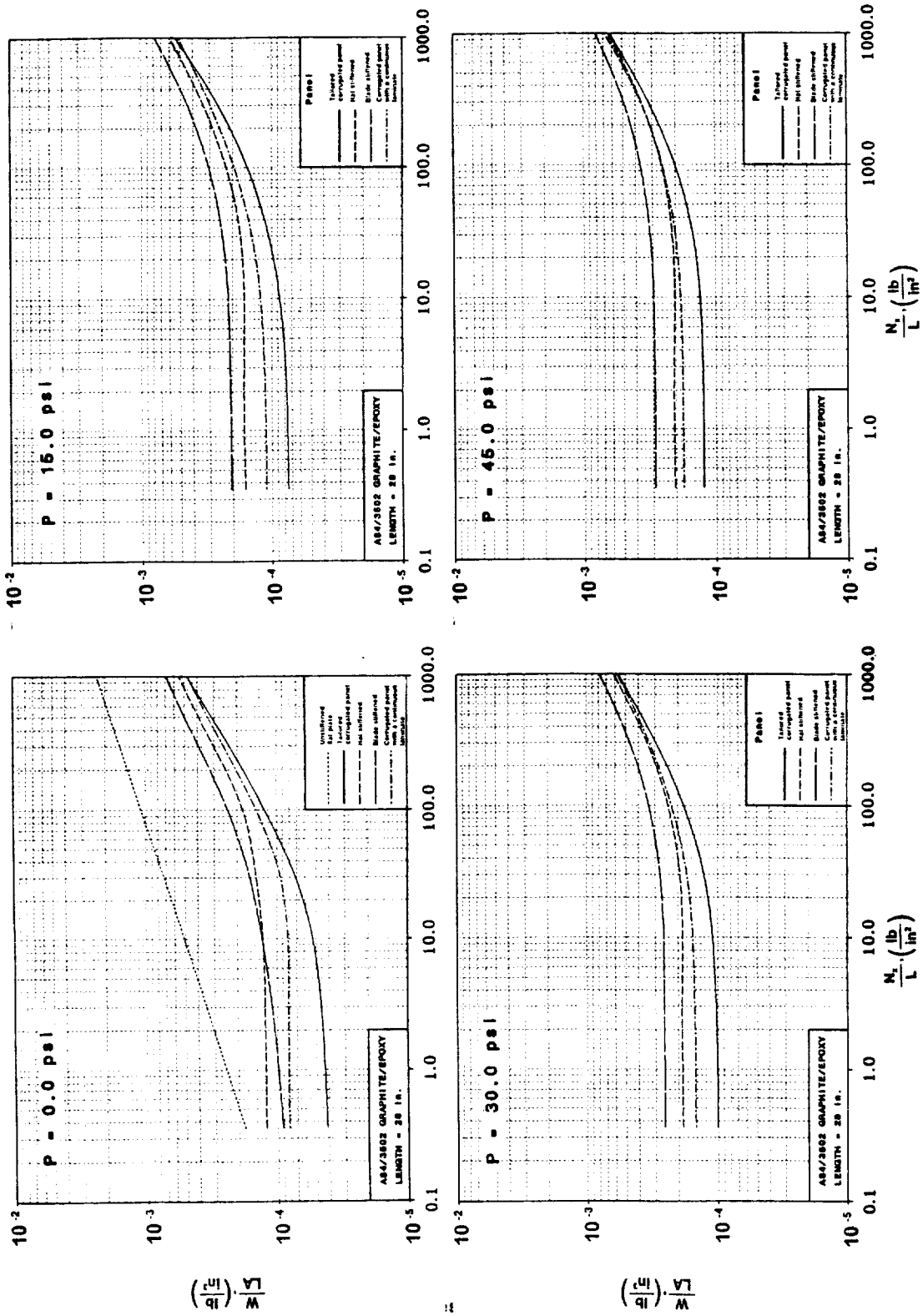
Figure 34. Structural Efficiency Curves for the Configurations Loaded by Pressure.

corrugated panel with a continuous laminate. For N_x/L less than 10 lb/in², the blade stiffened panel is lighter than the hat stiffened panel, and both are heavier than the corrugated panels. For applied pressure of up to 45 lb/in², three of the panel configurations, the tailored corrugated panel, the corrugated panel with a continuous laminate, and the hat stiffened panel, approach a similar weight for increasing N_x/L while the blade stiffened panel weight is always heavier than the others. The blade stiffened panel, a common configuration in many metal designs and the least efficient of the configurations considered presently for composite materials applications, is the most widely used panel configuration for the wing sub-component. Factors such as the attachment of sub-components to each other, maintainability, and manufacturing considerations, may constrain the designer such that composite materials are not be used to their fullest potential. However, if weight is of primary importance, the present design study shows that some weight savings can be obtained by considering different panel configurations. Also, as a result of the recent advances in manufacturing technology, these configurations currently being studied may be cheaper to manufacture than the commonly used blade stiffened panel and may contain fewer free edges, giving further incentive to consider the alternatives.

The axially loaded panels presented with and without applied pressure can be used for other sub-components, such as a wing skin, since the loading range considered includes typical loads for these sub-components. The trends provided by PASCO add insight into the sensitivity of the configuration geometry to this type of loading. However, the design process is not final until the effects of the interaction of the boundary conditions on a finite length panel and the effect of nonlinearity due to applied pressure are addressed.

3.3 Axial Compression and Shear Loadings

For the design cases considered so far (panels loaded in axial compression and combined compression and out-of-plane pressure), the only limitation in the PASCO analysis is the omission of nonlinear effects on the buckling response due to interaction of the in-plane axial compression and the out-of-plane pressure loads. As is discussed earlier, PASCO has other shortcomings in its analysis. When a shear load is applied, the skewing of the nodal lines in a semi-infinite panel violates the simply supported boundary condition assumed at the loaded ends and results in an underestimation of the overall buckling load. A typical wing rib is loaded heavily with shear, therefore, the shortcoming in PASCO when shear is present must be accounted for. Since wing ribs are typically short in height (constrained by the thickness of the wing), the effects of the boundary conditions on the global buckling mode is an important consideration.

As is discussed in Chapter 2, the overall buckling load incorrectly calculated by PASCO in the presence of shear is corrected for in the present study using the program VICON [29]. PASCO and VICON are used together iteratively to account for the shortcomings in the PASCO analysis when shear is applied. However, the analysis procedure common to both PASCO and VICON (VIPASA) assumes a simply supported boundary condition and the results must be used carefully since the boundary conditions in a real structure may be different. The VICON correction to the PASCO panel design is of interest because it provides a better solution when shear is applied than the PASCO solution obtained with the optional smeared orthotropic stiffness method used to evaluate the overall buckling load. The iterative addition of the VICON solution to the PASCO design capabilities provides an economical solution to the shortcomings which currently exist in PASCO when shear loads are applied. The design and analysis of composite structures must be both accurate and economical for composite material applications to be competitive with metallic structures.

3.3.1 Tailored Corrugated Panel

Shear is applied, along with an axial compression load, to the corrugated panel with op-
timally tailored laminates and the results are presented in Figure 35 and Figure 36. Shear
loading is represented as a fraction of the applied axial compression load levels. Ratios of
the shear load to the axial compression load studied include $N_{xy}/N_x=0.0$, 0.3, 0.6, and 1.0, al-
though only $N_{xy}/N_x=0.0$ and 1.0 are included in Figure 35. Panels designed with PASCO alone
show little change in structural efficiency due to shear at the lower applied loadings of N_x/L
less than 5 lb/in^2 where minimum gage constraints are active. At increased loadings above
$N_x/L=20$ lb/in^2, the structural efficiency penalty due to the VICON correction for $N_{xy}/N_x=1.0$
increases to a consistent amount of 15%. At the high end of the loading range near
$N_x/L=1000$ lb/in^2, the material failure constraints are critical and the effect of the VICON cor-
rections on the structural efficiency becomes insignificant. However, in the load range where
only the buckling criteria are affecting the design, between $N_x/L=20$ and 200 lb/in^2, changes
in the structural efficiency due to the VICON corrections are observed. The error in the
PASCO analysis for a corrugated panel as compared to a general finite element solution was
shown in Reference 24 to be conservative for the non-optimum designs. These errors are
shown in the present study to be less critical for the tailored corrugated panel when multiple
constraints affect the optimum design. As a further comparison, the present results are
compared to the results of the simplified buckling analysis design study [22]. The comparison
is included in Figure 35 and shows fairly good correlation considering slightly different mate-
rial properties and geometric constraints for the corrugated panel with an applied axial com-
pression load only. However, lower weight designs are obtained for those cases in which a
shear load of $N_{xy}/N_x=1.0$ is applied. Changes in the geometry of the repeating elements as
a result of applied shear on the panel are presented in Figure 36 for the tailored corrugated
panels (designed both with and without the VICON correction) under combined axial com-
pression load and increasing percentages of applied shear. For lightly loaded panels (N_x/L

Figure 35.   Structural Efficiency Curves for a Tailored Corrugated Panel Loaded in Shear.

Figure 36. Geometry of Tailored Corrugated Panels Loaded in Shear.

Refer to Tables 3 and 4 in Appendix A for actual dimensions.

less than 10 lb/in^2), the effect on the designs of increasing shear is minor, regardless of the VICON correction. For increasing shear with light axial compression loadings, the minimum gage constraint is active and the geometry shows a shortening of the repeating element width and a slight increase of the corrugation angle in the bent plate type design described earlier. The material necessary to satisfy the minimum gage constraints is sufficient to carry the increased shearing loads without significant geometrical changes. For the higher axial compression loadings (N_x/L greater than 100 lb/in^2), the minimum gage constraints are inactive, and the application of shear widens the repeating element width of the configuration, reduce the web angles, increase the cap widths, and increase the ply thicknesses for both the 0° and 45 ° plies. The wider cap widths may be attributed to the tendency of an individual plate element with a larger aspect ratio to carry larger shearing loads. For the higher loads (N_x/L above 100 lb/in^2), the effect of the VICON correction on the geometry can be significant when compared to the PASCO design. At these higher load levels, the VICON correction to the PASCO design (smeared orthotropic stiffness solution) results in panel designs with relatively shorter repeating element widths and corrugation depths.

3.3.2 Corrugated Panel with a Continuous Laminate

For the corrugated panel with a single, continuous laminate throughout its length and width, the VICON corrections are not carried out. Since this configuration is similar to the corrugated panel with tailored laminates, the effects of the VICON corrections are assumed to be similar. The effect of shear on the structural efficiency of the corrugated panel with a continuous laminate is very similar to the effect on the tailored corrugated panels designed by using PASCO without the VICON correction, and is shown in Figure 37 and Figure 38, respectively. At low load levels (N_x/L less than 50 lb/in^2), the weight in all cases is heavier than the tailored corrugated panel due to an increased number of minimum gage plies necessary to define the laminate. As the load increases to $N_x/L = 1000$ lb/in^2, the structural efficiency of
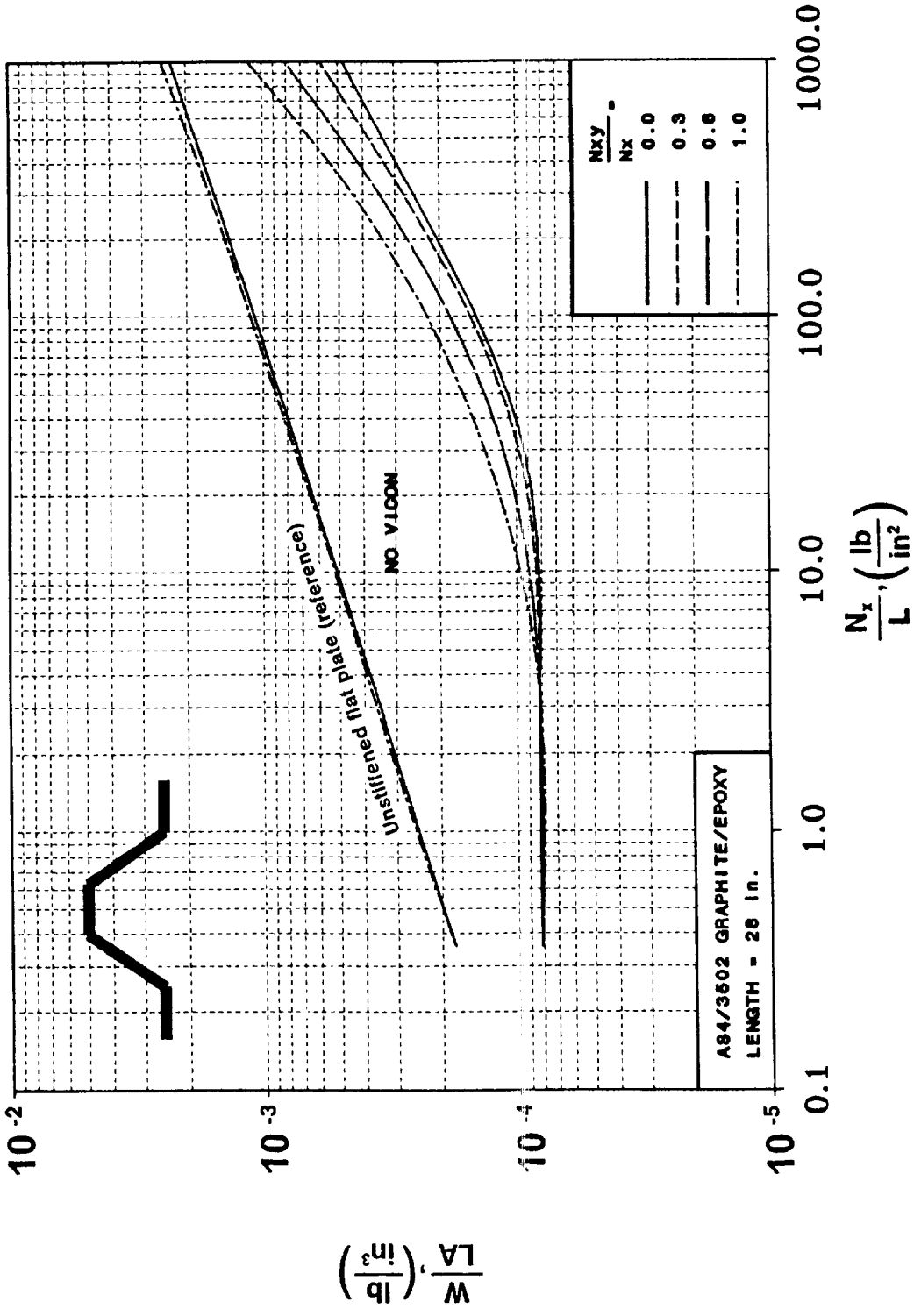
Figure 37. Structural Efficiency Curves for a Corrugated Panel with a Continuous Laminate Loaded in Shear.
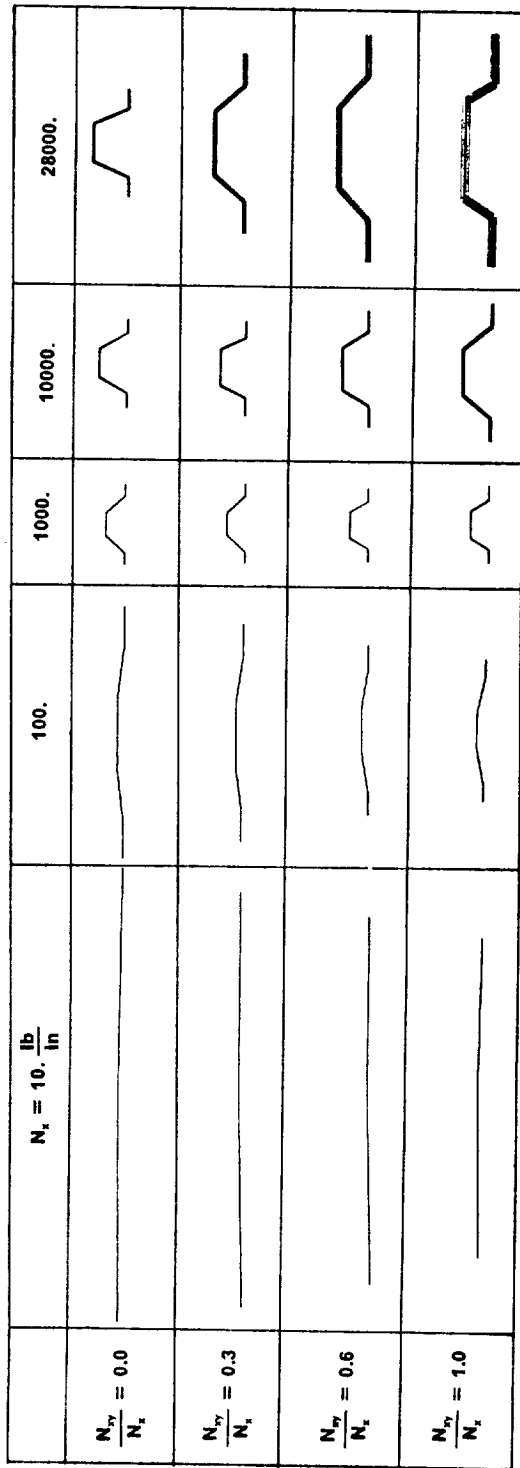
Refer to Table 36 in Appendix D for actual dimensions.

Figure 38. Geometry of Corrugated Panels with Continuous Laminates Loaded in Shear.

the panel approaches the structural efficiency of the tailored corrugated panel for each level of applied shear. The 90° plies in the laminate remain at minimum gage for all levels of loading and is discussed in Chapter 4. The effects of shear on the panel geometry are similar to the tailored corrugated panel for all the loading levels.

3.3.3 Hat Stiffened Panel

For the hat stiffened panel, the effect of the shearing load on the the structural efficiency and geometry is, in general, similar to that described earlier for the two corrugated panel geometries and is shown in Figure 39 and Figure 40, respectively. The results of the hat stiffened panel design using the simplified analysis [22], are included for reference. For applied shear loads, the results from the simplified analysis are unconservative for much of the loading range, yet still follow trends similar to those formed in the present study. The effect of the VICON correction on the hat stiffened panel design over the entire loading range, indicates a negligible difference when compared to the design using PASCO alone. The effect of the VICON correction on the geometry as compared to PASCO designs is also negligible. The ineffectiveness of the VICON correction is of interest because the PASCO shortcomings may not be critical for certain panel design configurations if the critical buckling mode for that design is not affected severely by the overall buckling mode.

3.3.4 Blade Stiffened Panel

The blade stiffened panel response to applied shear is similar to the response of the previous configurations discussed. The effect of applied shear on the structural efficiency and geometry of the blade stiffened panel is shown in Figure 41 and Figure 42, respectively. The VICON corrections to the analysis have little effect on the structural efficiency of the designs
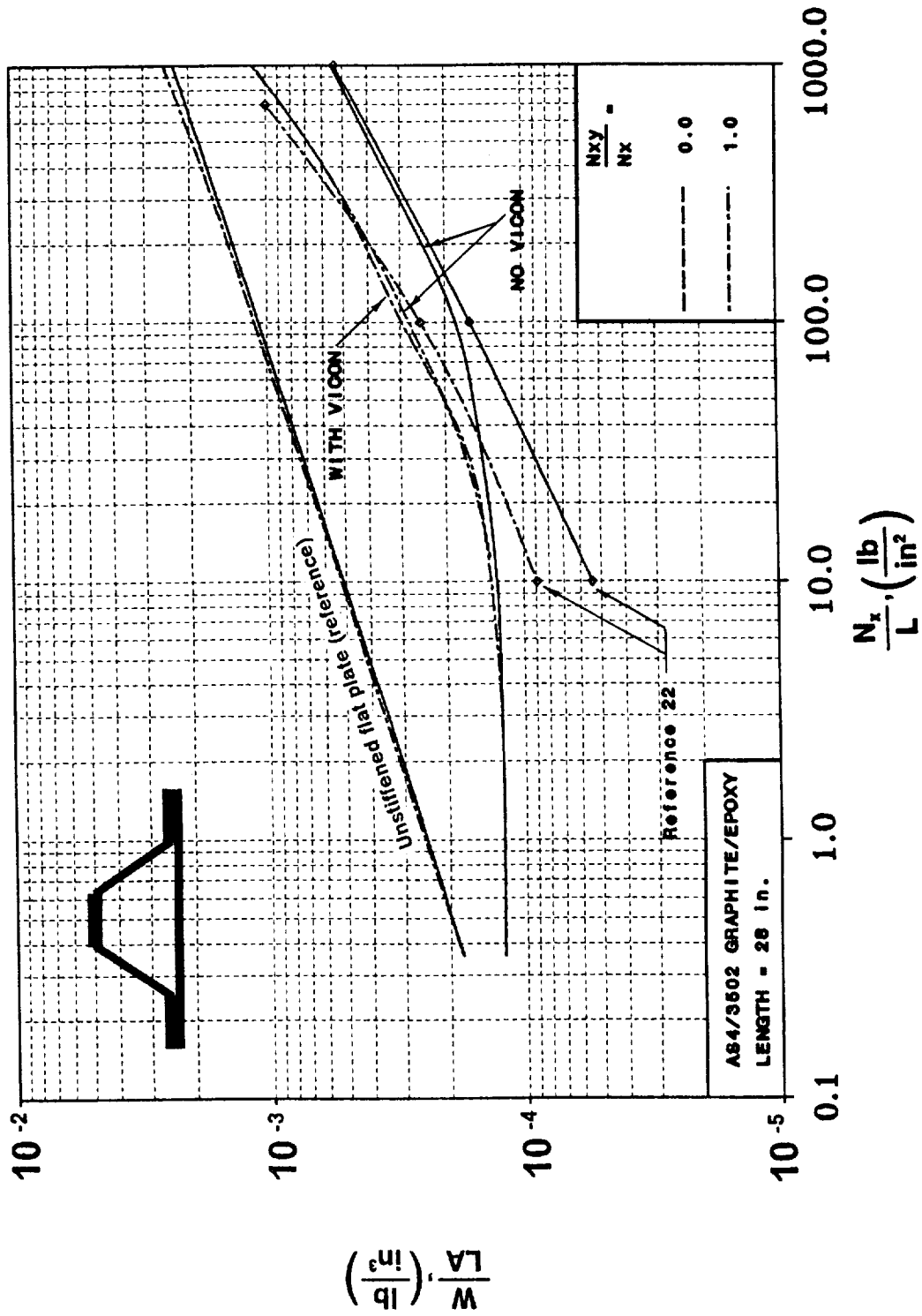
Figure 39.   Structural Efficiency Curves for a Hat Stiffened Panel Loaded in Shear.

$N_x = 10. \frac{lb}{in}$	100.	350.	1000.	2800.	10000.	28000.
$\frac{N_{xy}}{N_x} = 0.0$ NO VICON						
$\frac{N_{xy}}{N_x} = 0.3$ NO VICON						
VICON						
$\frac{N_{xy}}{N_x} = 0.6$ NO VICON						
VICON						
$\frac{N_{xy}}{N_x} = 1.0$ NO VICON						
VICON						

Refer to Tables 15 and 16 in Appendix B for actual dimensions.

Figure 40. Geometry of Hat Stiffened Panels Loaded in Shear.
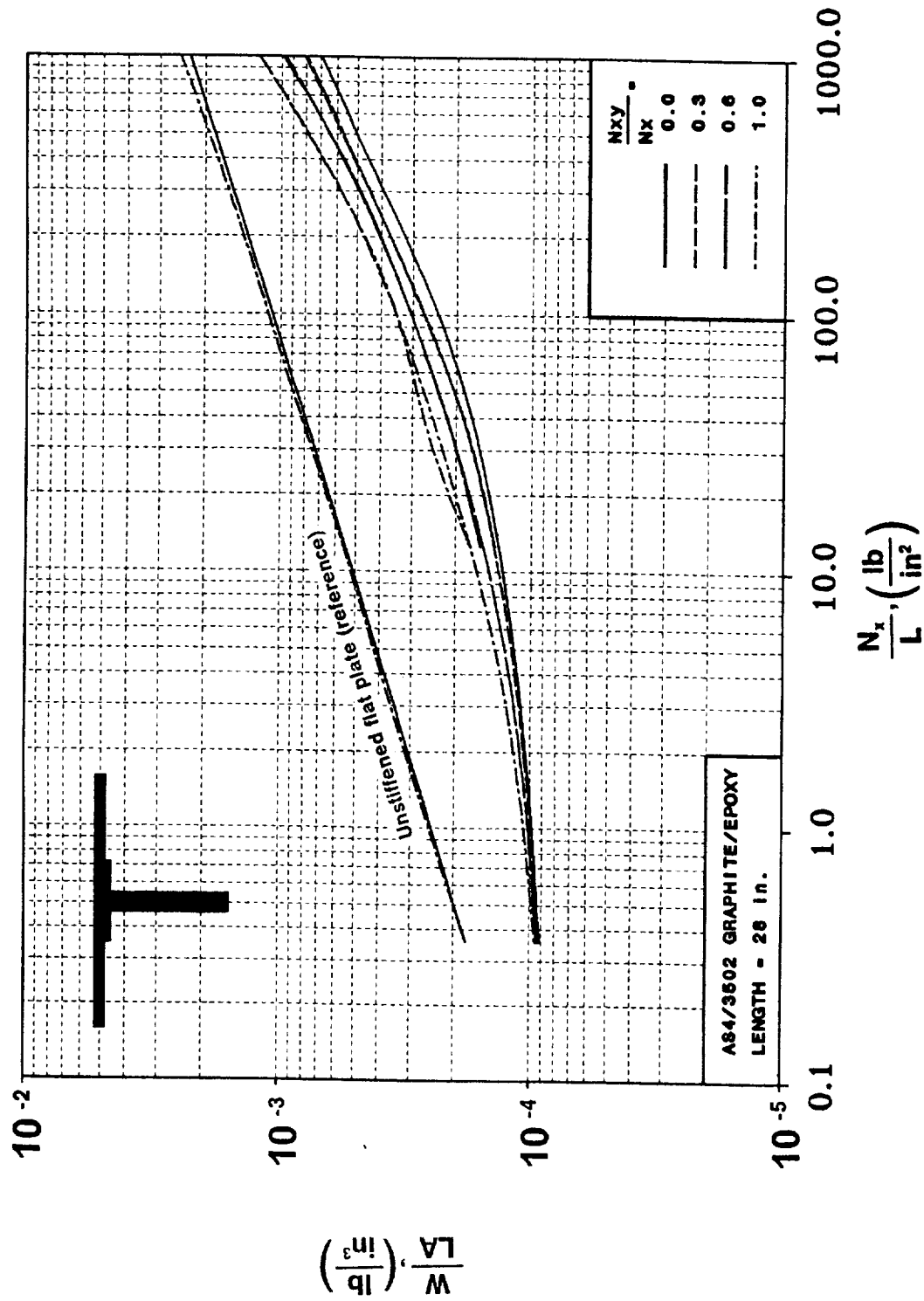
Figure 41.   Structural Efficiency Curves for a Blade Stiffened Panel Loaded in Shear.

Figure 42. Geometry of Blade Stiffened Panels Loaded in Shear.

Refer to Tables 26 and 27 in Appendix C for actual dimensions.

over the entire loading range. The addition of shear to the blade stiffened panel design in the lightly loaded range has little effect on the structural efficiency and can be attributed to the minimum gage constraint active at this loading level. At the higher end of the loading range (above $N_x/L = 100$ lb/in^2), the additional shear has a noticeable effect on the structural efficiency. At this higher loading level, both the buckling and the material strength constraints are active in the design. The addition of the shear loading is accounted for by minor adjustments in the geometry and by the addition of extra material which results in heavier weight. The geometric effects of the additional shear loading on the blade stiffened panel are again similar to the other configurations. For the light loading level (N_x/L less than 50 lb/in^2), the minimum gage thicknesses and wide repeating element widths dominate the panel design for no shear applied. For a light axial compression load with a N_{xy}/N_x ratio increasing to 1.0, the repeating element widths decrease, the blade depth increases, and the plies remain at minimum gage ply thickness. These geometric trends hold until an increased axial compression loading near $N_x/L = 100$ lb/in^2 causes the minimum gage constraints to become inactive. At load levels where the minimum gage constraints are active, the repeating element widths become smaller as the shear increases and the blade depths increase. Again, the effect of the VICON correction on the cross sectional geometry is negligible for the entire loading range.

3.3.5 Unstiffened Flat Plate Results and Comments

For comparison, an unstiffened flat plate is subjected to similar axial compression and shear loads. For all loading conditions, material failure is not critical. The shear loads have little effect on the structural efficiency except at the highest load levels near $N_x/L = 1000$ lb/in^2 where a small increase in the structural efficiency due to shear is noticeable. The VICON corrections to the design are negligible for all load levels considered.

The VICON correction described in Chapter 2 has its biggest effect on the structural efficiency when a buckling constraint alone is critical and is significant only for specific configurations. If other constraints, such as material strength or minimum gage, are critical, the effect of the improved analysis on structural efficiency is negligible. It is shown that the VICON correction has a noticeable effect on the tailored corrugated panel and creates geometry changes which are significant for the higher loading levels and tend to reduce the corrugation size. The VICON correction is not significant for the hat stiffened panel, the blade stiffened panel, and the unstiffened flat plate. To further illustrate the effect of the VICON correction on the panel weight, the structural efficiencies of the panel configurations are plotted in Figure 43 as a function of N_{xy}/N_x for $N_x = 1000$ lb/in. The effect of the shear load on the VICON correction to the overall buckling mode is largest for the corrugated panel. When PASCO is used without the VICON correction (smeared orthotropic stiffness solution) the local buckling of the stiffeners for the overall buckling mode is neglected. Although the design does not change significantly as a result of the VICON correction, the local stiffener buckling mode should not be ignored. In summary, the effect of shear for all lightly loaded panel configurations (N_x/L less than 10 lb/in²) is negligible since the material needed to satisfy the minimum gage constraint active at this loading level is sufficient to carry the applied shear without significant geometric changes. For higher axial compression loads approaching $N_x/L = 1000$ lb/in², the structural efficiencies of the configurations for each level of applied shear ($N_{xy}/N_x = 0.0, 0.3, 0.6,$ and 1.0) approach similar values. Thus, other considerations and criteria such as cost, maintainability, manufacturability, and imperfection sensitivity, among others, may influence the selection of a configuration for a design.
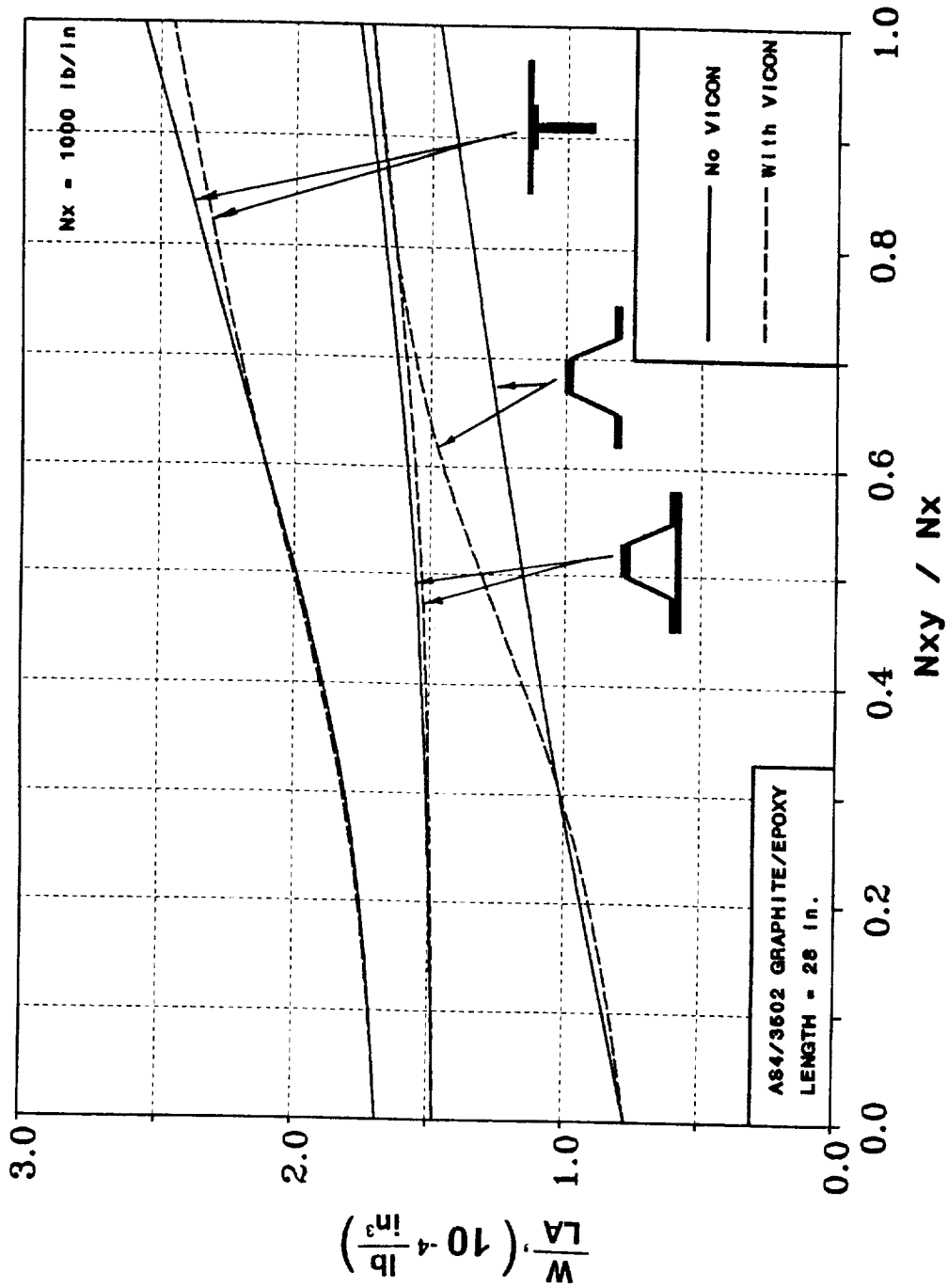
Figure 43.   Effect of the VICON Correction on the Structural Efficiency: $N_X = 1000$ lb/in.

3.4 Axial Compression, Shear, and Pressure Loading

The importance of considering lateral pressure loads on a wing rib design has been discussed. The effect of the pressure, along with axial compression and shear is determined for the configurations studied and is presented in the following section. PASCO uses a beam column approach to account for the interaction of the in-plane loads with the out-of-plane pressure load. The effect of the interaction is included during the analysis as a magnification factor, β, on an applied moment discussed earlier in Section 2.3.1. Since the overall buckling mode in the PASCO analysis is not critical for designs in which pressure is applied, and the VICON correction on the moment resulting from the applied pressure has little effect on the design trends, the VICON corrections to the PASCO analysis are not carried out for this loading condition.

The results of applying a combination of axial compression, shear, and out-of-plane pressure loads to the panel configurations using the smeared orthotropic stiffness solution in PASCO, are presented in the following sections. The data presented shows the effect of axial compression (N_x) and shear (N_{xy}/N_x) for pressure loads including 0, 15, 30, and 45 lb/in^2. Each figure has two parts, a) and b). Part a) is the structural efficiency diagram which presents the effect of axial compression and shear on the structural efficiency of the optimized panel for a specific pressure level. Part b) presents the geometric changes in the repeating element of the cross section resulting from the applied loading conditions.

3.4.1 Tailored Corrugated Panel

The results for the combined loading of axial compression, shear, and lateral pressure for the tailored corrugated panel are shown in Figure 44 through Figure 47 for four levels of pressure, P = 0, 15, 30, and 45 lb/in^2, respectively, and for increasing levels of shear (N_{xy}/N_x).

Some of the data presented are repeated for completeness. The trends for the structural weight for various levels of N_x, N_{xy}/N_x, and P behave similarly to those mentioned earlier. In essence, the behavior of the applied pressure in the presence of axial compression and shear is similar, at all levels of applied shear, to the trends that were discussed for the effect of pressure on the panel loaded in axial compression alone. Likewise, the effect of shear in the presence of axial compression and pressure, is similar at all pressure levels to the trends discussed for the effect of shear on the panel loaded in axial compression without pressure. For each level of pressure, however, the stiffeners did become deeper and more closely spaced.

3.4.2 Other Configurations

The trends for the other configurations considered in the present study (the corrugated panel with a continuous laminate, the hat stiffened panel, and the blade stiffened panel) are also presented. The discussion of the effect of the loading is the same as that for the tailored corrugated panel in that similar trends hold for each panel configuration. The data for the corrugated panel with a continuous laminate are presented in Figure 48 through Figure 51. The data for the hat stiffened panel are presented in Figure 52 through Figure 55, and the data for the blade stiffened panel are presented in Figure 56 through Figure 59. The sensitivity of the panel configurations studied to applied pressure at a loading level of N_x= 1000. lb/in is compared in Figure 60 by normalizing the panel weight of a configuration by its weight for no applied pressure. For axial compression load only, the sensitivity of the hat stiffened panel weight is much less for an applied pressure of 45 lb/in² (42% heavier compared to the design for P= 0 lb/in²) than the sensitivity of the other configurations considered in the present study (between 90% and 110% heavier compared to panels designed for P= 0 lb/in²). When shear is applied (N_{xy}/N_x = 1.0), all of the configurations show similar weight sensitivities compared to the panel designed for P= 0 lb/in² (40% to 60% weight increase). The corrugated panel

with a continuous laminate is the most sensitive configuration to applied pressure for all levels of applied shear considered in the present study.

The present study presents trends and design sensitivities of common configurations to loading conditions common for a wing rib application, including combinations of axial compression, shear, and out-of-plane pressure. Constraints such as minimum attachment widths, maximum stiffener depths, minimum laminate thicknesses, minimum corrugation web angles, maximum and minimum number of stiffeners, and many other detailed design parameters are not applied to the present designs in order to provide as much generality as possible to the study. The data presented so far can be used to provide information on a best choice for a preliminary design which can then be studied in detail to reach the final design.

a)

b)
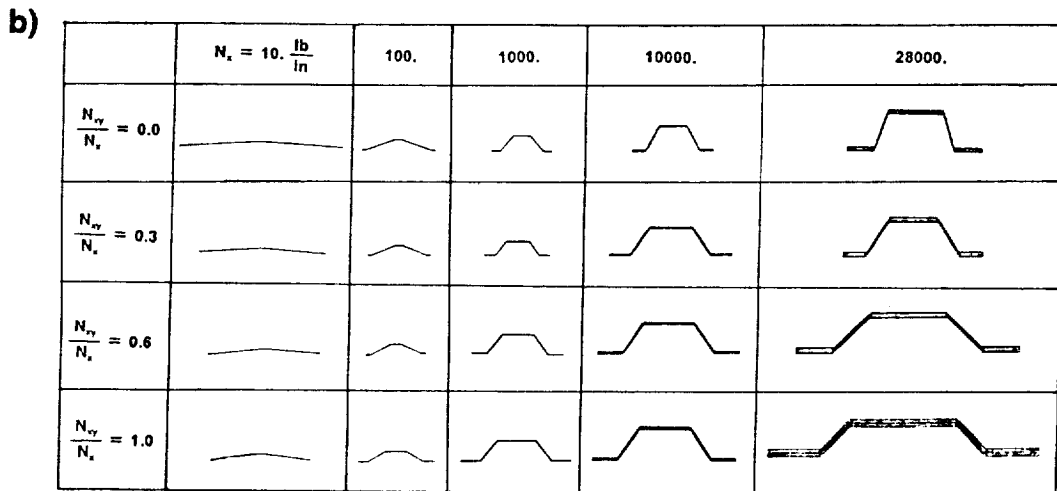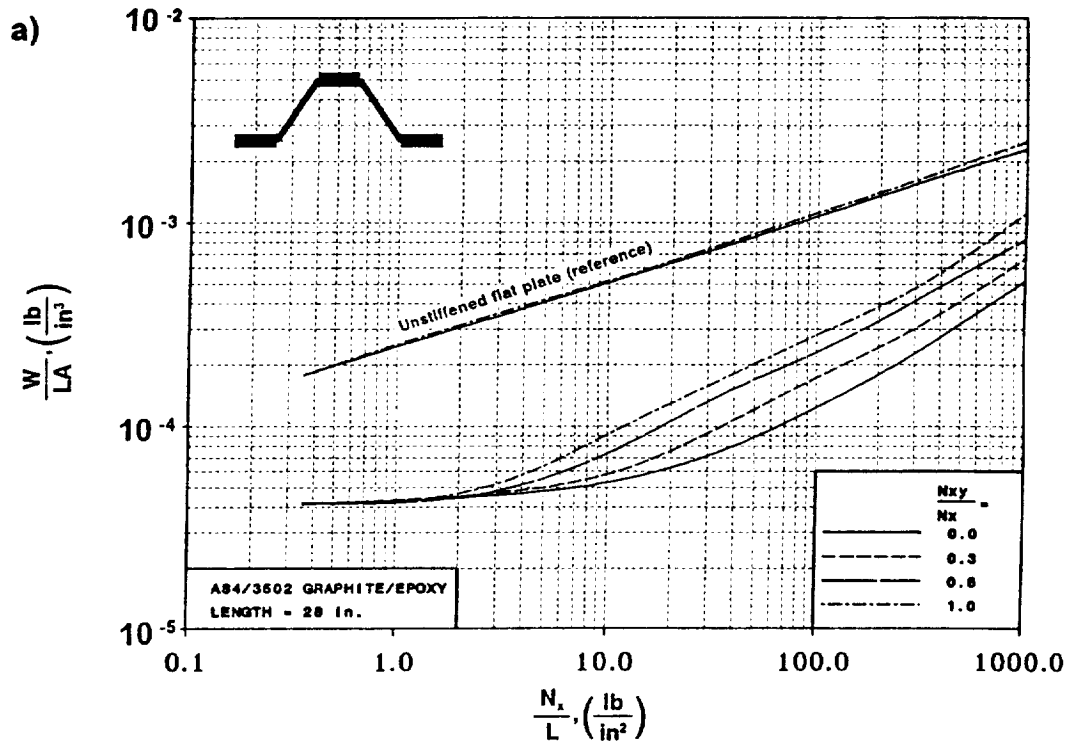
Refer to Table 3 in Appendix A for actual dimensions.

Figure 44.   Tailored Corrugated Panel Loaded in Shear (P=0 lb/in²):   a) Structural Efficiency and
b) Geometry.

a)

A84/3602 GRAPHITE/EPOXY
LENGTH = 28 In.

	Nxy/Nx
——	0.0
– – –	0.3
——	0.6
–·–·–	1.0

b)
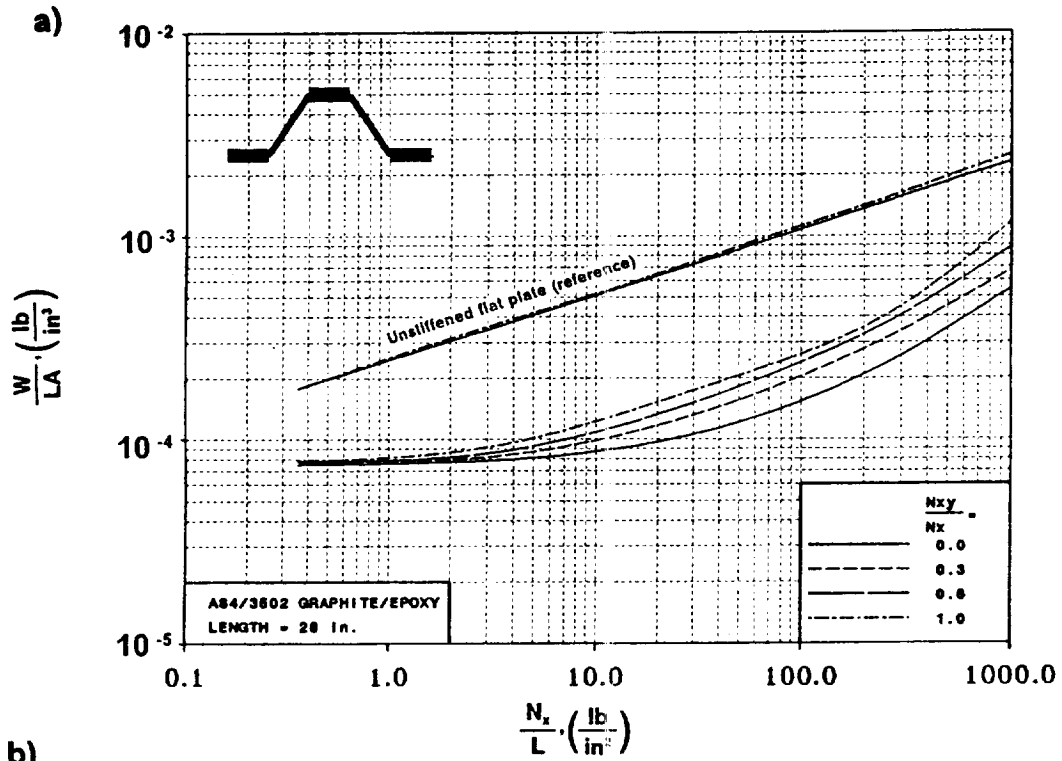
	$N_x = 10.$	100.	1000.	10000.	28000. $\frac{lb}{In}$
$\frac{N_{xy}}{N_x} = 0.0$					
$\frac{N_{xy}}{N_x} = 0.3$					
$\frac{N_{xy}}{N_x} = 0.6$					
$\frac{N_{xy}}{N_x} = 1.0$					

Refer to Table 7 in Appendix A for actual dimensions.

Figure 45. Tailored Corrugated Panel Loaded in Shear (P = 15 lb/In²):   a) Structural Efficiency and b) Geometry.

a)

b)
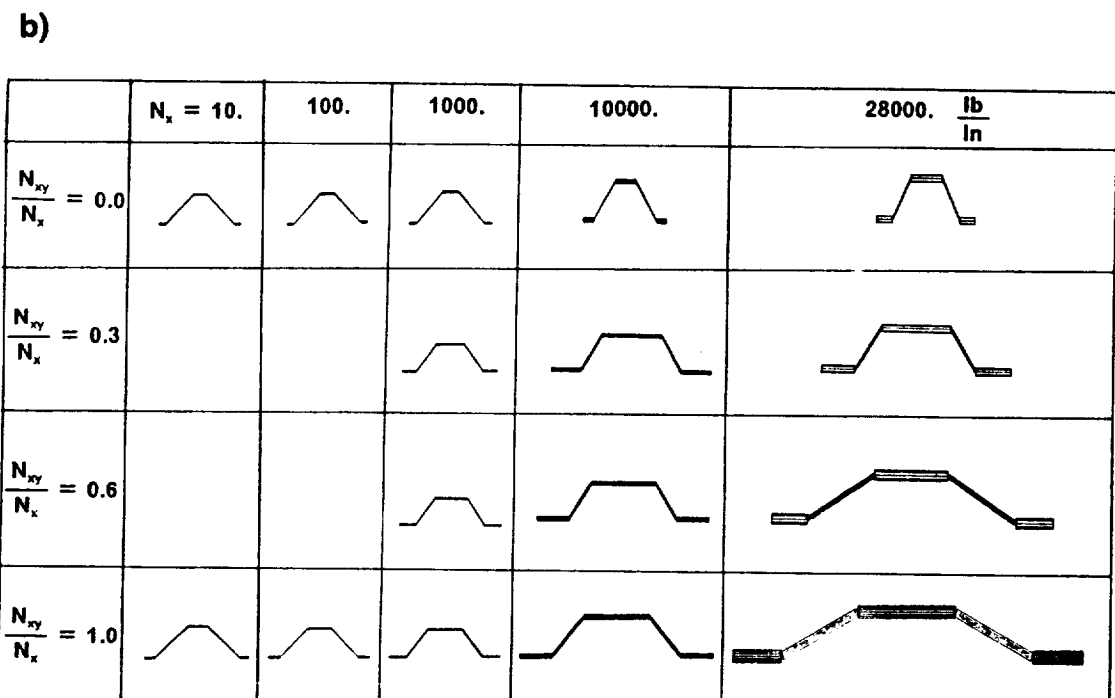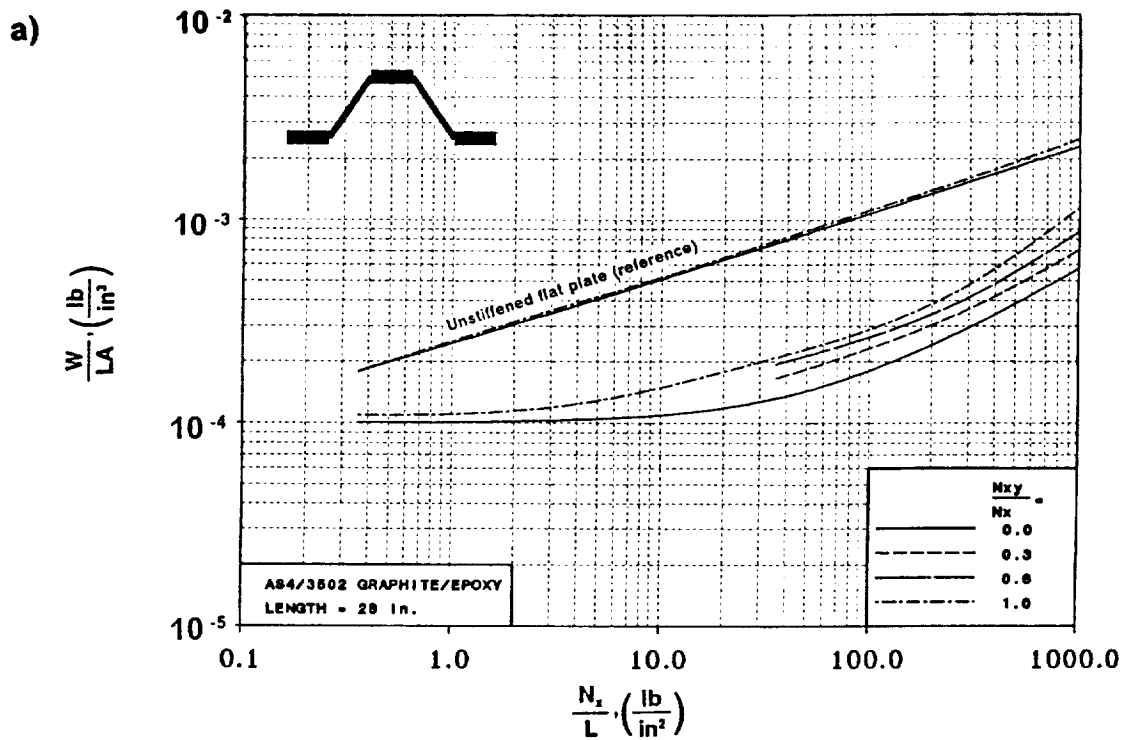
Refer to Table 8 In Appendix A for actual dimensions.

Figure 46. Tailored Corrugated Panel Loaded In Shear (P=30 lb/in²):   a) Structural Efficiency and b) Geometry.
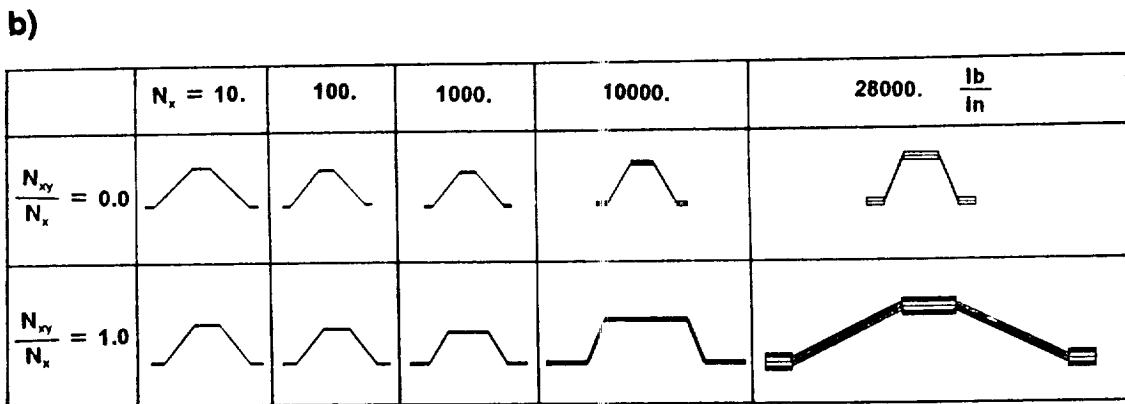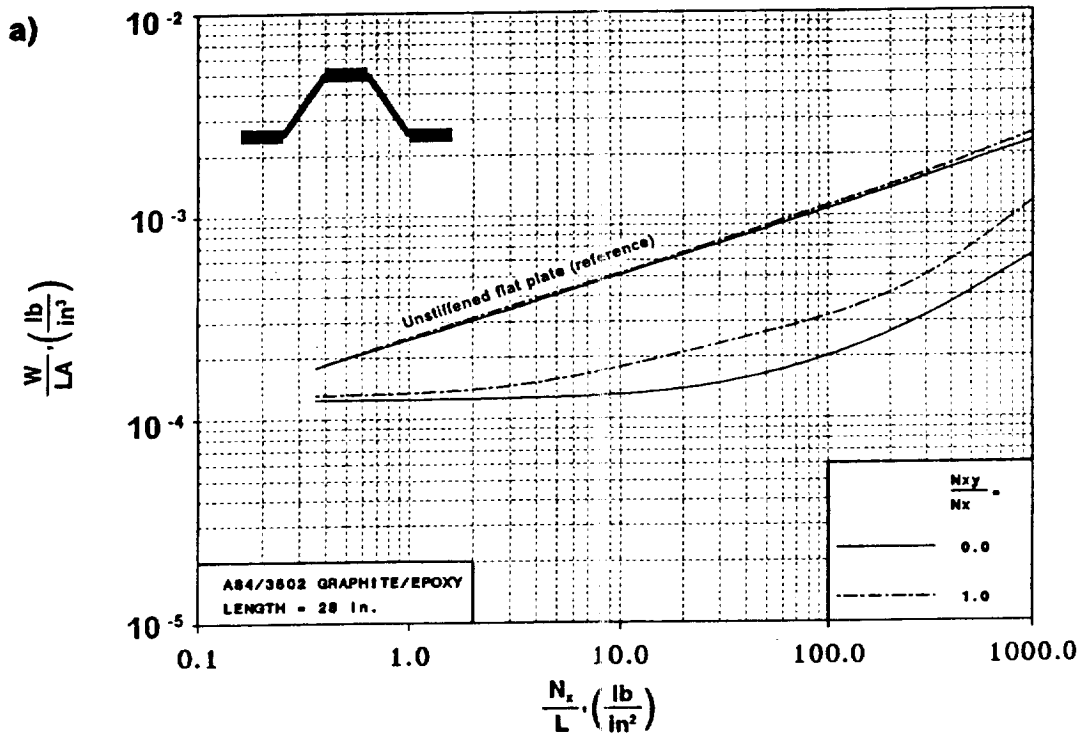
Design Study Results

Figure 47. Tailored Corrugated Panel Loaded In Shear (P=45 lb/in²): a) Structural Efficiency and b) Geometry.

a)

$\dfrac{W}{LA}\left(\dfrac{lb}{in^2}\right)$

10^{-2}

10^{-3}

Unstiffened flat plate (reference)

10^{-4}

A94/3602 GRAPHITE/EPOXY
LENGTH = 28 in.

$\dfrac{Nxy}{Nx}$	
———	0.0
– – – –	0.3
———	0.6
–·–·–·	1.0

10^{-5}

0.1   1.0   10.0   100.0   1000.0

$\dfrac{N_x}{L}\cdot\left(\dfrac{lb}{in^2}\right)$

b)

	$N_x = 10.\ \frac{lb}{in}$	100.	1000.	10000.	28000.
$\dfrac{N_{xy}}{N_x} = 0.0$					
$\dfrac{N_{xy}}{N_x} = 0.3$					
$\dfrac{N_{xy}}{N_x} = 0.6$					
$\dfrac{N_{xy}}{N_x} = 1.0$					

Refer to Table 36 in Appendix D for actual dimensions.

Figure 48.   Corrugated Panel with a Continuous Laminate Loaded in Shear (P=0 lb/in^2):   a) Structural Efficiency and b) Geometry.

a)

b)
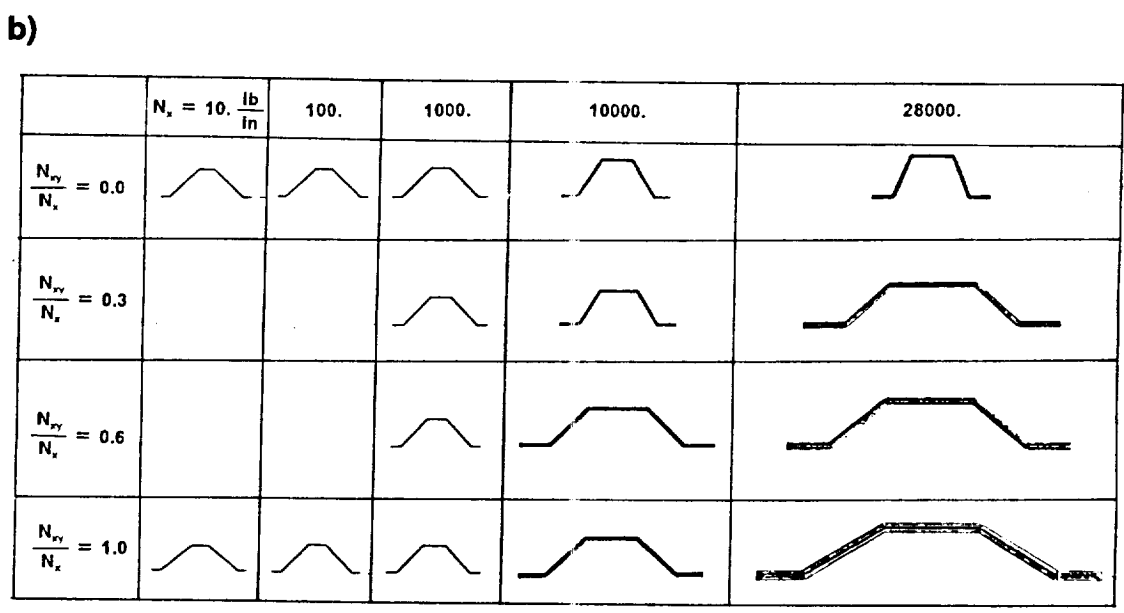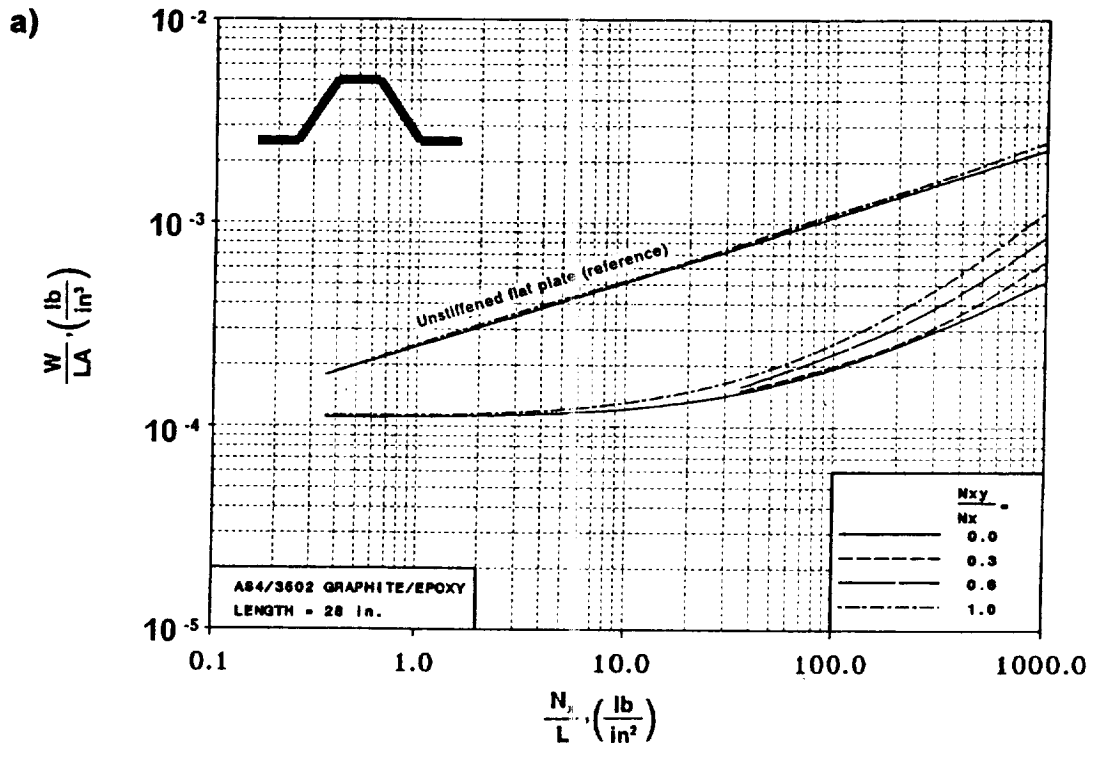
Refer to Table 37 in Appendix D for actual dimensions.

Figure 49. Corrugated Panel with a Continuous Laminate Loaded in Shear (P=15 lb/in²): a) Structural Efficiency and b) Geometry.

Design Study Results

10^{-2}

10^{-3}

$\dfrac{W}{LA}\cdot\left(\dfrac{lb}{in^3}\right)$

10^{-4}

Unstiffened flat plate (reference)

$\dfrac{Nxy}{Nx}$ =

_____ 0.0

—·—·— 1.0

A84/3502 GRAPHITE/EPOXY
LENGTH = 28 In.

10^{-5}

0.1   1.0   10.0   100.0   1000.0

$\dfrac{N_x}{L}\cdot\left(\dfrac{lb}{in^2}\right)$

b)

	N_x = 10.	100.	1000.	10000.	28000. $\dfrac{lb}{in}$
$\dfrac{N_{xy}}{N_x}$ = 0.0					
$\dfrac{N_{xy}}{N_x}$ = 1.0					
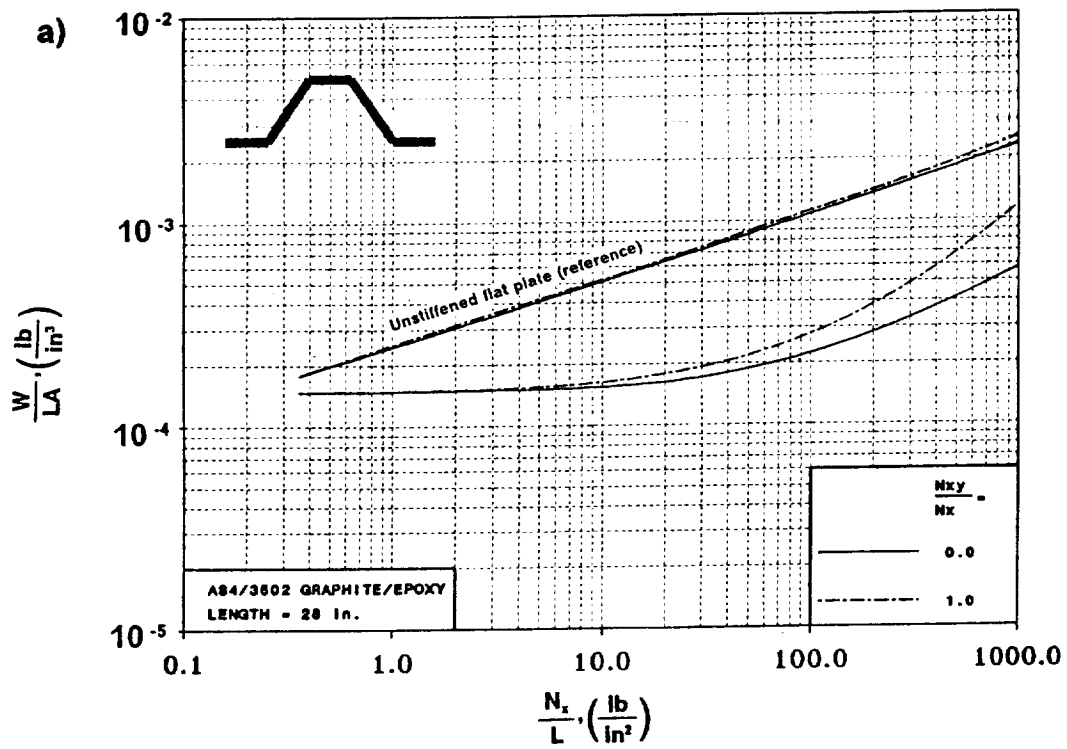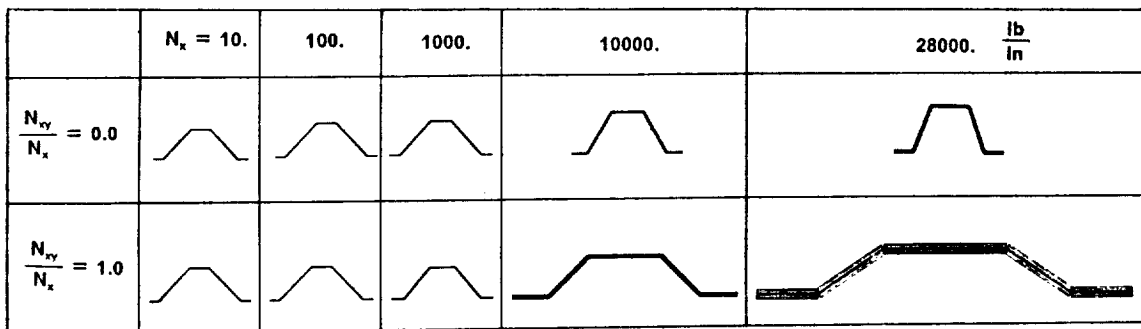
Refer to Table 38 in Appendix D for actual dimensions.

Figure 50.   Corrugated Panel with a Continuous Laminate Loaded in Shear ($P=30$ lb/in²):   a) Structural Efficiency and b) Geometry.

a)

$\dfrac{W}{LA} \cdot \left(\dfrac{lb}{in^3}\right)$

10^{-2}

10^{-3}

10^{-4}

10^{-5}

Unstiffened flat plate (reference)

AS4/3502 GRAPHITE/EPOXY
LENGTH = 28 in.

$\dfrac{Nxy}{Nx}$ =
0.0
1.0

$\dfrac{N_t}{L} \cdot \left(\dfrac{lb}{in^2}\right)$

0.1   1.0   10.0   100.0   1000.0

b)

	$N_x = 10. \dfrac{lb}{in}$	100.	1000.	10000.	28000.
$\dfrac{N_{xy}}{N_x} = 0.0$					
$\dfrac{N_{xy}}{N_x} = 1.0$					
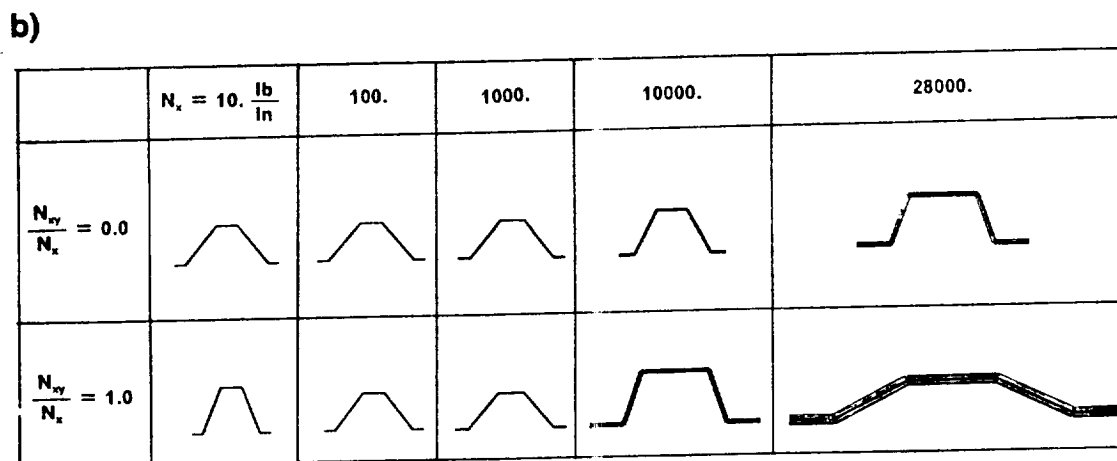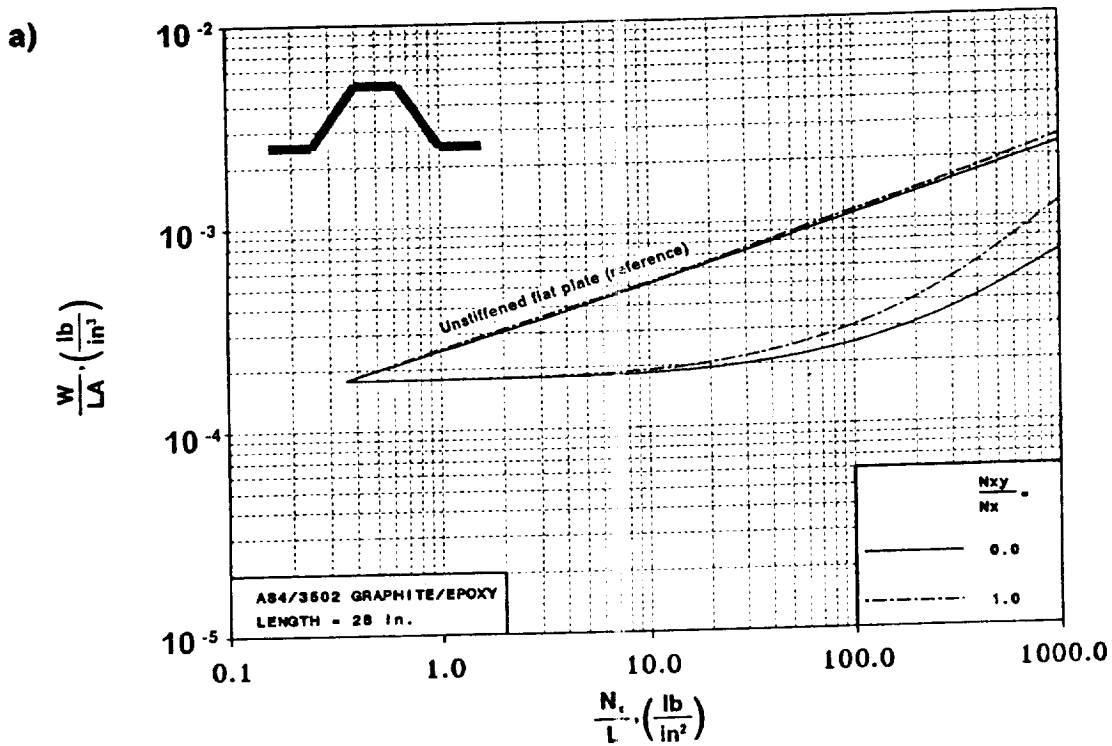
Refer to Table 39 in Appendix D for actual dimensions.

Figure 51. Corrugated Panel with a Continuous Laminate Loaded in Shear (P=45 lb/in²): a) Structural Efficiency and b) Geometry.

a)

10^{-2}

10^{-3}

$\frac{W}{LA} \cdot \left(\frac{lb}{in^3}\right)$

Unstiffened flat plate (reference)

10^{-4}

	$\frac{Nxy}{Nx}$ =
	0.0
	0.3
	0.6
	1.0

A84/3602 GRAPHITE/EPOXY
LENGTH = 28 in.

10^{-5}

0.1   1.0   10.0   100.0   1000.0

$\frac{N_z}{L} \cdot \left(\frac{lb}{in^2}\right)$

b)

	$N_x = 10. \frac{lb}{in}$	100.	350.	1000.	2800.	10000.	28000.
$\frac{N_{ry}}{N_z}$ = 0.0							
$\frac{N_{ry}}{N_z}$ = 0.3							
$\frac{N_{ry}}{N_z}$ = 0.6							
$\frac{N_{ry}}{N_z}$ = 1.0							
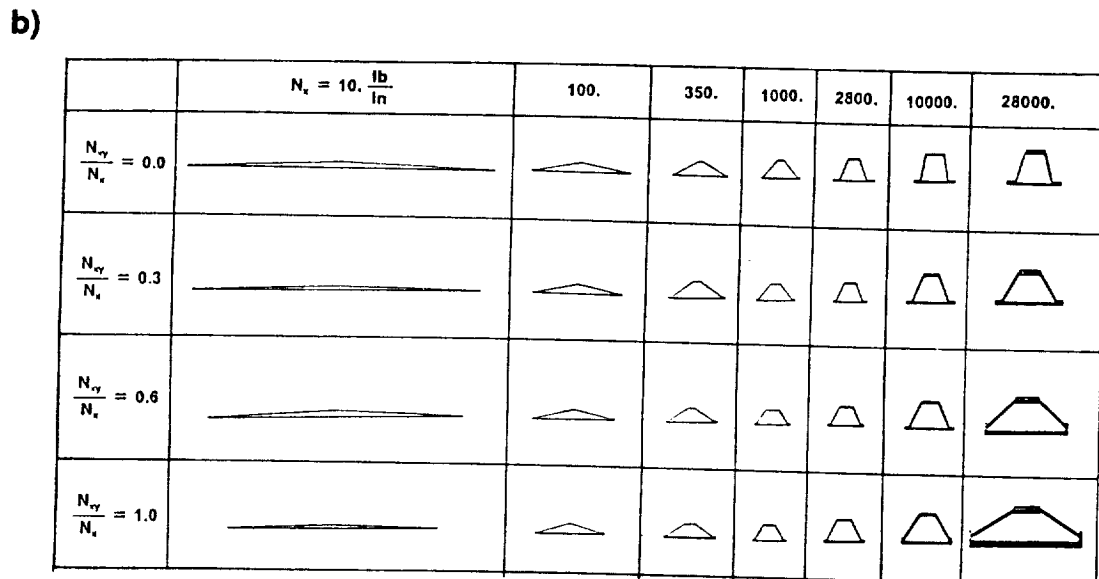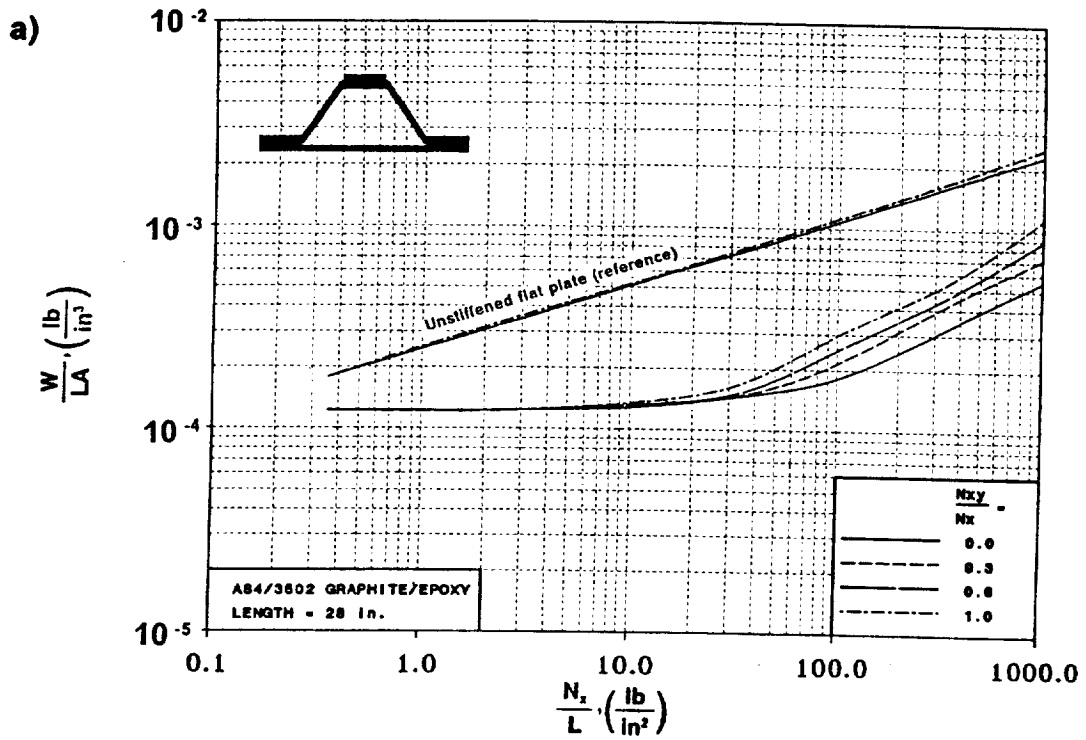
Refer to Table 15 in Appendix B for actual dimensions.

Figure 52. Hat Stiffened Panel Loaded in Shear ($P=0$ lb/in²):   a) Structural Efficiency and b) Geometry.

a)

A84/3602 GRAPHITE/EPOXY
LENGTH = 28 In.

b)

	$N_x = 10.$	100	1000.	10000.	28000. $\frac{lb}{in}$
$\frac{N_{xy}}{N_x} = 0.0$					
$\frac{N_{xy}}{N_x} = 0.3$					
$\frac{N_{xy}}{N_x} = 0.6$					
$\frac{N_{xy}}{N_x} = 1.0$					
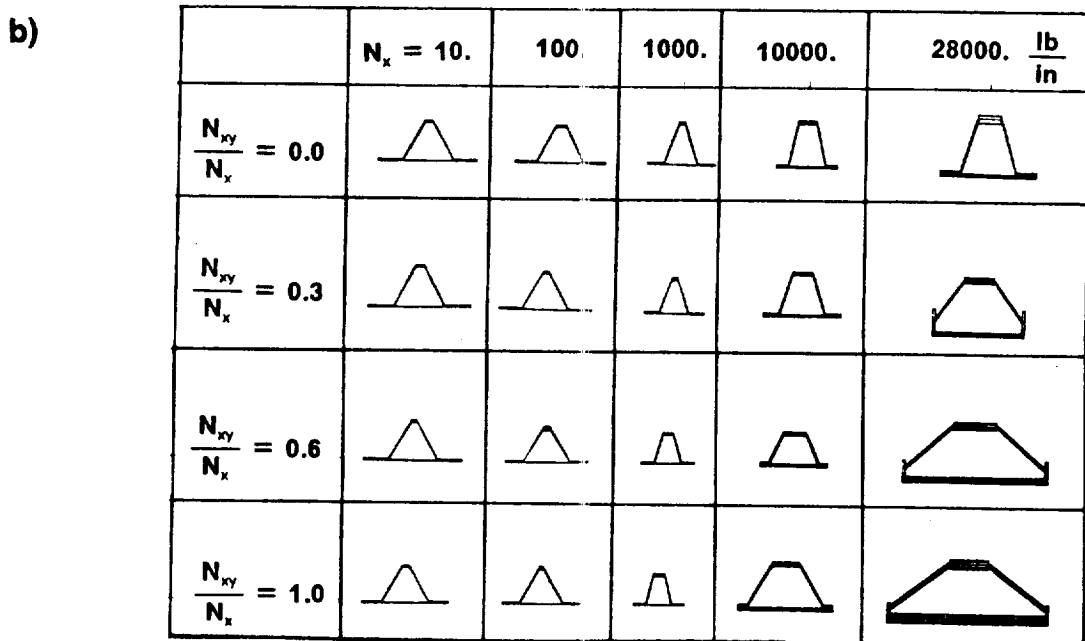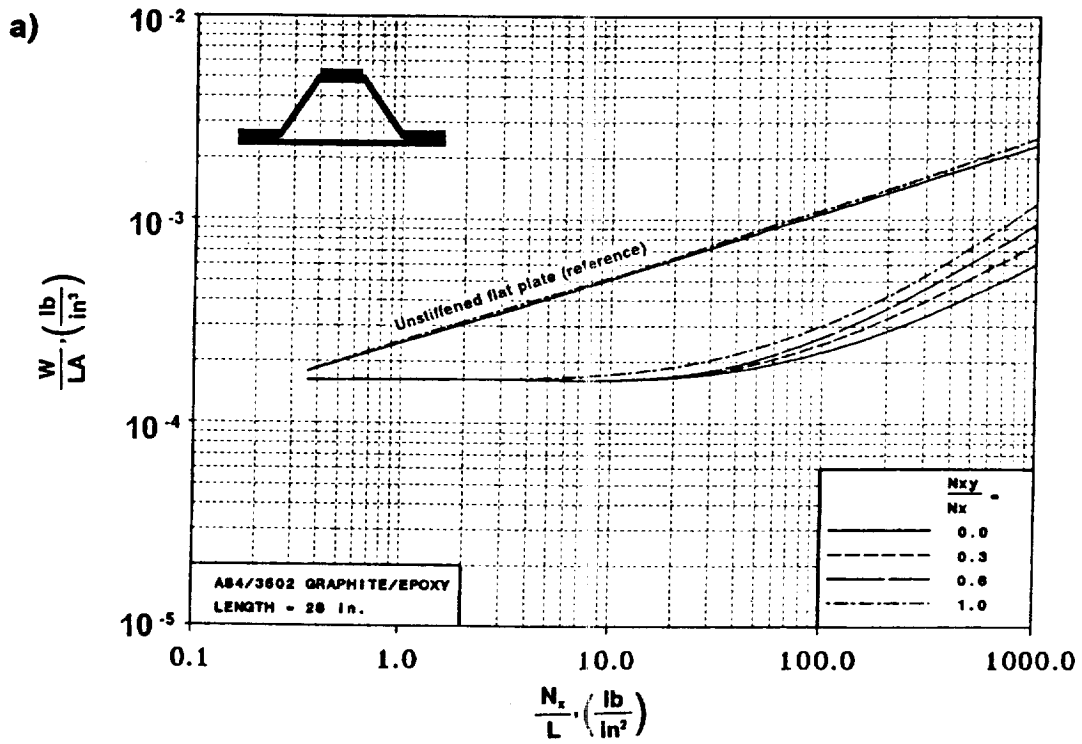
Refer to Table 19 In Appendix B for actual dimensions.

Figure 53. Hat Stiffened Panel Loaded in Shear ($P = 15$ lb/in²): a) Structural Efficiency and b) Geometry.

a)

Chart axes:
- Y-axis: $\frac{W}{LA} \cdot \left(\frac{lb}{in^3}\right)$, ranging from 10^{-5} to 10^{-2}
- X-axis: $\frac{N_x}{L} \cdot \left(\frac{lb}{in^2}\right)$, ranging from 0.1 to 1000.0

Labels on chart:
- Unstiffened flat plate (reference)
- A84/3602 GRAPHITE/EPOXY LENGTH = 28 in.

Legend:
$\frac{Nxy}{Nx}$ =
0.0
0.3
0.6
1.0

b)

	$N_x = 10.$	100.	1000.	10000.	28000. $\frac{lb}{in}$
$\frac{N_{xy}}{N_x} = 0.0$	△	△	△	△	△
$\frac{N_{xy}}{N_x} = 0.3$			△	△	△
$\frac{N_{xy}}{N_x} = 0.6$			△	△	△
$\frac{N_{xy}}{N_x} = 1.0$	△	△	△	△	△
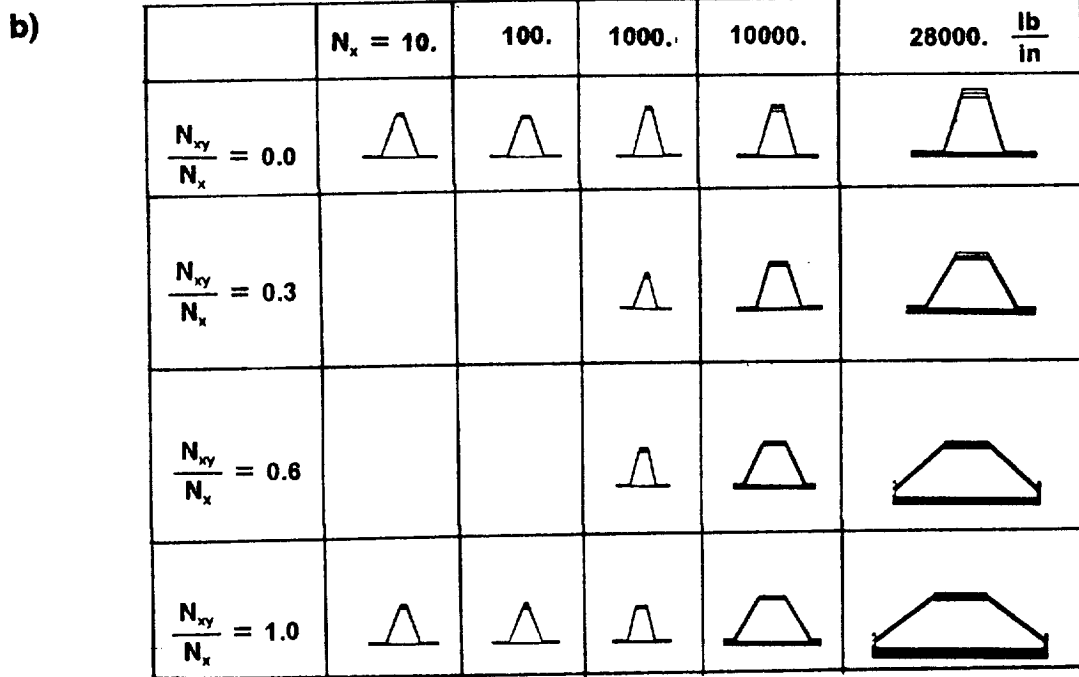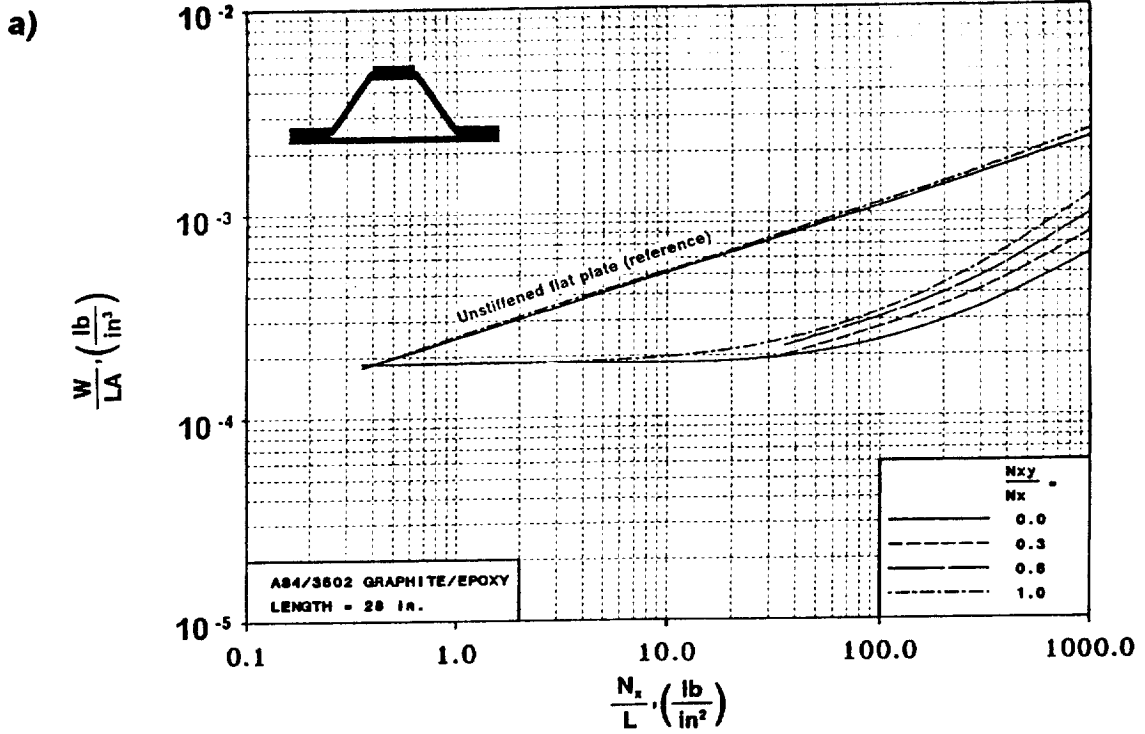
Refer to Table 20 in Appendix B for actual dimensions.

Figure 54. Hat Stiffened Panel Loaded in Shear (P=30 lb/in²): a) Structural Efficiency and b) Geometry.

a)

b)

	$N_x = 10.$	100.	1000.	10000.	28000. $\frac{lb}{in}$
$\frac{N_{xy}}{N_x} = 0.0$					
$\frac{N_{xy}}{N_x} = 1.0$					
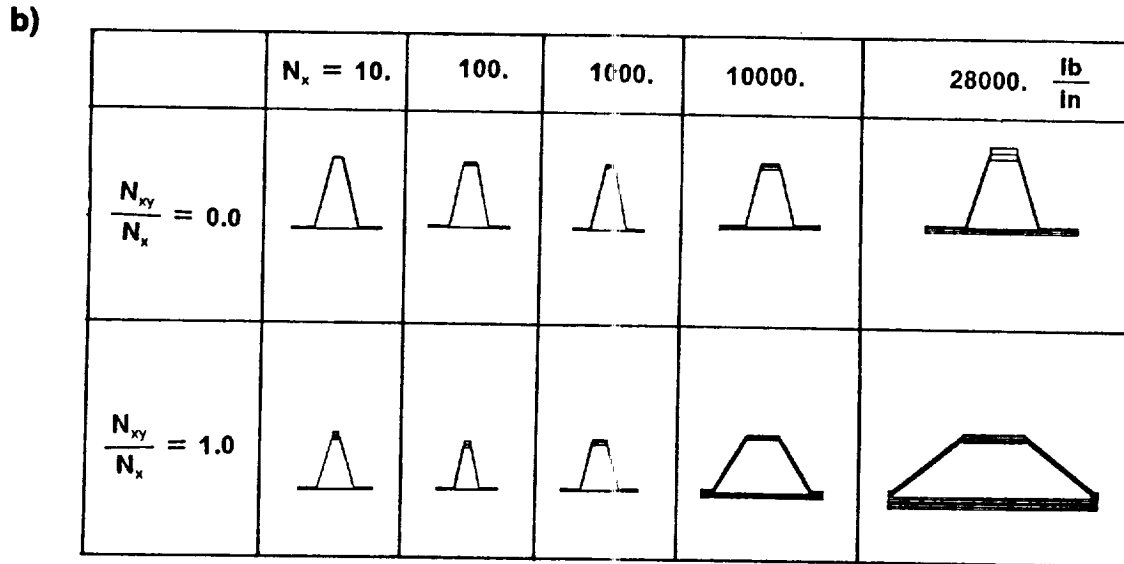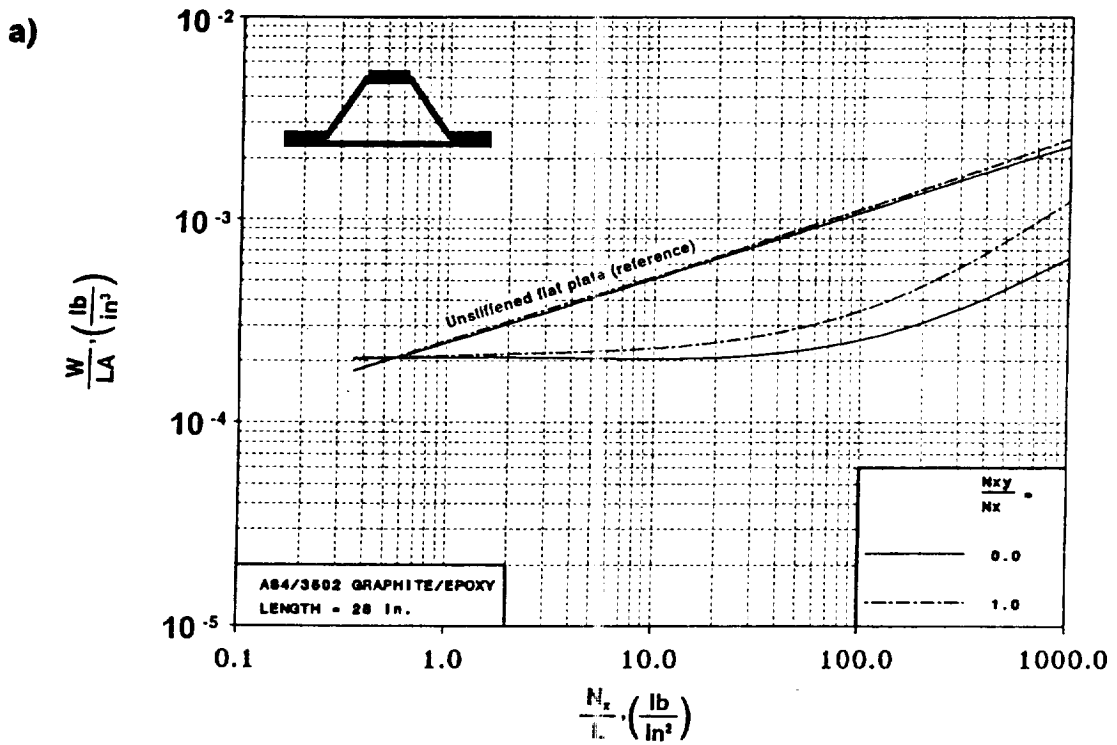
Refer to Table 21 in Appendix B for actual dimensions.

Figure 55. Hat Stiffened Panel Loaded in Shear ($P = 45$ lb/in²): a) Structural Efficiency and b) Geometry.

Figure 56. Blade Stiffened Panel Loaded in Shear (P=0 lb/in²): a) Structural Efficiency and b) Geometry.
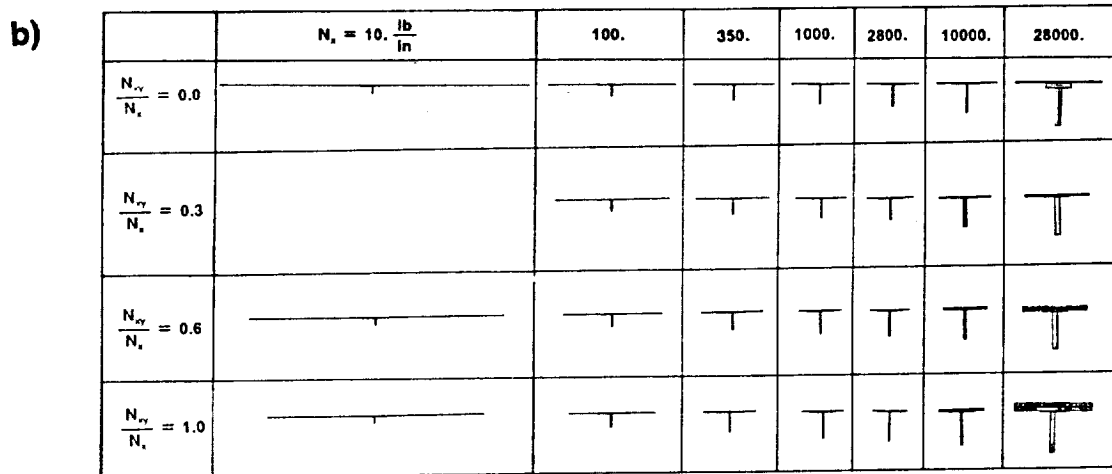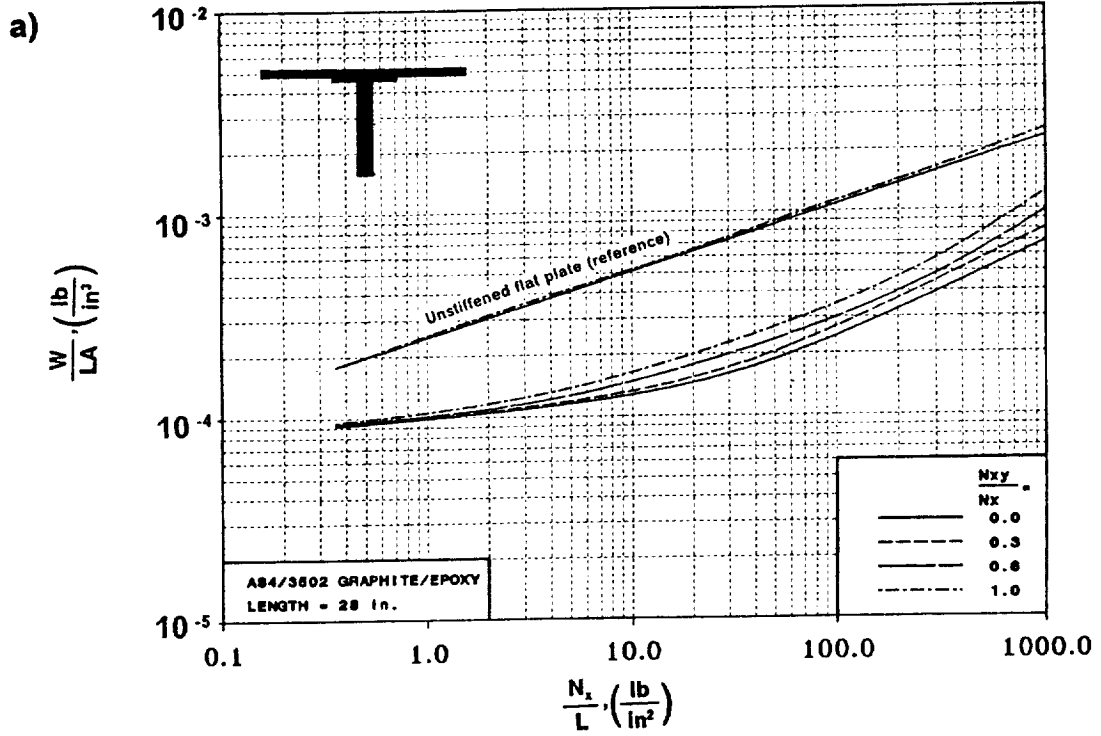
Refer to Table 26 in Appendix C for actual dimensions.

a)

b)
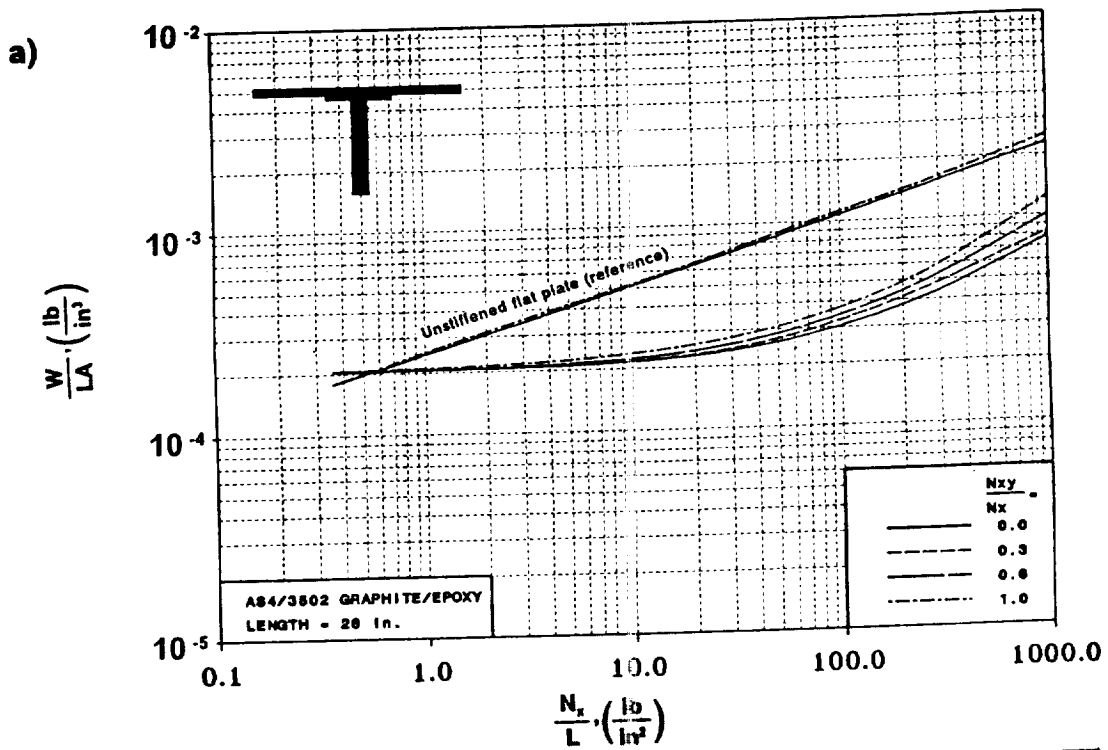
Refer to Table 30 in Appendix C for actual dimensions.

Figure 57. Blade Stiffened Panel Loaded in Shear ($P = 15$ lb/in^2): a) Structural Efficiency and b) Geometry.

Figure 58. Blade Stiffened Panel Loaded in Shear (P=30 lb/in²): a) Structural Efficiency and b) Geometry.

a)

A84/3602 GRAPHITE/EPOXY
LENGTH = 28 in.

$\frac{W}{LA}\left(\frac{lb}{in^3}\right)$

Unstiffened flat plate (reference)

$\frac{N_x}{L}\left(\frac{lb}{in^2}\right)$

$\frac{Nxy}{Nx}$ =

———— 0.0

—·—·— 1.0

b)
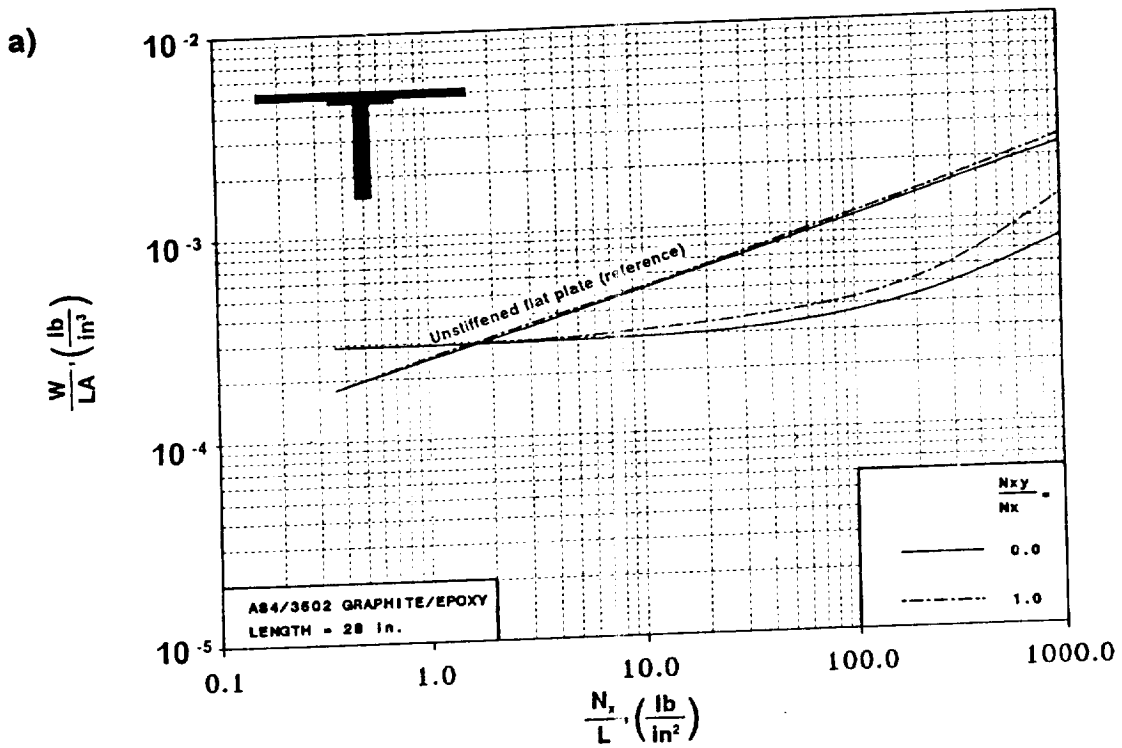
	$N_x = 10.$	100.	1000.	10000.	28000. $\frac{lb}{in}$
$\frac{N_{xy}}{N_x} = 0.0$					
$\frac{N_{xy}}{N_x} = 1.0$					

Refer to Table 32 in Appendix C for actual dimensions.

Figure 59. Blade Stiffened Panel Loaded in Shear (P=45 lb/in²): a) Structural Efficiency and b) Geometry.
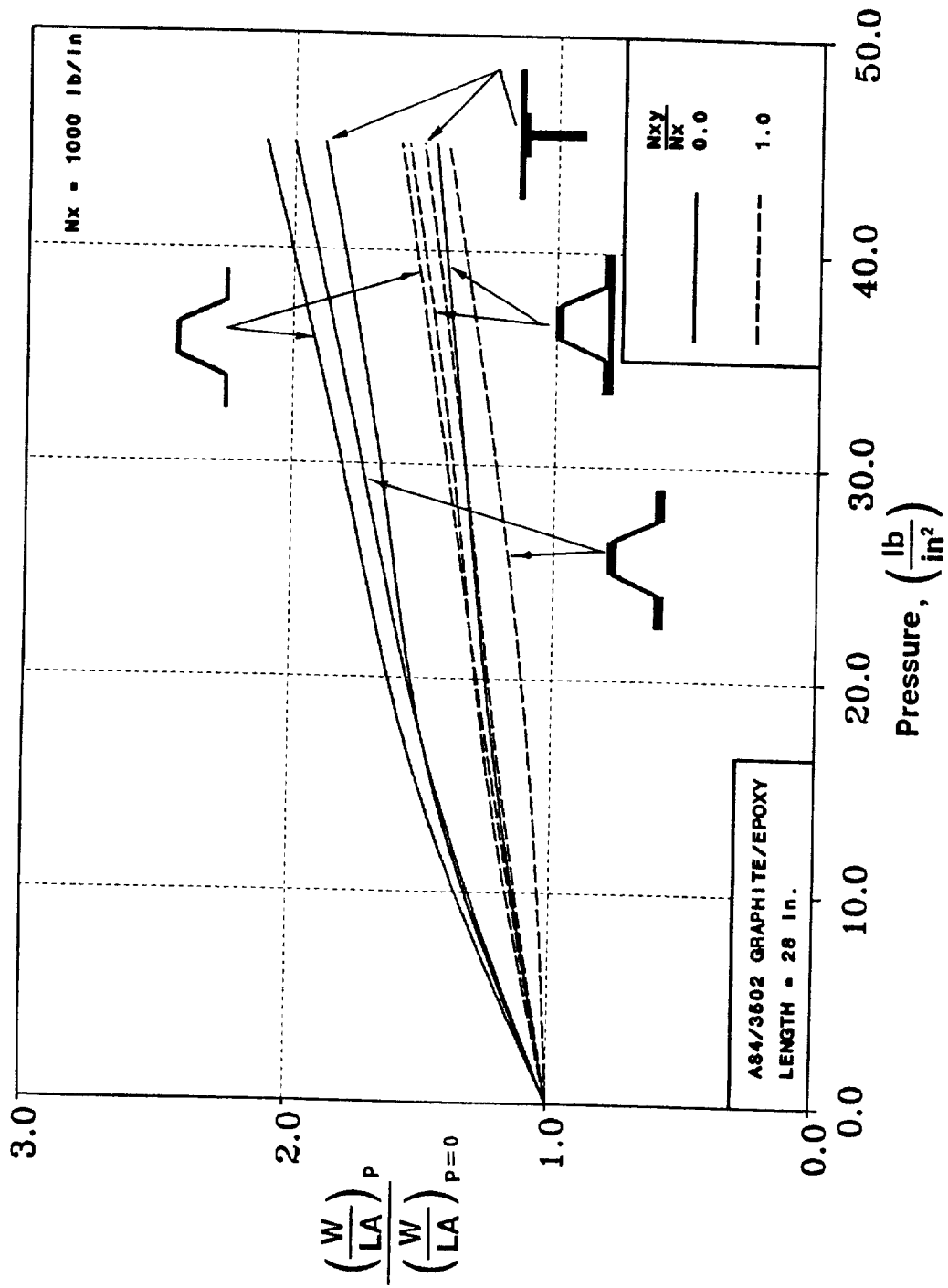
Figure 60. Sensitivity of Panel Weights for all Configurations to Pressure (Nx=1000 lb/in).

4.0 Design Sensitivities and Comments

Many factors present in the design and manufacturing of a stiffened panel can affect the expected performance level. To better understand what factors are most critical, the sensitivity of the structural efficiency to changes in optimum geometric design parameters is considered. Stiffened panel weight and cross sectional geometry trends are discussed in Chapter 3 for optimum panels designed for various in-plane loading combinations of axial compression (N_x) and shear (N_{xy}). Many of the panel configurations studied earlier in Reference 22 by using a simplified analysis are similar in many ways to those discussed in the current design study. Since these similar panels were shown in Reference 22 to be insensitive to small changes in geometry, the effect on the optimum panel weight of a small variation in any individual dimension in the current study is assumed to be small. However, practical limitations in the manufacturing and design process may cause panel dimensions to be significantly different from the optimum dimensions, making the effect of large, non-optimum dimensional changes on structural efficiency trends of interest. Thus, the effect of increasing the blade stiffener spacing and of forming a beaded corrugated panel on both the panel geometry and the structural efficiency is discussed in the following sections.

4.1 Blade Stiffener Spacing

The blade stiffened panel (the most common configuration currently being used) is studied for stiffener spacing larger than the optimum spacing. To understand better the effects of large spacing on the design, the optimum spacing trends are first considered.

4.1.1 Optimum Stiffener Spacing Trends

The trends of the optimum stiffener spacing of blade stiffened panels under combined axial compression (N_x) and shear (N_{xy}/N_x) are shown in Figure 61. The optimum blade spacing for very light axial compression loads in the range near $N_x/L = 1.0$ lb/in^2 is about 18 inches, a relatively large value compared to the panel width of 80 inches. The minimum gage laminate which makes up the skin portion of the panel configuration can carry the light load without the need for closely spaced stiffeners. As the ratio of the shear load to axial compression load, for constant axial compression loading, is increased, the spacing reduces slightly to account for the extra load. For example, for a ratio of $N_{xy}/N_x = 1.0$, with N_x/L near 1.0 lb/in^2, the stiffener spacing is reduced to 13 inches. As the axial compression loads increase to a moderate value (near 100 lb/in^2), the blade spacing decreases to a minimum value near 3 inches. For increasing shear loads of up to $N_{xy}/N_x = 1.0$, the stiffener spacing reduces further to about 2 inches. The cross section is defined by the minimum gage constraint with relatively small, closely spaced, stiffeners to provide the necessary panel bending stiffness. For large values of axial compression, greater than $N_x/L = 200$ lb/in^2, the minimum gage constraint becomes inactive and both the spacing and stiffener size increase steadily with the axial loading, reaching a spacing of about 5 inches for $N_x/L = 1000$ lb/in^2. The response of the optimum blade stiffener spacing to the added shearing load is again relatively small at $N_x/L = 1000$ lb/in^2. The spacing first reduces for increasing values of N_{xy}/N_x and approaches 4 inches for $N_{xy}/N_x = 0.6$.
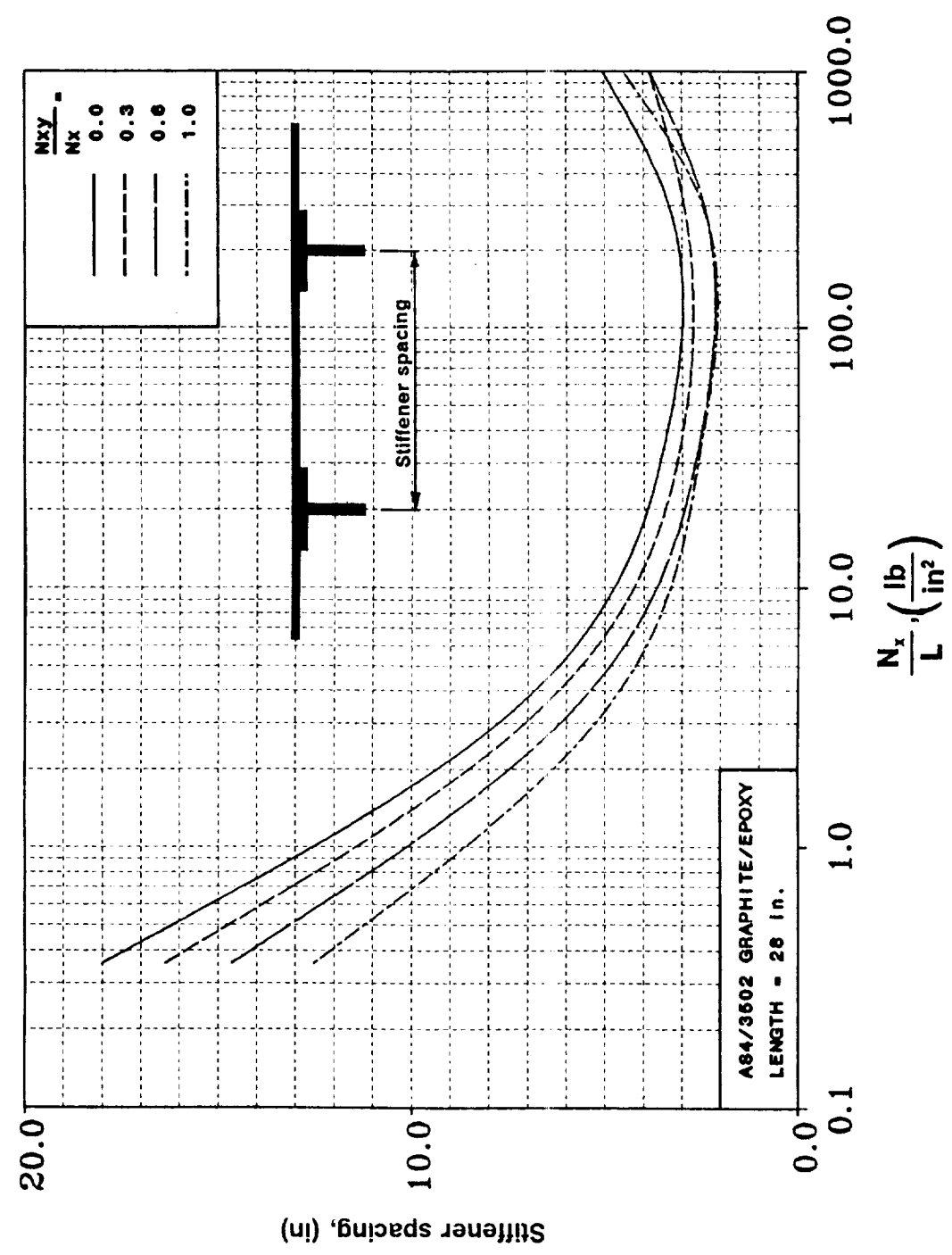
Figure 61. Effect of Axial Compression and Shear Loadings on Optimum Stiffener Spacing (Blade Stiffened Panel).

Further increases in N_{xy}/N_x greater than 0.6 result in a slightly increased spacing. In general, the optimum blade spacing is a function of both load level and minimum ply thickness constraints on the panel section. As long as the minimum gage constraint is active, the blade stiffeners remain small and decrease in spacing to resist increased axial load. Once the minimum gage constraint becomes inactive, near N_x /L = 200 lb/in^2, larger stiffeners are needed to carry the load, and they are spaced farther apart.

4.1.2 Non-optimum Stiffener Spacing

To assess the effect of increasing the stiffener spacing to a value much larger than the optimum spacing determined by PASCO, the dimension for the stiffener spacing is increased in multiples of the optimum spacing until the spacing between two adjacent blades approaches the panel width of 80 inches, essentially emulating an unstiffened flat plate. Loading cases of axial compression (N_x = 100, 1000, 10000, and 28000 lb/in) and shear (N_{xy}/N_x = 0.0, 0.3, 0.6, and 1.0) are investigated. Stiffener spacings considered are 2.0, 4.0, and 8.0 times the optimum spacing for all load cases, with other stiffener spacings considered as needed to define the trends, shown in Figure 62. The structural efficiency curves tend to flatten out near the optimum spacing suggesting that the optimum spacing is a minimum. That is, a small change in the stiffener spacing, either a smaller or a larger spacing, increases the structural weight only slightly. Large changes in the stiffener spacing (less than the panel width) cause a significant increase in the structural weight. When the stiffener spacing approaches the panel width (80 inches), the efficiency of the panels approaches the efficiency of an unstiffened flat plate indicated by symbols in Figure 62. The blade stiffener geometry changes significantly for the non-optimum spacing and is shown in Figure 63 for various loading levels. The stiffener appears to approach a Tee-stiffener configuration for spacings on the order of 8 times the optimum spacing, implying that the Tee-stiffener is providing the configuration with a more efficient cross section. Since the initial PASCO model is intended to be used for blade stiff-
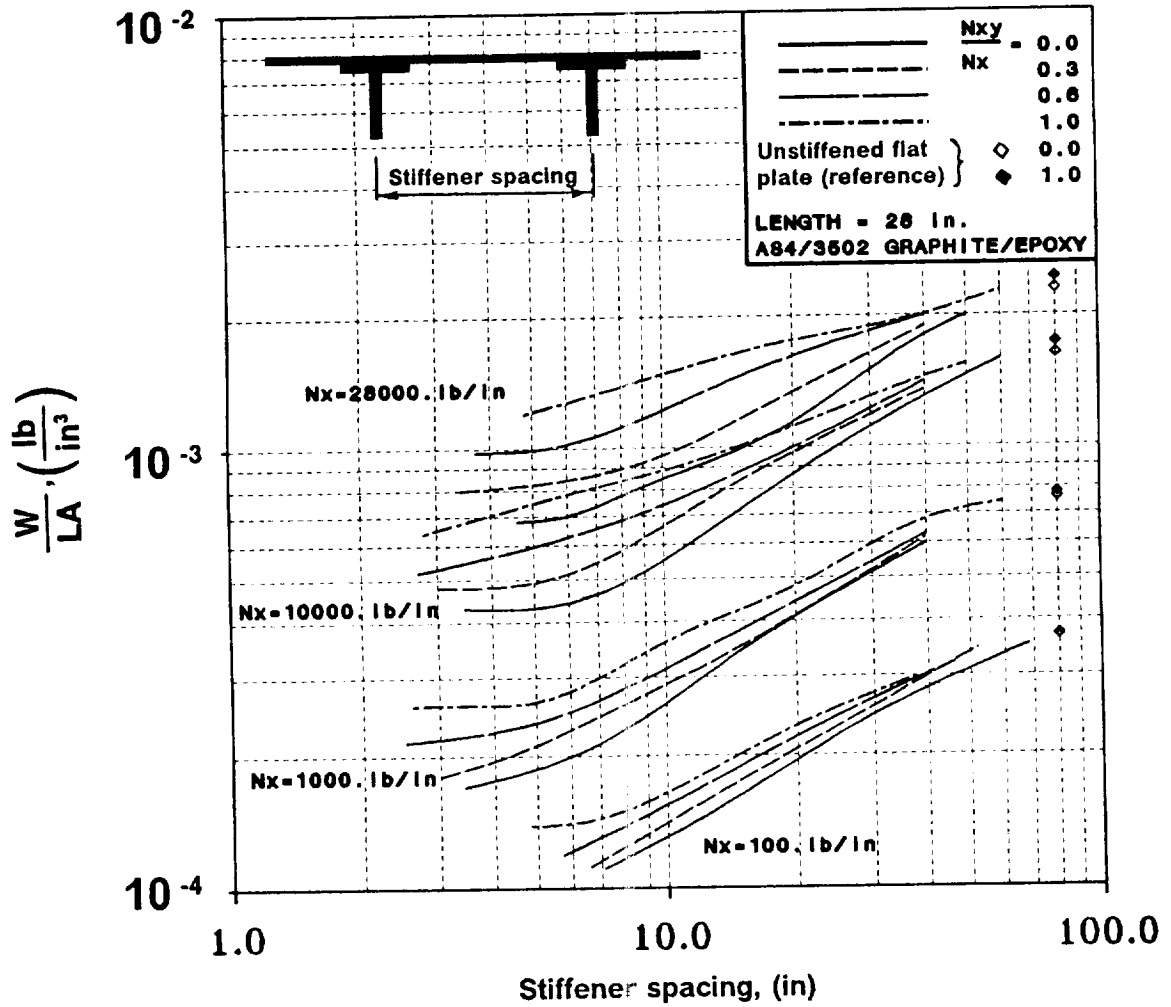
Figure 62. Effect of Stiffener Spacing on Blade Stiffened Panel Weight For Axial Compression (N_x) and Shear (N_{xy}) Loadings.

	$N_x = 10. \frac{lb}{in}$	100.	1000.	10000.	28000.
Optimum Spacing					
2x					
4x					
8x					

Refer to Tables 32 through 35 in Appendix C for actual dimensions.

For each entry: Upper figure denotes the repeating element geometry
Lower figure denoted the stiffener detail

Figure 63. Effect of Non-Optimum Stiffener Spacing on Blade Stiffened Panel Geometry: For Axial Compression Loadings (N_x).

ened panels (the flange width of the blade stiffener is constrained to be 1.5 inches wide, and the laminate in the blade itself is oriented perpendicular to the skin), the use of the same model for Tee-stiffened panels may be inappropriate. As modeled, the Tee-stiffener web is constrained to be 1.5 inches in thickness. The high load level and large spacing which cause this drastic configuration change, even with these unrealistic constraints, suggest that a stiffener configuration other than the blade may be more suited for these extreme cases.

4.1.3 Anisotropic Effects

For the case of axial compression load only, PASCO ignores, by default, the anisotropic terms which may be present in the analysis. The anisotropic terms include terms from the [A] and [D] matrices that couple normal forces and shearing strains and normal moments and twisting. These terms are often referred to in the literature as A_{16}, A_{26}, D_{16}, and D_{26}. By ignoring these terms, the buckling load which is used to size the panel may have been calculated unconservatively. The effect of the anisotropic terms on the buckling load is investigated by taking the optimum blade stiffened panel configuration, designed by PASCO without the anisotropic terms, and analyzing it with the anisotropic terms included. This analysis, an option within PASCO, is repeated for blade stiffener spacings greater than the optimum. The loading cases considered are limited to only an axial compression load level of $N_x = 1000$ lb/in, and a longitudinal panel length of 28 inches. The results shown in Table 2 indicate that for the optimum design, the anisotropic terms have little if any effect on the buckling analysis. However, for stiffener spacings greater than optimum, the anisotropic terms have a larger effect on the local buckling loads, while the effect on the overall buckling load remains small. The optimum design has many closely spaced stiffeners, which dominate the response. As the spacing increases to 2, 4, and 8 times the optimum spacing, a larger unstiffened flat plate area is exposed between the stiffeners, making the stiffener less effective in the local buckling of the skin between the stiffeners, and thus results in the increased effect of the anisotropic

Table 2. Anisotropic Effects on Blade Stiffened Panel.

	Global Buckling Load		Local Buckling Load	
N_x = 1000. lb/in N_{xy} = 0.0 lb/in P = 0. lb/in^2 L = 28 in				
Spacing	**Global Buckling Load**		**Local Buckling Load**	
Factor times optimum (actual dimension in inches)	without anisotropy (design)	with anisotropy (analysis)	without anisotropy (design)	with anisotropy (analysis)
opt. (3.5)	1.00	1.04	1.00	1.00
2x (7.0)	1.00	1.00	1.00	0.93
4x (14.0)	1.00	1.00	1.00	0.89
8x (28.0)	1.00	0.95	1.00	0.85

terms on the buckling response. When the anisotropic terms are included in the analysis of panels designed without the anisotropic terms, a reduction in the local buckling load of about 15% is obtained for a stiffener spacing of 8 times the optimum spacing. It is known that the effect of anisotropy on the buckling response of laminates can be minimized by increasing the number of thin ply groups rather than having them in thick ply groups. However, lumping the plies with the same orientation increases the efficiency of the PASCO optimization by reducing the number of design variables. Thicker sections of the actual panel will likely contain repeating sub-laminates [56], effectively making the anisotropic terms negligible. The reordering of the laminate does not have any effect on the rest of the extensional stiffness matrix, [A], other than reducing the values of A_{16} and A_{26}. The bending stiffness matrix, [D], will also have reduced anisotropic bending terms, D_{16} and D_{26}.

4.2 Length Effects in PASCO

PASCO treats the panel length, L, as a finite segment of an infinitely long panel. The buckling load for the global mode is essentially the load at which the buckling half wavelength, λ, equals the panel length, L. Local buckling loads are determined by loads corresponding to λ less than L. Optimum PASCO designs are obtained for loading conditions of axial compression (N_x/L between 0.3 and 1000 lb/in²) and shear ($N_{xy}/N_x = 0.0$ and 1.0). The effect on the panel weight of shorter panel lengths is shown in Figure 64, Figure 65, and Figure 66 for the tailored corrugated panel, the hat stiffened pane , and the blade stiffened panel, respectively. Panel lengths of 5, 15, and 28 inches are considered. For load levels below $N_x/L = 100$ lb/in², the structural efficiency of the panels with decreased length appears to degrade as the length is shortened. However, the minimum gage ply thickness constraint is active at this loading level for the configurations presented in Figure 64 through Figure 66. Thus, at this low loading level (N_x/L below 100 lb/in²), the tailored corrugated panel, for all three lengths considered,
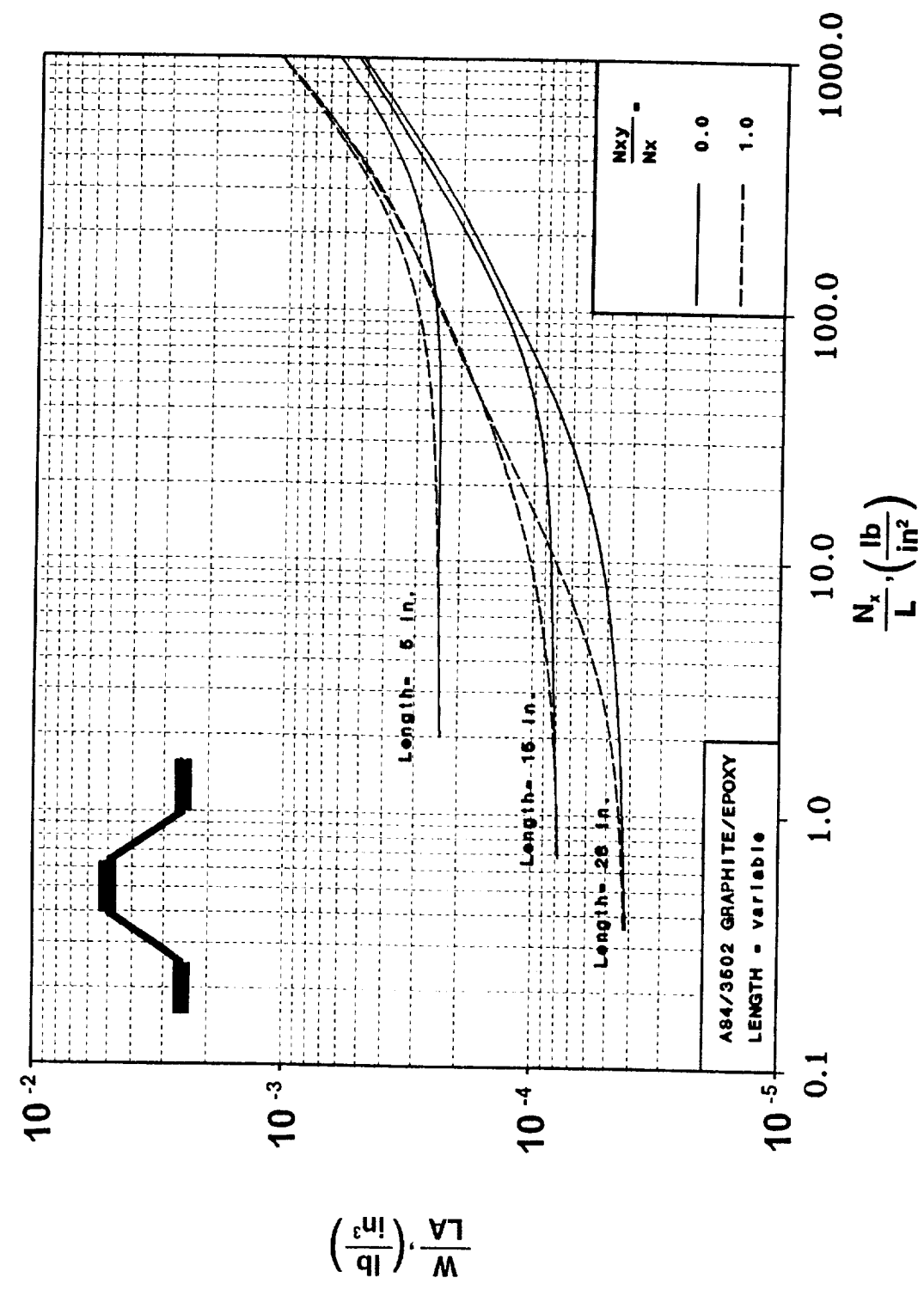
Figure 64. Effect of Panel Length on Structural Efficiency of the Tailored Corrugated Panel.
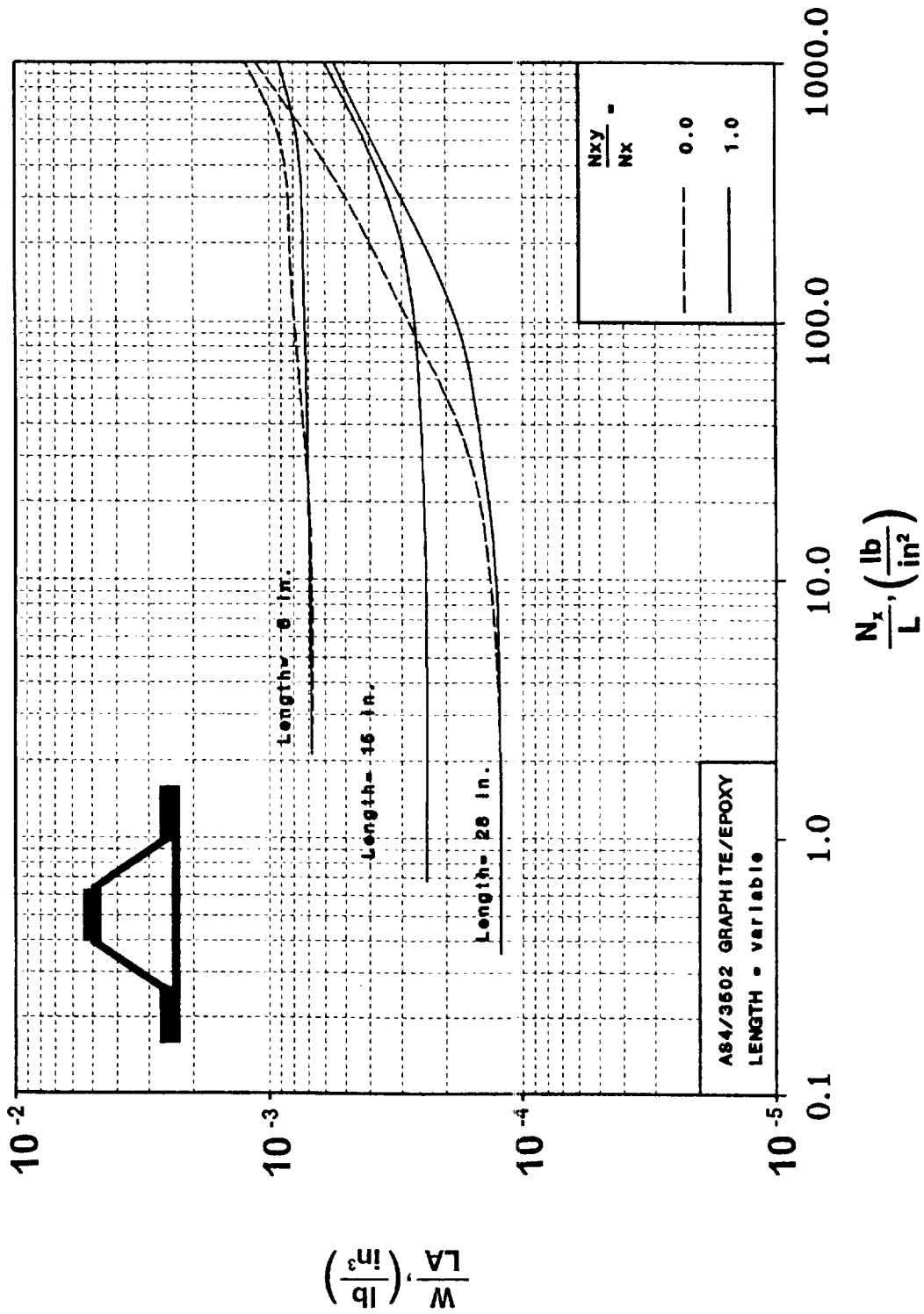
Figure 65. Effect of Panel Length on Structural Efficiency of the Hat Stiffened Panel.
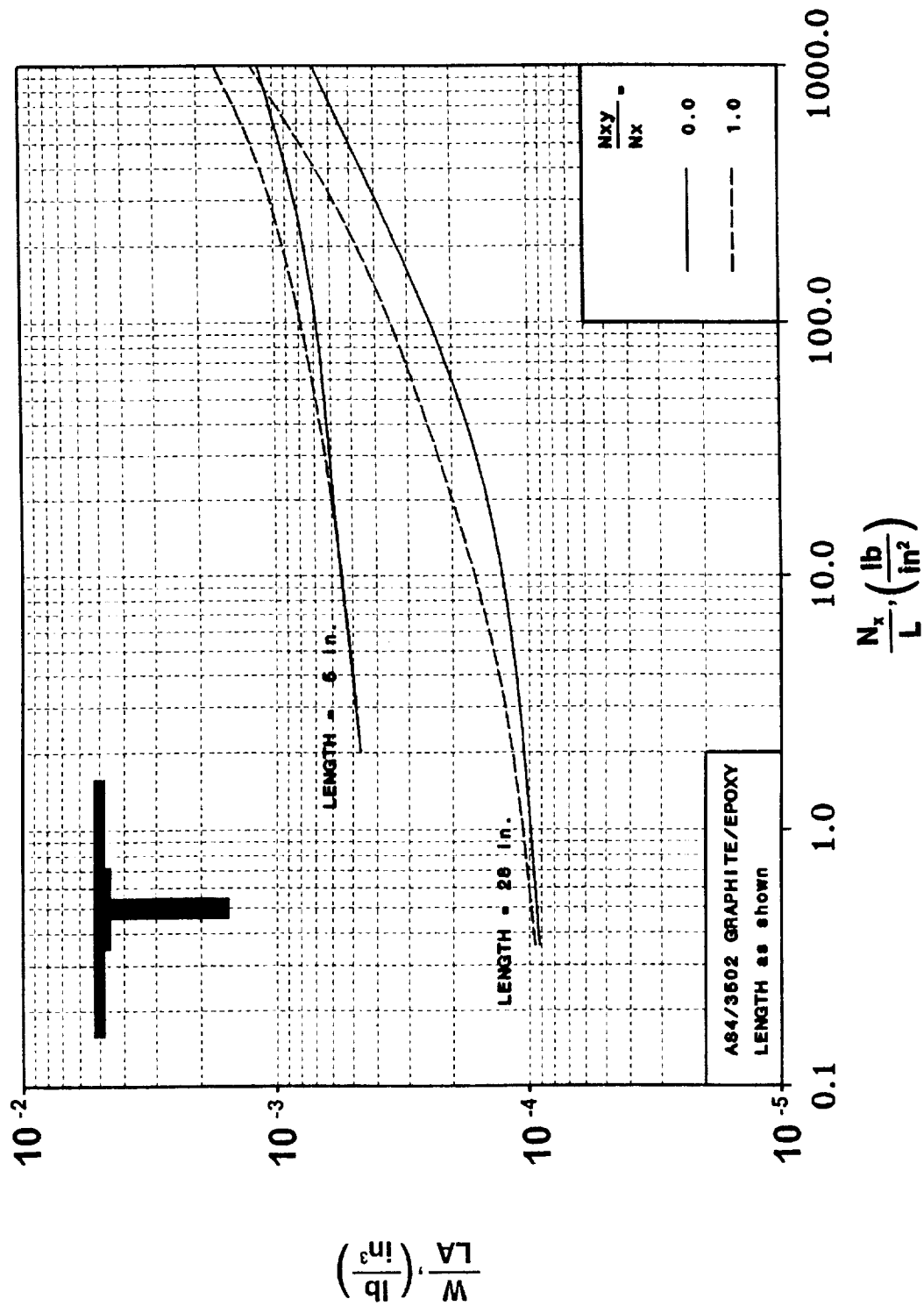
Figure 66. Effect of Panel Length on Structural Efficiency of the Blade Stiffened Panel.

is made up of essentially the same thickness laminates, based on the number of plies needed to define the laminate in the model. The same holds true for the hat stiffened panel. For the lightly loaded panels (N_x/L less than 10 lb/in^2), this observation leads to the conclusion that the weight per unit area of the panel is the same, regardless of the length. Since the structural efficiency is defined in this study as the weight per unit area over the length, a $1/L$ factor causes the discrepancy at this low loading level (N_x/L less than 10 lb/in^2). As N_x/L increases above 10 lb/in^2, the structural efficiency of the panels with different lengths approaches a common value. As it was discussed earlier, for highly loaded panels the material failure criterion is active. Figure 67 shows the effect of length on the panel weight for a constant loading index of $N_x/L = 35.7$ lb/in^2. For longer lengths (L greater than 15 inches), the minimum gage constraint is no longer active and the effect of the length on the panel weight appears to be small for both $N_{xy}/N_x = 0.0$ and 1.0. For the loading level considered in Figure 67, the adjustment to the PASCO analysis using VICON (for $N_{xy}/N_x = 1.0$) approximates a simple support for the longer lengths (L greater than 20 inches). The boundary conditions modeled for shorter lengths at this load level are not clear because VICON inherently includes a moment at the panel ends to satisfy the imposed constraints. This suggests that the effect of the boundary conditions and the panel length should be handled with a more accurate analysis for very short panels, since PASCO designs are not affected by a change in length and the VICON correction is limited.

4.3 Effect of Flange Width on Design

When designing the blade stiffened panel, the parameter in the PASCO model representing the flange width is not constrained and, therefore, is reduced to a very small, unrealistic value by the optimizer. This flange width reduction occurs because a perfect bond between the flange and skin is assumed in the analysis. In a real structure, the flange is necessary to
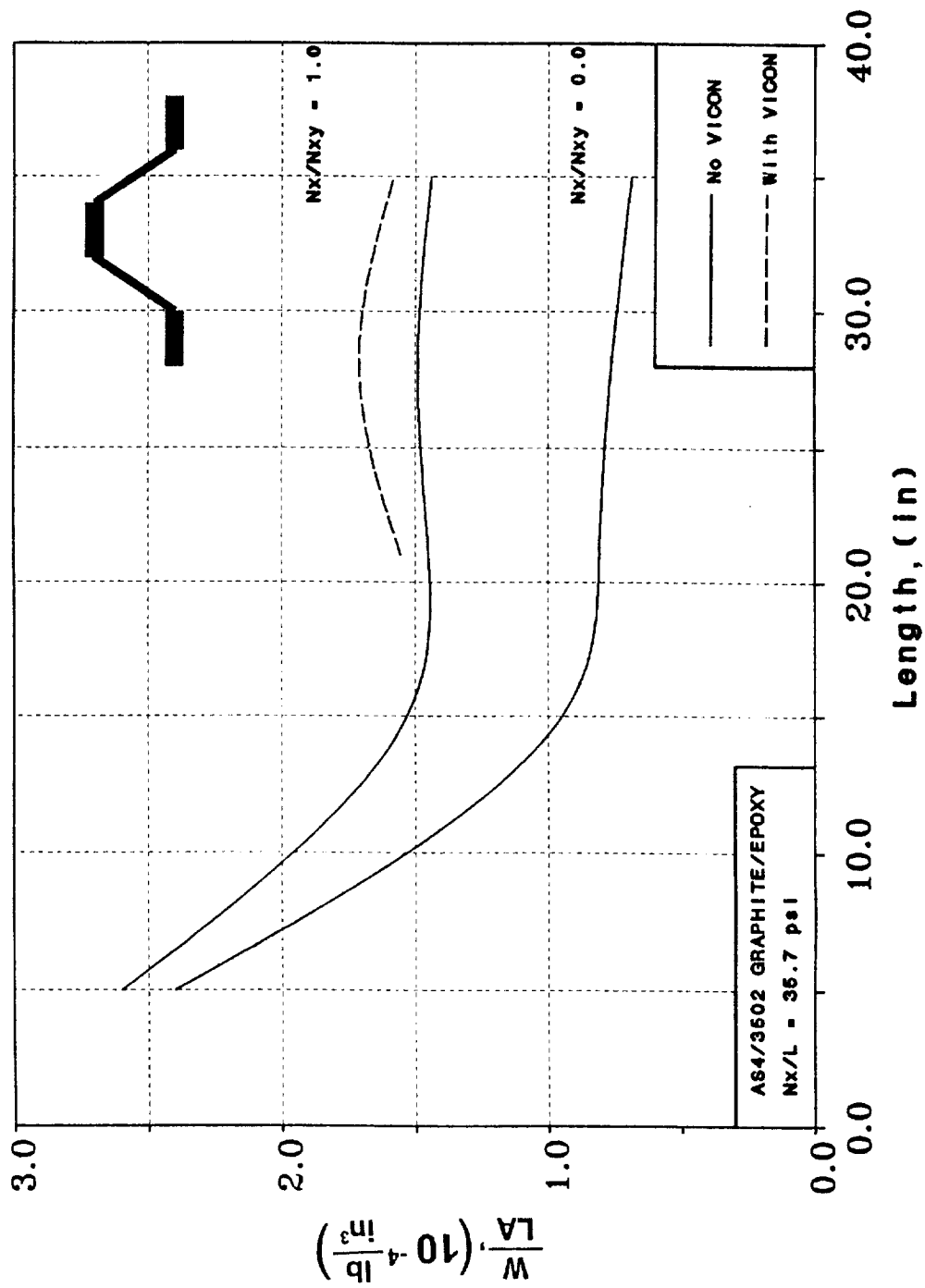
Figure 67. Length Effects with VICON on the Tailored Corrugated Panel Weight ($N_x/L =$ 35.7 lb/in²).

attach the blade stiffener to the panel and must be able to transfer the loads without failure. Designs using PASCO are obtained for different flange widths, including 0.75 and 1.50 inches. The structural efficiency of these designs show little change due to the different flange widths. Since there is little effect due to the flange width, a value of 0.75 inches is arbitrarily chosen for the width of a single flange for all of the design cases. The flange width should be investigated using a more detailed analysis that can take into account the interlaminar normal and shear stresses in the flange-skin interaction area to assure a properly designed structure.

4.4 Evaluation of the Beaded Panel Concept

Optimum panel designs are not always applicable to actual wing rib applications because of practical geometric constraints imposed on the design, making the sensitivity of the optimum panel weight to geometric changes of considerable interest. As was discussed in Section 4.1, the spacing of stiffeners is often required by a design constraint to be larger than optimum. When considering an optimum corrugated panel, the upper and lower cap widths of the corrugation are assumed to be equal, creating symmetry about the mid-plane of the cross section. In design practice, it is sometimes desirable for the spacing between the corrugations to be increased such that the cap widths are no longer equal. This spacing increase is achieved in the present study by using the concept of a beaded panel. A beaded panel refers to a panel with a corrugated type geometry that is designed such that the distance between corrugations is a multiple of the corrugation width itself, henceforth called a bead ratio. The modeling of this concept was discussed briefly in Chapter 2 (Figure 20) and is further illustrated in Figure 68. By studying the effect of this type of geometrical constraint on the panel design, a better understanding of the sensitivities of the corrugated panel weight to changes in cross sectional geometry can be gained. The concept of a beaded panel is also of interest because of its potential for using economical manufacturing techniques, specifically
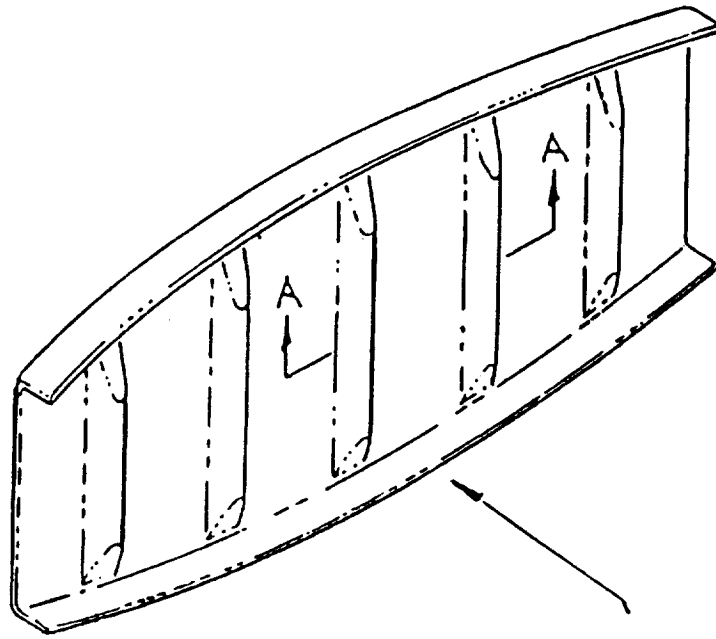
ONE-PIECE FORMED RIB

$\psi =$ **Bead Ratio**
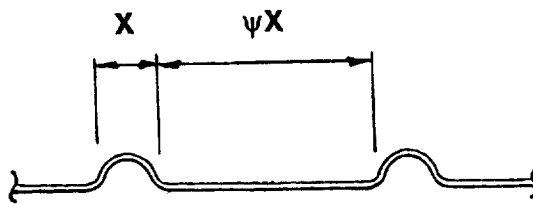
Section A-A

Figure 68.   Beaded Panel Illustration

Design Sensitivities and Comments   118

thermoplastic thermoforming, to create integrally stiffened panels with potential cost savings that may prove to be significant.

To assess the effect of beading, bead ratios of 1.0, 3.0, and 10.0, are considered for the tailored corrugated panel and the hat stiffened panel. The hat stiffened panel is considered to be a tailored corrugated panel attached to a face sheet. For all loading conditions considered so far, both the corrugated panel with a tailored laminate and the panel with a continuous laminate, have similar structural efficiency and geometric trends. Based on this observation, the trends for the beading of the tailored corrugated panel are assumed to be the same as those for the beaded corrugated panel with a continuous laminate. A number of cases are investigated to confirm this assumption.

The beaded panel is only studied for combinations of in-plane axial compression (N_x) and shear (N_{xy}) loads. The designs that include axial compression loads only ignore all anisotropic effects, an assumption discussed earlier in this chapter. Nevertheless, a few cases are investigated using the beaded corrugated panels to assess the effect of the anisotropic terms on the buckling load. The results indicate similar trends to those obtained for a blade stiffened panel. That is, the corrugated panel configurations show little sensitivity of the buckling loads to the anisotropic terms for the optimum design. However, as the bead ratio increases, the effect of these anisotropic terms on the buckling load increase. Thus, the results imply that, in general, the anisotropic terms have little effect on designs which are optimized without any geometric spacing constraints. It is assumed that for the cases in which these terms do affect the buckling analysis, this effect can be accounted for in the panel manufacturing by the use of repeating sub-laminates that are dispersed throughout the laminate thickness as discussed previously.

4.4.1 Beaded Panels under Axial Compression Load

The tailored corrugated panel and the hat stiffened panel configurations with different bead ratios are investigated for various levels of applied axial compression load. Bead ratios of 1.0, 3.0, and 10.0 times the corrugation width are considered along with axial compression loads of $N_x = 10, 100, 1000,$ and 28000 lb/in^2.

The cross sectional geometries of the tailored corrugated beaded panel configurations under axial compression are presented in Figure 69 along with the blade stiffened panel for comparison. As the bead ratio increases to a value of 10.0, the highest value considered in the present study, the geometry of the beaded panel configuration approaches a configuration that resembles the blade stiffened panel, yet slightly more efficient. The structural efficiency of the tailored corrugated beaded panel for various bead ratios is shown in Figure 70 as a function of the axial loading, with the structural efficiency curve for the optimum blade stiffened panel included for reference. The cross sectional geometries and the structural efficiencies, respectively, of the beaded hat stiffened panel, are shown in Figure 71 and Figure 72 as a function of the axial compression loading. Again, the beaded panel geometry resembles the geometry of the optimum blade stiffened panel, yet is slightly more efficient. For N_x/L of less than 30. lb/in^2, the beaded hat stiffened panel is heavier than the blade stiffened panel. The increased weight can be attributed to the minimum gage constraint effect as discussed in Chapter 3.

The approach of using a beaded panel to evaluate the sensitivity of different geometric parameters serves many purposes. It shows the sensitivity of the panel weight to non-optimum changes of various geometric spacing parameters which may occur in actual composite material applications. In the case of the hat stiffened panel, for example, the space between the hat stiffeners is the bonding surface between the corrugated panel and the un-stiffened flat plate sheet used to construct the panel. The width of this connection will most likely be based on the peel strength of the joint between the two sections, and should be de-

$N_x = 10. \frac{lb}{in}$	100.	1000.	10000.	28000.
BEAD RATIO = OPTIMUM				
1.0				
3.0				
10.0				
Blade (Reference)				

Refer to Tables 3, 12, 13, 14, and 26 for actual dimensions.

Figure 69. Beading Effect on Corrugated Panel Geometry (Blade stiffened panel included for comparison).
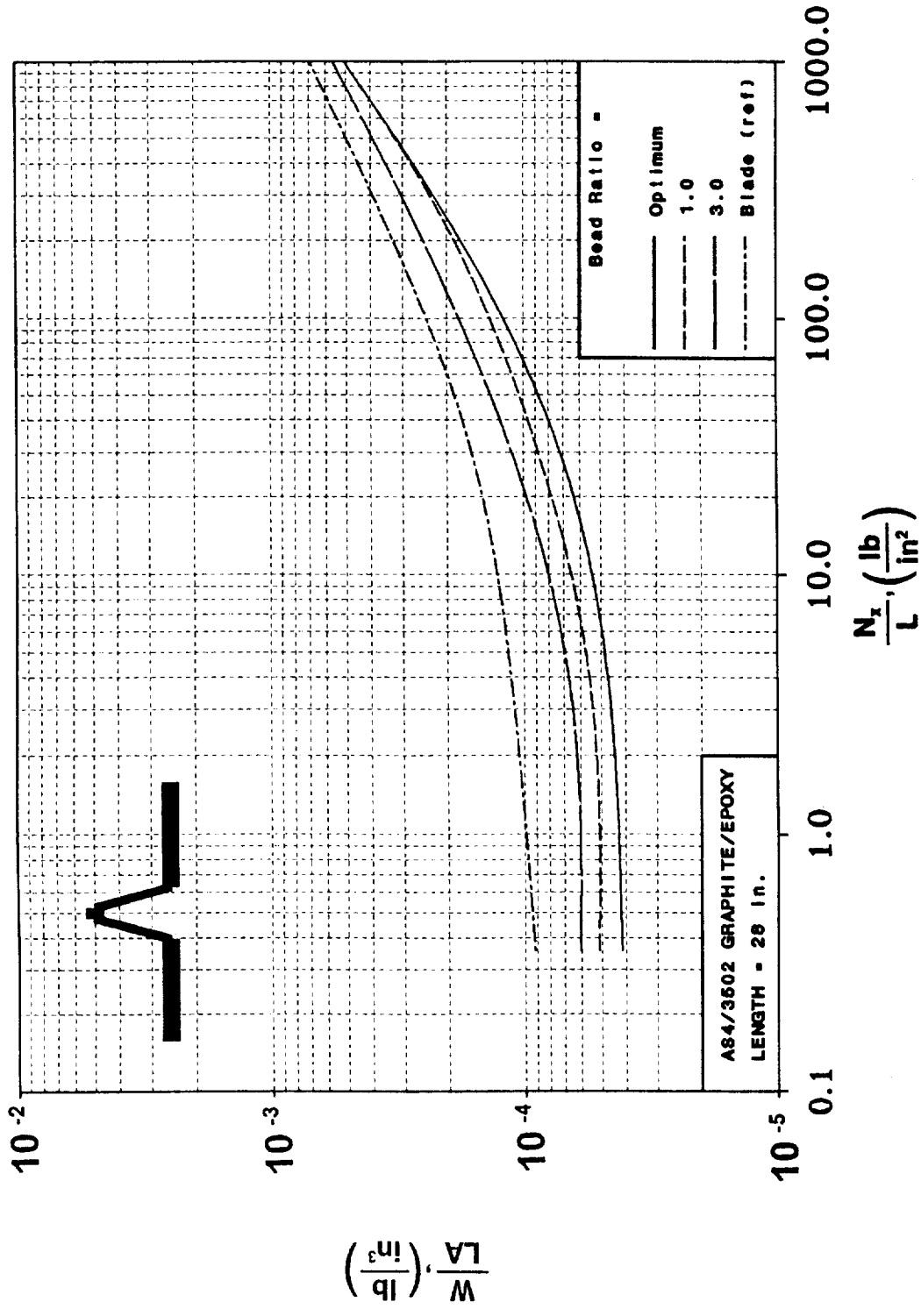
Figure 70. Beading Effect on Corrugated Panel Structural Efficiency (Blade stiffened panel included for comparison).

Figure 71. Beading Effect on the Hat Stiffened Panel Geometry (Blade stiffened panel included for comparison).

Refer to Tables 15, 23, 24, 25, and 26 for actual dimensions.
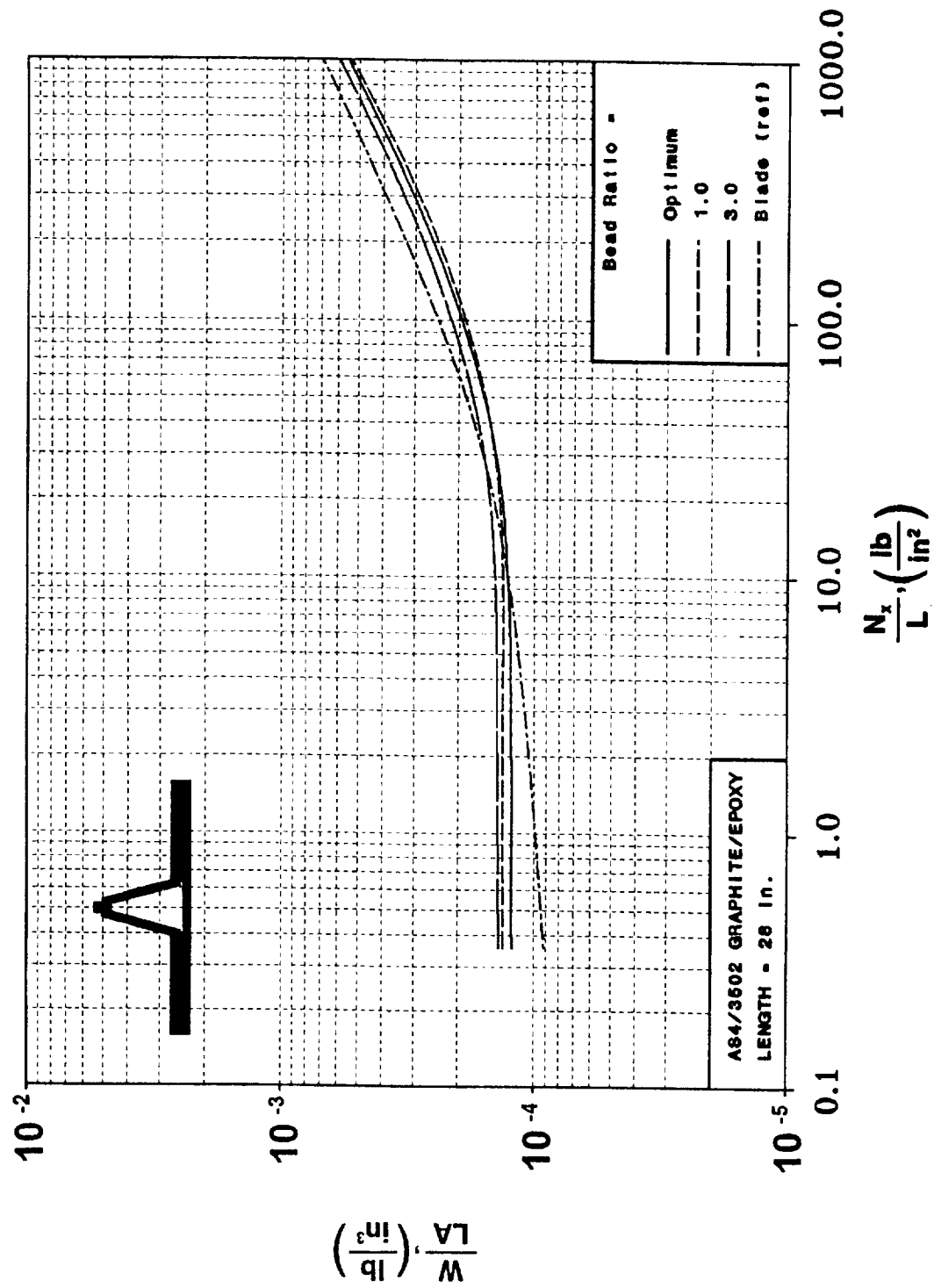
Figure 72. Beading Effect on the Hat Stiffened Panel Structural Efficiency (Blade stiffened panel included for comparison)

termined by a more detailed analysis than PASCO provides. Manufacturing constraints may also provide a realistic value for the attachment width constraint. In general, the panels which are subjected to the beading process in this study resemble the optimum blade stiffened panel geometry yet appear to be more efficient for bead ratios of up to 10.0. Since the stiffeners are formed from thin sheets, the material is more efficiently used to resist the loads since it is located away from the reference surface, a concept often used to justify the usage of a honeycomb core for the stiffeners. For bead ratios which are greater than 10.0, the combination of the local minimum width constraints imposed on the design and the large bead ratio may force the resulting design to a configuration defined by those constraints.

The results of the study suggest that when a corrugated type panel is formed into a beaded panel, it can perform similarly to (if not better than) a blade type stiffened panel, with potential reductions in the manufacturing and fabrication costs of the panel. These are important factors when dealing with an aircraft component such as a wing rib.

4.4.2 Beaded Panels with Axial Compression and Shear Loads

The effects of the shear load on the cross sectional geometry and efficiency of the beaded panel configurations with the bead ratios of 1.0, 3.0, and 10.0 are shown in Figure 73 through Figure 76 for a fixed ratio of shear load to axial compression load, $N_{xy}/N_x = 1.0$. Figure 73 and Figure 74 are for the tailored corrugated panel and Figure 75 and Figure 76 are for the hat stiffened panel. In all cases, the design trends are similar to the ones observed for the beaded panels loaded in axial compression only. Each configuration resembles the design of the optimum blade stiffened panel geometry for the given loading combination. Many similar characteristics exist between the beaded panel and the blade stiffened panel. However, the beaded panel has fewer constraints applied to the fabrication procedure and should be considered as a potential candidate for aircraft structures applications. The beaded panel contains fewer parts to manufacture and assemble, and the stiffeners are formed in a single

	$N_x = 10. \frac{lb}{in}$	100.	1000.	10000.	28000.
BEAD RATIO = OPTIMUM					
1.0					
3.0					
10.0					
Blade (Reference)					
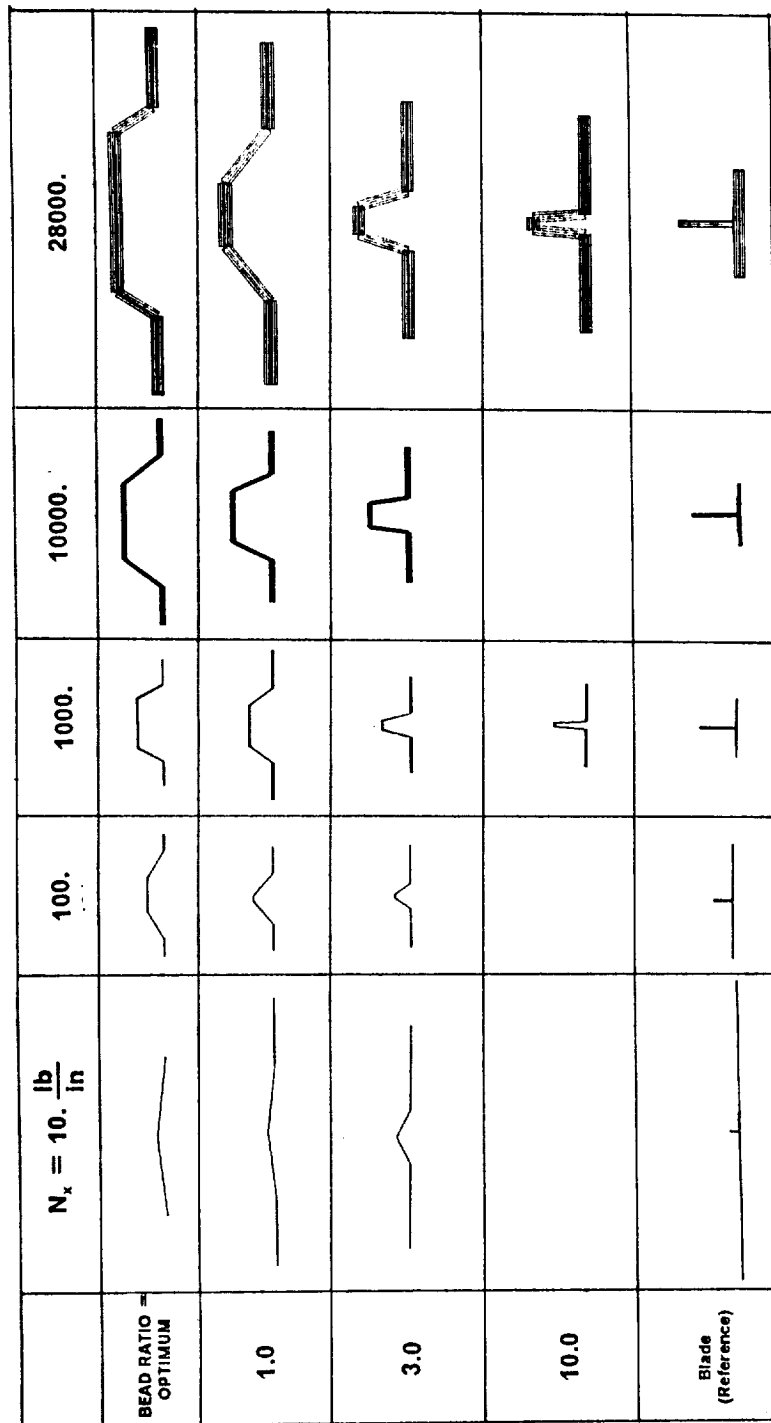
$$\frac{N_{xy}}{N_x} = 1.0$$

Refer to Tables 3, 12, 13, 14, and 26 for actual dimensions.

Figure 73. Beading Effect on the Corrugated Panel Geometry for applied Axial Compression and Shear Loadings. (Blade stiffened panel included for comparison).
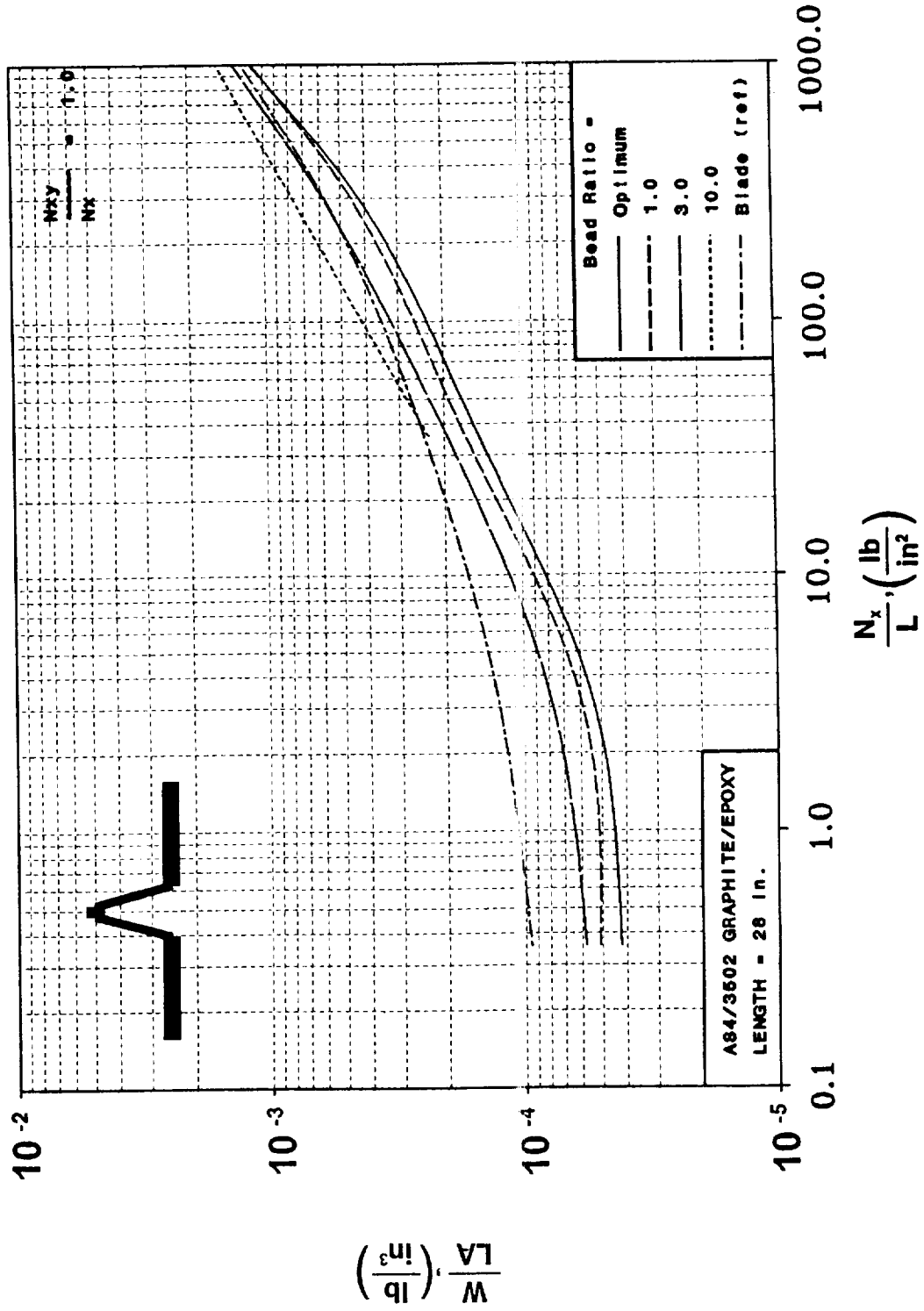
Figure 74. Beading Effect on the Corrugated Panel Structural Efficiency for applied Axial Compression and Shear Loadings (Blade stiffened panel included for comparison).

$$N_x = 10. \frac{lb}{in}$$

BEAD RATIO = Optimum		100.	1000.	10000.	28000.
1.0					
3.0					
10.0					
Blade (Reference)					

$$\frac{N_{xy}}{N_x} = 1.0$$

Refer to Tables 15, 23, 24, 25, and 26 for actual dimensions.

Figure 75. Beading Effect on the Hat Stiffened Panel Geometry for applied Axial Compression and Shear Loadings (Blade stiffened panel included for comparison).
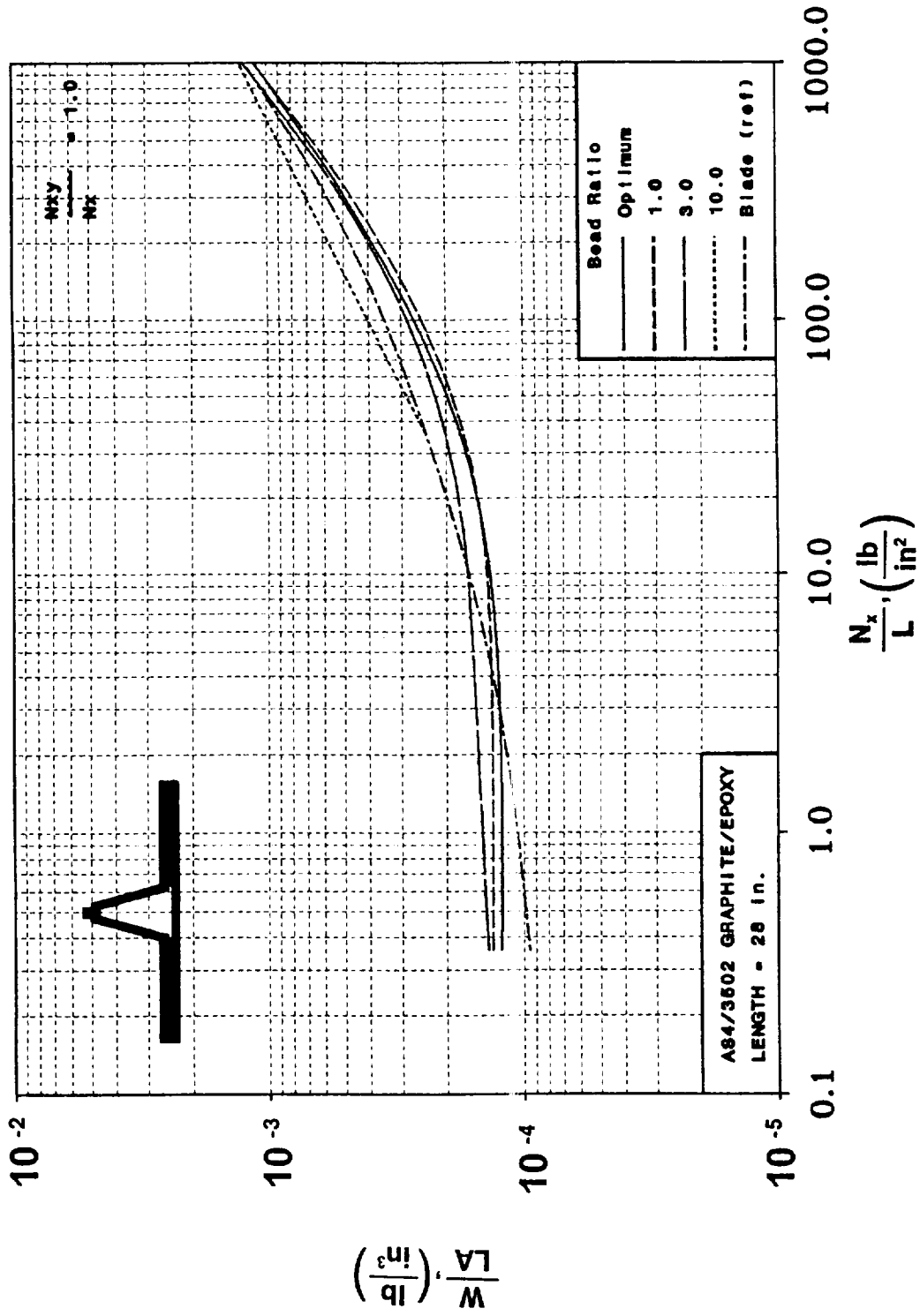
Figure 76. Beading Effect on the Hat Stiffened Panel Structural Efficiency for applied Axial Compression and Shear Loadings (Blade stiffened panel included for comparison).

manufacturing process, reducing handling and increasing the potential for automation. Further analytical study and experimental evaluation is necessary, however, to fully assure the applicability and cost effectiveness of this type of configuration.

4.5 Design Sensitivities

4.5.1 Laminates used in PASCO Model

The PASCO models used in the design and analysis of the stiffened panels are based on many practical constraints such as using continuous $\pm45°$ plies for the corrugated panel to reduce any stress concentrations that would occur at the ply termination points. As previously discussed, in the tailored corrugated panel and hat stiffened panel models, the $\pm45°$ plies run continuously throughout the corrugated panel with $0°$ plies added to the caps, leaving only a $[\pm45°]_s$ laminate in the webs. To assess the completeness and accuracy of the models used in the PASCO study, variations to the original laminates are made. The effects on the structural efficiency of including $\pm45°$, $0°$, and $90°$ plies in each of the tailored corrugated panel laminates is studied. More specifically, the effects on the structural efficiency of adding $0°$ plies to the tailored corrugated panel web laminate and $90°$ plies to both the web and cap laminates are assessed in the following sections for various loading conditions.

4.5.1.1 0° Plies Added to the Corrugated Panel Web

Tailored corrugated and hat stiffened panels are redesigned for various loadings after altering the PASCO models to allow an independent $0°$ ply thickness in the web laminate. For

loading levels less than $N_x/L = 200$ lb/in², the minimum gage ply thickness constraint is active for all of the plies originally considered, thus sizing the 0° fibers added to the web (without any constraints applied) such that they are essentially omitted. For axial compression loading levels above 200 lb/in², the minimum gage constraint is no longer active and the effect of the added 0° fibers in the web on the panel geometry becomes significant, resulting in a more even load distribution between the caps and webs, rather than being concentrated predominantly in the caps. The geometry and structural efficiency of the panels, with and without this layup change, are shown in Figure 77 and Figure 78, respectively. The results indicate that, for all load levels above $N_x/L = 200$ lb/in², adding the 0° plies in the web changes the cross sectional geometry but does not affect the panel weight of either the tailored corrugated panel or the hat stiffened panel. Since PASCO determines the load distribution by assuming a constant strain throughout the panel width, the addition of a 0° lamina to the web significantly increases the local load carried by the web due to increased stiffness. Much of the load in the web is carried by the 0° fibers in the web laminate, noticeably reducing the thickness requirement of the ±45° fibers in the web laminate relative to the thickness of 45° fibers without the 0° layer. Because the ±45° plies run continuously throughout the panel, the part of the panel requiring the largest ±45° ply thicknesses defines these thicknesses for all other panel elements, creating possible weight penalties in some elements. Since the 45° ply thicknesses defined in the web are reduced when 0° plies are included in the web laminate, the 45° plies in the cap are also reduced, increasing the structural efficiency of the corrugation and offsetting much of the weight due to the added 0° fibers in the web. Thus, this change in modeling of the panel configuration laminates shifts the load distribution from the cap to the web, and alters the optimum cross sectional configuration slightly but does not significantly change the structural efficiency.

Refer to Tables 3, 11, 15, and 22 for actual dimensions.

Figure 77. Effect of Including 0° Plies In the Corrugation Web on the Geometry (Tailored Corrugated Panel and Hat Stiffened Panel).
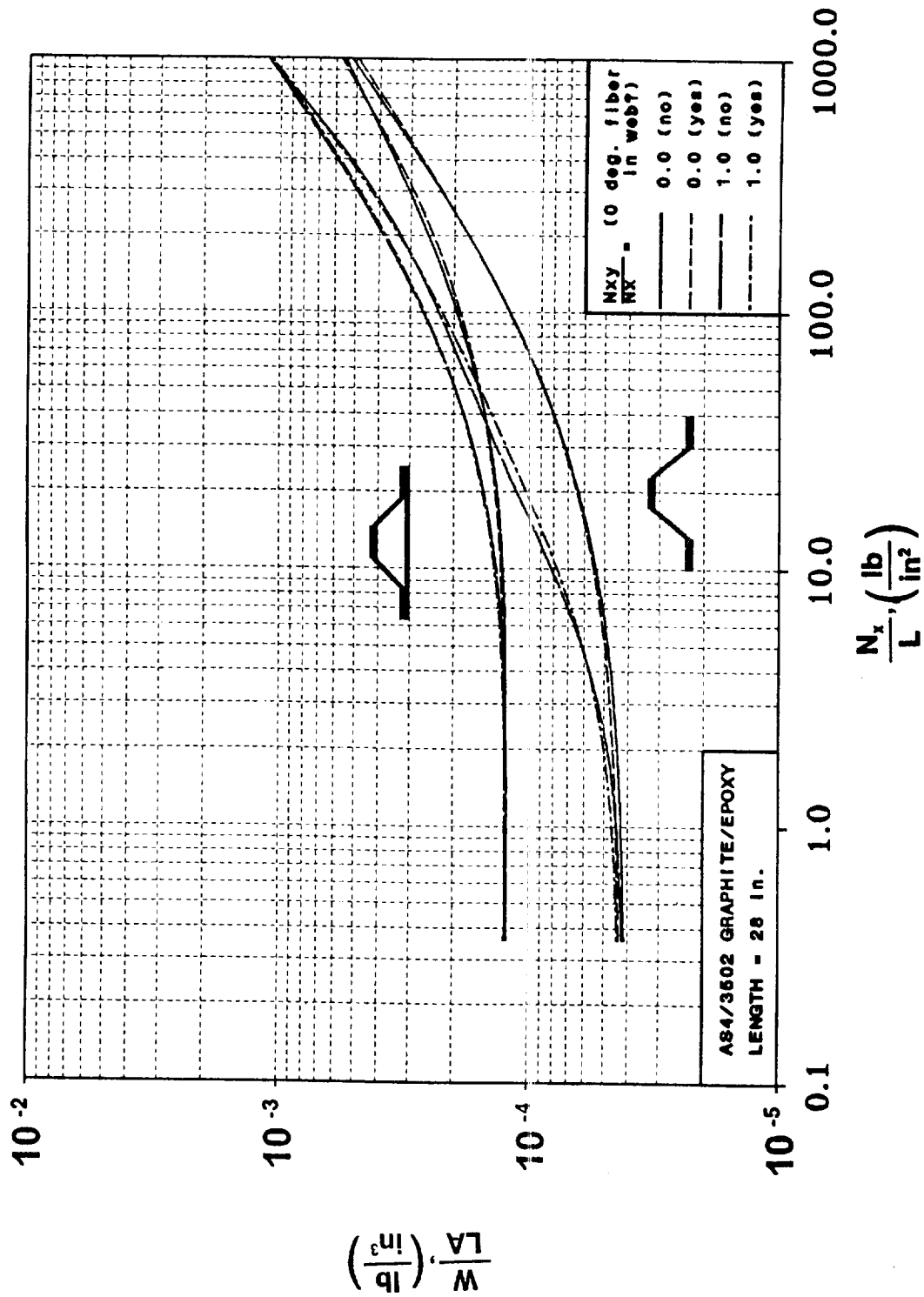
Figure 78. Effect of Including 0° Plies in the Corrugation Web on the Structural Efficiency (Tailored Corrugated Panel and Hat Stiffened Panel).

4.5.1.2 90° Plies in the Corrugated Panel

The effect of adding 90° plies to a corrugated panel structure is considered next. In a global sense, a corrugated panel has very little extensional or bending stiffness in the transverse direction due to the accordion-like nature of the panel geometry. The 90° plies follow the corrugation geometry, adding little transverse bending or extensional stiffness. Thus, it is unnecessary to include the 90° plies in the laminates which make up the corrugated panel unless they are included to control local thermal effects or damage tolerance, neither of which are considered in the present study. The assessment of the effect of this particular ply angle on the panel efficiency can be seen in the results of the corrugated panel with a continuous laminate (for example, Figure 23). For all load levels, the 90° ply in the continuous $[\pm 45°, 0°, 90°]_s$ laminate is sized by the optimizer to remain at a minimum gage thickness of 0.005 inches. The ineffectiveness of the 90° plies on the corrugated panel design suggests that the omission of the 90° plies from the tailored corrugated panel laminates is justified.

4.5.2 Corrugation Angles

Another geometric parameter whose sensitivity to change is assessed is the corrugation angle, θ, shown in Figure 79. Since manufacturing tolerances may effect the accuracy to which the optimum cross section can be fabricated, the sensitivity of the structural response to changes in the corrugation angle is of interest. Variations in the corrugation angles from the optimum are imposed and panels are redesigned with a fixed corrugation angle. The structural efficiencies of the panel for various corrugation angles are presented in Figure 80, and show that moderate changes in the angle have only a small effect on the panel weight.
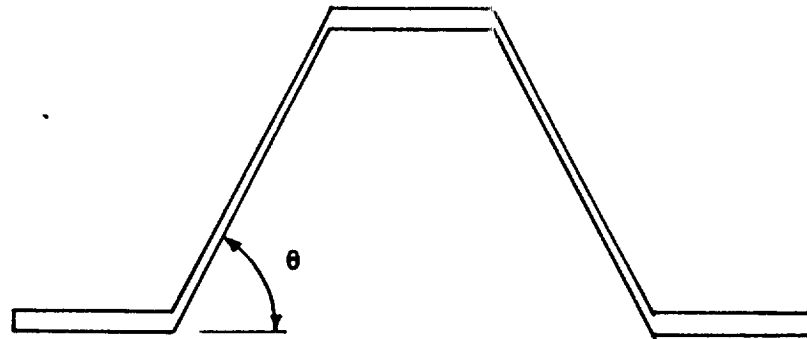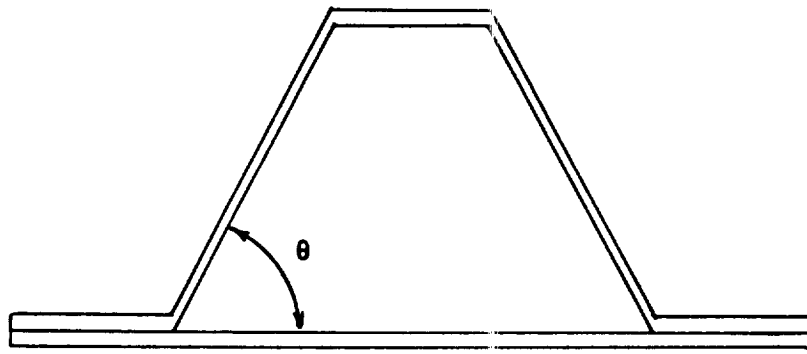
Figure 79. Definition of the Corrugation Angle.
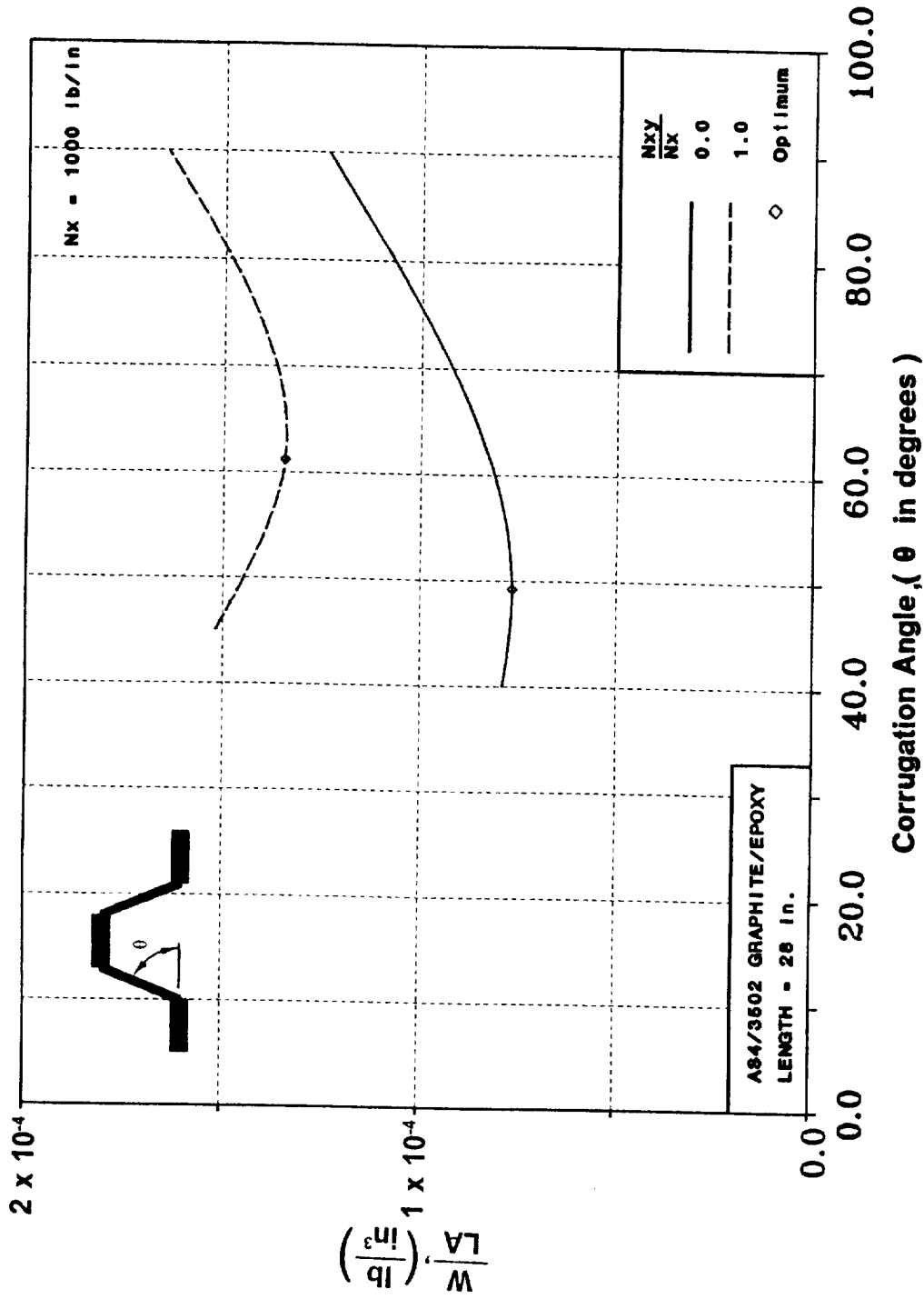
Figure 80.   Effect of the Corrugation Angle, θ, on the Structural Efficiency.

4.5.3 Discrete Ply Thicknesses

Another important realistic consideration that must be addressed is the availability of material in discrete ply thicknesses. PASCO sizes the individual ply thicknesses by allowing them to assume any value within the specified bounds. The optimum value of the ply thickness almost never corresponds to a multiple of the available discrete ply thickness which is typically about 0.005 inches. Since a panel can only be manufactured with these discrete ply thicknesses, the effect on the panel design of rounding the optimum ply thickness up to the nearest discrete ply thickness on structural efficiency and geometry is considered. The panel configurations currently being studied are altered to force the optimum ply thickness to the next highest discrete ply thickness and then are redesigned again by PASCO to obtain the optimum geometry for the new, discrete thicknesses. The results for the tailored corrugated panel are presented in Figure 81 and Figure 82. The conclusion reached is that the effects of these discrete ply thicknesses on the structural efficiency are negligible. Small changes in the panel geometry are observed in the design procedure to account for the slight changes in ply thicknesses necessary to reach the next discrete thickness. This same observation is made for all of the other panel configurations currently being considered, including the corrugated panel with a continuous laminate, the hat stiffened panel, and the blade stiffened panel. Loading conditions including axial compression (N_x), shear (N_{xy}), and pressure (P) are considered along with both optimum and non-optimum geometries and the results indicate that the small geometric changes in the panel cross sectional geometry are sufficient to account for the minor changes in ply thicknesses created as a result of rounding up to the nearest discrete ply thickness.
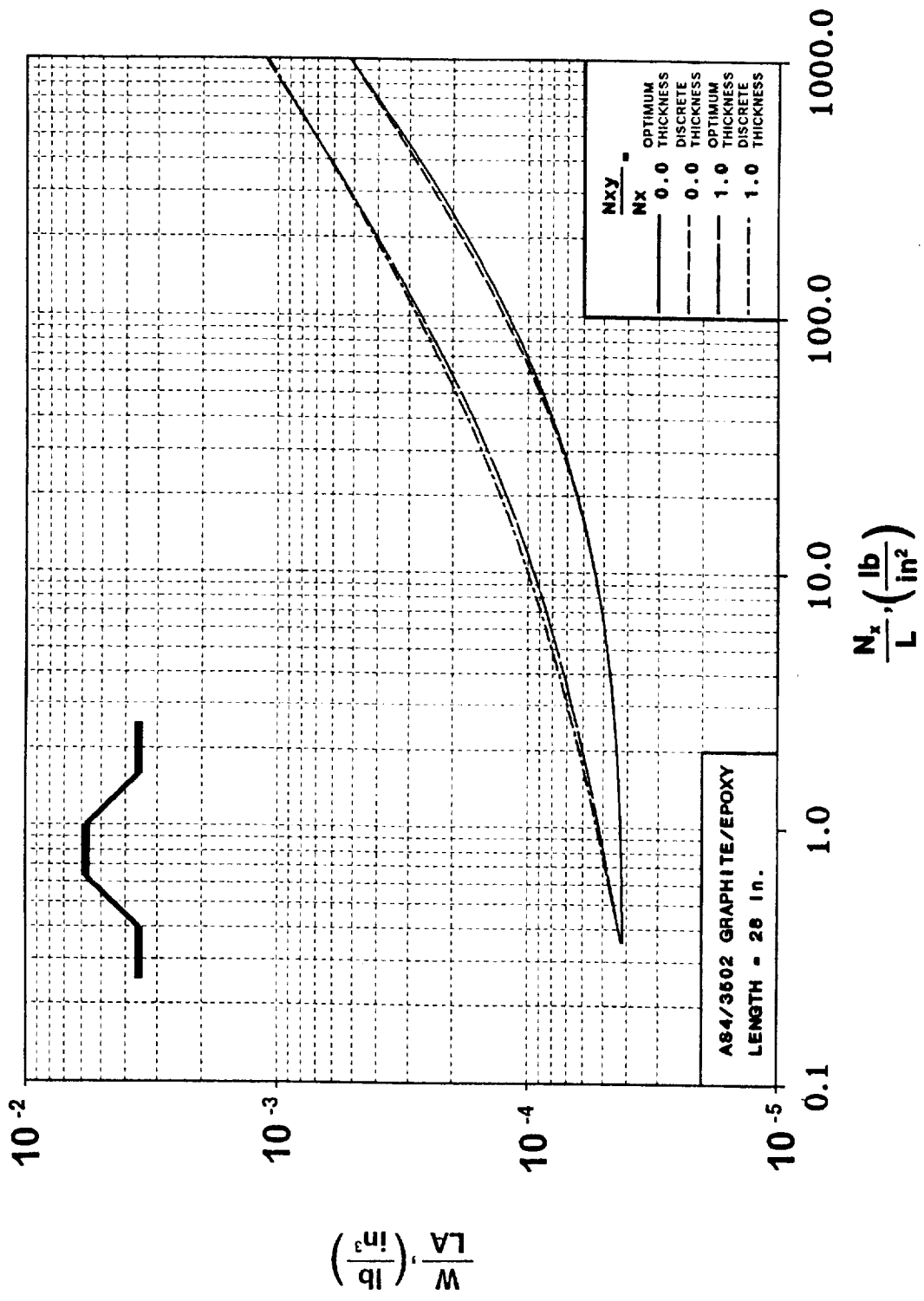
Figure 81. Effect of the Discrete Ply Thickness on Structural Efficiency.
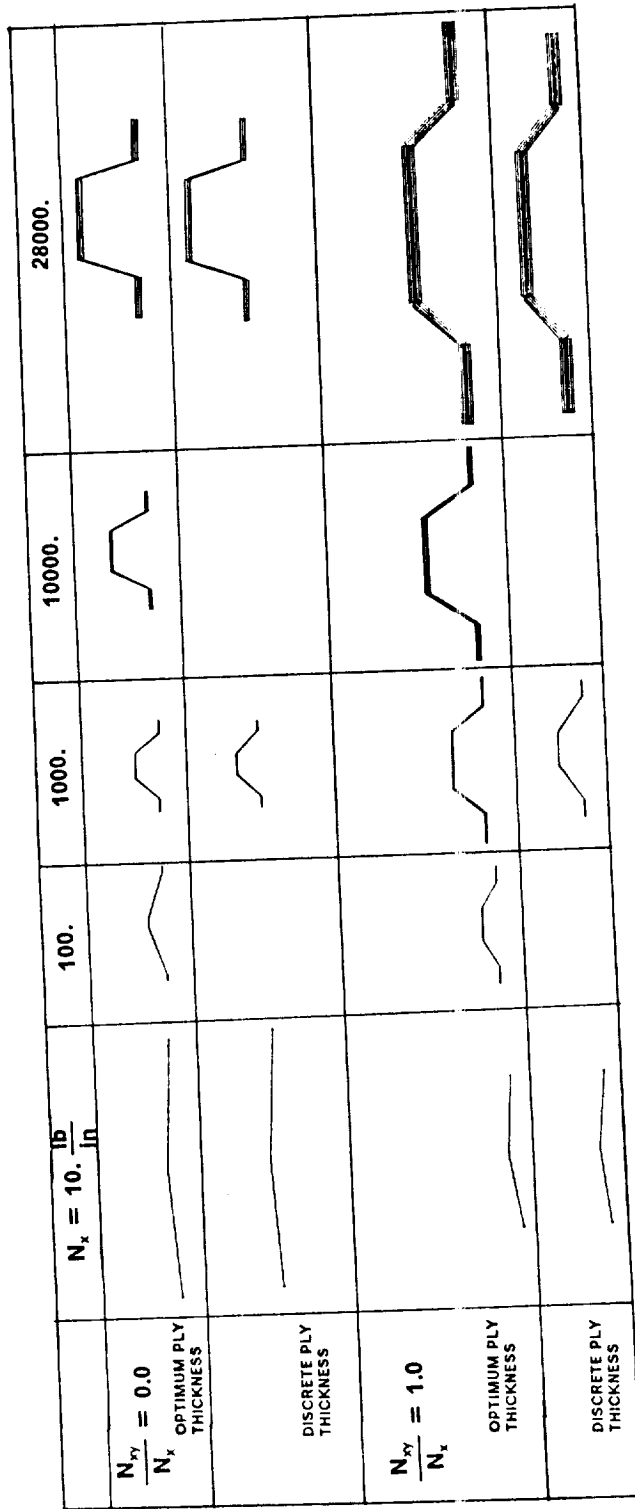
Refer to Tables 3 and 10 for actual dimensions.

Figure 82. Effect of the Discrete Ply Thickness on Geometry.

Design Sensitivities and Comments

139

5.0 Summary and Conclusions

In the present study, a series of stiffened panel designs is presented which may be used for a preliminary design assessment of an aircraft primary structure, namely a wing rib. In order to efficiently use composites in aircraft primary structures, the acquisition costs of the components must be reduced by incorporating economical manufacturing methods into the design process. The present study considers the structural efficiency and geometric trends of several configurations which lend themselves to existing economical manufacturing techniques under various combinations of axial compression, shear, and out-of-plane pressure. Understanding the effects of these combined loads on the structural efficiency and geometry of the stiffened panel configurations considered will enable the designer to utilize composite materials more efficiently for the design of a wing rib. The configurations considered in the present study which show potential for use in economical manufacturing processes include a tailored corrugated panel, a corrugated panel with a continuous laminate, a hat stiffened panel, a blade stiffened panel, and an unstiffened flat plate, the latter two being included for reference. Axial compression loading is applied to the panels for a range of the loading index (N_x/L) from 0.3 to 1000 lb/in². Shear is applied as a fraction of the applied axial compression load (N_{xy}/N_x) from 0.0 to 1.0. Pressure is applied from 0 to 45 lb/in².

The computer program PASCO is used as the primary design tool for the study. As the loading combinations are varied, minimum weight designs of the configurations are obtained. Variables including the spacing and cross sectional dimensions of the stiffeners and individual ply thicknesses are optimized to achieve the most efficient buckling resistant design for the applied loads. Design constraints on the minimum allowable ply thickness and the material failure properties are applied. Limitations in the PASCO analysis when shear is applied make it necessary to correct the buckling load corresponding to the buckling half wavelength equal to the panel length. The correction to the overall buckling load is accomplished by using the computer program VICON in a two step iterative process. The results of the study show that the effect of the PASCO analysis shortcoming is most pronounced on the corrugated panel configuration at a load level greater than the load at which a minimum gage constraint is active and at a load level less than that required to cause the material failure constraint to be active. The effect of the VICON correction on the design of the hat stiffened panel, the blade stiffened panel, and the unstiffened flat plate are small. The design trends generated in this study for combinations of axial compression, shear, and out-of-plane pressure loadings, can be used to better understand the sensitivities of the optimized designs to variations in applied loads for stiffened panels used in a wing rib application.

The lightly loaded (N_x/L less than 10 lb/in²) corrugated panel with no applied pressure is most efficient when a minimum gage material thickness constraint is active and the panel cross section is defined by a series of slight bends along the width of the panel. The optimum panel design must be used with caution because the global and local buckling modes occur simultaneously, a very dangerous design practice resulting in a lower buckling load than predicted due to modal interaction. Variations in the optimum local plate element width result in a dominant global buckling mode for shorter plate element widths and a dominant local buckling mode for increased plate element widths. When pressure is applied, the caps of the corrugation become wider and the cross section becomes deeper to account for the bending load and satisfy the material failure constraints that result from the additional pressure load.

Summary and Conclusions

141

When pressure is applied to the panel, PASCO uses a beam column approach to account for the interaction of the in-plane loads with the out-of-plane pressure load. The interaction between the in-plane and out-of-plane loads is included as an additional moment with a magnification factor. The effect of the magnification factor is such that the overall buckling load is increased to a point where it is no longer critical, causing the local buckling mode to become critical. Thus, the PASCO shortcoming in the analysis of the overall buckling mode when shear is applied is not significant when pressure is applied, making the correction to the overall buckling load unnecessary for this case. Panels designed using PASCO reflect the presence of the applied pressure, and generally have deeper, more closely spaced stiffeners that are required to resist the additional pressure loads. This approach, however, does not consider any geometrically nonlinear attributes that will likely accompany the lateral pressure.

The effect of changes in the layup used in the PASCO models on the panel weight and geometry is considered. The effect of 0° plies in the corrugation web, both with and without a face sheet, on the structural efficiency is negligible. When no 0° plies are present in the web, a higher percentage of the load is carried in the caps. When 0° plies are included in the web, the ±45° ply thicknesses decrease and the load is distributed such that the web carries more load, without changing the panel weight. The effect of including a 90° ply in a corrugated panel is shown not to have any significant effect on the structural efficiency. The sensitivity of the corrugated panel structural efficiency to small variations in the corrugation web angle which may occur in the manufacturing process is shown to have only a small effect on the panel weight.

For PASCO design studies, the effect of length on the structural efficiency of heavily loaded panels is shown to be negligible. However, as a result of the active minimum gage constraint for the lightly loaded panels, structural weight increases proportional to the panel weight. For heavily loaded panels (N_x/L for which the material failure constraint is active), no difference due to panel length is observed in the weight index (W/LA) plotted against the loading index (N_x/L) in the structural efficiency diagrams.

The effect of stiffener spacing on the blade stiffened panel suggests that small variations from the optimum spacing has little effect on the weight. Large increases in spacing increase the panel weight until it approaches the weight of an unstiffened flat plate without stiffeners. These data can be used to better understand the weight penalties associated with non-optimum stiffener spacing which may be required by specific design requirements.

The effect of the anisotropic bending terms, D_{16} and D_{26}, on the design of the panels is considered because of assumptions made in the modeling of the stiffened panels which included grouping plies with similar orientations together to reduce the number of design variables. For optimum stiffener spacing of a blade stiffened panel, the effect of these terms on the buckling analysis is negligible. However, as the stiffener spacing is increased above the optimum stiffener spacing, the anisotropic terms become more important, reducing the buckling load of the panel by up to 15%. The effect of these terms on an unstiffened flat plate can be reduced by using many repeating sub-laminates in the laminate, a procedure that will likely be done in the actual manufacturing of the panels.

Increasing the spacing between the stiffeners in a corrugated panel is accomplished by using a beaded panel concept, modeled by requiring the spacing between the corrugations to be a multiple of the size of the corrugation. The corrugated and hat stiffened panel geometries approach a configuration similar to an optimized blade stiffened panel configuration, suggesting that the beaded panel is similar to (if not better than) a blade stiffened panel, most likely with a lower manufacturing cost.

Conclusions

- The design trends generated in this study for combinations of axial compression, shear, and out-of-plane pressure loadings, can be used to better understand the design sensitivities of various stiffened panel configurations used in a wing rib application to changes in the loading and geometry.

- For panel configurations designed to resist applied pressure, deeper, more closely spaced stiffeners are required to resist the additional bending moments due to the pressure loads.

- The effect of 0° plies in the corrugation web, both with and without a face sheet, on the structural efficiency is negligible. The effect of including a 90° ply in a corrugated panel is shown to not have any significant effect on the structural efficiency. Small perturbations in the corrugation web angle are shown to have only a small effect on the panel weight.

- The effect of stiffener spacing on the blade stiffened panel suggests that small variations from the optimum spacing has little effect on the weight. Large increases in spacing increase the panel weight until it approaches the weight of an unstiffened flat plate.

- As the stiffener spacing is increased above the optimum stiffener spacing, the anisotropic terms become more important and reduce the buckling load of the panel by up to 15%.

- For increased axial compression loads, the beaded corrugated and beaded hat stiffened panel geometries approach a configuration similar to an optimized blade stiffened panel configuration, suggesting that the beaded panel is similar to (if not better than) a blade stiffened panel, most likely with a lower manufacturing cost.

Recommendations for Further Study

- A finite element analysis of the panels designed in this study needs to be investigated to verify the use of the VICON correction to PASCO.

- Non-linear finite element analysis of the panels with applied pressure should be investigated to assess the validity of the beam column assumption used in PASCO.

- The effect of boundary conditions on the panel design (other than simple support) should be investigated by using a more detailed analysis.

- A detailed analysis of the effects of the flange width on the panel design should be investigated, including a constraint dealing with the interface stresses between the attachment flange and the skin.

- The panels which are analyzed and designed in the current study should be experimentally verified.

References

1. Vosteen, Louis F., "Composite Aircraft Structures", Fiberous Composites in Structural Design, Plenum Press, New York, 1978, pp. 7-24.

2. Lackman, L.M., O'Brien, W.L., and Loyd, M.S., "Advanced Composites Integral Structures Meet the Challenge of Future Aircraft Systems", Fiberous Composites in Structural Design, Plenum Press, New York, 1978, pp. 125-144.

3. McMullen, P., "Fibre/Resin Composites for Aircraft Primary Structures: A Short History, 1936-1984", Composites, July, 1984, pp. 222-230.

4. Huttrop, M.L., "Composite Wing Substructure Technology on the AV-8B Advanced Aircraft", Fiberous Composites in Structural Design, Plenum Press, New York, 1978, pp. 25-40.

5. Jackson, A.C., Campion, M.C., and Pei, G., "Study of Utilization of Advanced Composites in Fuselage Structures of Large Transports, Final Report", NASA Contractor Report 173404, September, 1984.

6. Davis, G.W., and Sakata, I.F., "Design Considerations for Composite Fuselage Structure of Commercial Transport Aircraft", NASA Contractor Report 159296, March, 1981.

7. Dickson, J.N., and Biggers, S.B., "Design and Analysis for a Stiffened Composite Fuselage Panel", NASA Contractor Report 159302, August, 1980.

8. Watts, D.J., "A Study on the Utilization of Advanced Composites in Commercial Aircraft Wing", NASA Contractor Report 158902-2, July, 1978.

9. Harvey, S.T., and Michaelson, G.L., "Advanced Composites Wing Study Program, Volume 2 - Final Report", NASA Contractor Report 145382-2, July, 1978.

10. Agarwal, B.L., and Davis, R.C., "Minimum-Weight Designs for Hat-Stiffened Compostie Panels Under Uniaxial Compression", NASA Technical Note D-7779, November, 1974.

11. Agarwal, B.L., and Sobel, L.H., "Optimization of a Corrugated Stiffened Composite Panel Under Uniaxial Compression", NASA Contractor Report 132314, 1973.

12. Viswanathan, A.V., and Takekuni, M., "Elastic Buckling Analysis for Composite Stiffened Panels and Other Structures Subjected to Biaxial Inplane Loads," NASA Contractor Report 2216, September, 1973.

13. Williams, J.G., and Mikulas, M.M., "Analytical and Experimental Study of Structural Efficient Composite Hat-Stiffened Panels Loaded in Axial Compression", NASA Technical Memorandum X-72813, January, 1976.

14. Williams, J.G., and Stein, M., "Buckling Behavior and Structural Efficiency of Open-Section Stiffened Composite Compression Panels", AIAA Journal, Volume 14, Number 11, November, 1976, pp. 1618-1626.

15. Stein, M., and Williams, J.G., "Buckling and Structural Efficiency of Sandwich Blade Stiffened Composite Compression Panels", NASA TP-1269, September 1978.

16. Bushnell, D., "PANDA2 - Program for Minimum Weight Design of Stiffened, Composite, Locally Buckled Panels", AIAA/ASME/ASCE/AHS 27th Structures, Structural Dynamics, and Materials Conference, Part 1, San Antonio, TX, May 19-21, 1986, pp. 29-58.

17. Williams, F.W., and Anderson, M.E., "User's Guide to VIPASA, Vibration and Instability of Plate Assemblies including Shear and Anisotropy", Department of Civil Engineering, University of Birmingham, January, 1973.

18. Anderson, M.S., Hennessy, K.W., and Heard, Walter L. Jr., "Addendum to User's Guide to VIPASA, Vibration and Instability of Plate Assemblies including Shear and Anisotropy", NASA Technical Memorandum X-73914, May, 1976.

19. Anderson, M.S., Stroud, W.J., Durling, B.J., and Hennessy, K.W., "PASCO: Structural Panel Analysis and Sizing Code, User's Manual", NASA Technical Memorandum 80182, November, 1981.

20. Stroud, W.J. and Anderson, M.S., "PASCO: Structural Panel Analysis and Sizing Code, Capability and Analytical Foundations", NASA Technical Memorandum 80801, November, 1981.

21. Anderson, M.S. and Stroud, W.J., "General Panel Sizing Computer Code and Its Application to Composite Structural Panels", AIAA Journal, Volume 17, Number 8, August 1979, pp. 892-897.

22. Stroud, W.J. and Agranoff, N., "Minimum-Mass Design of Filamentary Composite Panels Under Combined Loads: Design Procedure Based on Simplified Buckling Equations", NASA Technical Note D-8257, 1976.

23. Stroud, W.J., Agranoff, N., and Anderson, M.S., "Minimum-Mass Design of Filamentary Composite Panels Under Combined Loads: Design Procedure Based on a Rigorous Buckling Analysis," NASA Technical Note D-8417, July 1977.

24. Stroud, W.J., Greene, W.H., and Anderson, M.S., "Buckling Loads of Stiffened Panels Subjected to Combined Longitudinal Compression and Shear: Results Obtained With PASCO, EAL, and STAGS Computer Programs", NASA Technical Paper 2215, January 1984.

25. Whetstone, W.D., "SPAR Structural Analysis System Reference Manual, Volume 1, Program Execution", NASA CR-145098, 1976.

26. Almroth, B.O., Brogan, F.A., and Stanley, G.M., "Structural Analysis of General Shells", Volume 2, Applied Mechanics Laboratory, Lockheed Palo Alto Research Laboratory, Palo Alto, CA, December 1982.

27. Davis, R.C., Mills, C.T., Prabhakaran, R., and Jackson, L.R., "Structural Efficiency Studies of Corrugated Compression Panels with Curved Caps and Beaded Webs", NASA Technical Paper 2272, 1984.

28. Stroud, W.J., Greene, W.H., and Anderson, M.S., "Current Research on Shear Buckling and Thermal Loads with PASCO; Panel Analysis and Sizing Code", NASA Technical Memorandum 83206, September, 1981.

29. Williams, F.W. and Kennedy, D., "User's Guide to VICON, VIPASA with Constraints", Department of Civil Engineering and Building Technology, University of Wales Institute of Science and Technology, August, 1984.

30. Anderson, M.S., Williams, F.W., and Wright, C.J., "Buckling and Vibration of Any Prismatic Assembly of Shear and Compression Loaded Anisotropic Plates with an Arbitrary Supporting Structure", International Journal fo Mechanical Science, Volume 25, Number 8, 1983, pp. 585-596.

31. Williams, F.W. and Anderson, M.S., "Incorporation of Lagrangian Multipliers into an Algorithm for Finding Exact Natural Frequencies or Critical Buckling Loads", International Journal of Mechanical Science, Volume 25, Number 8, pp. 579-584, 1983.

32. Williams, F.W., and Anderson, M.S., "Buckling and Vibration Analysis of Shear-Loaded Prismatic Plate Assemblies with Supporting Structures Utilizing Symmetric or Repetitive Cross-Sections", Aspects of the Analysis of Plate Structures, A Volume in Honour of W.H. Wittrick, Edited by D.J. Dawe, R.W. Horsington, A.G. Kametekar and G.H. Little, Oxford University Press, 1985, pp. 51-71.

33. Anderson, M.S. and Williams, F.W., "Buckling of Simply Supported Plate Assemblies Subject to Shear Loading", Aspects of the Analysis of Plate Structures, A Volume in Honour of W.H. Wittrick, Edited by D.J. Dawe, R.W. Horsington, A.G. Kamtekar, G.H. Little, Oxford University Press, 1985, pp. 39-49.

34. Peterson, J.P., and Card, M.F., "Investigation of the Buckling Strength of Corrugated Webs in Shear", NASA TN-D-424, June 1960.

35. Rothwell, A., "The Buckling of Shallow Corrugated Webs in Shear", The Aeronautical Journal of the Royal Aeronautical Society, Volume 72, October, 1968, pp. 883-886.

36. Libove, C., "Survey of Recent Work on the Analysis of Discretely Attached Corrugated Shear Webs", AIAA/ASME/SAE Structures, Structural Dynamics, and Materials Conference, 13th, San Antonio, TX, April 10-12, 1972.

37. Libove, C., "Buckling of Corrugated Plates in Shear", International Colloquium on Stability of Structures Under Static and Dynamic Loads, Washington, D.C., May 17-19, 1977, Proceedings, NY, ASCE, 1977, pp. 435-462.

38. Libove, C., "Asymptotic Behavior of Discretely Attached Corrugated Shear Webs", AIAA Journal, Vol. 13, December, 1975, pp. 1557-1561.

39.   Perel, D., and Libove, C., "Elastic Buckling of Infinitely Long Trapeziodally Corru-gated Plates in Shear", ASME, Transactions, Journal of Applied Mechanics, Vol. 45, September, 1978, pp. 579-582.

40.   Toda, S., "Buckling of Sinusiodally Corrugated Plates under Axial Compression", AIAA Journal, Volume 21, Number 8, August, 1983, pp. 1211-1213.

41.   Toda, S., and Sanbongi, S., "Buckling of Quasisinusiodally Corrugated Plates in Shear", AIAA Journal, Volume 24, Number 1, January 1986, pp 138-143.

42.   Tada, Y., Ishikawa, T., and Nakai, E., "Tests of CFRP Spar/Rib Models with Corru-gated Web", Composite Materials, K. Kawata and T. Akasaka, Editors, Proceedings Japan-U.S. Conference, Tokyo, 1981.

43.   Johnston, N.J., O'Brien, T.K., Morris, D.H., and Simonds, R.A., "Interlaminar Fracture Toughness of Composites. II - Refinement of the Edge Delamination Test and Appli-cation to Thermoplastics", 28th National SAMPE Symposium and Exhibition, Anaheim, California, April 12-14, 1983.

44.   Johnston, N.J., and Hergenrother, P.M "High Performance Thermoplastics: A Re-view of Neat Resin and Composite Properties", 32nd SAMPE International Sympo-sium and Exhibition, Anaheim, California, April 6-9, 1987.

45.   Christensen, S., and Clark, L.P., "Thermoplastic Composites for Structural Applica-tions, An Emerging Technology", 31st International SAMPE Symposium, April 7-10, 1986, pp. 1747-1754.

46.   Goad, R.C., "Development of Thermoplastic Composite Aircraft Structural Elements, Final Report", NADC-77187-30, May, 1977.

47.   Hoggatt, J.T., Oken, S., and House, E.E , "Advanced Fiber Reinforced Thermoplastic Structures", AFWAL-TR-80-3023, April, 1980.

48.   Srinivasan, R.S., and Thiruvenkatachari, V., "Static Analysis of Stiffened Plates", AIAA Journal, Volume 22, Number 6, September, 1984, pp. 1342-1344.

49.   Rehfield, L.W. and Reddy, A.D.: "Damage Tolerance of Continuous Filament Com-posite Isogrid Structures: A Preliminary Assessment", Composite Materials, K. Kawata, T. Akaska, Editors, Proceedings US-Japan Conference, Tokyo, 1981.

50.   Rehfield, L.W., Deo, R.B., and Renieri, G.D., "Continuous Filament Advanced Com-posite Isogrid: A Promising Structural Concept", Fiberous Composites in Structural Design, Plenum Press, New York, 1978, pp. 215-239.

51.   Reddy, A.D., "Behavior of Continuous Filament Advanced Composite Isogrid Struc-ture", Ph.D Thesis, Georgia Institute of Technology, November, 1980.

52.   Reddy, A.D., Valisetty, R.R., and Rehfield, L.W., "Continuous Filament Wound Com-posite Concepts for Aircraft Fuselage Structures", Journal of Aircraft, Volume 22, Number 3, March, 1985, pp. 249-255.

53.   Jones, R.M., "Mechanics of Composite Materials", McGraw Hill, 1975.

54.   Vanderplaats, G.N., "CONMIN - A Fortran Program for Constrained Function Minimi-zation. User's Manual", NASA TM X-62, 282, 1973.

55.   Giles, G.L., and Anderson, M.S., "Effects of Eccentricities and Lateral Pressure on the Design of Stiffened Compression Panels", NASA Technical Note D-6784, 1972.

56.   Nemeth, M.P., "Importance of Anisotropy on Buckling of Compression Loaded Symmetric Composite Plates", AIAA Journal, Volume 24, Number 11, November, 1986, pp. 1831-1835.

Appendix A. Tailored Corrugated Panel Data
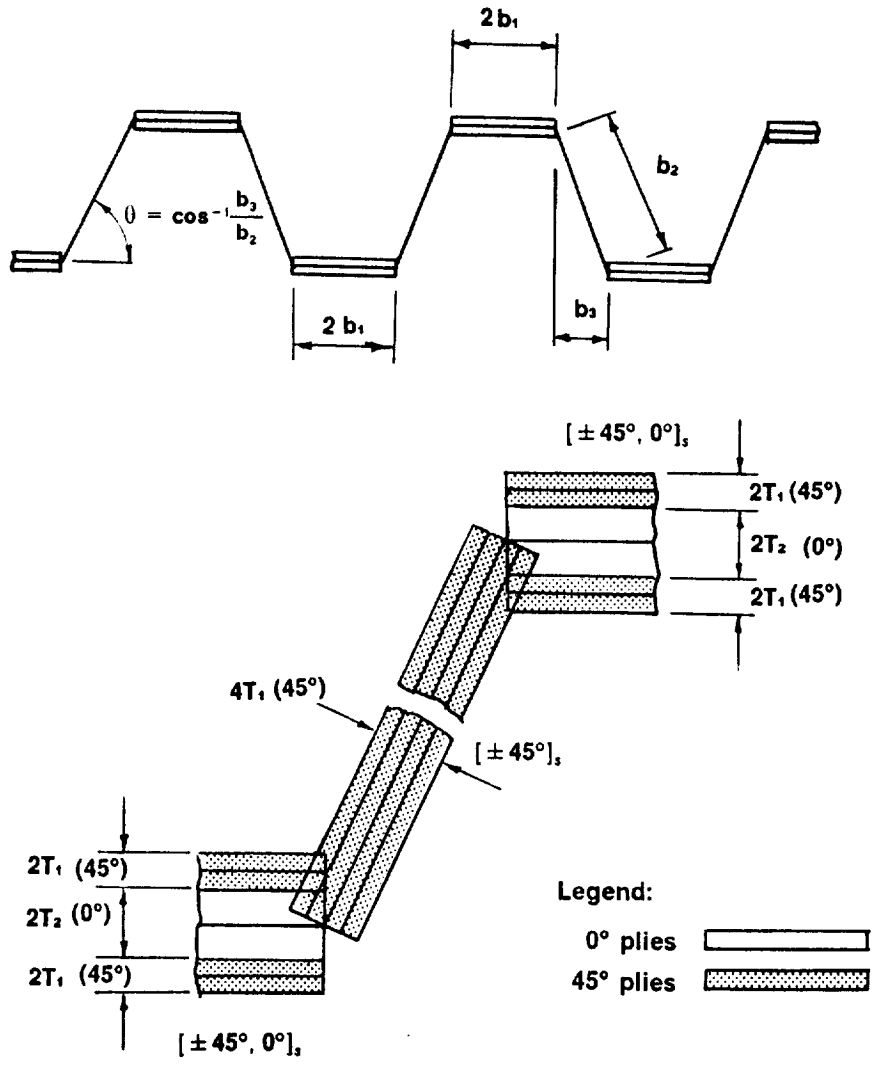
Figure 83. Tailored Corrugated Panel Model

Table 3. Tailored Corrugated Panel (P= 0.0 psi   L= 28 in)

	Nx= 10 (lb/in)	Nx= 100 (lb/in)	Nx= 350 (lb/in)	Nx= 1000 (lb/in)	Nx= 2800 (lb/in)	Nx= 10000 (lb/in)	Nx= 28000 (lb/in)
$\frac{N_{xy}}{N_x} = 0.0$							
B_1 (in.)[x]	0.1000	0.2296	0.5295	0.5807	0.7164	0.9008	1.8259
B_2	5.4424	2.1751	1.5900	1.4032	1.3726	1.8728	2.6897
Angle, θ	3.5	19.1	36.4	49.3	61.7	62.5	72.7
T_1 (in.)[xx]	0.0050	0.0050	0.0050	0.0050	0.0055	0.0118	0.0148
T_2	0.0050	0.0050	0.0050	0.0115	0.0225	0.0440	0.1041
$\frac{W}{LA}$(10⁻⁴ lb/in³)	0.4151	0.4637	0.5533	0.7653	1.2399	2.5290	5.1955
$\frac{N_{xy}}{N_x} = 0.3$							
B_1 (in.)[x]	0.1000	0.2492	0.6122	0.7942	1.0643	1.4116	1.6129
B_2	4.1374	1.7634	1.1266	1.1650	1.5657	2.2071	2.7767
Angle, θ	4.4	21.8	44.6	53.6	54.1	56.5	58.3
T_1 (in.)[xx]	0.0050	0.0050	0.0050	0.0067	0.0117	0.0227	0.0333
T_2	0.0050	0.0050	0.0061	0.0122	0.0205	0.0359	0.1152
$\frac{W}{LA}$(10⁻⁴ lb/in³)	0.4177	0.4787	0.6228	1.0115	1.7337	3.3273	6.7101
$\frac{N_{xy}}{N_x} = 0.6$							
B_1 (in.)[x]	0.1000	0.3039	0.9111	1.0652	1.3687	1.7313	2.5112
B_2	3.6291	1.5638	1.2249	1.6775	2.0784	2.3950	3.3742
Angle, θ	5.1	25.8	39.3	53.2	48.2	56.1	45.0
T_1 (in.)[xx]	0.0050	0.0050	0.0060	0.0109	0.0180	0.0334	0.0591
T_2	0.0050	0.0050	0.0088	0.0136	0.0217	0.0424	0.1037
$\frac{W}{LA}$(10⁻⁴ lb/in³)	0.4194	0.5000	0.8217	1.4515	2.3020	4.5648	8.3220
$\frac{N_{xy}}{N_x} = 1.0$							
B_1 (in.)[x]	0.1000	0.7189	1.0833	1.3053	1.4486	1.6915	3.5376
B_2	3.1494	1.3354	1.4274	1.8812	1.9800	2.5928	2.8713
Angle, θ	6.6	31.5	47.7	51.3	56.4	56.5	47.2
T_1 (in.)[xx]	0.0050	0.0050	0.0082	0.0134	0.0205	0.0370	0.0986
T_2	0.0050	0.0050	0.0093	0.0153	0.0257	0.0546	0.0727
$\frac{W}{LA}$(10⁻⁴ lb/in³)	0.4219	0.5517	1.0290	1.7194	2.7999	5.2993	11.165

[x] Reference dimensions to Figure 83.
[xx] Minimum gage ply thickness = 0.005 inches

Table 4. Tailored Corrugated Panel - No VICON Corrections (P= 0.0 psi   L= 28 in)

	Nx= 10 (lb/in)	Nx= 100 (lb/in)	Nx= 350 (lb/in)	Nx= 1000 (lb/in)	Nx= 2800 (lb/in)	Nx= 10000 (lb/in)	Nx= 28000 (lb/in)
$\frac{N_{xy}}{N_x} = 0.0$ B_1 (in.)^x B_2 Angle, θ T_1 (in.)^{xx} T_2 $\frac{W}{LA}(10^{-4}$ lb/in^3)	n/c	n/c	n/c	n/c	n/c	n/c	n/c
$\frac{N_{xy}}{N_x} = 0.3$ B_1 (in.)^x B_2 Angle, θ T_1 (in.)^{xx} T_2 $\frac{W}{LA}(10^{-4}$ lb/in^3)	n/c	n/c	0.6196 1.1409 44.7 0.0050 0.0063 0.6293	0.8024 1.1746 53.8 0.0068 0.0121 1.0150	1.0020 1.4702 55.7 0.0112 0.0196 1.6790	1.3319 2.0110 56.0 0.0212 0.0355 3.1512	2.1952 1.9620 55.6 0.0297 0.1014 6.0870
$\frac{N_{xy}}{N_x} = 0.6$ B_1 (in.)^x B_2 Angle, θ T_1 (in.)^{xx} T_2 $\frac{W}{LA}(10^{-4}$ lb/in^3)	n/c	n/c	0.7912 0.9879 36.9 0.0051 0.0084 0.7390	0.9729 1.2720 52.7 0.0087 0.0132 1.2208	1.1917 1.4788 59.2 0.0134 0.0217 2.0139	1.4421 1.7898 63.0 0.0232 0.0439 3.7779	3.1275 2.2836 45.7 0.0591 0.0894 8.1366
$\frac{N_{xy}}{N_x} = 1.0$ B_1 (in.)^x B_2 Angle, θ T_1 (in.)^{xx} T_2 $\frac{W}{LA}(10^{-4}$ lb/in^3)	n/c	n/c	0.6916 1.1409 44.7 0.0050 0.0063 0.6293	0.8024 1.1746 53.8 0.0068 0.0121 1.0150	1.0020 1.4702 55.7 0.0112 0.0196 1.6790	1.3319 2.0110 56.0 0.0212 0.0355 3.1512	2.1952 1.9620 55.6 0.0297 0.1014 6.0870

^{x} Reference dimensions to Figure 83.
^{xx} Minimum gage ply thickness = 0.005 inches.
n/c Loading condition not considered.

Table 5.   Tailored Corrugated Panel (P= 5.0 psi   L= 28 in)

	Nx = 10 (lb/in)	Nx = 100 (lb/in)	Nx = 350 (lb/in)	Nx = 1000 (lb/in)	Nx = 2800 (lb/in)	Nx = 10000 (lb/in)	Nx = 28000 (lb/in)
$\dfrac{N_{xy}}{N_x} = 0.0$ B_1 (in.)* B_2 Angle, θ T_1 (in.)** T_2 $\dfrac{W}{LA}$ (10^{-4} lb/in³)	0.3064 1.9320 32.4 0.0050 0.0082 0.5525	0.3133 1.8594 35.4 0.0050 0.0100 0.5917	n/c	0.4063 1.5408 49.8 0.0050 0.0204 1.6300	n/c	n/c	n/c
$\dfrac{N_{xy}}{N_x} = 0.3$ B_1 (in.)* B_2 Angle, θ T_1 (in.)** T_2 $\dfrac{W}{LA}$ (10^{-4} lb/in³)	n/c	n/c	n/c	n/c	n/c	n/c	n/c
$\dfrac{N_{xy}}{N_x} = 0.6$ B_1 (in.)* B_2 Angle, θ T_1 (in.)** T_2 $\dfrac{W}{LA}$ (10^{-4} lb/in³)	n/c	n/c	n/c	n/c	n/c	n/c	n/c
$\dfrac{N_{xy}}{N_x} = 1.0$ B_1 (in.)* B_2 Angle, θ T_1 (in.)** T_2 $\dfrac{W}{LA}$ (10^{-4} lb/in³)	0.2953 1.7019 34.2 0.0050 0.0088 0.5731	0.3457 1.2888 43.3 0.0050 0.0125 0.7105	n/c	n/c	n/c	n/c	n/c

* Reference dimensions to Figure 83.
** Minimum gage ply thickness = 0.005 inches.
n/c Loading condition not considered.

Table 6.   Tailored Corrugated Panel (P= 10.0 psi   L= 28 In)

	Nx = 10 (lb/in)	Nx = 100 (lb/in)	Nx = 350 (lb/in)	Nx = 1000 (lb/in)	Nx = 2800 (lb/in)	Nx = 10000 (lb/in)	Nx = 28000 (lb/in)
$\dfrac{N_{xy}}{N_x} = 0.0$ B_1 (in.)[x] B_2 Angle, θ T_1 (in.)[xx] T_2 $\dfrac{W}{LA}$(10^{-4} lb/in^3)	0.3407 1.9926 37.4 0.0050 0.0142 0.6553	0.3443 1.9203 40.5 0.0050 0.0150 0.6904	n/c	0.3357 1.6179 49.2 0.0050 0.0295 1.0063	n/c	n/c	n/c
$\dfrac{N_{xy}}{N_x} = 0.3$ B_1 (in.)[x] B_2 Angle, θ T_1 (in.)[xx] T_2 $\dfrac{W}{LA}$(10^{-4} lb/in^3)	n/c	n/c	n/c	n/c	n/c	n/c	n/c
$\dfrac{N_{xy}}{N_x} = 0.6$ B_1 (in.)[x] B_2 Angle, θ T_1 (in.)[xx] T_2 $\dfrac{W}{LA}$(10^{-4} lb/in^3)	n/c	n/c	n/c	n/c	n/c	n/c	n/c
$\dfrac{N_{xy}}{N_x} = 1.0$ B_1 (in.)[x] B_2 Angle, θ T_1 (in.)[xx] T_2 $\dfrac{W}{LA}$(10^{-4} lb/in^3)	0.3407 1.7526 39.4 0.0050 0.0144 0.6832	0.3965 1.3986 46.6 0.0052 0.0165 0.8333	n/c	0.8490 1.7538 47.2 0.01266 0.02127 1.7398	n/c	n/c	n/c

[x] Reference dimensions to Figure 83.
[xx] Minimum gage ply thickness = 0.005 inches.
n/c Loading condition not considered.

Appendix A. Tailored Corrugated Panel Data   156

Table 7. Tailored Corrugated Panel (P= 15.0 psi L = 28 in)

	Nx= 10 (lb/in)	Nx= 100 (lb/in)	Nx=350 (lb/in)	Nx=1000 (lb/in)	Nx=2800 (lb/in)	Nx=10000 (lb/in)	Nx=26000 (lb/in)
$\dfrac{N_{xy}}{N_x} = 0.0$							
B_1 (in.)[*]	0.3496	0.2723		0.2747		0.6035	0.8240
B_2	2.0120	1.9596		1.6659		2.1969	2.2890
Angle, θ	39.0	43.6	n/c	52.1	n/c	57.6	65.6
T_1 (in.)[**]	0.0050	0.0050		0.0050		0.01042	0.0126
T_2	0.0209	0.0241		0.0373		0.07885	0.1514
$\dfrac{W}{LA}(10^{-4}$ lb/in^3)	0.7516	0.7912		1.1040		2.8369	5.4679
$\dfrac{N_{xy}}{N_x} = 0.3$							
B_1 (in.)[*]	0.3760	0.3831		0.6301		1.2308	1.7957
B_2	1.7829	1.6455		1.6461		2.1594	2.2884
Angle, θ	43.6	45.6	n/c	48.6	n/c	56.1	58.1
T_1 (in.)[**]	0.0050	0.0050		0.0084		0.0213	0.0303
T_2	0.01803	0.01967		0.0252		0.0560	0.1212
$\dfrac{W}{LA}(10^{-4}$ lb/in^3)	0.7755	0.8325		1.3934		3.7241	6.7124
$\dfrac{N_{xy}}{N_x} = 0.6$							
B_1 (in.)[*]	0.3689	0.4014		0.7183		1.1091	1.4075
B_2	1.7802	1.5201		1.6968		2.7069	3.2037
Angle, θ	44.1	47.5	n/c	49.1	n/c	51.8	41.0
T_1 (in.)[**]	0.0050	0.0050		0.0104		0.0312	0.0591
T_2	0.0183	0.0200		0.0247		0.0736	0.1454
$\dfrac{W}{LA}(10^{-4}$ lb/in^3)	0.7813	0.8738		1.6125		4.4839	8.7234
$\dfrac{N_{xy}}{N_x} = 1.0$							
B_1 (in.)[*]	0.3645	0.4441		0.8303		1.4472	1.6979
B_2	1.7751	1.5444		1.7685		2.3634	3.5883
Angle, θ	40.9	45.8	n/c	49.4	n/c	52.4	37.1
T_1 (in.)[**]	0.0050	0.0056		0.0126		0.0347	0.0985
T_2	0.0204	0.0206		0.0251		0.0588	0.1206
$\dfrac{W}{LA}(10^{-4}$ lb/in^3)	0.7857	0.9431		1.8487		5.0225	11.6148

[*] Reference dimensions to Figure 83.
[**] Minimum gage ply thickness = 0.005 inches.
n/c Loading condition not considered.

Table 8. Tailored Corrugated Panel (P= 30.0 psi   L= 28 in)

	Nx= 10 (lb/in)	Nx= 100 (lb/in)	Nx= 350 (lb/in)	Nx=1000 (lb/in)	Nx=2800 (lb/in)	Nx=10000 (lb/in)	Nx=28000 (lb/in)
$\dfrac{N_{xy}}{N_x} = 0.0$ B_1 (in.)[x] B_2 Angle, θ T_1 (in.)[xx] T_2 $\dfrac{W}{LA}(10^{-4}$ lb/in^3)	0.3391 2.0310 46.9 0.0050 0.0353 1.0056	0.3458 2.0151 47.4 0.0050 0.0363 1.0376	n/c	0.3915 2.0676 50.4 0.0060 0.0439 1.3250	n/c	0.5211 2.2407 61.4 0.0106 0.0931 3.2097	0.8034 2.2773 66.5 0.0132 0.1566 5.7346
$\dfrac{N_{xy}}{N_x} = 0.3$ B_1 (in.)[x] B_2 Angle, θ T_1 (in.)[xx] T_2 $\dfrac{W}{LA}(10^{-4}$ lb/in^3)	n/c	n/c	n/c	0.7219 1.6431 53.4 0.0081 0.0338 1.6598	n/c	1.5036 2.0229 60.4 0.0200 0.0627 3.9573	1.7823 2.4312 58.2 0.0315 0.1304 7.0732
$\dfrac{N_{xy}}{N_x} = 0.6$ B_1 (in.)[x] B_2 Angle, θ T_1 (in.)[xx] T_2 $\dfrac{W}{LA}(10^{-4}$ lb/in^3)	n/c	n/c	n/c	0.8343 1.6206 55.3 0.0099 0.0355 1.9505	n/c	1.6305 2.0802 59.4 0.0252 0.0650 4.5354	1.8752 4.1460 34.1 0.0594 0.1599 8.7170
$\dfrac{N_{xy}}{N_x} = 1.0$ B_1 (in.)[x] B_2 Angle, θ T_1 (in.)[xx] T_2 $\dfrac{W}{LA}(10^{-4}$ lb/in^3)	0.4941 2.2911 43.8 0.0065 0.0283 1.0929	0.5952 2.0394 45.9 0.0070 0.0281 1.2239	n/c	0.8942 1.7478 53.1 0.0120 0.0343 2.1014	n/c	1.6493 2.5335 51.6 0.0367 0.0632 5.3158	2.4869 4.5636 30.3 0.0983 0.1290 11.4945

[x] Reference dimensions to Figure 83.
[xx] Minimum gage ply thickness = 0.005 inches.
n/c Loading condition not considered.

Table 9. Tailored Corrugated Panel (P = 45.0 psi L = 28 in)

	Nx = 10 (lb/in)	Nx = 100 (lb/in)	Nx = 350 (lb/in)	Nx = 1000 (lb/in)	Nx = 2000 (lb/in)	Nx = 10000 (lb/in)	Nx = 28000 (lb/in)
$\frac{N_{xy}}{N_x} = 0.0$ B_1 (in.)* B_2 Angle, θ T_1 (in.)** T_2 $\frac{W}{LA}(10^{-4}$ lb/in^3)	0.4539 2.7393 44.5 0.0068 0.0417 1.2421	0.3810 2.3552 48.7 0.0058 0.0464 1.2637	n/c	0.4028 2.2107 50.4 0.0061 0.0575 1.5317	n/c	0.5497 2.3556 59.4 0.0116 0.1050 3.4679	0.8815 2.4753 67.0 0.0149 0.1667 6.2701
$\frac{N_{xy}}{N_x} = 0.3$ B_1 (in.)* B_2 Angle, θ T_1 (in.)** T_2 $\frac{W}{LA}(10^{-4}$ lb/in^3)	n/c	n/c	n/c	n/c	n/c	n/c	n/c
$\frac{N_{xy}}{N_x} = 0.6$ B_1 (in.)* B_2 Angle, θ T_1 (in.)** T_2 $\frac{W}{LA}(10^{-4}$ lb/in^3)	n/c	n/c	n/c	n/c	n/c	n/c	n/c
$\frac{N_{xy}}{N_x} = 1.0$ B_1 (in.)* B_2 Angle, θ T_1 (in.)** T_2 $\frac{W}{LA}(10^{-4}$ lb/in^3)	0.6517 2.4288 50.3 0.0068 0.0318 1.3102	0.6809 2.2050 50.3 0.0073 0.0355 1.4798	n/c	1.0198 1.8159 57.8 0.0124 0.0410 2.4268	n/c	2.0717 2.2791 67.4 0.0345 0.0581 5.5476	1.3728 6.2283 25.0 0.0984 0.2269 11.5907

* Reference dimensions to Figure 83.
** Minimum gage ply thickness = 0.005 inches.
n/c Loading condition not considered.

Table 10. Tailored Corrugated Panel - Discrete Ply Thickness (P= 0.0 psi L= 28 in)

	Nx= 10 (lb/in)	Nx= 100 (lb/in)	Nx= 350 (lb/in)	Nx= 1000 (lb/in)	Nx= 2800 (lb/in)	Nx= 10000 (lb/in)	Nx= 28000 (lb/in)
$\dfrac{N_{xy}}{N_x} = 0.0$ B_1 (in.)[x] B_2 Angle, θ T_1 (in.)[xx] T_2 $\dfrac{W}{LA}(10^{-4}$ lb/in³)	0.1000 5.4424 3.46 0.0050 0.0050 0.4151	n/c	n/c	0.4572 1.4769 44.5 0.0050 0.0150 0.7785	n/c	n/c	1.8412 2.6714 71.6 0.0150 0.1050 5.1923
$\dfrac{N_{xy}}{N_x} = 0.3$ B_1 (in.)[x] B_2 Angle, θ T_1 (in.)[xx] T_2 $\dfrac{W}{LA}(10^{-4}$ lb/in³)	n/c	n/c	n/c	n/c	n/c	n/c	n/c
$\dfrac{N_{xy}}{N_x} = 0.6$ B_1 (in.)[x] B_2 Angle, θ T_1 (in.)[xx] T_2 $\dfrac{W}{LA}(10^{-4}$ lb/in³)	n/c	n/c	n/c	n/c	n/c	n/c	n/c
$\dfrac{N_{xy}}{N_x} = 1.0$ B_1 (in.)[x] B_2 Angle, θ T_1 (in.)[xx] T_2 $\dfrac{W}{LA}(10^{-4}$ lb/in³)	0.1000 3.1486 6.3 0.0050 0.0050 0.4217	n/c	n/c	0.7418 1.9797 35.1 0.0150 0.0150 1.6548	n/c	n/c	3.2536 2.5876 39.9 0.1000 0.0750 11.0607

[x] Reference dimensions to Figure 83.
[xx] Minimum gage ply thickness = 0.005 inches.
n/c Loading condition not considered.

Table 11. Tailored Corrugated Panel - 0° Plies in Web (P= 0.0 psi   L= 28 in)

	Nx= 10 (lb/in)	Nx= 100 (lb/in)	Nx= 350 (lb/in)	Nx= 1000 (lb/in)	Nx= 2800 (lb/in)	Nx= 10000 (lb/in)	Nx= 28000 (lb/in)
$\dfrac{N_{xy}}{N_x} = 0.0$							
B_1 (in.)*	0.1000	0.1620		0.5609		1.0337	1.0425
B_2	5.7454	2.0543		1.4008		1.9346	2.0354
Angle, θ	2.98	20.7	n/c	49.1	n/c	60.0	69.7
T_1 (in.)**	0.0050	0.0050		0.0050		0.0126	0.0126
T_2	0.0050	0.0050		0.0118		0.0366	0.0970
T_3	0.0005	0.0005		0.0001		0.0048	0.0148
$\dfrac{W}{LA}$(10⁻⁴ lb/in³)	0.4357	0.4805		0.7708		2.4968	4.9020
$\dfrac{N_{xy}}{N_x} = 0.3$							
B_1 (in.)*							
B_2							
Angle, θ	n/c	n/c	n/c	n/c	n/c	n/c	n/c
T_1 (in.)**							
T_2							
$\dfrac{W}{LA}$(10⁻⁴ lb/in³)							
$\dfrac{N_{xy}}{N_x} = 0.6$							
B_1 (in.)*							
B_2							
Angle, θ	n/c	n/c	n/c	n/c	n/c	n/c	n/c
T_1 (in.)**							
T_2							
$\dfrac{W}{LA}$(10⁻⁴ lb/in³)							
$\dfrac{N_{xy}}{N_x} = 1.0$							
B_1 (in.)*	0.1000	0.6033		0.8186		1.5127	2.5221
B_2	3.1466	1.5928		1.2517		2.1953	4.1288
Angle, θ	5.3	25.3	n/c	58.5	n/c	52.3	26.7
T_1 (in.)**	0.0050	0.0050		0.0050		0.0353	0.1002
T_2	0.0050	0.0050		0.0180		0.0376	0.0677
T_3	0.0005	0.0010		0.0138		0.0191	0.0378
$\dfrac{W}{LA}$(10⁻⁴ lb/in³)	0.4409	0.5585		1.3449		4.8845	10.8869

* Reference dimensions to Figure 83.
** Minimum gage ply thickness = 0.005 inches.
n/c Loading condition not considered.

Table 12.   Tailored Corrugated Panel - Bead Ratio = 1.0   (P= 0.0 psi   L= 28 in)

	Nx= 10 (lb/in)	Nx= 100 (lb/in)	Nx=350 (lb/in)	Nx=1000 (lb/in)	Nx=2800 (lb/in)	Nx=10000 (lb/in)	Nx=28000 (lb/in)
$\dfrac{N_{xy}}{N_x}=0.0$							
B_1 (in.)*	3.8063	1.2937		0.6690		0.9939	1.3721
B_2	3.7687	1.3500		1.1992		1.8725	2.0925
B_3	0.1000	0.2474		0.4551		0.9023	1.2633
Angle, θ	4.7	29.9	n/c	68.1	n/c	73.1	69.3
T_1 (in.)**	0.0050	0.0050		0.0050		0.0100	0.0116
T_2	0.0050	0.0050		0.0107		0.0414	0.1211
$\dfrac{W}{LA}$(10⁻⁴ lb/in³)	0.5109	0.5470		0.9273		2.5837	5.0122
$\dfrac{N_{xy}}{N_x}=0.3$							
B_1 (in.)*	3.4213	1.1649		0.8509		1.3886	2.3460
B_2	3.3830	1.2149		0.9572		1.7188	2.1761
B_3	0.1000	0.2731		1.0316		1.5810	2.1037
Angle, θ	4.77	32.2	n/c	69.5	n/c	69.6	56.5
T_1 (in.)**	0.0050	0.0050		0.0055		0.0184	0.0296
T_2	0.0050	0.0050		0.0139		0.0387	0.1115
$\dfrac{W}{LA}$(10⁻⁴ lb/in³)	0.5111	0.5535		1.0718		3.3369	6.1486
$\dfrac{N_{xy}}{N_x}=0.6$							
B_1 (in.)*	3.2035	1.0649		1.0534		1.5986	3.0402
B_2	3.1661	1.2626		1.0714		1.6588	2.7023
B_3	0.1000	0.1723		1.2677		2.1954	2.1242
Angle, θ	5.11	39.2	n/c	66.9	n/c	72.4	42.9
T_1 (in.)**	0.0050	0.0050		0.0075		0.0217	0.0591
T_2	0.0050	0.0050		0.0153		0.0446	0.1047
$\dfrac{W}{LA}$(10⁻⁴ lb/in³)	0.5113	0.5715		1.2951		3.9428	8.2657
$\dfrac{N_{xy}}{N_x}=1.0$							
B_1 (in.)*	2.7889	1.1065		1.5859		1.8315	3.5851
B_2	2.7560	1.2799		1.2255		1.8204	2.9406
B_2	0.1000	0.2661		1.7271		2.1554	2.6220
Angle, θ	6.38	40.5	n/c	53.9	n/c	65.5	39.3
T_1 (in.)**	0.0050	0.0050		0.0095		0.0333	0.0988
T_2	0.0050	0.0066		0.0241		0.0483	0.0838
$\dfrac{W}{LA}$(10⁻⁴ lb/in³)	0.5120	0.6139		1.6573		5.0605	11.1200

* Reference dimensions to Figure 83.
** Minimum gage ply thickness = 0.005 inches.
n/c Loading condition not considered.

Table 13. Tailored Corrugated Panel - Bead Ratio = 3.0 (P= 0.0 psi   L= 28 in)

	Nx= 10 (lb/in)	Nx= 100 (lb/in)	Nx= 350 (lb/in)	Nx= 1000 (lb/in)	Nx= 2800 (lb/in)	Nx= 10000 (lb/in)	Nx= 28000 (lb/in)
$\dfrac{N_{xy}}{N_x} = 0.0$							
B_1 (in.)*	5.2567	1.7136		0.7576		1.1372	1.6476
B_2	1.7066	0.6977		1.0963		1.7720	2.2689
B_3	0.1235	0.2901		0.3050		0.5015	0.7310
Angle, θ	7.9	52.3	n/c	84.8	n/c	85.8	85.3
T_1 (in.)**	0.0050	0.0050		0.0050		0.0093	0.0143
T_2	0.0050	0.0050		0.0100		0.0408	0.0587
T_3	0.0040	0.0030		0.0002		0.0041	0.0040
$\dfrac{W}{LA}$ (10⁻⁴ lb/in³)	0.6050	0.6587		1.1873		3.3014	5.6393
$\dfrac{N_{xy}}{N_x} = 0.3$							
B_1 (in.)*	4.2161	1.6555		0.9238		1.3541	2.2512
B_2	1.3984	0.6961		0.9810		1.5374	2.0181
B_3	0.1000	0.2829		0.4159		0.6578	1.1162
Angle, θ	14.2	53.9	n/c	84.1	n/c	85.4	84.5
T_1 (in.)**	0.0050	0.0050		0.0050		0.0100	0.0305
T_2	0.0050	0.0070		0.0151		0.0495	0.0765
T_3	0.0005	0.0006		0.0010		0.0125	0.0059
$\dfrac{W}{LA}$ (10⁻⁴ lb/in³)	0.5702	0.7001		1.2965		3.7583	7.0778
$\dfrac{N_{xy}}{N_x} = 0.6$							
B_1 (in.)*	3.9167	1.5193		1.0170		1.8724	2.9187
B_2	1.3824	0.7361		1.0501		1.6592	2.1757
B_3	0.1000	0.2380		0.4780		0.8890	1.1354
Angle, θ	24.7	58.2	n/c	84.5	n/c	83.7	79.2
T_1 (in.)**	0.0050	0.0050		0.0050		0.0213	0.0604
T_2	0.0050	0.0068		0.0180		0.0561	0.0582
T_3	0.0005	0.0012		0.0038		0.0231	0.0189
$\dfrac{W}{LA}$ (10⁻⁴ lb/in³)	0.5775	0.7198		1.4948		4.8834	9.7141
$\dfrac{N_{xy}}{N_x} = 1.0$							
B_1 (in.)*	3.5256	1.6116		1.5262		2.1642	3.7256
B_2	1.2557	0.8057		1.2701		1.6491	2.1874
B_3	0.1000	0.1504		0.4026		1.0027	1.1877
Angle, θ	26.3	55.0	n/c	76.0	n/c	82.3	72.8
T_1 (in.)**	0.0050	0.0050		0.0071		0.0356	0.1004
T_2	0.0050	0.0080		0.0246		0.0485	0.0514
T_3	0.0005	0.0040		0.0101		0.0155	0.0358
$\dfrac{W}{LA}$ (10⁻⁴ lb/in³)	0.5791	0.8033		1.9544		6.5213	13.1678

* Reference dimensions to Figure 83.
** Minimum gage ply thickness = 0.005 inches.
n/c Loading condition not considered.

	Nx = 10 (lb/in)	Nx = 100 (lb/in)	Nx = 350 (lb/in)	Nx = 1000 (lb/in)	Nx = 2800 (lb/in)	Nx = 10000 (lb/in)	Nx = 28000 (lb/in)
$\dfrac{N_{xy}}{N_x} = 0.0$							
B_1 (in.)*	5.3129			0.7684			1.9961
B_2	0.6180			1.1597			2.3303
B_3	0.1455			0.1335			0.2971
Angle, θ	42.1	n/c	n/c	89.5	n/c	n/c	88.7
T_1 (in.)**	0.0050			0.0050			0.0168
T_2	0.0050			0.0079			0.0844
T_3	0.0005			0.0017			0.0251
$\dfrac{W}{LA}(10^{-4}$ lb/in$^3)$	0.6082			1.3733			7.2291
$\dfrac{N_{xy}}{N_x} = 0.3$							
B_1 (in.)*				1.5090			3.3804
B_2				0.9993			2.3944
B_3				0.1018			0.4110
Angle, θ	n/c	n/c	n/c	84.2	n/c	n/c	86.8
T_1 (in.)**				0.0050			0.0296
T_2				0.0232			0.1261
T_3				0.0080			0.0165
$\dfrac{W}{LA}(10^{-4}$ lb/in$^3)$				1.7192			9.2584
$\dfrac{N_{xy}}{N_x} = 0.6$							
B_1 (in.)*				1.4455			3.2343
B_2				1.1190			2.3412
B_3				0.1980			0.4469
Angle, θ	n/c	n/c	n/c	87.7	n/c	n/c	87.6
T_1 (in.)**				0.0069			0.0596
T_2				0.0202			0.0722
T_3				0.0055			0.0289
$\dfrac{W}{LA}(10^{-4}$ lb/in$^3)$				1.8976			11.5487
$\dfrac{N_{xy}}{N_x} = 1.0$							
B_1 (in.)*				1.5955			4.1304
B_2				1.3733			2.2185
B_3				0.1527			0.5289
Angle, θ	n/c	n/c	n/c	86.5	n/c	n/c	86.1
T_1 (in.)**				0.0067			0.0981
T_2				0.0299			0.0635
T_3				0.0084			0.0606
$\dfrac{W}{LA}(10^{-4}$ lb/in$^3)$				2.3709			15.3326

* Reference dimensions to Figure 83.
** Minimum gage ply thickness = 0.005 inches.
n/c Loading condition not considered.

Appendix B. Hat Stiffened Panel Data

Figure 84. Hat Stiffened Panel Model

Table 15. Hat Stiffened Panel (P= 0.0 psi   L= 28 in)

	Nx = 10 (lb/in)	Nx = 100 (lb/in)	Nx = 350 (lb/in)	Nx = 1000 (lb/in)	Nx = 2800 (lb/in)	Nx = 10000 (lb/in)	Nx = 28000 (lb/in)
$\dfrac{N_{xy}}{N_x} = 0.0$							
B_1 (in.)*	0.1000	0.1000	0.1000	0.1000	0.3940	0.3914	0.5013
B_2	8.5988	2.6454	1.5681	1.2899	1.2691	1.5111	1.7568
B_3	0.1000	0.1000	0.1832	0.3358	0.6086	1.0105	1.0549
Angle, θ	2.0	10.6	29.5	49.7	69.4	80.5	75.9
T_1 (in.)**	0.0050	0.0050	0.0050	0.0050	0.0050	0.0074	0.0097
T_2	0.0050	0.0050	0.0050	0.0050	0.0050	0.0089	0.0254
T_3	0.0050	0.0050	0.0050	0.0108	0.0217	0.0314	0.0910
T_4	0.0050	0.0050	0.0050	0.0050	0.0056	0.0056	0.0050
T_5	0.0050	0.0050	0.0050	0.0050	0.0050	0.0165	0.0423
T_6	0.0050	0.0050	0.0050	0.0050	0.0050	0.0050	0.0050
$\dfrac{W}{LA}(10^{-4}$ lb/in$^3)$	1.2252	1.2392	1.2995	1.4747	1.8185	3.2898	5.5260
$\dfrac{N_{xy}}{N_x} = 0.3$							
B_1 (in.)*	0.1000	0.1000	0.1238	0.1294	0.1964	0.3626	0.4038
B_2	7.9686	2.4558	1.5685	1.1383	1.0972	1.5692	1.8213
B_3	0.1000	0.1000	0.3608	0.5063	0.6189	0.8687	1.1525
Angle, θ	1.4	11.5	35.5	51.2	67.8	69.0	60.3
T_1 (in.)**	0.0050	0.0050	0.0050	0.0050	0.0066	0.0130	0.0196
T_2	0.0050	0.0050	0.0050	0.0050	0.0050	0.0050	0.0173
T_3	0.0050	0.0050	0.0050	0.0101	0.0225	0.0469	0.1000
T_4	0.0050	0.0050	0.0050	0.0050	0.0050	0.0088	0.0170
T_5	0.0050	0.0050	0.0050	0.0050	0.0062	0.0195	0.0417
T_6	0.0050	0.0050	0.0050	0.0050	0.0050	0.0500	0.0050
$\dfrac{W}{LA}(10^{-4}$ lb/in$^3)$	1.2253	1.2412	1.3358	1.4977	2.1533	4.2195	7.1500
$\dfrac{N_{xy}}{N_x} = 0.6$							
B_1 (in.)*	0.1000	0.1000	0.1095	0.1000	0.1629	0.2822	0.1000
B_2	7.0656	2.2686	1.3810	0.9428	1.1234	1.5403	2.1722
B_3	0.1000	0.1000	0.3415	0.7379	0.7126	0.9572	1.2461
Angle, θ	2.7	13.1	34.0	56.2	65.6	66.3	44.0
T_1 (in.)**	0.0050	0.0050	0.0050	0.0050	0.0084	0.0154	0.0262
T_2	0.0050	0.0050	0.0050	0.0050	0.0050	0.0050	0.1667
T_3	0.0050	0.0050	0.0050	0.0091	0.0197	0.0386	0.1111
T_4	0.0050	0.0050	0.0050	0.0050	0.0056	0.0122	0.0390
T_5	0.0050	0.0050	0.0050	0.0050	0.0090	0.0202	0.0293
T_6	0.0050	0.0050	0.0050	0.0050	0.0050	0.0050	0.0050
$\dfrac{W}{LA}(10^{-4}$ lb/in$^3)$	1.2258	1.2446	1.3289	1.5551	2.4920	4.7014	8.8097
$\dfrac{N_{xy}}{N_x} = 1.0$							
B_1 (in.)*	0.1000	0.1000	0.1000	0.1087	0.1662	0.1000	0.1000
B_2	5.7727	1.8798	1.2784	0.9562	1.2466	1.6128	2.7123
B_3	0.1000	0.1000	0.5890	0.6660	0.7836	0.8694	1.4018
Angle, θ	1.7	16.2	33.3	59.3	63.7	58.3	32.0
T_1 (in.)**	0.0050	0.0050	0.0050	0.0061	0.0061	0.0175	0.0352
T_2	0.0050	0.0050	0.0050	0.0050	0.0050	0.0594	0.2089
T_3	0.0050	0.0050	0.0050	0.0098	0.0098	0.0348	0.1152
T_4	0.0050	0.0050	0.0080	0.0050	0.0050	0.0241	0.0687
T_5	0.0050	0.0050	0.0050	0.0050	0.0050	0.0123	0.0219
T_6	0.0050	0.0050	0.0050	0.0050	0.0050	0.0050	0.0050
$\dfrac{W}{LA}(10^{-4}$ lb/in$^3)$	1.2268	1.2526	1.5790	1.7225	2.9543	5.5072	11.2702

* Reference dimensions to Figure 84.
** Minimum gage ply thickness = 0.005 inches.

Table 16. Hat Stiffened Panel - No VICON Corrections (P= 0.0 psi   L= 28 in)

	Nx= 10 (lb/in)	Nx= 100 (lb/in)	Nx= 350 (lb/in)	Nx= 1000 (lb/in)	Nx= 2800 (lb/in)	Nx= 10000 (lb/in)	Nx= 28000 (lb/in)
$\frac{N_{xy}}{N_x} = 0.0$							
B_1 (in.)*	n/c	n/c	n/c	n/c	n/c	n/c	n/c
B_2							
B_3							
Angle, θ							
T_1 (in.)**							
T_2							
T_3							
T_4							
T_5							
T_6							
$\frac{W}{LA}$ (10⁻⁴ lb/in³)							
$\frac{N_{xy}}{N_x} = 0.3$							
B_1 (in.)*	n/c	n/c	0.1000	0.1247	0.2047	0.1987	0.4991
B_2			1.4615	1.1421	1.1421	1.4702	1.7841
B_3			0.2898	0.5341	0.5341	0.7940	1.2809
Angle, θ			32.1	52.0	66.5	67.3	60.3
T_1 (in.)**			0.0050	0.0050	0.0070	0.0123	0.0192
T_2			0.0050	0.0050	0.0050	0.0145	0.0050
T_3			0.0050	0.0101	0.0232	0.0434	0.0970
T_4			0.0050	0.0050	0.0050	0.0088	0.0174
T_5			0.0050	0.0050	0.0067	0.0183	0.0441
T_6			0.0050	0.0050	0.0050	0.0050	0.0050
$\frac{W}{LA}$ (10⁻⁴ lb/in³)			1.3167	1.5080	2.2034	4.1580	6.9719
$\frac{N_{xy}}{N_x} = 0.6$							
B_1 (in.)*	n/c	n/c	0.2433	0.1000	0.1645	0.2732	0.1000
B_2			1.3769	0.9790	1.1107	1.4832	2.0473
B_3			0.5096	0.6999	0.7039	0.9278	1.3404
Angle, θ			30.7	55.9	65.9	65.9	38.4
T_1 (in.)**			0.0050	0.0052	0.0083	0.0152	0.0255
T_2			0.0050	0.0050	0.0050	0.0051	0.3672
T_3			0.0050	0.0097	0.0196	0.0379	0.0911
T_4			0.0050	0.0050	0.0056	0.0116	0.0385
T_5			0.0050	0.0050	0.0088	0.0204	0.0266
T_6			0.0050	0.0050	0.0050	0.0050	0.0050
$\frac{W}{LA}$ (10⁻⁴ lb/in³)			1.3286	1.5828	2.4685	4.6062	8.5673
$\frac{N_{xy}}{N_x} = 1.0$							
B_1 (in.)*	n/c	n/c	0.2368	0.1031	0.1662	0.1000	0.1000
B_2			1.1276	0.9685	1.1369	1.6193	2.5959
B_3			0.5948	0.6685	0.7221	0.8465	1.5772
Angle, θ			35.9	59.1	65.0	55.7	30.1
T_1 (in.)**			0.0050	0.0062	0.0097	0.0177	0.0343
T_2			0.0050	0.0052	0.0051	0.1525	0.2241
T_3			0.0050	0.0098	0.0179	0.0340	0.0984
T_4			0.0050	0.0051	0.0073	0.0246	0.0687
T_5			0.0050	0.0051	0.0091	0.0084	0.0233
T_6			0.0050	0.0051	0.0050	0.0050	0.0050
$\frac{W}{LA}$ (10⁻⁴ lb/in³)			1.3567	1.7662	2.7657	5.4858	11.1539

* Reference dimensions to Figure 84.
** Minimum gage ply thickness = 0.005 inches.
n/c Loading condition not considered.

Appendix B. Hat Stiffened Panel Data

Table 17. Hat Stiffened Panel (P= 5.0 psi   L= 28 in)

	Nx= 10 (lb/in)	Nx= 100 (lb/in)	Nx= 350 (lb/in)	Nx= 1000 (lb/in)	Nx= 2800 (lb/in)	Nx= 10000 (lb/in)	Nx= 28000 (lb/in)
$\dfrac{N_{xy}}{N_x} = 0.0$							
B_1 (in.)*	0.4303	0.6289		0.7768			
B_2	1.4775	1.4691		1.4937			
B_3	0.1000	0.1436		0.1425			
Angle, θ	39.6	43.8	n/c	62.7	n/c	n/c	n/c
T_1 (in.)**	0.0050	0.0050		0.0050			
T_2	0.0050	0.0050		0.0050			
T_3	0.0363	0.0295		0.0451			
T_4	0.0050	0.0050		0.0050			
T_5	0.0050	0.0050		0.0050			
T_6	0.0050	0.0050		0.0050			
$\dfrac{W}{LA}$(10^{-4} lb/in³)	1.4068	1.4376		1.6250			
$\dfrac{N_{xy}}{N_x} = 0.3$							
B_1 (in.)*							
B_2							
B_3							
Angle, θ	n/c	n/c	n/c	n/c	n/c	n/c	n/c
T_1 (in.)**							
T_2							
T_3							
T_4							
T_5							
T_6							
$\dfrac{W}{LA}$(10^{-4} lb/in³)							
$\dfrac{N_{xy}}{N_x} = 0.6$							
B_1 (in.)*							
B_2							
B_3							
Angle, θ	n/c	n/c	n/c	n/c	n/c	n/c	n/c
T_1 (in.)**							
T_2							
T_3							
T_4							
T_5							
T_6							
$\dfrac{W}{LA}$(10^{-4} lb/in³)							
$\dfrac{N_{xy}}{N_x} = 1.0$							
B_1 (in.)*	0.6769	0.3782		0.2351			
B_2	1.5387	1.3380		0.9249			
B_3	0.1088	0.1294		0.4551			
Angle, θ	40.3	44.1	n/c	73.2	n/c	n/c	n/c
T_1 (in.)**	0.0050	0.0050		0.0051			
T_2	0.0050	0.0050		0.0050			
T_3	0.0381	0.0287		0.0185			
T_4	0.0050	0.0050		0.0050			
T_5	0.0050	0.0050		0.0050			
T_6	0.0050	0.0050		0.0050			
$\dfrac{W}{LA}$(10^{-4} lb/in³)	1.4162	1.4394		1.9036			

* Reference dimensions to Figure 84.
** Minimum gage ply thickness = 0.005 inches.
n/c Loading condition not considered.

Table 18. Hat Stiffened Panel (P= 10.0 psi   L= 28 in)

	Nx= 10 (lb/in)	Nx= 100 (lb/in)	Nx= 350 (lb/in)	Nx= 1000 (lb/in)	Nx= 2800 (lb/in)	Nx= 10000 (lb/in)	Nx= 28000 (lb/in)
$\frac{N_{xy}}{N_x} = 0.0$							
B_1 (in.)*	1.1276	0.9765		0.7768			
B_2	1.7316	1.5564		1.4937			
B_3	0.1659	0.2345		0.1425			
Angle, θ	53.7	55.5	n/c	62.7	n/c	n/c	n/c
T_1 (in.)**	0.0050	0.0050		0.0050			
T_2	0.0050	0.0050		0.0050			
T_3	0.0475	0.0338		0.0451			
T_4	0.0050	0.0050		0.0050			
T_5	0.0050	0.0050		0.0050			
T_6	0.0050	0.0050		0.0050			
$\frac{W}{LA}$ (10^{-4} lb/in^3)	1.5241	1.5432		1.6250			
$\frac{N_{xy}}{N_x} = 0.3$							
B_1 (in.)*							
B_2							
B_3							
Angle, θ	n/c	n/c	n/c	n/c	n/c	n/c	n/c
T_1 (in.)**							
T_2							
T_3							
T_4							
T_5							
T_6							
$\frac{W}{LA}$ (10^{-4} lb/in^3)							
$\frac{N_{xy}}{N_x} = 0.6$							
B_1 (in.)*							
B_2							
B_3							
Angle, θ	n/c	n/c	n/c	n/c	n/c	n/c	n/c
T_1 (in.)**							
T_2							
T_3							
T_4							
T_5							
T_6							
$\frac{W}{LA}$ (10^{-4} lb/in^3)							
$\frac{N_{xy}}{N_x} = 1.0$							
B_1 (in.)*	0.8698	0.8464		0.4542			
B_2	1.4988	1.5180		1.0080			
B_3	0.1423	0.1000		0.4669			
Angle, θ	51.5	54.4	n/c	75.8	n/c	n/c	n/c
T_1 (in.)**	0.0050	0.0050		0.0054			
T_2	0.0050	0.0050		0.0050			
T_3	0.0573	0.0808		0.0277			
T_4	0.0050	0.0050		0.0051			
T_5	0.0050	0.0050		0.0050			
T_6	0.0050	0.0050		0.0050			
$\frac{W}{LA}$ (10^{-4} lb/in^3)	1.5277	1.5562		2.0000			

* Reference dimensions to Figure 84.
** Minimum gage ply thickness = 0.005 inches.
n/c Loading condition not considered.

Appendix B. Hat Stiffened Panel Data

170

Table 19. Hat Stiffened Panel (P= 15.0 psi   L= 28 in)

	Nx = 10 (lb/in)	Nx = 100 (lb/in)	Nx = 350 (lb/in)	Nx = 1000 (lb/in)	Nx = 2800 (lb/in)	Nx = 10000 (lb/in)	Nx = 28000 (lb/in)
$\dfrac{N_{xy}}{N_x} = 0.0$							
B_1 (in.)*	0.8942	0.8254		0.6591		0.4536	0.7608
B_2	1.6155	1.4631		1.5696		1.6056	2.0562
B_3	0.2890	0.3839		0.2400		0.6815	2.6562
Angle, θ	60.8	62.9	n/c	70.5	n/c	77.5	72.9
T_1 (in.)**	0.0050	0.0050		0.0050		0.0071	0.0107
T_2	0.0050	0.0050		0.0050		0.0111	0.0165
T_3	0.0344	0.0266		0.0350		0.0599	0.1358
T_4	0.0050	0.0050		0.0050		0.0050	0.0050
T_5	0.0050	0.0050		0.0050		0.0220	0.0538
T_6	0.0050	0.0050		0.0050		0.0050	0.0050
$\dfrac{W}{LA}$(10⁻⁴ lb/in³)	1.6158	1.6367		1.7821		3.6058	6.0113
$\dfrac{N_{xy}}{N_x} = 0.3$							
B_1 (in.)*	0.9709	0.8587		0.5878		0.5993	0.1000
B_2	1.6713	1.5456		1.3569		1.5798	1.8474
B_3	0.3364	0.2167		0.2007		0.7503	1.1258
Angle, θ	62.7	61.1	n/c	69.7	n/c	72.2	54.5
T_1 (in.)**	0.0050	0.0050		0.0050		0.0125	0.0198
T_2	0.0050	0.0050		0.0050		0.0050	0.3906
T_3	0.0287	0.0466		0.0535		0.0559	0.0781
T_4	0.0050	0.0050		0.0050		0.0079	0.0166
T_5	0.0050	0.0050		0.0050		0.0253	0.0433
T_6	0.0050	0.0050		0.0050		0.0500	0.0050
$\dfrac{W}{LA}$(10⁻⁴ lb/in³)	1.6221	1.6336		1.8245		4.3361	7.6008
$\dfrac{N_{xy}}{N_x} = 0.6$							
B_1 (in.)*	0.9125	0.6860		0.5222		0.3284	0.1000
B_2	1.6130	1.4271		1.1043		1.6185	2.3670
B_3	0.2174	0.2468		0.3965		0.8638	1.6312
Angle, θ	60.2	58.7	n/c	73.0	n/c	65.6	41.1
T_1 (in.)**	0.0050	0.0050		0.0050		0.0152	0.0282
T_2	0.0050	0.0050		0.0050		0.0050	0.2369
T_3	0.0466	0.0734		0.0323		0.0445	0.0842
T_4	0.0050	0.0050		0.0050		0.0139	0.0389
T_5	0.0050	0.0050		0.0050		0.0259	0.0419
T_6	0.0050	0.0050		0.0050		0.0050	0.0097
$\dfrac{W}{LA}$(10⁻⁴ lb/in³)	1.6177	1.6390		1.8773		5.0459	9.4565
$\dfrac{N_{xy}}{N_x} = 1.0$							
B_1 (in.)*	0.7259	0.6579		0.5006		0.3466	0.1000
B_2	1.5117	1.4766		1.1091		1.7817	2.7258
B_3	0.2525	0.1733		0.4746		0.9975	1.4453
Angle, θ	60.1	60.6	n/c	76.6	n/c	59.6	37.1
T_1 (in.)**	0.0050	0.0050		0.0058		0.0182	0.0393
T_2	0.0050	0.0050		0.0050		0.0050	0.1287
T_3	0.0375	0.0547		0.0320		0.0417	0.1045
T_4	0.0050	0.0050		0.0053		0.0258	0.0707
T_5	0.0050	0.0050		0.0050		0.0205	0.0340
T_6	0.0050	0.0050		0.0050		0.0050	0.0050
$\dfrac{W}{LA}$(10⁻⁴ lb/in³)	1.6254	1.6518		2.1287		5.8904	11.8563

* Reference dimensions to Figure 84.
** Minimum gage ply thickness = 0.005 inches.
n/c Loading condition not considered.

Appendix B. Hat Stiffened Panel Data

Table 20. Hat Stiffened Panel (P= 30.0 psi L= 28 in)

	Nx= 10 (lb/in)	Nx= 100 (lb/in)	Nx= 350 (lb/in)	Nx= 1000 (lb/in)	Nx= 2800 (lb/in)	Nx= 10000 (lb/in)	Nx= 28000 (lb/in)
$\frac{N_{xy}}{N_x} = 0.0$							
B_1 (in.)*	0.7227	0.6819		0.6138		0.7973	1.2274
B_2	1.6680	1.5243		1.8171		1.8123	2.2764
B_3	0.2700	0.3525		0.2314		0.4623	0.9193
Angle, θ	70.0	71.4	n/c	74.9	n/c	74.1	73.0
T_1 (in.)**	0.0050	0.0050		0.0050		0.0078	0.0116
T_2	0.0050	0.0050		0.0050		0.0050	0.0096
T_3	0.0554	0.0438		0.0496		0.1056	0.1529
T_4	0.0050	0.0050		0.0050		0.0050	0.0050
T_5	0.0050	0.0050		0.0050		0.0280	0.0633
T_6	0.0050	0.0050		0.0050		0.0050	0.0050
$\frac{W}{LA}$(10^{-4} lb/in^3)	1.8500	1.8725		1.9751		3.6905	6.2051
$\frac{N_{xy}}{N_x} = 0.3$							
B_1 (in.)*				0.5255		0.7692	0.7125
B_2				1.2558		1.6620	2.1813
B_3				0.1483		0.7079	1.1945
Angle, θ	n/c	n/c	n/c	72.3	n/c	72.5	59.9
T_1 (in.)**				0.0050		0.0131	0.0224
T_2				0.0050		0.0050	0.0050
T_3				0.0985		0.0676	0.1040
T_4				0.0050		0.0064	0.0150
T_5				0.0050		0.0308	0.0660
T_6				0.0050		0.0500	0.0050
$\frac{W}{LA}$(10^{-4} lb/in^3)				2.0037		4.5035	7.8499
$\frac{N_{xy}}{N_x} = 0.6$							
B_1 (in.)*				0.5235		0.4023	0.1000
B_2				1.3854		1.7211	2.5245
B_3				0.3084		0.8749	1.6428
Angle, θ	n/c	n/c	n/c	76.4	n/c	65.1	42.2
T_1 (in.)**				0.0058		0.0160	0.0296
T_2				0.0050		0.0050	0.2411
T_3				0.0544		0.0454	0.0780
T_4				0.0050		0.0132	0.0381
T_5				0.0050		0.0317	0.0489
T_6				0.0050		0.0050	0.0103
$\frac{W}{LA}$(10^{-4} lb/in^3)				2.2261		5.2614	9.7733
$\frac{N_{xy}}{N_x} = 1.0$							
B_1 (in.)*	0.6577	0.6239		0.6075		0.3993	0.1000
B_2	1.4832	1.4691		1.3002		1.8837	2.7747
B_3	0.2469	0.1680		0.4208		1.0069	1.9568
Angle, θ	69.0	68.4	n/c	76.1	n/c	58.4	36.5
T_1 (in.)**	0.0050	0.0050		0.0063		0.0192	0.0350
T_2	0.0050	0.0050		0.0050		0.0050	0.2090
T_3	0.0640	0.0948		0.0487		0.0434	0.0820
T_4	0.0050	0.0050		0.0063		0.0247	0.0694
T_5	0.0050	0.0050		0.0058		0.0257	0.0397
T_6	0.0050	0.0050		0.0050		0.0050	0.0050
$\frac{W}{LA}$(10^{-4} lb/in^3)	1.8652	1.8846		2.3868		6.1084	12.0380

* Reference dimensions to Figure 84.
** Minimum gage ply thickness = 0.005 inches.
n/c Loading condition not considered.

Table 21. Hat Stiffened Panel (P= 45.0 psi L= 28 in)

	Nx= 10 (lb/in)	Nx= 100 (lb/in)	Nx= 350 (lb/in)	Nx= 1000 (lb/in)	Nx= 2800 (lb/in)	Nx= 10000 (lb/in)	Nx= 28000 (lb/in)
$\frac{N_{xy}}{N_x} = 0.0$							
B_1 (in.)*	0.7014	0.6674		0.5647		0.8503	1.2584
B_2	2.2593	2.0031		2.0061		1.9068	2.4078
B_3	0.2772	0.4301		0.2887		0.5837	0.8428
Angle, θ	75.8	77.9	n/c	77.7	n/c	75.4	72.4
T_1 (in.)**	0.0050	0.0050		0.0050		0.0079	0.0121
T_2	0.0050	0.0050		0.0050		0.0054	0.0121
T_3	0.0056	0.0375		0.0488		0.0850	0.1694
T_4	0.0051	0.0050		0.0052		0.0050	0.0050
T_5	0.0050	0.0050		0.0050		0.0319	0.0693
T_6	0.0050	0.0050		0.0050		0.0050	0.0050
$\frac{W}{LA}$ (10^{-4} lb/in^3)	2.0527	2.0744		2.1590		3.8590	6.4068
$\frac{N_{xy}}{N_x} = 0.3$							
B_1 (in.)*							
B_2							
B_3							
Angle, θ	n/c	n/c	n/c	n/c	n/c	n/c	n/c
T_1 (in.)**							
T_2							
T_3							
T_4							
T_5							
T_6							
$\frac{W}{LA}$ (10^{-4} lb/in^3)							
$\frac{N_{xy}}{N_x} = 0.6$							
B_1 (in.)*							
B_2							
B_3							
Angle, θ	n/c	n/c	n/c	n/c	n/c	n/c	n/c
T_1 (in.)**							
T_2							
T_3							
T_4							
T_5							
T_6							
$\frac{W}{LA}$ (10^{-4} lb/in^3)							
$\frac{N_{xy}}{N_x} = 1.0$							
B_1 (in.)*	0.5750	0.5703		0.6383		0.4171	0.1000
B_2	1.7220	1.4046		1.5135		1.9659	2.8026
B_3	0.1750	0.1978		0.4522		1.0222	1.9723
Angle, θ	73.2	77.5	n/c	75.1	n/c	58.6	38.5
T_1 (in.)**	0.0050	0.0050		0.0070		0.0198	0.0348
T_2	0.0050	0.0050		0.0050		0.0050	0.0351
T_3	0.1027	0.0972		0.0616		0.0447	0.0724
T_4	0.0050	0.0050		0.0067		0.0243	0.0702
T_5	0.0050	0.0050		0.0077		0.0304	0.0394
T_6	0.0050	0.0050		0.0050		0.0050	0.0050
$\frac{W}{LA}$ (10^{-4} lb/in^3)	2.0681	2.2050		2.7006		6.3232	12.2139

* Reference dimensions to Figure 84.
** Minimum gage ply thickness = 0.005 inches.
n/c Loading condition not considered.

Appendix B. Hat Stiffened Panel Data

Table 22. Hat Stiffened Panel - 0° Plies in Web (P= 0.0 psi   L= 28in)

	Nx= 10 (lb/in)	Nx= 100 (lb/in)	Nx=350 (lb/in)	Nx=1000 (lb/in)	Nx=2800 (lb/in)	Nx=10000 (lb/in)	Nx=28000 (lb/in)
$\dfrac{N_{xy}}{N_x} = 0.0$							
B_1 (in.)*	0.1000	0.1000		0.2291		0.7504	0.6034
B_2	8.9152	2.7218		1.3981		1.5232	1.7857
B_3	0.1000	0.1108		0.3059		0.7185	1.1273
Angle, θ	1.9	9.5	n/c	49.0	n/c	78.1	76.8
T_1 (in.)**	0.0050	0.0050		0.0050		0.0079	0.0114
T_2	0.0050	0.0050		0.0050		0.0050	0.0071
T_3	0.0050	0.0050		0.0104		0.0611	0.0810
T_4	0.0050	0.0050		0.0050		0.0050	0.0050
T_5	0.0050	0.0050		0.0050		0.0154	0.0444
T_6	0.0050	0.0050		0.0050		0.0050	0.0050
T (0° web)	0.0005	0.0005		0.0005		0.0005	0.0054
$\dfrac{W}{LA}$ (10⁻⁴ lb/in³)	1.2465	1.2591		1.4816		3.1729	5.7062
$\dfrac{N_{xy}}{N_x} = 0.3$							
B_1 (in.)*							
B_2							
B_3							
Angle, θ	n/c	n/c	n/c	n/c	n/c	n/c	n/c
T_1 (in.)**							
T_2							
T_3							
T_4							
T_5							
T_6							
$\dfrac{W}{LA}$ (10⁻⁴ lb/in³)							
$\dfrac{N_{xy}}{N_x} = 0.6$							
B_1 (in.)*							
B_2							
B_3							
Angle, θ	n/c	n/c	n/c	n/c	n/c	n/c	n/c
T_1 (in.)**							
T_2							
T_3							
T_4							
T_5							
T_6							
$\dfrac{W}{LA}$ (10⁻⁴ lb/in³)							
$\dfrac{N_{xy}}{N_x} = 1.0$							
B_1 (in.)*	0.1000	0.1000		0.1690		0.1000	0.0010
B_2	6.2451	2.0459		0.9900		1.6508	2.5918
B_3	0.1000	0.1102		0.7946		0.8675	1.8301
Angle, θ	1.7	13.4	n/c	59.3	n/c	57.6	29.4
T_1 (in.)**	0.0050	0.0050		0.0050		0.0132	0.0227
T_2	0.0050	0.0050		0.0050		0.1073	0.5809
T_3	0.0050	0.0050		0.0050		0.0313	0.0376
T_4	0.0050	0.0050		0.0050		0.0270	0.0798
T_5	0.0050	0.0050		0.0052		0.0068	0.0052
T_6	0.0050	0.0050		0.0052		0.0050	0.0050
T (0° web)	0.0005	0.0007		0.0064		0.0070	0.0246
$\dfrac{W}{LA}$ (10⁻⁴ lb/in³)	1.2477	1.2722		1.7763		5.3625	10.9018

* Reference dimensions to Figure 84.
** Minimum gage ply thickness = 0.005 inches.
n/c Loading condition not considered.

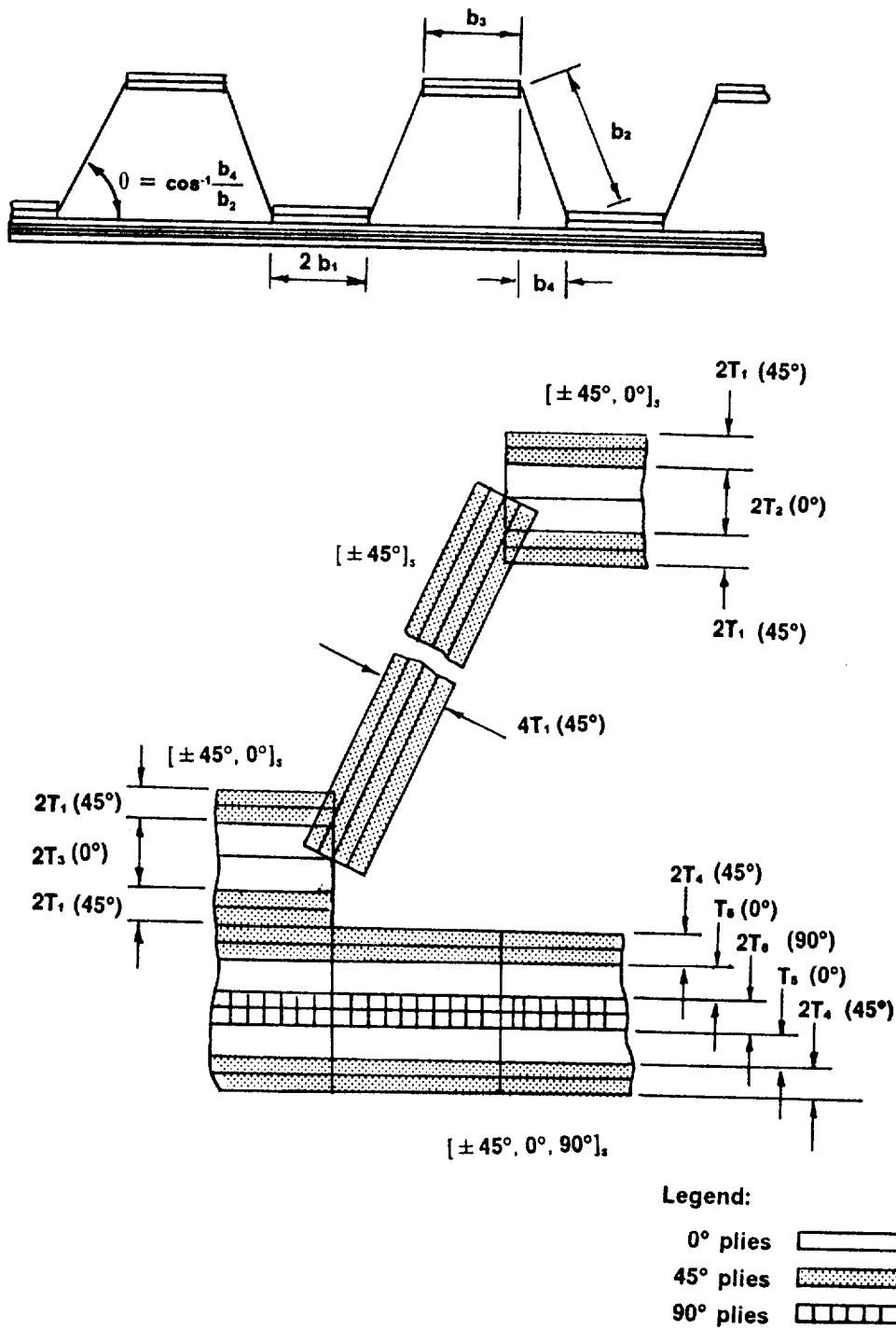**Appendix B. Hat Stiffened Panel Data**   174

Table 23. Hat Stiffened Panel - Bead Ratio = 1.0 (p = 0.0 psi   L= 28 in)

	Nx = 10 (lb/in)	Nx = 100 (lb/in)	Nx = 350 (lb/in)	Nx = 1000 (lb/in)	Nx = 2800 (lb/in)	Nx = 10000 (lb/in)	Nx = 28000 (lb/in)
$\frac{N_{xy}}{N_x} = 0.0$							
B_1 (in.)*	8.9994.	3.1920		1.0899		0.7298	0.9099
B_2	8.9550	3.2477		1.4453		1.5337	1.8177
B_3	0.1000	0.1000		0.1817		0.6068	0.2706
Angle, θ	2.0	14.7	n/c	46.3	n/c	73.9	64.8
T_1 (in.)**	0.0050	0.0050		0.0050		0.0075	0.0100
T_2	0.0050	0.0050		0.0050		0.0050	0.0050
T_3	0.0050	0.0050		0.0420		0.0748	0.5424
T_4	0.0050	0.0050		0.0050		0.0050	0.0050
T_6	0.0050	0.0050		0.0050		0.0176	0.0420
T_8	0.0050	0.0050		0.0050		0.0050	0.0050
$\frac{W}{LA}(10^{-4}\ \text{lb/in}^3)$	1.3239	1.3316		1.4778		3.1317	5.3470
$\frac{N_{xy}}{N_x} = 0.3$							
B_1 (in.)*	6.3134	2.9326		0.8979		0.8446	1.4753
B_2	6.2684	3.0056		1.1585		1.5044	1.7380
B_3	0.1000	0.1000		0.3684		0.9062	1.4056
Angle, θ	2.3	16.4	n/c	52.8	n/c	74.9	63.6
T_1 (in.)**	0.0050	0.0050		0.0050		0.0129	0.0189
T_2	0.0050	0.0050		0.0050		0.0050	0.0050
T_3	0.0050	0.0050		0.0222		0.0594	0.1416
T_4	0.0050	0.0050		0.0050		0.0086	0.0173
T_6	0.0050	0.0050		0.0050		0.0106	0.0410
T_8	0.0050	0.0050		0.0050		0.0073	0.0050
$\frac{W}{LA}(10^{-4}\ \text{lb/in}^3)$	1.3242	1.3335		1.5219		3.9257	6.7842
$\frac{N_{xy}}{N_x} = 0.6$							
B_1 (in.)*	6.3134	2.2919		0.6986		0.9048	2.1123
B_2	6.2864	2.3774		0.9881		1.5026	1.9807
B_3	0.1000	0.1000		0.3745		1.0032	1.6660
Angle, θ	2.3	19.4	n/c	58.8	n/c	74.4	49.8
T_1 (in.)**	0.0050	0.0050		0.0050		0.0145	0.0239
T_2	0.0050	0.0050		0.0050		0.0050	0.0056
T_3	0.0050	0.0050		0.0240		0.0530	0.1610
T_4	0.0050	0.0050		0.0050		0.0147	0.0403
T_6	0.0050	0.0050		0.0050		0.0090	0.0333
T_8	0.0050	0.0050		0.0050		0.0050	0.0050
$\frac{W}{LA}(10^{-4}\ \text{lb/in}^3)$	1.3242	1.3375		1.5929		4.3711	8.5158
$\frac{N_{xy}}{N_x} = 1.0$							
B_1 (in.)*	5.9923	2.2890		0.6046		1.1862	2.4305
B_2	5.9473	2.3236		0.8774		1.6627	2.3914
B_3	0.1000	0.1107		0.6287		1.0669	1.2753
Angle, θ	2.3	16.0	n/c	70.6	n/c	66.9	41.1
T_1 (in.)**	0.0050	0.0055		0.0051		0.0173	0.0295
T_2	0.0050	0.0050		0.0050		0.0050	0.0050
T_3	0.0050	0.0209		0.0171		0.0588	0.1895
T_4	0.0050	0.0050		0.0050		0.0263	0.0750
T_6	0.0050	0.0050		0.0050		0.0050	0.0275
T_8	0.0050	0.0050		0.0050		0.0055	0.0050
$\frac{W}{LA}(10^{-4}\ \text{lb/in}^3)$	1.3242	1.3863		1.7110		5.1968	11.2411

* Reference dimensions to Figure 84.
** Minimum gage ply thickness = 0.005 inches.
n/c Loading condition not considered.

Table 24. Hat Stiffened Panel - Bead Ratio = 3.0 (P= 0.0 psi   L= 28 in)

	Nx= 10 (lb/in)	Nx= 100 (lb/in)	Nx= 350 (lb/in)	Nx= 1000 (lb/in)	Nx= 2800 (lb/in)	Nx= 10000 (lb/in)	Nx= 28000 (lb/in)
$\dfrac{N_{xy}}{N_x} = 0.0$							
B_1 (in.)*	11.8032.	3.6841		1.2667		0.9026	1.1512
B_2	3.9571	1.3636		1.0677		1.4031	1.8376
B_3	0.1000	0.2151		0.1148		0.2929	0.2926
Angle, θ	11.0	34.7	n/c	70.0	n/c	83.4	82.6
T_1 (in.)**	0.0050	0.0050		0.0050		0.0063	0.0116
T_2	0.0050	0.0050		0.0050		0.0050	0.0091
T_3	0.0050	0.0060		0.0594		0.1344	0.2512
T_4	0.0050	0.0050		0.0050		0.0050	0.0057
T_6	0.0050	0.0050		0.0050		0.0168	0.0411
T_8	0.0050	0.0050		0.0050		0.0050	0.0051
$\dfrac{W}{LA}(10^{-4}$ lb/in$^3)$	1.3822	1.4057		1.6395		3.5924	5.9847
$\dfrac{N_{xy}}{N_x} = 0.3$							
B_1 (in.)*		2.7387		1.1411		0.8443	1.6041
B_2		1.0415		1.0429		1.3744	1.8497
B_3		0.2209		0.1737		0.3552	0.3287
Angle, θ	n/c	39.6	n/c	73.7	n/c	85.7	78.4
T_1 (in.)**		0.0050		0.0050		0.0072	0.0127
T_2		0.0050		0.0050		0.0058	0.0119
T_3		0.0061		0.0325		0.1112	0.2451
T_4		0.0050		0.0050		0.0083	0.0260
T_6		0.0050		0.0050		0.0116	0.0329
T_8		0.0050		0.0050		0.0050	0.0050
$\dfrac{W}{LA}(10^{-4}$ lb/in$^3)$		1.4145		1.6711		3.9165	7.0025
$\dfrac{N_{xy}}{N_x} = 0.6$							
B_1 (in.)*	9.7281	2.1076		1.0225		1.0590	1.5970
B_2	3.2734	0.7049		1.0380		1.5435	1.8522
B_3	0.1000	0.1000		0.1488		0.4436	0.3805
Angle, θ	12.7	46.6	n/c	75.1	n/c	85.1	79.4
T_1 (in.)**	0.0050	0.0050		0.0050		0.0081	0.0139
T_2	0.0050	0.0050		0.0050		0.0077	0.0093
T_3	0.0050	0.0050		0.0399		0.1103	0.2120
T_4	0.0050	0.0050		0.0050		0.0194	0.0559
T_6	0.0050	0.0050		0.0050		0.0050	0.0269
T_8	0.0050	0.0050		0.0050		0.0050	0.0050
$\dfrac{W}{LA}(10^{-4}$ lb/in$^3)$	1.3796	1.4273		1.7266		4.6790	9.2399
$\dfrac{N_{xy}}{N_x} = 1.0$							
B_1 (in.)*	8.5911	2.9462		0.8946		1.4609	2.4725
B_2	2.8706	1.0843		1.0183		1.7323	1.9411
B_3	0.1000	0.1254		0.2554		0.4317	0.4132
Angle, θ	13.6	32.0	n/c	80.4	n/c	81.0	71.4
T_1 (in.)**	0.0050	0.0050		0.0050		0.0087	0.0217
T_2	0.0050	0.0090		0.0050		0.0127	0.0138
T_3	0.0050	0.0096		0.0217		0.1134	0.2759
T_4	0.0050	0.0050		0.0050		0.0335	0.0924
T_6	0.0050	0.0050		0.0050		0.0050	0.0142
T_8	0.0050	0.0050		0.0050		0.0050	0.0050
$\dfrac{W}{LA}(10^{-4}$ lb/in$^3)$	1.3836	1.5534		2.0170		5.6897	12.4035

* Reference dimensions to Figure 84.
** Minimum gage ply thickness = 0.005 inches.
n/c Loading condition not considered.

Table 25. Hat Stiffened Panel - Bead Ratio = 10.0 (P= 0.0 psi L= 28 in)

	Nx= 10 (lb/in)	Nx= 100 (lb/in)	Nx= 350 (lb/in)	Nx= 1000 (lb/in)	Nx= 2800 (lb/in)	Nx= 10000 (lb/in)	Nx= 28000 (lb/in)
$\frac{N_{xy}}{N_x} = 0.0$ B_1 (in.)* B_2 B_3 Angle, θ T_1 (in.)** T_2 T_3 T_4 T_5 T_6 $\frac{W}{LA}$(10⁻⁴ lb/in³)	9.4451. 0.9969 0.1000 26.2 0.0050 0.0050 0.0050 0.0050 0.0050 0.0050 1.4136	n/c	n/c	1.3512 0.9315 0.1000 84.7 0.0050 0.0050 0.0723 0.0050 0.0050 0.0050 1.7648	n/c	n/c	n/c
$\frac{N_{xy}}{N_x} = 0.3$ B_1 (in.)* B_2 B_3 Angle, θ T_1 (in.)** T_2 T_3 T_4 T_5 T_6 $\frac{W}{LA}$(10⁻⁴ lb/in³)	n/c	n/c	n/c	1.5274 1.0809 0.1055 84.7 0.0050 0.0050 0.0375 0.0064 0.0084 0.0050 2.0027	n/c	n/c	1.8646 1.7891 0.2816 88.5 0.0136 0.0138 0.2273 0.0264 0.0374 0.0050 7.9493
$\frac{N_{xy}}{N_x} = 0.6$ B_1 (in.)* B_2 B_3 Angle, θ T_1 (in.)** T_2 T_3 T_4 T_5 T_6 $\frac{W}{LA}$(10⁻⁴ lb/in³)	n/c	n/c	n/c	1.5300 1.0179 0.1000 84.7 0.0050 0.0073 0.0537 0.0068 0.0052 0.0096 2.2195	n/c	n/c	2.2328 1.9201 0.3831 89.0 0.0133 0.0248 0.1891 0.0580 0.0219 0.0076 9.9011
$\frac{N_{xy}}{N_x} = 1.0$ B_1 (in.)* B_2 B_3 Angle, θ T_1 (in.)** T_2 T_3 T_4 T_5 T_6 $\frac{W}{LA}$(10⁻⁴ lb/in³)	n/c	n/c	n/c	1.5487 1.3300 0.1000 85.5 0.0050 0.0102 0.0402 0.0072 0.0050 0.0105 2.4141	n/c	n/c	2.3299 1.9682 0.3280 88.0 0.0150 0.0232 0.2249 0.1007 0.0050 0.0050 12.8550

* Reference dimensions to Figure 84.
** Minimum gage ply thickness = 0.005 inches.
n/c Loading condition not considered.

Appendix C. Blade Stiffened Panel Data

Figure 85. Blade Stiffened Panel Model

Table 26. Blade Stiffened Panel (P= 0.0 psi   L= 28 in)

	Nx = 10 (lb/in)	Nx = 100 (lb/in)	Nx = 350 (lb/in)	Nx = 1000 (lb/in)	Nx = 2800 (lb/in)	Nx = 10000 (lb/in)	Nx = 28000 (lb/in)
$\dfrac{N_{xy}}{N_x} = 0.0$							
B_1 (in.)*	8.2548	2.8307	1.5940	0.9786	0.8097	1.0024	1.7784
B_2	0.7500	0.7500	0.7500	0.7500	0.7500	0.7500	0.7500
B_3	0.4107	0.6489	0.9009	1.1408	1.2741	1.6649	2.1819
T_1 (in.)**	0.0050	0.0050	0.0050	0.0050	0.0050	0.0076	0.0194
T_2	0.0050	0.0050	0.0050	0.0050	0.0050	0.0050	0.0050
T_3	0.0050	0.0050	0.0050	0.0108	0.0050	0.0050	0.0050
T_4	0.0050	0.0050	0.0050	0.0050	0.0050	0.0090	0.0195
T_5	0.0050	0.0050	0.0050	0.0050	0.0070	0.0240	0.1146
T_6	0.0050	0.0050	0.0050	0.0050	0.0050	0.0050	0.0050
T_7	0.0050	0.0060	0.0050	0.0050	0.0050	0.0051	0.0050
T_8	0.0050	0.0052	0.0050	0.0086	0.0346	0.0680	0.0050
$\dfrac{W}{LA}(10^{-4}\ \text{lb/in}^3)$	0.9146	1.1146	1.3487	1.6858	2.3655	4.2552	6.9498
$\dfrac{N_{xy}}{N_x} = 0.3$							
B_1 (in.)*	7.3463	2.5089	1.3621	0.7695	0.6281	0.7664	1.1701
B_2	0.7500	0.7500	0.7500	0.7500	0.7500	0.7500	0.7500
B_3	0.4073	0.6173	0.8792	1.0800	1.2417	1.6378	2.1890
T_1 (in.)**	0.0050	0.0050	0.0050	0.0050	0.0050	0.0157	0.0287
T_2	0.0050	0.0050	0.0050	0.0050	0.0050	0.0098	0.0215
T_3	0.0050	0.0050	0.0050	0.0050	0.0110	0.0050	0.0050
T_4	0.0050	0.0050	0.0050	0.0050	0.0050	0.0050	0.0050
T_5	0.0050	0.0050	0.0050	0.0050	0.0050	0.0050	0.0050
T_6	0.0050	0.0050	0.0050	0.0050	0.0050	0.0050	0.0050
T_7	0.0050	0.0050	0.0050	0.0050	0.0050	0.0107	0.0263
T_8	0.0050	0.0058	0.0058	0.0115	0.0337	0.0756	0.1039
$\dfrac{W}{LA}(10^{-4}\ \text{lb/in}^3)$	0.9243	1.1399	1.4067	1.8170	2.6780	4.8601	8.1116
$\dfrac{N_{xy}}{N_x} = 0.6$							
B_1 (in.)*	6.5759	2.0834	1.0306	0.5315	0.4109	0.5285	1.1653
B_2	0.7500	0.7500	0.7500	0.7500	0.7500	0.7500	0.7500
B_3	0.3864	0.6651	0.9887	1.2752	1.4562	1.6971	2.1506
T_1 (in.)**	0.0050	0.0050	0.0050	0.0063	0.0090	0.0199	0.0603
T_2	0.0050	0.0050	0.0050	0.0050	0.0080	0.0205	0.0153
T_3	0.0050	0.0050	0.0050	0.0050	0.0050	0.0050	0.0050
T_4	0.0050	0.0050	0.0050	0.0050	0.0050	0.0050	0.0050
T_5	0.0050	0.0050	0.0050	0.0050	0.0050	0.0050	0.0194
T_6	0.0050	0.0050	0.0050	0.0050	0.0050	0.0050	0.0050
T_7	0.0050	0.0050	0.0050	0.0050	0.0050	0.0059	0.0050
T_8	0.0050	0.0051	0.0050	0.0050	0.0180	0.0484	0.1110
$\dfrac{W}{LA}(10^{-4}\ \text{lb/in}^3)$	0.9352	1.1975	1.5529	2.1057	3.0358	5.3022	9.8432
$\dfrac{N_{xy}}{N_x} = 1.0$							
B_1 (in.)*	5.5173	1.6752	0.7532	0.5057	0.3061	0.5776	1.5095
B_2	0.7500	0.7500	0.7500	0.7500	0.7500	0.7500	0.7500
B_3	0.3532	0.7599	1.1103	1.5050	1.6686	1.9086	2.3214
T_1 (in.)**	0.0050	0.0050	0.0050	0.0057	0.0103	0.0357	0.1027
T_2	0.0050	0.0050	0.0050	0.0050	0.0108	0.0096	0.0081
T_3	0.0050	0.0050	0.0050	0.0096	0.0050	0.0050	0.0050
T_4	0.0050	0.0050	0.0080	0.0050	0.0050	0.0050	0.0100
T_5	0.0050	0.0050	0.0050	0.0050	0.0050	0.0050	0.0055
T_6	0.0050	0.0050	0.0050	0.0050	0.0050	0.0050	0.0050
T_7	0.0050	0.0050	0.0050	0.0050	0.0050	0.0079	0.0050
T_8	0.0050	0.0050	0.0050	0.0050	0.0139	0.0464	0.1000
$\dfrac{W}{LA}(10^{-4}\ \text{lb/in}^3)$	0.9519	1.2894	1.7468	2.4019	3.4755	6.3650	12.2014

* Reference dimensions to Figure 85.
** Minimum gage ply thickness = 0.005 inches.

Appendix C. Blade Stiffened Panel Data

Table 27. Blade Stiffened Panel - No VICON Corrections (P= 0.0 psi   L= 28 in)

	Nx = 10 (lb/in)	Nx = 100 (lb/in)	Nx = 350 (lb/in)	Nx = 1000 (lb/in)	Nx = 2800 (lb/in)	Nx = 10000 (lb/in)	Nx = 28000 (lb/in)
$\dfrac{N_{xy}}{N_x} = 0.0$							
B_1 (in.)*	n/c	n/c	n/c	n/c	n/c	n/c	n/c
B_2							
B_3							
T_1 (in.)**							
T_2							
T_3							
T_4							
T_5							
T_6							
T_7							
T_8							
$\dfrac{W}{LA}$ (10⁻⁴ lb/in³)							
$\dfrac{N_{xy}}{N_x} = 0.3$							
B_1 (in.)*	n/c	n/c	1.3593	0.764?	0.6414	0.7421	1.0816
B_2			0.7500	0.750?	0.7500	0.7500	0.7500
B_3			0.8158	1.067?	1.2568	1.6239	2.0947
T_1 (in.)**			0.0050	0.005?	0.0050	0.0148	0.0289
T_2			0.0050	0.005?	0.0050	0.0110	0.0213
T_3			0.0050	0.005?	0.0114	0.0050	0.0050
T_4			0.0050	0.005?	0.0050	0.0050	0.0050
T_5			0.0050	0.005?	0.0050	0.0050	0.0050
T_6			0.0050	0.005?	0.0050	0.0050	0.0050
T_7			0.0050	0.005?	0.0050	0.0110	0.0240
T_8			0.0059	0.011?	0.0345	0.0731	0.1118
$\dfrac{W}{LA}$ (10⁻⁴ lb/in³)			1.3989	1.807?	2.6976	4.8185	7.9405
$\dfrac{N_{xy}}{N_x} = 0.6$							
B_1 (in.)*	n/c	n/c	1.0940	0.5060	0.4186	0.5962	1.0598
B_2			0.7500	0.7500	0.7500	0.7500	0.7500
B_3			1.1418	1.280?	1.4568	1.7294	2.0487
T_1 (in.)**			0.0050	0.0060	0.0093	0.0199	0.0621
T_2			0.0050	0.0050	0.0082	0.0211	0.0190
T_3			0.0050	0.0050	0.0050	0.0050	0.0050
T_4			0.0050	0.0050	0.0050	0.0050	0.0050
T_5			0.0050	0.0050	0.0050	0.0050	0.0086
T_6			0.0050	0.0050	0.0050	0.0050	0.0050
T_7			0.0050	0.0050	0.0050	0.0056	0.0050
T_8			0.0055	0.0050	0.0179	0.0536	0.1090
$\dfrac{W}{LA}$ (10⁻⁴ lb/in³)			1.5933	2.1050	3.0346	5.3556	9.6367
$\dfrac{N_{xy}}{N_x} = 1.0$							
B_1 (in.)*	n/c	n/c	0.7515	0.5478	0.3229	0.6642	1.5363
B_2			0.7500	0.7500	0.7500	0.7500	0.7500
B_3			1.1075	1.7827	1.6790	1.9504	2.3273
T_1 (in.)**			0.0050	0.0059	0.0102	0.0355	0.1023
T_2			0.0050	0.0050	0.0116	0.0113	0.0100
T_3			0.0050	0.0111	0.0050	0.0050	0.0050
T_4			0.0050	0.0050	0.0050	0.0050	0.0100
T_5			0.0050	0.0050	0.0050	0.0050	0.0050
T_6			0.0050	0.0050	0.0050	0.0050	0.0050
T_7			0.0050	0.0050	0.0050	0.0074	0.0050
T_8			0.0050	0.0060	0.0138	0.0509	0.1003
$\dfrac{W}{LA}$ (10⁻⁴ lb/in³)			1.7466	2.6085	3.4726	6.3956	12.2508

* Reference dimensions to Figure 85.
** Minimum gage ply thickness = 0.005 inches.
n/c Loading condition not considered.

Table 28. Blade Stiffened Panel (P= 5.0 psi   L= 28 in)

	Nx = 10 (lb/in)	Nx = 100 (lb/in)	Nx = 350 (lb/in)	Nx = 1000 (lb/in)	Nx = 2800 (lb/in)	Nx = 10000 (lb/in)	Nx = 28000 (lb/in)
$\frac{N_{xy}}{N_x}=0.0$							
B_1 (in.)*	0.8904	0.7932		0.6133			
B_2	0.7500	0.7500		0.7500			
B_3	0.9246	0.9696		1.5396			
T_1 (in.)**	0.0050	0.0050	n/c	0.0050	n/c	n/c	n/c
T_2	0.0050	0.0050		0.0050			
T_3	0.0050	0.0050		0.0050			
T_4	0.0050	0.0050		0.0050			
T_5	0.0050	0.0050		0.0054			
T_6	0.0050	0.0050		0.0050			
T_7	0.0050	0.0050		0.0050			
T_8	0.0050	0.0050		0.0050			
$\frac{W}{LA}$ (10^{-4} lb/in³)	1.5883	1.6578		2.0840			
$\frac{N_{xy}}{N_x}=0.3$							
B_1 (in.)*							
B_2							
B_3							
T_1 (in.)**	n/c	n/c	n/c	n/c	n/c	n/c	n/c
T_2							
T_3							
T_4							
T_5							
T_6							
T_7							
T_8							
$\frac{W}{LA}$ (10^{-4} lb/in³)							
$\frac{N_{xy}}{N_x}=0.6$							
B_1 (in.)*							
B_2							
B_3							
T_1 (in.)**	n/c	n/c	n/c	n/c	n/c	n/c	n/c
T_2							
T_3							
T_4							
T_5							
T_6							
T_7							
T_8							
$\frac{W}{LA}$ (10^{-4} lb/in³)							
$\frac{N_{xy}}{N_x}=1.0$							
B_1 (in.)*	0.8662	0.7336		0.5553			
B_2	0.7500	0.7500		0.7500			
B_3	0.9315	1.0722		1.6140			
T_1 (in.)**	0.0050	0.0071	n/c	0.0050	n/c	n/c	n/c
T_2	0.0050	0.0050		0.0050			
T_3	0.0050	0.0050		0.0137			
T_4	0.0050	0.0050		0.0050			
T_5	0.0050	0.0050		0.0050			
T_6	0.0050	0.0051		0.0050			
T_7	0.0050	0.0050		0.0050			
T_8	0.0050	0.0050		0.0060			
$\frac{W}{LA}$ (10^{-4} lb/in³)	1.6028	1.7477		2.5443			

* Reference dimensions to Figure 85.
** Minimum gage ply thickness = 0.005 inches.
n/c Loading condition not considered.

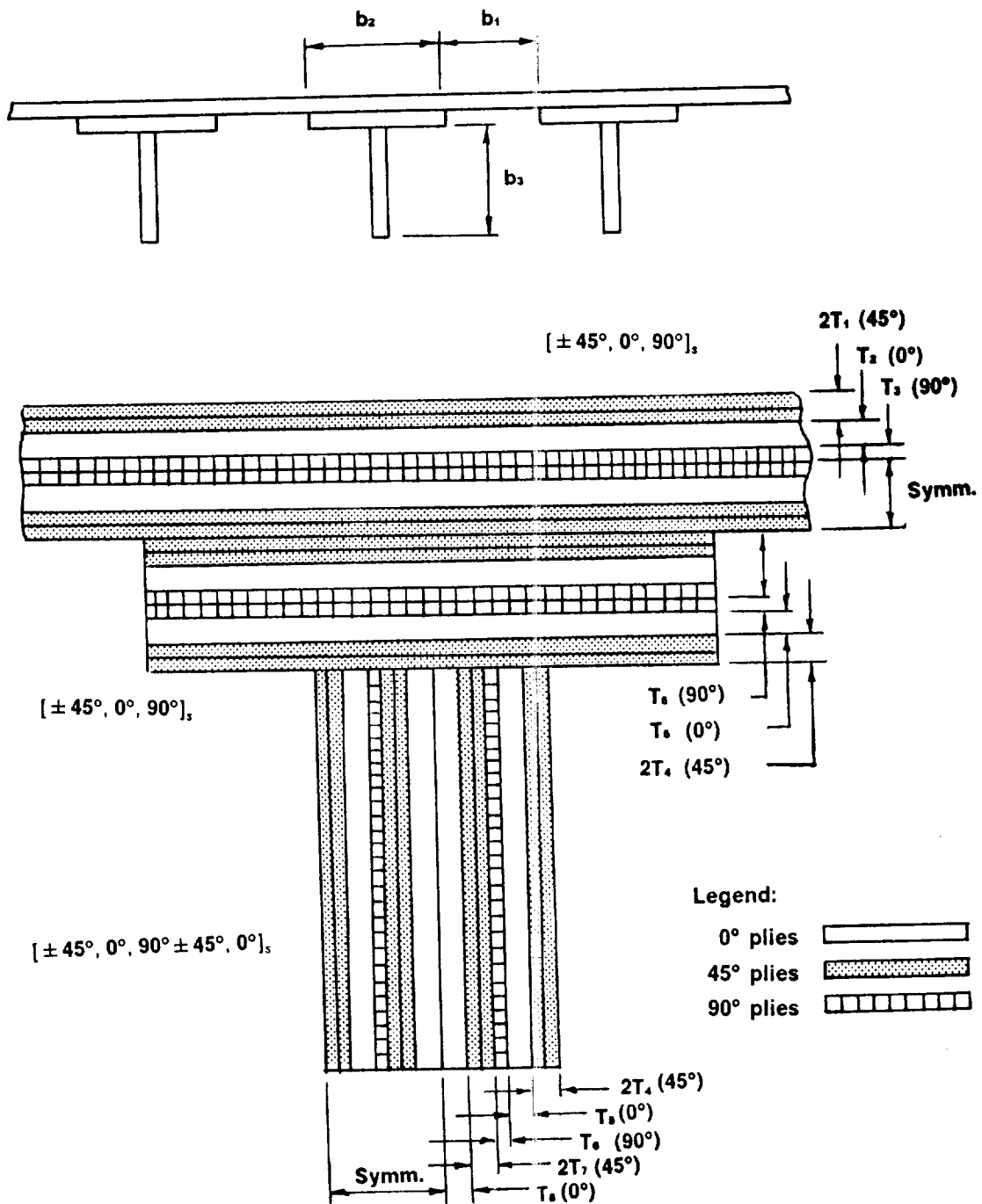Appendix C. Blade Stiffened Panel Data

Table 29. Blade Stiffened Panel (P= 10.0 psi   L= 28 in)

	Nx = 10 (lb/in)	Nx = 100 (lb/in)	Nx = 350 (lb/in)	Nx = 1000 (lb/in)	Nx = 2800 (lb/in)	Nx = 10000 (lb/in)	Nx = 28000 (lb/in)
$\frac{N_{xy}}{N_x} = 0.0$							
B_1 (in.)*	0.7135	0.6583		0.5476			
B_2	0.7500	0.7500		0.7500			
B_3	1.2597	1.2732		1.5381			
T_1 (in.)**	0.0050	0.0050	n/c	0.0050	n/c	n/c	n/c
T_2	0.0050	0.0050		0.0050			
T_3	0.0050	0.0050		0.0050			
T_4	0.0050	0.0050		0.0050			
T_5	0.0050	0.0050		0.0080			
T_6	0.0050	0.0050		0.0050			
T_7	0.0050	0.0050		0.0050			
T_8	0.0050	0.0050		0.0050			
$\frac{W}{LA}$ (10⁻⁴ lb/in³)	1.8448	1.8921		2.2793			
$\frac{N_{xy}}{N_x} = 0.3$							
B_1 (in.)*							
B_2							
B_3							
T_1 (in.)**	n/c	n/c	n/c	n/c	n/c	n/c	n/c
T_2							
T_3							
T_4							
T_5							
T_6							
T_7							
T_8							
$\frac{W}{LA}$ (10⁻⁴ lb/in³)							
$\frac{N_{xy}}{N_x} = 0.6$							
B_1 (in.)*							
B_2							
B_3							
T_1 (in.)**	n/c	n/c	n/c	n/c	n/c	n/c	n/c
T_2							
T_3							
T_4							
T_5							
T_6							
T_7							
T_8							
$\frac{W}{LA}$ (10⁻⁴ lb/in³)							
$\frac{N_{xy}}{N_x} = 1.0$							
B_1 (in.)*	0.6961	0.5922		0.5967			
B_2	0.7500	0.7500		0.7500			
B_3	1.2669	1.3506		1.8403			
T_1 (in.)**	0.0050	0.0050	n/c	0.0052	n/c	n/c	n/c
T_2	0.0050	0.0050		0.0051			
T_3	0.0050	0.0050		0.0112			
T_4	0.0050	0.0050		0.0050			
T_5	0.0050	0.0050		0.0050			
T_6	0.0050	0.0050		0.0050			
T_7	0.0050	0.0050		0.0050			
T_8	0.0050	0.0050		0.0052			
$\frac{W}{LA}$ (10⁻⁴ lb/in³)	1.8609	2.0404		2.8016			

* Reference dimensions to Figure 85.
** Minimum gage ply thickness = 0.005 inches.
n/c Loading condition not considered.

Table 30. Blade Stiffened Panel (P= 15.0 psi L= 28 In)

	Nx= 10 (lb/in)	Nx= 100 (lb/in)	Nx= 350 (lb/in)	Nx= 1000 (lb/in)	Nx= 2800 (lb/in)	Nx= 10000 (lb/in)	Nx= 28000 (lb/in)
$\frac{N_{xy}}{N_x} = 0.0$							
B_1 (in.)*	0.7200	0.5855		0.5169		1.1284	1.4707
B_2	0.7500	0.7500		0.7500		0.7500	0.7500
B_3	1.1460	1.4901		1.7109		1.8129	2.4444
T_1 (in.)**	0.0061	0.0050	n/c	0.0068	n/c	0.0138	0.0141
T_2	0.0050	0.0050		0.0050		0.0050	0.0468
T_3	0.0050	0.0050		0.0050		0.0050	0.0050
T_4	0.0050	0.0050		0.0050		0.0079	0.0299
T_5	0.0086	0.0055		0.0058		0.0565	0.0036
T_6	0.0050	0.0050		0.0050		0.0050	0.0052
T_7	0.0050	0.0050		0.0050		0.0050	0.0050
T_8	0.0142	0.0050		0.0050		0.0131	0.0325
$\frac{W}{LA}$ (10⁻⁴ lb/in³)	2.1525	2.0903		2.4429		4.7574	7.8484
$\frac{N_{xy}}{N_x} = 0.3$							
B_1 (in.)*	0.6018	0.5645		0.5043		1.0424	1.4561
B_2	0.7500	0.7500		0.7500		0.7500	0.7500
B_3	1.5036	1.4940		1.6800		1.7766	2.1390
T_1 (in.)**	0.0050	0.0050	n/c	0.0057	n/c	0.0129	0.0294
T_2	0.0050	0.0050		0.0050		0.0070	0.0438
T_3	0.0050	0.0050		0.0098		0.0227	0.0061
T_4	0.0050	0.0050		0.0050		0.0080	0.0135
T_5	0.0050	0.0053		0.0050		0.0252	0.0351
T_6	0.0050	0.0050		0.0050		0.0050	0.0050
T_7	0.0050	0.0050		0.0050		0.0050	0.0050
T_8	0.0050	0.0050		0.0050		0.0521	0.0742
$\frac{W}{LA}$ (10⁻⁴ lb/in³)	2.0585	2.1016		2.5058		5.2281	8.3371
$\frac{N_{xy}}{N_x} = 0.6$							
B_1 (in.)*	0.6012	0.5665		0.5641		0.7498	1.9569
B_2	0.7500	0.7500		0.7500		0.7500	0.7500
B_3	1.5045	1.5084		1.8333		1.8957	2.3838
T_1 (in.)**	0.0050	0.0050	n/c	0.0050	n/c	0.0228	0.0614
T_2	0.0050	0.0050		0.0050		0.0123	0.0351
T_3	0.0466	0.0052		0.0141		0.0062	0.0102
T_4	0.0050	0.0050		0.0050		0.0084	0.0129
T_5	0.0050	0.0054		0.0050		0.0209	0.0301
T_6	0.0050	0.0050		0.0050		0.0050	0.0050
T_7	0.0050	0.0050		0.0050		0.0050	0.0055
T_8	0.0050	0.0050		0.0050		0.0365	0.0703
$\frac{W}{LA}$ (10⁻⁴ lb/in³)	2.0596	2.1197		2.6447		5.7822	10.0791
$\frac{N_{xy}}{N_x} = 1.0$							
B_1 (in.)*	0.5975	0.5127		0.5920		1.0653	2.3704
B_2	0.7500	0.7500		0.7500		0.7500	0.7500
B_3	1.5114	1.5939		2.0550		2.1150	2.7603
T_1 (in.)**	0.0050	0.0051	n/c	0.0050	n/c	0.0352	0.1009
T_2	0.0050	0.0050		0.0050		0.0276	0.0246
T_3	0.0050	0.0050		0.0172		0.0069	0.0050
T_4	0.0050	0.0050		0.0050		0.0050	0.0112
T_5	0.0050	0.0050		0.0050		0.0050	0.0050
T_6	0.0050	0.0050		0.0050		0.0050	0.0050
T_7	0.0050	0.0050		0.0050		0.0100	0.0138
T_8	0.0050	0.0050		0.0050		0.0415	0.0896
$\frac{W}{LA}$ (10⁻⁴ lb/in³)	2.0667	2.1197		2.8564		6.5383	12.4338

* Reference dimensions to Figure 85.
** Minimum gage ply thickness = 0.005 inches.
n/c Loading condition not considered.

Appendix C. Blade Stiffened Panel Data

Table 31. Blade Stiffened Panel (P= 30.0 psi   L= 28 in)

	Nx = 10 (lb/in)	Nx = 100 (lb/in)	Nx = 350 (lb/in)	Nx = 1000 (lb/in)	Nx = 2800 (lb/in)	Nx = 10000 (lb/in)	Nx = 28000 (lb/in)
$\dfrac{N_{xy}}{N_x} = 0.0$							
B_1 (in.)*	0.5710	0.5265	n/c	0.5650	n/c	1.0022	1.2366
B_2	0.7500	0.7500		0.7500		0.7500	0.7500
B_3	1.7346	1.8819		2.0753		1.9167	2.2320
T_1 (in.)**	0.0050	0.0050		0.0089		0.0118	0.0098
T_2	0.0050	0.0050		0.0050		0.0050	0.0461
T_3	0.0050	0.0050		0.0050		0.0050	0.0050
T_4	0.0050	0.0050		0.0050		0.0090	0.0179
T_5	0.0105	0.0089		0.0055		0.0593	0.0606
T_6	0.0050	0.0050		0.0050		0.0050	0.0050
T_7	0.0050	0.0050		0.0050		0.0050	0.0050
T_8	0.0073	0.0050		0.0050		0.0050	0.0393
$\dfrac{W}{LA}$ (10^{-4} lb/in³)	2.5470	2.5550		2.8013		4.9667	7.8840
$\dfrac{N_{xy}}{N_x} = 0.3$							
B_1 (in.)*	n/c	n/c	n/c	0.5164	n/c	0.5603	1.3993
B_2				0.7500		0.7500	0.7500
B_3				2.0690		1.7658	2.2479
T_1 (in.)**				0.0061		0.0126	0.0278
T_2				0.0050		0.0296	0.0598
T_3				0.0106		0.0050	0.0050
T_4				0.0050		0.0051	0.0050
T_5				0.0053		0.0050	0.0051
T_6				0.0050		0.0050	0.0050
T_7				0.0050		0.0050	0.0132
T_8				0.0050		0.0526	0.1066
$\dfrac{W}{LA}$ (10^{-4} lb/in³)				2.8558		5.1732	8.4415
$\dfrac{N_{xy}}{N_x} = 0.6$							
B_1 (in.)*	n/c	n/c	n/c	0.5095	n/c	0.8564	1.9348
B_2				0.7500		0.7500	0.7500
B_3				2.0611		1.9149	2.4744
T_1 (in.)**				0.0053		0.0211	0.0589
T_2				0.0050		0.0299	0.0467
T_3				0.0150		0.0050	0.0050
T_4				0.0051		0.0050	0.0070
T_5				0.0053		0.0050	0.0050
T_6				0.0050		0.0050	0.0050
T_7				0.0051		0.0051	0.0097
T_8				0.0064		0.0597	0.1081
$\dfrac{W}{LA}$ (10^{-4} lb/in³)				3.0864		5.7030	10.0484
$\dfrac{N_{xy}}{N_x} = 1.0$							
B_1 (in.)*	0.4235	0.5600	n/c	0.5929	n/c	1.0688	2.4349
B_2	0.7500	0.7500		0.7500		0.7500	0.7500
B_3	2.0322	2.1735		2.0619		2.1153	2.7774
T_1 (in.)**	0.0050	0.0065		0.0050		0.0360	0.1004
T_2	0.0050	0.0050		0.0050		0.0247	0.0304
T_3	0.0050	0.0057		0.0188		0.0050	0.0050
T_4	0.0050	0.0050		0.0050		0.0050	0.0106
T_5	0.0050	0.0050		0.0050		0.0050	0.0050
T_6	0.0050	0.0050		0.0050		0.0050	0.0050
T_7	0.0050	0.0050		0.0050		0.0009	0.0093
T_8	0.0050	0.0050		0.0086		0.0556	0.1033
$\dfrac{W}{LA}$ (10^{-4} lb/in³)	2.5685	2.6154		3.0204		6.5914	12.6333

* Reference dimensions to Figure 85.
** Minimum gage ply thickness = 0.005 inches
n/c Loading condition not considered.

Table 32. Blade Stiffened Panel (P= 45.0 psi   L= 28 in)

	$N_x = 10$ (lb/in)	$N_x = 100$ (lb/in)	$N_x = 350$ (lb/in)	$N_x = 1000$ (lb/in)	$N_x = 2800$ (lb/in)	$N_x = 10000$ (lb/in)	$N_x = 28000$ (lb/in)
$\frac{N_{xy}}{N_x} = 0.0$							
B_1 (in.)*	0.5885	0.5882		0.5051		1.0551	1.2759
B_2	0.7500	0.7500		0.7500		0.7500	0.7500
B_3	2.1015	2.0871		2.0442		1.9962	2.2977
T_1 (in.)**	0.0050	0.0050	n/c	0.0076	n/c	0.0131	0.0096
T_2	0.0050	0.0050		0.0050		0.0064	0.0458
T_3	0.0050	0.0050		0.0050		0.0050	0.0050
T_4	0.0050	0.0050		0.0050		0.0084	0.0162
T_5	0.0141	0.0148		0.0110		0.0632	0.0891
T_6	0.0050	0.0050		0.0050		0.0050	0.0050
T_7	0.0050	0.0050		0.0050		0.0050	0.0050
T_8	0.0050	0.0050		0.0100		0.0050	0.0050
$\frac{W}{LA}$ (10⁻⁴ lb/in³)	2.8857	2.9164		3.1790		5.2199	8.0376
$\frac{N_{xy}}{N_x} = 0.3$							
B_1 (in.)*							
B_2							
B_3	n/c	n/c	n/c	n/c	n/c	n/c	n/c
T_1 (in.)**							
T_2							
T_3							
T_4							
T_5							
T_6							
T_7							
T_8							
$\frac{W}{LA}$ (10⁻⁴ lb/in³)							
$\frac{N_{xy}}{N_x} = 0.6$							
B_1 (in.)*							
B_2							
B_3	n/c	n/c	n/c	n/c	n/c	n/c	n/c
T_1 (in.)**							
T_2							
T_3							
T_4							
T_5							
T_6							
T_7							
T_8							
$\frac{W}{LA}$ (10⁻⁴ lb/in³)							
$\frac{N_{xy}}{N_x} = 1.0$							
B_1 (in.)*	0.5989	0.6263		0.5290		1.1492	2.6398
B_2	0.7500	0.7500		0.7500		0.7500	0.7500
B_3	2.3583	2.5005		2.6160		2.1615	2.8680
T_1 (in.)**	0.0067	0.0071	n/c	0.0054	n/c	0.0358	0.0997
T_2	0.0050	0.0050		0.0052		0.0260	0.0388
T_3	0.0050	0.0065		0.0186		0.0050	0.0050
T_4	0.0050	0.0050		0.0052		0.0050	0.0101
T_5	0.0095	0.0085		0.0052		0.0050	0.0050
T_6	0.0050	0.0050		0.0052		0.0050	0.0050
T_7	0.0050	0.0050		0.0052		0.0050	0.0098
T_8	0.0050	0.0050		0.0102		0.0658	0.1037
$\frac{W}{LA}$ (10⁻⁴ lb/in³)	2.9142	2.9880		3.6292		6.7213	12.8173

* Reference dimensions to Figure 85.
** Minimum gage ply thickness = 0.005 inches.
n/c Loading condition not considered.

Appendix C. Blade Stiffened Panel Data

Table 33. Blade Stiffened Panel - Increased Spacing (P= 0.0 psi   L= 28 in)

	Nx = 10 (lb/in)	Nx = 100 (lb/in)	Nx = 350 (lb/in)	Nx = 1000 (lb/in)	Nx = 2800 (lb/in)	Nx = 10000 (lb/in)	Nx = 28000 (lb/in)
$\dfrac{N_{xy}}{N_x} = 0.0$							
B_1 (in.)*	17.3000	6.4650	n/c	2.7000	n/c	2.3800	3.5000
B_2	0.7500	0.7500		0.7500		0.7500	0.7500
B_3	0.6584	0.4043		0.9055		1.7401	2.0673
T_1 (in.)**	0.0095	0.0103		0.0116		0.0213	0.0419
T_2	0.0050	0.0050		0.0050		0.0050	0.0240
T_3	0.0050	0.0050		0.0050		0.0050	0.0050
T_4	0.0051	0.0050		0.0050		0.0078	0.0169
T_5	0.0397	0.0055		0.0311		0.0870	0.1539
T_6	0.0050	0.0397		0.0050		0.0050	0.0050
T_7	0.0050	0.0050		0.0050		0.0050	0.0050
T_8	0.0369	0.0369		0.0285		0.0050	0.0234
$\dfrac{W}{LA}$ (10⁻⁴ lb/in³)	1.3460	1.5909		2.2002		4.5757	8.2195
$\dfrac{N_{xy}}{N_x} = 0.3$							
B_1 (in.)*	15.5200	5.7700	n/c	1.4750	n/c	2.2100	4.5500
B_2	0.7500	0.7500		0.7500		0.7500	0.7500
B_3	0.3979	0.4224		0.8136		1.7146	1.8186
T_1 (in.)**	0.0050	0.0050		0.0050		0.0076	0.0316
T_2	0.0050	0.0050		0.0050		0.0050	0.0050
T_3	0.0126	0.0162		0.0296		0.0478	0.0080
T_4	0.0112	0.0057		0.0076		0.0159	0.0313
T_5	0.0248	0.0320		0.0295		0.0162	0.1902
T_6	0.0061	0.0050		0.0076		0.0050	0.0050
T_7	0.0230	0.0050		0.0050		0.0070	0.0050
T_8	0.0342	0.0311		0.0640		0.0970	0.0684
$\dfrac{W}{LA}$ (10⁻⁴ lb/in³)	1.2904	1.6168		2.6578		5.2453	9.8674
$\dfrac{N_{xy}}{N_x} = 0.6$							
B_1 (in.)*	13.8200	4.8650	n/c	1.8100	n/c	2.2100	1.9020
B_2	0.7500	0.7500		0.7500		0.7500	0.7500
B_3	0.4774	0.4730		1.1550		1.7335	2.4675
T_1 (in.)**	0.0050	0.0050		0.0050		0.0182	0.0570
T_2	0.0128	0.0050		0.0050		0.0050	0.0503
T_3	0.0055	0.0154		0.0261		0.0593	0.0067
T_4	0.0050	0.0091		0.0050		0.0140	0.0148
T_5	0.0050	0.0199		0.0050		0.0085	0.0050
T_6	0.0050	0.0050		0.0050		0.0050	0.0050
T_7	0.0050	0.0050		0.0050		0.0067	0.0117
T_8	0.0156	0.0425		0.0214		0.0937	0.0608
$\dfrac{W}{LA}$ (10⁻⁴ lb/in³)	1.2249	1.6357		2.3839		6.3000	9.7674
$\dfrac{N_{xy}}{N_x} = 1.0$							
B_1 (in.)*	11.7500	2.6390	n/c	1.1250	n/c	2.7700	2.2500
B_2	0.7500	0.7500		0.7500		0.7500	0.7500
B_3	0.3041	0.7023		1.7668		1.7714	1.8883
T_1 (in.)**	0.0050	0.0050		0.0063		0.0340	0.0191
T_2	0.0100	0.0050		0.0051		0.0103	0.0123
T_3	0.0090	0.0097		0.0206		0.0409	0.0094
T_4	0.0050	0.0050		0.0050		0.0408	0.0195
T_5	0.0050	0.0050		0.0050		0.0352	0.0261
T_6	0.0050	0.0050		0.0050		0.0088	0.0095
T_7	0.0050	0.0050		0.0050		0.0089	0.0097
T_8	0.0370	0.0290		0.0074		0.0703	0.1553
$\dfrac{W}{LA}$ (10⁻⁴ lb/in³)	1.2546	1.4345		2.6044		8.1329	13.7230

* Reference dimensions to Figure 85.
** Minimum gage ply thickness = 0.005 inches.
n/c Loading condition not considered.

Appendix C. Blade Stiffened Panel Data

187

Table 34. Blade Stiffened Panel - Increased Spacing (P= 0.0 psi   L= 28 in)

	Nx = 10 (lb/in)	Nx = 100 (lb/in)	Nx = 350 (lb/in)	Nx = 1000 (lb/in)	Nx = 2800 (lb/in)	Nx = 10000 (lb/in)	Nx = 28000 (lb/in)
$\dfrac{N_{xy}}{N_x} = 0.0$							
B_1 (in.)*	35.3000	13.5700	n/c	6.1460	n/c	6.2600	5.5950
B_2	0.7500	0.7500		0.7500		0.7500	0.7500
B_3	0.1823	0.7700		0.6712		1.3415	1.9613
T_1 (in.)**	0.0104	0.0187		0.0236		0.0512	0.0640
T_2	0.0050	0.0050		0.0050		0.0050	0.0062
T_3	0.0050	0.0050		0.0050		0.0050	0.0096
T_4	0.0050	0.0073		0.0073		0.0070	0.0195
T_5	0.1161	0.0572		0.0060		0.2060	0.2248
T_6	0.0050	0.0050		0.0050		0.0050	0.0050
T_7	0.0050	0.0130		0.0050		0.0050	0.0050
T_8	0.1480	0.1450		0.0903		0.0728	0.0652
$\dfrac{W}{LA}$ (10⁻⁴ lb/in³)	1.3965	2.3683		3.2068		6.7698	9.3176
$\dfrac{N_{xy}}{N_x} = 0.3$							
B_1 (in.)*	31.9900	12.2900	n/c	5.3280	n/c	5.1360	6.9300
B_2	0.7500	0.7500		0.7500		0.7500	0.7500
B_3	0.2710	0.3844		0.7522		1.4322	1.2987
T_1 (in.)**	0.0050	0.0064		0.0050		0.0357	0.0265
T_2	0.0050	0.0056		0.0050		0.0111	0.0050
T_3	0.0147	0.0318		0.0430		0.0495	0.1297
T_4	0.0050	0.0050		0.0050		0.0225	0.0181
T_5	0.0584	0.0509		0.0217		0.0483	0.4494
T_6	0.0050	0.0050		0.0050		0.0050	0.0051
T_7	0.0237	0.0194		0.0066		0.0184	0.0050
T_8	0.1270	0.1806		0.2029		0.2330	0.0122
$\dfrac{W}{LA}$ (10⁻⁴ lb/in³)	1.3215	2.3672		3.1844		7.6393	11.3589
$\dfrac{N_{xy}}{N_x} = 0.6$							
B_1 (in.)*	28.5500	10.5800	n/c	4.3760	n/c	4.3640	6.9110
B_2	0.7500	0.7500		0.7500		0.7500	0.7500
B_3	0.3223	0.3610		0.8025		1.4363	3.3843
T_1 (in.)**	0.0050	0.0050		0.0050		0.0155	0.0621
T_2	0.0061	0.0050		0.0050		0.0050	0.1628
T_3	0.0127	0.0339		0.0441		0.0840	0.0396
T_4	0.0050	0.0050		0.0051		0.0357	0.0136
T_5	0.0137	0.0395		0.0061		0.0246	0.0088
T_6	0.0050	0.0050		0.0050		0.0050	0.0050
T_7	0.0137	0.0250		0.0195		0.0160	0.0133
T_8	0.0050	0.2164		0.1486		0.2170	0.0537
$\dfrac{W}{LA}$ (10⁻⁴ lb/in³)	1.2398	2.3475		3.1965		7.4916	14.5439
$\dfrac{N_{xy}}{N_x} = 1.0$							
B_1 (in.)*	24.3200	8.9510	n/c	4.2730	n/c	4.5600	8.2880
B_2	0.7500	0.7500		0.7500		0.7500	0.7500
B_3	0.3562	0.5305		0.9370		2.5173	1.6477
T_1 (in.)**	0.0050	0.0050		0.0050		0.0293	0.1068
T_2	0.0050	0.0050		0.0050		0.0050	0.0766
T_3	0.0203	0.0350		0.0490		0.1181	0.0670
T_4	0.0050	0.0050		0.0051		0.0208	0.0697
T_5	0.0050	0.0050		0.0050		0.0296	0.0926
T_6	0.0050	0.0050		0.0050		0.0050	0.0181
T_7	0.0139	0.0332		0.0050		0.0050	0.0182
T_8	0.2222	0.1445		0.0288		0.0368	0.2440
$\dfrac{W}{LA}$ (10⁻⁴ lb/in³)	1.5410	2.3545		3.5776		9.0213	17.3530

* Reference dimensions to Figure 85.
** Minimum gage ply thickness = 0.005 Inches.
n/c Loading condition not considered.

Appendix C. Blade Stiffened Panel Data

Table 35. Blade Stiffened Panel - Increased Spacing (P= 0.0 psi   L= 28 in)

	Nx= 10 (lb/in)	Nx= 100 (lb/in)	Nx= 350 (lb/in)	Nx= 1000 (lb/in)	Nx= 2800 (lb/in)	Nx= 10000 (lb/in)	Nx= 28000 (lb/in)
$\frac{N_{xy}}{N_x}=0.0$							
B_1 (in.)*	39.2500	27.8900		19.2560		19.2500	19.2500
B_2	0.7500	0.7500		0.7500		0.7500	0.7500
B_3	0.1828	0.6127		0.9363		1.5783	0.8413
T_1 (in.)**	0.0115	0.0331	n/c	0.0554	n/c	0.1187	0.1676
T_2	0.0050	0.0050		0.0086		0.0050	0.0050
T_3	0.0050	0.0050		0.0077		0.0090	0.0050
T_4	0.0050	0.0050		0.0087		0.0172	0.0180
T_5	0.1229	0.1730		0.3166		0.7457	1.5200
T_6	0.0050	0.0050		0.0050		0.0050	0.0050
T_7	0.0050	0.0050		0.0050		0.0050	0.0050
T_8	0.1840	0.5218		0.3235		0.2610	0.3798
$\frac{W}{LA}$ (10⁻⁴ lb/in³)	1.4837	3.6147		6.3365		13.1657	18.1199
$\frac{N_{xy}}{N_x}=0.3$							
B_1 (in.)*	39.2500	25.3300		19.2500		19.2500	19.2500
B_2	0.7500	0.7500		0.7500		0.7500	0.7500
B_3	0.1797	0.4423		1.0715		1.9812	1.9391
T_1 (in.)**	0.0057	0.0078	n/c	0.0115	n/c	0.0395	0.0431
T_2	0.0050	0.0050		0.0050		0.0114	0.0072
T_3	0.0172	0.0515		0.0947		0.1788	0.2778
T_4	0.0050	0.0050		0.0113		0.0354	0.0446
T_5	0.0998	0.1579		0.0942		0.1807	0.7240
T_6	0.0050	0.0050		0.0050		0.0169	0.0066
T_7	0.0278	0.0050		0.0108		0.0184	0.0067
T_8	0.1277	0.6470		0.7270		0.8372	0.2681
$\frac{W}{LA}$ (10⁻⁴ lb/in³)	1.4839	3.2481		6.1330		13.6755	18.5410
$\frac{N_{xy}}{N_x}=0.6$							
B_1 (in.)*	39.2500	21.9100		19.2500		19.2500	19.2500
B_2	0.7500	0.7500		0.7500		0.7500	0.7500
B_3	0.3496	0.3724		1.1503		2.3149	5.1685
T_1 (in.)**	0.0051	0.0050	n/c	0.0159	n/c	0.0352	0.0598
T_2	0.0050	0.0050		0.0137		0.0300	0.2526
T_3	0.0186	0.0536		0.0938		0.1950	0.1032
T_4	0.0053	0.0050		0.0152		0.0415	0.0145
T_5	0.0430	0.1110		0.0235		0.0474	0.0089
T_6	0.0050	0.0050		0.0051		0.0076	0.0069
T_7	0.0234	0.0177		0.0312		0.0188	0.0136
T_8	0.1005	0.6376		0.4198		0.5177	0.0805
$\frac{W}{LA}$ (10⁻⁴ lb/in³)	1.4387	3.2291		6.3954		13.8718	20.2277
$\frac{N_{xy}}{N_x}=1.0$							
B_1 (in.)*	39.2500	18.6500		19.2500		19.2500	19.2500
B_2	0.7500	0.7500		0.7500		0.7500	0.7500
B_3	0.3225	0.5848		1.7645		3.4564	2.8651
T_1 (in.)**	0.0050	0.0065	n/c	0.0186	n/c	0.0564	0.0775
T_2	0.0050	0.0190		0.0410		0.0286	0.1450
T_3	0.0190	0.0356		0.0741		0.2003	0.1616
T_4	0.0050	0.0050		0.0050		0.0120	0.0431
T_5	0.0104	0.0050		0.0055		0.0403	0.1289
T_6	0.0050	0.0050		0.0051		0.0050	0.0120
T_7	0.0093	0.0191		0.0051		0.0050	0.0131
T_8	0.2584	0.2106		0.0085		0.0786	0.2025
$\frac{W}{LA}$ (10⁻⁴ lb/in³)	1.4544	2.9516		6.4444		14.5685	20.4646

* Reference dimensions to Figure 85.
** Minimum gage ply thickness = 0.005 inches.
n/c Loading condition not considered.

Appendix C. Blade Stiffened Panel Data

189

Appendix D. Corrugated Panel with a Continuous Laminate Data

Figure 86. Corrugated Panel with a Continuous Laminate Model

$\theta = \cos^{-1}\dfrac{b_3}{b_2}$

$2b_1$

b_2

$2b_3$

b_1

$2T_1 (45°)$
$T_2 (0°)$
$2T_3 (90°)$
$T_2 (0°)$
$2T_1 (45°)$

$2T_1 (45°)$
$T_2 (0°)$
$2T_1 (45°)$
$T_2 (0°)$
$2T_3 (90°)$

Legend:

0° plies

45° plies

90° plies

$[\pm 45°, 0°, 90°]_s$

Table 36. Corrugated Panel with a Continuous Laminate - No VICON Corrections (P= 0.0 psi
L= 28 in)

	Nx= 10 (lb/in)	Nx= 100 (lb/in)	Nx=350 (lb/in)	Nx=1000 (lb/in)	Nx=2800 (lb/in)	Nx=10000 (lb/in)	Nx=28000 (lb/in)
$\dfrac{N_{xy}}{N_x} = 0.0$							
B_1 (in.)*	1.0750	2.3750		0.7241		0.9155	1.2341
B_2	12.8154	3.3064		1.6333		2.0384	2.4372
Angle, θ	0.9	6.9		46.7		59.7	65.8
T_1 (in.)**	0.0050	0.0050	n/c	0.0050	n/c	0.0071	0.0101
T_2	0.0050	0.0050		0.0050		0.0310	0.0578
T_3	0.0050	0.0050		0.0050		0.0050	0.0050
$\dfrac{W}{LA}$(10⁻⁴ lb/in³)	0.8144	0.8167		0.9769		2.7769	4.7830
$\dfrac{N_{xy}}{N_x} = 0.3$							
B_1 (in.)*	1.5141	2.1765		0.7154		1.1407	2.0729
B_2	10.0688	2.6617		1.5710		1.7568	2.5532
Angle, θ	0.9	8.1		46.7		64.7	48.3
T_1 (in.)**	0.0050	0.0050	n/c	0.0050	n/c	0.0095	0.0274
T_2	0.0050	0.0050		0.0061		0.0327	0.0661
T_3	0.0050	0.0050		0.0050		0.0050	0.0500
$\dfrac{W}{LA}$(10⁻⁴ lb/in³)	0.8144	0.8174		1.0267		3.0712	5.8748
$\dfrac{N_{xy}}{N_x} = 0.6$							
B_1 (in.)*	1.4195	1.4613		0.8328		1.3492	2.6296
B_2	8.7978	2.5048		1.3566		1.9479	2.8100
Angle, θ	0.9	9.4		58.4		58.2	41.8
T_1 (in.)**	0.0050	0.0050	n/c	0.0050	n/c	0.0187	0.0581
T_2	0.0050	0.0050		0.0080		0.0333	0.0592
T_3	0.0050	0.0050		0.0050		0.0050	0.0050
$\dfrac{W}{LA}$(10⁻⁴ lb/in³)	0.8144	0.8194		1.1908		3.8523	8.0584
$\dfrac{N_{xy}}{N_x} = 1.0$							
B_1 (in.)*	1.0746	1.0851		0.8499		1.4716	3.4180
B_2	7.9569	2.2402		1.3651		2.3513	2.1448
Angle, θ	1.1	11.5		57.4		49.9	56.6
T_1 (in.)**	0.0050	0.0050	n/c	0.0050	n/c	0.0339	0.0991
T_2	0.0050	0.0050		0.0127		0.0298	0.0440
T_3	0.0050	0.0050		0.0050		0.0050	0.0057
$\dfrac{W}{LA}$(10⁻⁴ lb/in³)	0.8144	0.8230		1.4220		4.9578	11.3240

* Reference dimensions to Figure 86.
** Minimum gage ply thickness = 0.005 inches.
n/c Loading condition not considered.
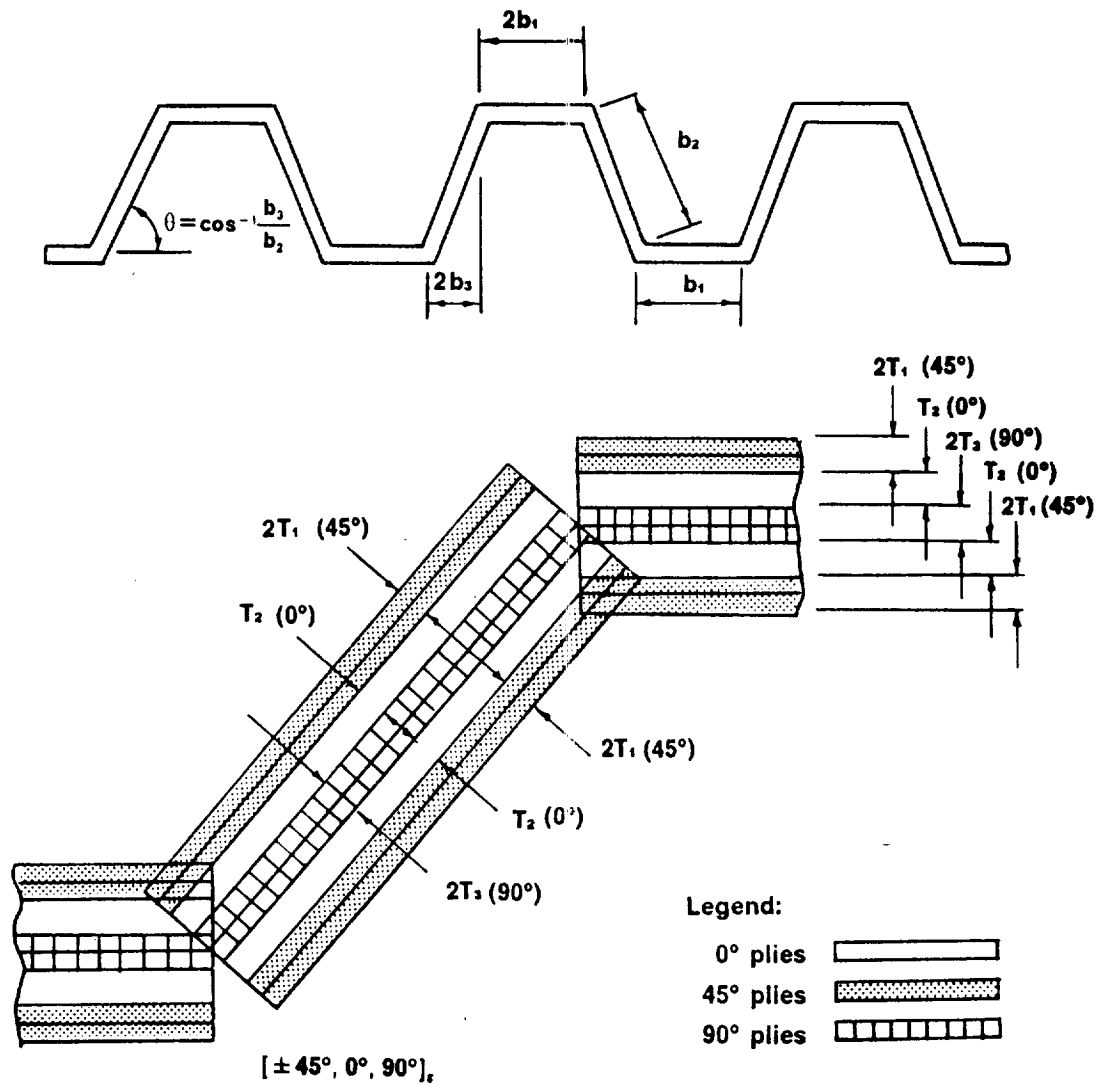
Table 37. Corrugated Panel with a Continuous Laminate (P= 15.0 psi   L= 28 in)

	Nx = 10 (lb/in)	Nx = 100 (lb/in)	Nx = 350 (lb/in)	Nx = 1000 (lb/in)	Nx = 2800 (lb/in)	Nx = 10000 (lb/in)	Nx = 28000 (lb/in)
$\frac{N_{xy}}{N_x} = 0.0$							
B_1 (in.)*	0.4598	0.4548		0.5096		0.8656	1.1388
B_2	2.1951	2.1933		2.2500		2.4120	2.4627
Angle, θ	43.7	44.4	n/c	45.2	n/c	57.7	68.4
T_1 (in.)**	0.0050	0.0050		0.0055		0.0073	0.0100
T_2	0.0069	0.0075		0.0127		0.0373	0.0637
T_3	0.0050	0.0050		0.0050		0.0050	0.0050
$\frac{W}{LA}$ (10⁻⁴ lb/in³)	1.1068	1.1458		1.4719		3.1792	5.1820
$\frac{N_{xy}}{N_x} = 0.3$							
B_1 (in.)*				0.5618		1.0480	2.2772
B_2				2.1267		2.1822	3.2460
Angle, θ	n/c	n/c	n/c	47.0	n/c	58.7	42.9
T_1 (in.)**				0.0057		0.0097	0.0265
T_2				0.0129		0.0383	0.0832
T_3				0.0050		0.0050	0.0060
$\frac{W}{LA}$ (10⁻⁴ lb/in³)				1.5091		3.3845	6.5295
$\frac{N_{xy}}{N_x} = 0.6$							
B_1 (in.)*				0.5272		1.6716	2.3520
B_2				2.0748		2.9037	3.8757
Angle, θ	n/c	n/c	n/c	47.7	n/c	44.9	40.2
T_1 (in.)**				0.0050		0.0186	0.0577
T_2				0.0153		0.0479	0.0672
T_2				0.0050		0.0051	0.0050
$\frac{W}{LA}$ (10⁻⁴ lb/in³)				1.5756		4.2478	8.5461
$\frac{N_{xy}}{N_x} = 1.0$							
B_1 (in.)*	0.4910	0.4654		0.5892		1.4464	2.5238
B_2	2.1462	2.1243		2.0442		2.9874	5.0283
Angle, θ	38.8	46.0	n/c	46.8	n/c	42.4	31.3
T_1 (in.)**	0.0051	0.0050		0.0051		0.0346	0.0981
T_2	0.0086	0.0079		0.0189		0.0388	0.0578
T_2	0.0050	0.0050		0.0050		0.0050	0.0050
$\frac{W}{LA}$ (10⁻⁴ lb/in³)	1.1355	1.1851		1.7342		5.3072	11.3821

* Reference dimensions to Figure 86.
** Minimum gage ply thickness = 0.005 inches.
n/c Loading condition not considered.

Table 38. Corrugated Panel with a Continuous Laminate (P= 30.0 psi   L= 28 in)

	Nx= 10 (lb/in)	Nx= 100 (lb/in)	Nx= 350 (lb/in)	Nx= 1000 (lb/in)	Nx= 2800 (lb/in)	Nx= 10000 (lb/in)	Nx= 28000 (lb/in)
$\dfrac{N_{xy}}{N_x} = 0.0$							
B_1 (in.)*	0.5154	0.5194		0.5516		0.8244	1.0083
B_2	2.4171	2.4192		2.4129		2.5446	2.6333
Angle, θ	47.8	47.8		49.3		60.8	70.2
T_1 (in.)**	0.0050	0.0050	n/c	0.0050	n/c	0.0085	0.0119
T_2	0.0129	0.0135		0.0180		0.0380	0.0596
T_3	0.0050	0.0050		0.0050		0.0050	0.0050
$\dfrac{W}{LA}$ (10^{-4} lb/in³)	1.4752	1.5048		1.7656		3.5486	5.7613
$\dfrac{N_{xy}}{N_x} = 0.3$							
B_1 (in.)*							
B_2							
Angle, θ							
T_1 (in.)**	n/c	n/c	n/c	n/c	n/c	n/c	n/c
T_2							
T_3							
$\dfrac{W}{LA}$ (10^{-4} lb/in³)							
$\dfrac{N_{xy}}{N_x} = 0.6$							
B_1 (in.)*							
B_2							
Angle, θ							
T_1 (in.)**	n/c	n/c	n/c	n/c	n/c	n/c	n/c
T_2							
T_3							
$\dfrac{W}{LA}$ (10^{-4} lb/in³)							
$\dfrac{N_{xy}}{N_x} = 1.0$							
B_1 (in.)*	0.5079	0.5084		0.6459		1.9109	3.2664
B_2	2.4366	2.4366		2.1456		2.9712	4.2183
Angle, θ	47.1	47.2		51.3		45.9	34.7
T_1 (in.)**	0.0050	0.0050	n/c	0.0053	n/c	0.0349	0.0975
T_2	0.0132	0.0142		0.0221		0.0409	0.0664
T_3	0.0050	0.0050		0.0050		0.0050	0.0050
$\dfrac{W}{LA}$ (10^{-4} lb/in³)	1.4827	1.5353		2.0039		5.4300	11.6618

* Reference dimensions to Figure 86.
** Minimum gage ply thickness = 0.005 inches.
n/c Loading condition not considered.

Table 39.   Corrugated Panel with a Continuous Laminate (P= 45.0 psi   L= 28 in)

	Nx = 10 (lb/in)	Nx = 100 (lb/in)	Nx = 350 (lb/in)	Nx = 1000 (lb/in)	Nx = 2800 (lb/in)	Nx = 10000 (lb/in)	Nx = 28000 (lb/in)
$\dfrac{N_{xy}}{N_x} = 0.0$ B_1 (in.)[x] B_2 Angle, θ T_1 (in.)[xx] T_2 T_3 $\dfrac{W}{LA}$ (10^{-4} lb/in³)	0.5541 2.6142 51.3 0.0050 0.0176 0.0050 1.7720	0.5761 2.6100 49.2 0.0050 0.0185 0.0050 1.7994	n/c	0.6328 2.5446 51.7 0.0050 0.0227 0.0050 2.0590	n/c	0.8133 2.6343 61.8 0.0089 0.0422 0.0050 3.9374	1.8201 2.7648 69.8 0.0112 0.0928 0.0050 6.8237
$\dfrac{N_{xy}}{N_x} = 0.3$ B_1 (in.)[x] B_2 Angle, θ T_1 (in.)[xx] T_2 $\dfrac{W}{LA}$ (10^{-4} lb/in³)	n/c	n/c	n/c	n/c	n/c	n/c	n/c
$\dfrac{N_{xy}}{N_x} = 0.6$ B_1 (in.)[x] B_2 Angle, θ T_1 (in.)[xx] T_2 $\dfrac{W}{LA}$ (10^{-4} lb/in³)	n/c	n/c	n/c	n/c	n/c	n/c	n/c
$\dfrac{N_{xy}}{N_x} = 1.0$ B_1 (in.)[x] B_2 Angle, θ T_1 (in.)[xx] T_2 T_3 $\dfrac{W}{LA}$ (10^{-4} lb/in³)	0.5561 2.6415 69.1 0.0050 0.0177 0.0050 1.7750	0.5785 2.4996 52.8 0.0050 0.0178 0.0050 1.8274	n/c	0.6884 2.4663 50.3 0.0050 0.0278 0.0050 2.2704	n/c	1.8008 2.9475 70.9 0.0346 0.0450 0.0050 5.6908	n/c

[x] Reference dimensions to Figure 86.
[xx] Minimum gage ply thickness = 0.005 inches.
n/c Loading condition not considered.

Table 40. Corrugated Panel with a Continuous Laminate - Bead Ratio = 1.0 (P= 0.0 psi   L= 28 in)
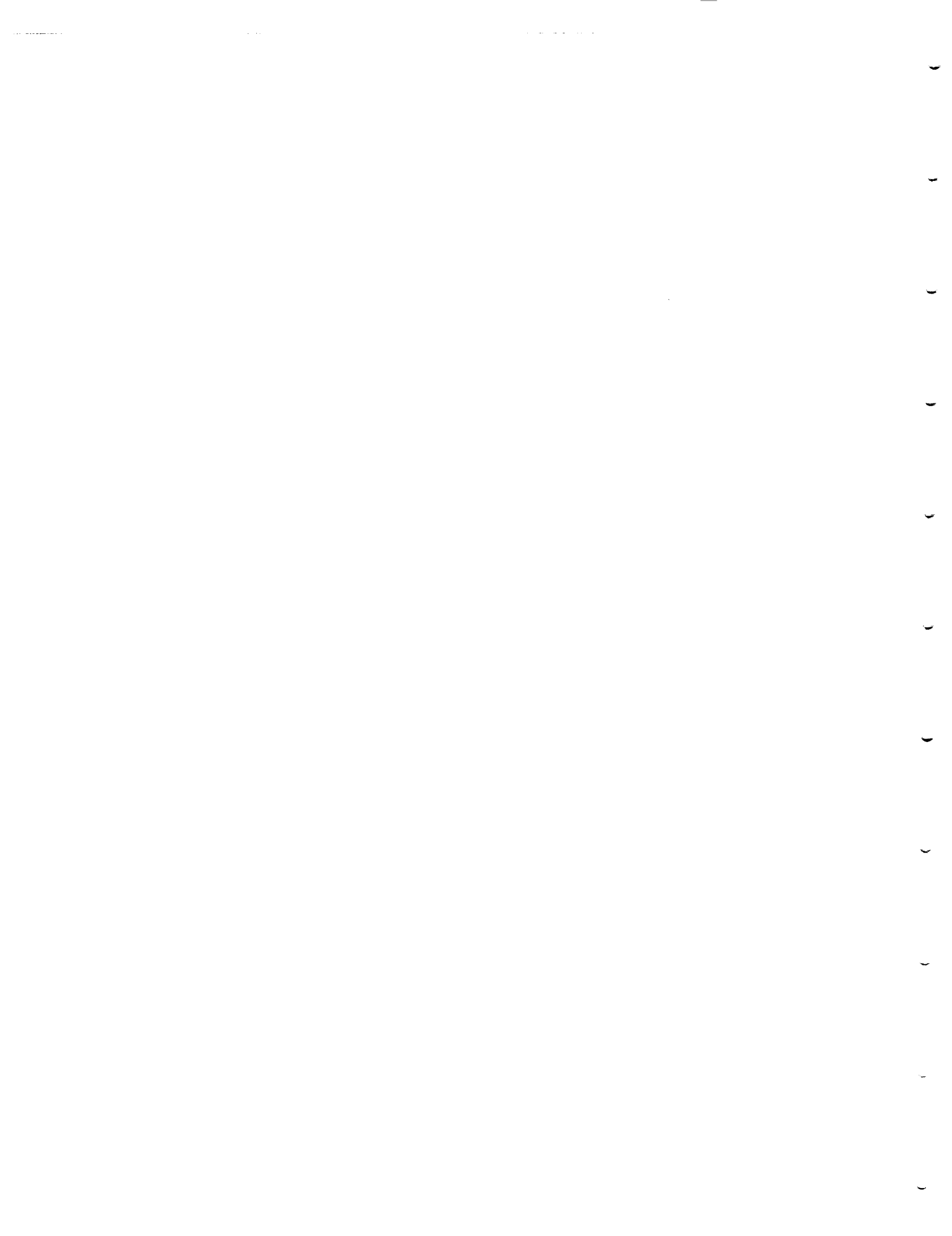
	Nx = 10 (lb/in)	Nx = 100 (lb/in)	Nx = 350 (lb/in)	Nx = 1000 (lb/in)	Nx = 2800 (lb/in)	Nx = 10000 (lb/in)	Nx = 28000 (lb/in)
$\dfrac{N_{xy}}{N_x} = 0.0$							
B_1 (in.)ˣ	6.8716	2.5446		0.9248		0.9547	1.1875
B_2	6.4012	1.9593		1.3725		1.8205	2.3075
B_3	0.9463	1.2665		0.4708		0.8534	1.2974
Angle, θ	1.7	12.7		59.8		73.1	76.5
T_1 (in.)ˣˣ	0.0050	0.0050	n/c	0.0050	n/c	0.0062	0.0162
T_2	0.0050	0.0050		0.0050		0.0273	0.0457
T_3	0.0050	0.0050		0.0050		0.0050	0.0050
$\dfrac{W}{LA}(10^{-4}$ lb/in³)	0.8145	0.8220		1.1151		3.0430	5.1093
$\dfrac{N_{xy}}{N_x} = 0.3$							
B_1 (in.)ˣ	6.1768	2.3300		0.9086		1.0482	2.1394
B_2	5.8836	1.7460		1.2184		1.6568	2.5344
B_3	0.5914	1.2665		0.7181		1.4037	1.4268
Angle, θ	1.7	13.6		63.4		77.9	55.7
T_1 (in.)ˣˣ	0.0050	0.0050	n/c	0.0050	n/c	0.0082	0.0278
T_2	0.0050	0.0050		0.0063		0.0285	0.0590
T_2	0.0050	0.0050		0.0050		0.0050	0.0050
$\dfrac{W}{LA}(10^{-4}$ lb/in³)	0.8145	0.8229		1.1878		3.3075	6.1381
$\dfrac{N_{xy}}{N_x} = 0.6$							
B_1 (in.)ˣ	4.9632	2.1313		0.9400		1.6034	2.9300
B_2	4.1349	1.5583		1.3076		1.8130	2.5456
B_2	1.6610	1.2665		0.6981		1.8875	2.6495
Angle, θ	1.9	16.0		63.1		68.7	50.9
T_1 (in.)ˣˣ	0.0050	0.0050	n/c	0.0050	n/c	0.0190	0.0583
T_2	0.0050	0.0050		0.0087		0.0309	0.0549
T_2	0.0050	0.0050		0.0050		0.0050	0.0050
$\dfrac{W}{LA}(10^{-4}$ lb/in³)	0.8145	0.8258		1.3364		4.0865	8.3405
$\dfrac{N_{xy}}{N_x} = 1.0$							
B_1 (in.)ˣ	4.1021	1.9111		0.9945		2.3775	3.5426
B_2	3.4663	1.3425		1.2945		1.8650	2.6563
B_3	1.2770	1.3231		0.9728		2.4998	3.4396
Angle, θ	2.3	21.4		66.9		52.8	46.7
T_1 (in.)ˣˣ	0.0050	0.0050	n/c	0.0050	n/c	0.0320	0.0991
T_2	0.0050	0.0050		0.0123		0.0433	0.0446
T_3	0.0050	0.0050		0.0050		0.0124	0.0050
$\dfrac{W}{LA}(10^{-4}$ lb/in³)	0.8146	0.8341		1.5517		5.6267	11.2756

ˣ Reference dimensions to Figure 86.
ˣˣ Minimum gage ply thickness = 0.005 inches.
n/c Loading condition not considered.

BIBLIOGRAPHIC DATA SHEET	1. Report No. CCMS-88-18; VPI-E-88-29	2.	3. Recipient's Accession No.

16. Abstracts

The present study focuses on the structural efficiencies of optimally designed composite wing rib panel configurations which have the potential for being economically manufactured. Panel analysis and design code PASCO, and VIPASA are chosen as the primary sizing and analysis tools for this study. The rib dimensions typical of a large transport aircraft are used. The configurations studied include a tailored corrugated panel, a corrugated panel with a continuous laminate throughout its length and width, and a hat-stiffened panel. Also included in the study are a blade stiffened panel and a flat unstiffened plate which are used as a baseline configurations for comparison.

The constraints considered in the present include those associated with material strength, buckling, and geometric limits. Postbuckling load carrying capability of the panels are neglected. Thicknesses of plies with different ply orientations in the different sections of the panel and detailed cross sectional dimensions are used as sizing variables to determine the best cross sectional geometry. The loads applied to the panels include the in-plane axial compression (N_x), shear (N_{xy}), and pressure (P) loads. The magnitude of the load range selected for study is based on a typical loading of an inboard wing rib fuel closeout cell for a large transport aircraft.

17. Key Words and Document Analysis.   17a. Descriptors

rib panels, combined loads, compression, shear, pressure, minimum weight, graphite-epoxy, structural efficiency, buckling, wing ribs, corrugated panel, beaded panel, stiffened panel

17b. Identifiers/Open-Ended Terms

17c. COSATI Field/Group

18. Availability Statement	19. Security Class (This Report) UNCLASSIFIED	21. No. of Pages 208
	20. Security Class (This Page) UNCLASSIFIED	22. Price

VIRGINIA TECH CENTER FOR
COMPOSITE MATERIALS AND STRUCTURES

The Center for Composite Materials and Structures is a coordinating organization for research and educational activity at Virginia Tech. The Center was formed in 1982 to encourage and promote continued advances in composite materials and composite structures. Those advances will be made from the base of individual accomplishments of the forty members who represent ten different departments in two colleges.

The Center functions through an Administrative Board which is elected yearly and a Director who is elected for a three-year term. The general purposes of the Center include:

- collection and dissemination of information about composites activities at Virginia Tech,
- contact point for other organizations and individuals,
- mechanism for collective educational and research pursuits,
- forum and agency for internal interactions at Virginia Tech.

The Center for Composite Materials and Structures is supported by a vigorous program of activity at Virginia Tech that has developed since 1963. Research expenditures for investigation of composite materials and structures total well over seven million dollars with yearly expenditures presently approximating two million dollars.

Research is conducted in a wide variety of areas including design and analysis of composite materials and composite structures, chemistry of materials and surfaces, characterization of material properties, development of new material systems, and relations between damage and response of composites. Extensive laboratories are available for mechanical testing, nondestructive testing and evaluation, stress analysis, polymer synthesis and characterization, material surface characterization, component fabrication, and other specialties.

Educational activities include eight formal courses offered at the undergraduate and graduate levels dealing with the physics, chemistry, mechanics, and design of composite materials and structures. As of 1984, some 43 Doctoral and 53 Master's students have completed graduate programs and several hundred Bachelor-level students have been trained in various aspects of composite materials and structures. A significant number of graduates are now active in industry and government.

Various Center faculty are internationally recognized for their leadership in composite materials and composite structures through books, lectures, workshops, professional society activities, and research papers.

MEMBERS OF THE CENTER

Aerospace and Ocean Engineering
Raphael T. Haftka
Eric R. Johnson
Rakesh K. Kapania

Chemical Engineering
Donald G. Baird

Chemistry
John G. Dillard
James E. McGrath
Thomas C. Ward
James P. Wightman

Civil Engineering
R. M. Barker

Electrical Engineering
Ioannis M. Besieris
Richard O. Claus

Engineering Science and Mechanics
Hal F. Brinson
Robert Czarnek
David Dillard
Norman E. Dowling
John C. Duke, Jr.
Daniel Frederick
O. Hayden Griffin, Jr.
Zafer Gurdal
Robert A. Heller
Edmund G. Henneke, II
Michael W. Hyer
Robert M. Jones
Liviu Librescu
Alfred C. Loos
Don H. Morris
John Morton
Ali H. Nayfeh
Marek Pindera
Daniel Post

J. N. Reddy
Kenneth L. Reifsnider
C. W. Smith
Wayne W. Stinchcomb
Surot Thangjitham

Industrial Engineering and Operations Research
Joel A. Nachlas

Materials Engineering
D. P. H. Hasselman
Robert E. Swanson

Mathematics
Werner E. Kohler

Mechanical Engineering
Charles E. Knight
John B. Kosmatka
J. Robert Mahan
Craig A. Rogers
Curtis H. Stern

Inquiries should be directed to:

Center for Composite Materials and Structures
College of Engineering
Virginia Tech
Blacksburg, VA 24061
Phone: (703) 961-4969